Abstracts 12,243-12,903

SOLID STATE ABSTRACTS

an abstract journal devoted to the theory, production and use of solid state materials and devices

VOLUME 2 NUMBERS 9 — 10

PHYSICS

METALLURGY

ELECTRONICS

SEMICONDUCTORS

PHOSPHORS

MAGNETICS

DIELECTRICS

SUPERCONDUCTORS

METALS

SOLID STATE ABSTRACTS

VOLUME 2, NUMBERS 9-10

December 1961/January 1962

Abstracts 12,243–12,903

TABLE OF CONTENTS

Abstracts of the Solid State Literature

Metallurgy and Chemistry of Solids

Thermodynamic Properties . . . 395
Crystal Structure . . . 396
General . . . 396
Point Defects . . . 397
Dislocations . . . 400
Grain Boundaries and Other Structures . . . 406
Chemical Impurities . . . 407
Structure of Surfaces and Special Crystal Forms 412
Crystal Growth . . . 413
Crystal Surfaces . . . 417
Environmental Effects . . . 418

Solid State Physics

Crystal Physics . . . 420
Binding Properties . . . 420
Energy Band Structure . . . 420
Lattice Potentials and Vibrations . . . 421
Electronic Properties . . . 422
Electrical Properties . . . 422
General . . . 422
Dielectric Properties . . . 422
Carrier Properties . . . 425
Conductivity (Resistivity) . . . 426
Superconductivity . . . 429
Breakdown . . . 430
Magnetoelectric (Galvanomagnetic) Properties . 430
Other Electrical Properties . . . 430
Magnetic Properties . . . 431
General . . . 431
Ferro- and Ferrimagnetism . . . 431
Paramagnetism . . . 434
Diamagnetism . . . 435
Optical Properties . . . 435
General . . . 435
Absorption (Transmission) . . . 436
Radiation and Luminescence . . . 438
Photoelectronic Properties . . . 440
Electromagnetic Properties . . . 442
Thermal Properties . . . 443
Mechanical Properties . . . 445

Solid State Devices

General . . . 448
Resistors . . . 448
Diodes . . . 448
Transistors . . . 451
Magnetoelectric Devices . . . 454
Other Conductive Devices . . . 455
Photodevices . . . 455
Thermal Devices . . . 456
Ferro- and Ferrimagnetic (Ferrite) Devices . . . 457
Paramagnetic Devices (Masers and Lasers) . . . 458
Dielectric Devices . . . 461
Other Solid State Devices . . . 461

Basic Solid State Device Circuits

General . . . 462
Amplifiers . . . 465
Oscillators . . . 469
Switching Circuits . . . 470
Signal Converters . . . 472
Wave Generators . . . 472
Pulse Circuits . . . 474
Other Circuits . . . 474

Applications of Solid State Devices

Communications and Related Applications . . . 475
Computers . . . 476
Digital Computers . . . 476
Analog Computers and Other Data Systems . . 480
Power . . . 481
Control . . . 482
Instrumentation . . . 482
Energy Conversion . . . 485

Subject Index . . . 486

Author Index . . . 496

Editor: GEOFFREY KNIGHT, JR., Ph.D.

Assistant Editor: JOHN A. MURPHY

PUBLISHED MONTHLY BY

Cambridge Communications Corporation, 238 Main Street, Cambridge 42, Massachusetts, Tel. 491-0710

Subscription Rate: $25.00 per year. Single Copies and Back Issues: $5.00. Advertising Rates on Request.

Cambridge Communications Corp. is not prepared to furnish copies of the articles abstracted. However, there are many libraries throughout the country which maintain photocopying services.

SYMBOLS USED IN THE ABSTRACTS

L: Letter to the Editor. A: Only an abstract is given in the reference. R: Only a review is given in the reference. E: Erratum.

The reference numbers in the indices are the abstract numbers, not the page numbers.

Copyright 1962 by Cambridge Communications Corp. Printed in the U.S.A. by the University Press, Inc.

ABSTRACTS OF THE SOLID STATE LITERATURE

METALLURGY AND CHEMISTRY OF SOLIDS

THERMODYNAMIC PROPERTIES

12,243 THE P-T-X PHASE DIAGRAM OF THE SYSTEM Sn-S by W. Albers and K. Schol (Philips); Philips Res. Rep., Vol. 16, pp. 329-342, Aug. 1961

Determination of the phase equilibria solid-liquid-vapor for the system Sn-S is reported. The maxima are found in the T-X_L diagram, one at the composition of SnS, the other at the composition of SnS_2. The compound SnS has a maximum melting point of 881.5 ± 2°C at a S pressure of 0.033 atm and SnS_2 has a maximum melting point of about 870°C at a S pressure of about 40 atm. A range of liquid immiscibility exists between about 10 and 47 atomic per cent S and possibly also between about 70 and 90 atomic per cent S. A new compound with a probable composition of Sn_3S_4 has been found.

12,244 THE ZIRCONIUM-RICH CORNERS OF THE TERNARY SYSTEMS Zr-Co-O AND Zr-Ni-O by M. V. Nevitt and J. W. Downey (Argonne Natl. Labs.); AIME Trans., Vol. 221, pp. 1014-1017, Oct. 1961

An investigation of the Zr-rich portions of the ternary systems Zr-Co-O and Zr-Ni-O is reported. The phase boundaries for the 950°C isothermal sections in these systems have been determined for the composition range from 50 to 100 atomic per cent Zr. The two systems show very similar relations, having no extensive solid solution phase fields. Each contains a ternary phase. These phases are apparently isostructural, but their structure has not been determined. Some aspects of the phase relations are discussed in terms of the alloying behavior of transition metals.

12,245 ABOUT THE DEPENDENCE OF THE EVAPORATION COEFFICIENT ON THE PARTIAL PRESSURE ABOVE THE EVAPORATING SINGLE CRYSTAL SURFACE [in German] by R. Jaeckel and W. Peperle (Phys. Inst., U. Bonn); Z. Phys. Chem., Leipzig, Vol. 217, pp. 321-336, Oct. 1961

Measurements of the partial vapor pressure above single crystal surfaces of NaCl, KI, Sb_2S_3 and S are reported. The evaporation rate is strongly affected by the degree of undersaturation. The Kossel-Shariski Model is used to explain the increase of the evaporation coefficient with decreasing pressure; increase in the coefficient is related to an increase of surface evaporation. Electro-optical techniques were employed in the study.

Dislocations and Substructures Produced during Solidification of Al - See 12,304

12,246 STRUCTURE AND PROPERTIES OF THE HgTe-CdTe SYSTEM by A. D. Schneider and I. V. Gavrishchak (L'vov State Pedagogical Inst.); Soviet Phys.-Solid State, Vol. 2, pp. 1865-1867, Mar. 1961

The formation and properties of a broad range of solid solutions in the system HgTe-CdTe are discussed. An optimum heat-treating schedule was necessary to effect a solid solution with each sample. For pure HgTe, the thermal EMF was negative throughout the temperature range studied, indicating that electrons are the majority carriers; all other specimens possessed hole majority conduction. Photoconductivity was observed in specimens in which the amount of CdTe was equal to or greater than 65 mole per cent.

12,247 SOLID SOLUBILITY OF ARSENIC IN GERMANIUM AT 865°C FROM A SATURATION DIFFUSION EXPERIMENT by F. A. Trumbore, W. G. Spitzer and R. A. Logan (Bell Labs.); J. Electrochem. Soc., Vol. 108, p. 263C (A), Dec. 1961

The diffusion of As into thin Ge slices (10-23 mils thick) at 865°C in a sealed-tube experiment lasting 97 days is discussed. The carrier concentration, n, in the As-diffused samples was $5 \times 10^{19} cm^{-3}$, as determined from optical reflectivity measurements. After heat treatment and quenching of these samples, n was $7.5 \times 10^{19} cm^{-3}$. The As concentration, determined chemically, agreed within experimental error with the quenched-in carrier concentration. These results indicate that the equilibrium solid solubility of As in Ge is almost a factor of two lower than previously reported.

12,248 DETERMINATION OF INTERSTITIAL SOLID-SOLUBILITY LIMIT IN TANTALUM AND IDENTIFICATION OF THE PRECIPITATE PHASES by D. A. Vaughan, O. M. Stewart and

C. M. Schwartz (Battelle); AIME Trans., Vol. 221, pp. 937-946, Oct. 1961

X-ray lattice parameter determinations of the solid-solubility limits for C, N and O in high purity Ta are presented. The phases of Ta_2C, the low temperature modification of Ta_2O_5 and Ta_xN of unknown composition but showing a super lattice structure based on the original bcc Ta lattice have been identified as the initial precipitates in the respective systems. Metallographic methods were employed to verify the X-ray analysis. The etching behavior of Ta is discussed in terms of lattice imperfection and precipitate phases.

Edge Dislocation Walls as Source of Diffusionless Phase Transformations - See 12,295

12,249 THE HIGH TEMPERATURE ELECTRICAL RESISTANCE OF IRON-ALUMINUM ALLOYS by R. Feder, P. H. Thornton and R. W. Cahn (U. Birmingham); Phil. Mag., Vol. 6, pp. 1093-1101, Sept. 1961

The use of electrical resistance, at temperatures from −196° to 700°C, as an indicator of crystallographic order to test the reality of certain anomalies in the long-range order in solid solutions near the composition Fe_3Al, which had previously been detected by X-ray diffraction, is discussed. Resistance anomalies were found in three alloys that contained 22.9, 23.5, and 24.8 atomic per cent Al; anomalies were not observed in alloys containing 22.2 and 25.5 atomic per cent Al. The significance of these results is briefly discussed.

12,250 MONTE CARLO CALCULATION OF THE ORDER-DISORDER TRANSFORMATION IN THE BODY-CENTERED CUBIC LATTICE by P. A. Flinn and G. M. McManus (Westinghouse Res. Labs.); Phys. Rev., Vol. 124, pp. 54-59, Oct. 1961

An investigation by a Monte Carlo method of the order-disorder transformation in the bcc structure is described. A critical temperature was observed at the point $(v/kT) = -0.315$. The results of the calculation are in close agreement with the best analytical approximations. The calculated variation of order with temperature is in good agreement with experimental data on β-brass and β-AgZn. Some information on the kinetics of the transformation was obtained. It appears likely that the rate-limiting process for diffusion in the ordered structure is the jumping of vacancies to second neighbor positions.

12,251 THE EFFECTS OF DEFORMATION AT 78°K ON THE ALLOY Cu_3Au by B. Roessler and M. B. Bever (MIT); AIME Trans., Vol. 221, pp. 1049-1055, Oct. 1961

The effects of deformation by wire drawing at 78°K on initially ordered and initially disordered specimens of the alloy Cu_3Au are reported. The resistivity, stored energy, drawing force, and microhardness were measured as functions of strain; microstructural changes were observed. The results are interpreted in terms of the structural imperfections and the changes in atomic configuration resulting from deformation. A few experiments on the effects of room-temperature annealing after deformation at 78°K were made; they suggest vacancy-promoted ordering in disordered alloys.

12,252 THE PHASE TRANSFORMATION IN THIN COBALT FILMS by E. Votava (European Res. Assoc.); J. Inst. Metals, Vol. 90, pp. 129-132, Dec. 1961

An investigation, by direct transmission electron microscopy, of the reversible phase transformation which takes place in Co at 417°C is discussed. It was found that in thin specimens considerable supercooling of the transition occurred and that the fcc phase could be retained to a considerable extent at room temperature. An explanation for this phenomenon is presented.

CRYSTAL STRUCTURE

GENERAL

12,253 PERFECTION OF THE LATTICE OF DISLOCATION-FREE SILICON, STUDIED BY THE LATTICE-CONSTANT AND DENSITY METHOD by M. E. Straumanis, P. Borgeaud and W. J. James (U. Missouri); J. Appl. Phys., Vol. 32, pp. 1382-1384, July 1961

Lattice-constant and density method studies of lattice perfection in Si ($n' = 8.0000$) using high purity, dislocation-free Si are described. Results obtained were in agreement with studies made by the decoration method. The lattice constant of vacuum heated Si powder of semiconductor purity was 5.43070 ± 0.00004 A; that of the nonheat-treated powder was 5.43081 A at 25°C. The constants determined from crystal chips by the rotating crystal method were lower, between 5.43028–5.43048 A at 25°C. As the constants of each series of measurements could be reproduced very well ($s = \pm 0.00004$ A), the lower values suggested the presence of some unknown systematic errors, the magnitude of which is outside the scope of errors due to absorption. The thermal expansion coefficients of all samples between 10°-60°C were $(2.6 \pm 0.4) \times 10^{-6}/°C$. The average density of etched crystal chips was 2.3289 ± 0.0001 g/cm^3. The lower density of the nonetched chips indicated the presence of microcracks, removable by etching, within the distorted surface layers. There was no significant difference in density of bars sawed, or of chips broken from the crystal and etched.

12,254 ANOMALOUS TEMPERATURE DEPENDENCE OF LATTICE CONSTANTS OF FERROELECTRIC SODIUM NITRITE by S. Hoshino and I. Shibuya (U. Tokyo); J. Phys. Soc. Japan, Vol. 16, pp. 1254-1255(L), June 1961

X-ray diffraction measurements of the $NaNO_2$ lattice constant temperature dependence are reported. Back reflection photographs were taken at various temperatures with a high-temperature X-ray camera. More precise measurements were made using an X-ray diffractometer with an electric furnace. The c axis was found to decrease in length while the a and b axes increased with the rise in temperature. Two anomalies, at 163° and 178°C, were observed, the former being the known transition point at which spontaneous polarization disappears, while the latter has not previously been reported. The nature of the anomaly cannot be explained without further structural investigations on the crystals. The transition at 163°C was deduced to be of the first order.

Irradiation Induced Lattice Expansion - See 12,281

12,255 THE SUPERSTRUCTURES OF IRON SELENIDE Fe_7Se_8 by A. Okazaki (Kyusyu U., Fukuoka); J. Phys. Soc. Japan, Vol. 16, pp. 1162-1170, June 1961

Iron vacancies in Fe_7Se_8 are confined to the alternate iron layers parallel to the c-plane of the fundamental lattice with the NiAs structure. The origin of the ferrimagnetism of Fe_7Se_8

(T_c = 187°C) may be attributed to this ordered arrangement as in the case of Fe_7Se_8. There are two types of superstructure: low- and high-temperature. The unit cell dimensions and the lattice symmetries of these structures are as follows: low-temperature type: $A = \sqrt{3}B$, $B = 2a$, $C = 4c$; triclinic, high-temperature type: $A = 2a$, $C = 3c$, hexagonal, where the capital and small letters designate the super- and fundamental lattices, respectively. The transition from the triclinic structure to the hexagonal one, which indicates a rearrangement of the iron vacancies upon heating, begins at 240°C, proceeds gradually, and ends at 298°C.

12,256 DIRECT STUDY OF IMPERFECTIONS IN NEARLY PERFECT CRYSTALS by R. H. Bragg (Armour Res. Found.) and L. V. Azaroff (Illinois Inst. Tech.); U.S. Gov. Res. Rep., Vol. 36, p. S-55(A), Aug. 20, 1961 PB 155 662 $2.60

Use of the Laue focussing geometry employed by Guinier and Tennevin to observe imperfections in deformed crystals is extended to the study of imperfections in nearly perfect crystals by interpreting the observed intensity distributions in terms of the dynamical theory of X-ray diffraction. A rather perfect Si crystal was examined by this method; it was found that neighboring regions of the same crystal slice consist of mosaic blocks approximately 1/1000 cm thick whose relative tilts range from 8 to 12 seconds of arc. As suggested by the more qualitative etch pit densities and diffraction line breadths, the central portions of the crystal contain larger blocks with smaller relative misorientations than those lying near the surfaces of the crystal. It is thus possible to use this method to accurately map the distribution of imperfections throughout as small or as large a region of a single crystal as is desired.

12,257 THE DIRECT OBSERVATION OF LATTICE DEFECTS BY FIELD ION MICROSCOPY by D. G. Brandon and M. Wald (U. Cambridge); Phil. Mag., Vol. 6, pp. 1035-1044, Aug. 1961

Observations made on Mo and W by a field ion microscope are discussed. In Mo, the structure of edge dislocations and a grain boundary have been observed. In W irradiated with 5-Mev α-particles, the production of vacancies at the surface has been observed. It is shown that this technique can be used to investigate the atomic structure at a grain boundary and around the core of a dislocation. It can also be applied to the study of radiation damage to provide information about the distribution and range of the damage produced by a single high-energy impact.

12,258 FIELD ION MICROSCOPY OF IRON WHISKERS by E. W. Müller (Pennsylvania State U.); U.S. Gov. Res. Rep., Vol. 35, p. 796(A), June 16, 1961 PB 171 598

The design, construction and operation of a complete field ion microscope unit are described. The restrictions due to the high rate of field evaporation of iron are considered. This microscope is used for the study of the atomic structure of iron whiskers. Indications of crystal defects such as screw dislocations and interstitials are found, although usually the whiskers did not have sufficient strength to withstand the extremely high field forces.

12,259 LATTICE STRAINS AND X-RAY STRESS MEASUREMENT by M. J. Donachie, Jr. and J. T. Norton (MIT); AIME Trans., Vol. 221, pp. 962-967, Oct. 1961

The production of residual lattice strains in 2024 Al and ingot Fe by uniaxial tensile deformation is reported. These strains were measured on the original surface and in depth below the surface. The strains conformed approximately to those from a macroscopic stress distribution but they were not truly macroscopic in nature. The exact mechanism which apparently causes the coherently diffracting region of each grain to behave as if macroscopically stressed was not determined.

Deformation of Cu_3Au Structure - See 12,251

POINT DEFECTS

12,260 RECENT ADVANCES IN THE THEORY OF DEFECTS IN CRYSTALS by A. Seeger (Max Planck Inst. Metall. and Tech. Hochsch., Stuttgart); Phys. Status Solidi, Vol. 1, No. 7, pp. 669-698, 1961

Recent advances in the theory of crystal defects are treated in a unified manner. The subject is divided into two areas: theoretical approaches which can be applied to all crystals, and methods which have been designed specifically for particular classes of crystals, e.g., metals, ionic crystals, homopolar crystals, etc. The first part almost coincides with the continuum theory of lattice defects, in which the individual properties of the crystals and their chemical and crystallographic nature enter essentially through the elastic constants. The second part comprises the methods based on the atomistic pictures of the various types of crystals. The atomistic part of this review deals only with metals. A treatment of the general theory of the continuum approach is followed by the application of the continuum theory to special problems and, finally, reports on the calculations based on electron theory and on models for point defects. Numerous references to summaries or to recent papers which reflect the present state of the field are given.

12,261 DEFORMATION-PRODUCED POINT DEFECTS by H. K. Birnbaum (U. Chicago) and F. R. Tuler (U. Illinois); J. Appl. Phys., Vol. 32, pp. 1403-1404(L), July 1961

Preliminary results of an investigation of the interaction of deformation-produced point defects in high purity copper are given. Specimens were strained at 77°K to a prestrain E_p, aged at a different temperature (T_a) for various periods of time (t_a) and then the strain was continued at 77°K. The magnitude of the yield point is compared with t for various values of T. Good agreement was obtained between the experimental data and the calculations based on a simple model. The analysis leads to an evaluation of the activation energy for diffusion of point defects and concludes that a considerable concentration of interstitials is produced by plastic deformation.

12,262 ENERGY-DEPENDENT BEHAVIOR OF INTRINSIC CLOSE-PAIR DEFECTS WITHIN COPPER by R. L. Chaplin and P. E. Shearin (U. North Carolina); Phys. Rev., Vol. 124, p. 1061, Nov. 15, 1961

Measurements of the low-temperature substages of high purity Cu which are associated with close-pair Frenkel defects following 2-Mev electron irradiations are discussed. Results are in the region of multiple defect production and show that a correlation exists between prior experimental work performed by lower energy electron and 10-Mev deuteron bombardments. It is evident that each intrinsic substage possesses a very definite dependence upon irradiation energy.

12,263 INVESTIGATIONS IN THE REGIONS OF CRYSTALLOCERAMICS. Part II. THE EFFECT OF ALL-ROUND PRESSURE ON THE KINETICS OF MACRODEFECT RECUPERATION IN IONIC CRYSTALS by Ya. E. Geguzin and L. M. Polyakov (Physiotech. Inst.); Soviet Phys.-Solid State, Vol. 3, pp. 381-386, Aug. 1961

The effect of pressure on the kinetics of the recuperation of defects which arise during plastic deformation is investigated. Experiments were carried out on a NaCl crystal. The recuperative process was investigated on the basis of variation in light scattering during the process of high temperature annealing. After annealing and slow cooling, the specimens were subjected to increasing pressure applied to an edge. Scattered light intensity increased during the loading. Two other series of experiments were conducted to determine the effect of pressure on microdefect recuperation. The observed effects are explained on the basis of a diffusion mechanism and the effect of pressure on the equilibrium vacancy concentration in the lattice. It is shown that equal recuperative effects, as observed by through-illumination of the crystal, may be obtained by increase of either temperature or pressure. Acceleration of the process of through-illumination of the crystal due to pressure is explained by the dependence of the vacancy concentration gradient on pressure.

12,264 VACANCY CONCENTRATION IN A SOLID [in Russian] by V. A. Iakovlev (Stalingrad Pedag. Inst.); Izv. VUZ Fiz., No. 1, pp. 143-146, 1961

The failure of most attempts at calculating the equilibrium number of vacancies in a solid to take adequate account of the dynamics of the crystal lattice is discussed. For example, the crystal is considered in the Einstein approximation and the influence of the defects is reduced to the change in frequency of vibration of a small number of neighbors. The changed frequency is not evaluated. It has been shown before that defects generate spatially localized vibrations whose frequencies lie beyond the acoustic and optical spectra. Moreover, without changing the dispersion law in the main bands, they change the distribution density of the number of vibrations in the frequency range. The influence of these effects affects the magnitude of γ in a crystal of the cubic system whose cell contains one atom.

Vacancy Concentrations in NiO - See 12,480

Formation of Dislocations by Vacancy Condensation - See 12,293

12,265 ELECTRON MICROSCOPIC OBSERVATION OF THE AGGREGATES OF VACANCIES IN GERMANIUM by K. Tanaka, M. Mannami, K. Izumi and H. Niwa (Kyoto U.); J. Phys. Soc. Japan, Vol. 16, p. 2070(L), Oct. 1961

Aggregates of vacancies observed in Ge crystals quenched after heating at temperatures between 750° and 800°C are discussed. Thin foils prepared by polishing the crystals in CP-4 were examined in an electron microscope by the transmission method. No annealing was carried out to precipitate the quenched-in vacancies since the foils were heated by the chemical polishing and by the electrons in the electron microscope. Depending on the direction of the incident electrons, the aggregate appears as a chain with either a dark region on one side, a dark region on both sides, or no dark region. These results indicate that elastic lattice distortion is dominant for about 200 A on both sides of the chain and that the chain is due to an irregularity in the lattice.

12,266 THE ELECTRON-MICROSCOPY INVESTIGATION OF THE AGGLOMERATES OF QUENCHED-IN VACANCIES IN F.C.C. LATTICES, PARTICULARLY IN NICKEL-COBALT ALLOYS [in German] by S. Mader, A. Seeger and E. Simsch (Max Planck Inst. Metall., Stuttgart); Z. Metallkde., Vol. 52, No. 12, pp. 785-794, 1961

The agglomeration of quenched-in vacancies in fcc Ni-Co, Ni-Cu and Au is discussed. In Ni-Cu and Ni-Co (up to 55 per cent Co content) only prismatic dislocation loops were observed. With higher Co content stacking fault tetrahedra occur. Tetrahedra form only in Ni-Co alloys of low stacking fault energy, where the total energy of a tetrahedron is less than the energy of a dislocation loop. The loops observed cannot be formed by condensation of vacancies on {111} planes and subsequent removal of the stacking fault by a Shockley partial. The nucleation of such a partial dislocation loop is only possible at stacking fault energies of $p \gtrsim 30 \cdot Co^{-3} G \cdot b$. In Ni and Ni-Co alloys the density of vacancy products visible in the electron microscope is rather low. This may be due to the segregation of vacancies into small invisible voids. In ferromagnetic metals the conversion of spherical voids into dislocation loops is presumably rendered difficult by the magnetic stray fields.

12,267 QUENCHED-IN VACANCY IN SOLID SOLUTION ALLOYS by Y. Hamaguchi (Japan Atomic Energy Res. Inst.); J. Phys. Soc. Japan, Vol. 16, pp. 1692-1697, Sept. 1961

From the difference in the electrical resistivity change induced by quenching between pure Au and Au-Pd solid solutions, the binding energy for a vacancy and a solute atom is determined. The rate of decrease of quenched-in additional resistivity with decreasing temperature in the alloy is more rapid than in the pure metal and the resistivity after quenching is smaller than that before quenching in high concentration alloys below a certain quenching temperature. It is concluded that the interaction of a Pd atom and a vacancy in Au-Pd alloys is attractive and that the additional resistivity of the solute atom is partly cancelled by the binding of the vacancy. The same observations are expected in Ag-Pd alloys.

12,268 QUENCHING OF CATION VACANCIES IN DOPED CRYSTALS OF SODIUM CHLORIDE by K. S. Krishnan and S. C. Jain (Natl. Phys. Lab., New Delhi); Nature, Vol. 191, pp. 162-164(L), July 8, 1961

The effective quenching of cation vacancies in NaCl is reported. NaCl crystals containing known concentrations, c, of $CdCl_2$ were grown from the melt in the usual manner, annealed at 1050°K, and then dropped into liquid nitrogen. The electrical conductivity σ was plotted against the ratio Cd/Na at four different temperatures, T, and also log T/c was plotted against T. All were straight lines, the first set passing through the origin. It follows from this that: (1) even at the highest temperatures the number of cation vacancies remains the same; (2) this number is proportional to c, and hence is the number of Cd^{2+} ions doped into the crystal; and (3) a low value for the energy of pairing of a cation vacancy with a Cd^{2+} ion is indicated. On annealing the crystal slowly, the effective number of cations drops. An explanation for this is proposed.

12,269 GRAVIMETRIC STUDIES OF THE DEFECT STRUCTURE OF α-Nb_2O_5 by P. Kofstad and P. B. Anderson (Central Inst. Ind. Res., Oslo); J. Phys. Chem. Solids, Vol. 21, pp. 280-

286, Dec. 1961

A gravimetric study of the defect structure of non-stoichiometric α-Nb_2O_5 in the temperature range 900°-1400°C is discussed. The relative, isothermal weight change of α-Nb_2O_5 equilibrated in mixtures of CO and CO_2 has been found to be proportional to $pO_2^{-1/6}$. This clearly establishes that the defect structure of oxygen-deficient α-Nb_2O_5 involves oxygen vacancies. Thermodynamic properties of the defect equilibrium and the partial molar thermodynamic properties of dissociation of oxygen in non-stoichiometric α-Nb_2O_5 have been calculated.

12,270 EFFECT OF BARDEEN-HERRING CORRELATION ON VACANCY DIFFUSION IN ANISOTROPIC CRYSTALS by J. G. Mullen (Argonne Natl. Lab.); Phys. Rev., Vol. 124, pp. 1723-1730, Dec. 15, 1961

The effect of correlation upon anisotropic self-diffusion is examined. From the Einstein relation, the principal diffusivities in anisotropic crystals are related to the atomic displacements. The effect of correlation is expressed in terms of correlation functions which are analogous to the correlation factor in isotropic diffusion. These correlation functions have been calculated for vacancy self-diffusion in the primitive tetragonal, body-centered tetragonal, and hexagonal close-packed lattices by a computer technique. The possible use of correlation to determine mechanisms of anisotropic self-diffusion is discussed.

12,271 MOBILITY OF VACANCY PAIRS IN IONIC CRYSTALS by K. Tharmalingam and A. B. Lidiard (U. Reading); Phil. Mag., Vol. 6, pp. 1157-1162, Sept. 1961

Calculations of activation energies for vacancy pair movements in NaCl and KCl using the approximation of a static lattice are presented. The numerical results indicate that these energies are comparable with, or greater than, the activation energies for single vacancy movement. Qualitative reasons for these results are given.

12,272 PRESSURE EFFECT ON VACANCY MIGRATION RATE IN GOLD by R. M. Emrick (U. Illinois); Phys. Rev., Vol. 122, pp. 1720-1733, June 15, 1961

The effect of hydrostatic pressures up to 10,000 kg/cm^2 on the annealing rate of vacancies quenched in gold is studied. High-purity gold wires are quenched from 700°C, trapping in the equilibrium concentration of vacancies at that temperature. The vacancies are then observed to anneal out in the vicinity of room temperature at various pressures by observing the decay of the quench-induced residual resistance increase. A simple relation for the temperature dependence of the annealing rate is derived, assuming a random distribution of vacancies and vacancy sinks. By applying thermodynamic relations to the expression for the vacancy annealing rate, a volume of motion is derived in terms of the experimentally determined pressure effect on the annealing rate. For gold, the motional volume is found to be 1.50 ± 0.14 cm^3/mole compared with the atomic volume of 10.2 cm^3/mole. A hard-spheres model for the jump process predicts about a one atomic volume increase of the lattice for the saddle-point configuration as well as a one atomic volume increase when a vacancy is formed. Many theoretical calculations of the lattice distortion around a vacancy and indirect experimental measurements of the volume change of the lattice on forming a vacancy indicate that there is considerable relaxation of the neighboring atoms about a vacancy. These results are used to explain the small value of the motional volume. Activation volumes derived from measurements of the effect of pressure on the rate of self-diffusion are seen to be consistent with the present experimental value.

Vacancy Mechanism of Atomic Diffusion - See 12,341

12,273 STRUCTURE AND PROPERTIES OF A-CENTERS IN KCl by K. Kojima, N. Nishimaki (Osaka Women's U.) and T. Kojima (Osaka City U.); J. Phys. Soc. Japan, Vol. 16, pp. 2033-2044, Oct. 1961; p. 2335, Nov. 1961

The irradiation of additively colored KCl crystals containing Na with F-band light is discussed. The F-light irradiation produces two absorption bands which are termed A_1 and A_2. By investigating their thermal, photochemical, and dichroic properties, these two bands are found to arise from a common species of centers called A-centers, and are identified with Petroff's A- and B-bands which have been found in nominally pure specimens. From the analysis of dichroic spectra, peak energy and half-width are determined for each band at several temperatures. The observed oscillator strength is 0.90 for the A_1-band and 0.81 for the A_2-band. The A-centers are destroyed thermally with an activation energy 0.43 ev. A model for the A-center is proposed and energy levels are calculated by the molecular orbital method.

12,274 NATURE OF THE V_1 CENTER by F. Seitz (U. Illinois); Phys. Rev. Lett., Vol. 7, pp. 282-283(L), Oct. 1, 1961

A proposed model for the V_1 center is discussed. It is suggested that the V_1 center is an interstitial negative ion which is probably surrounded tetrahedrally by like and unlike neighbors. It is assumed that the center migrates by interstitial diffusion when the V_1 band bleaches and that the conversion from H to V_1 in warming from liquid He temperature to liquid nitrogen temperature involves the transfer of an electron from an F center to an H center to form an energetically more stable vacancy-interstitial pair. Several features of the model are discussed. The experimental conditions under which the model may be tested in KBr are outlined.

12,275 PRODUCTION OF V_3 CENTERS IN KCl BY X-RAYS by R. W. Christy and D. H. Phelps (Dartmouth Coll.); Phys. Rev., Vol. 124, pp. 1053-1060, Nov. 15, 1961

The growth of the V_3 band has been studied in X-ray-irradiated KCl at room temperature by measuring the optical absorption as a function of X-ray dose. In the region in which the F band grows linearly with time (after the initial "fast coloration"), the V_3 band height increases approximately as the square root of the time. The V_3 band growth rate varies with X-ray intensity and depth in the crystal in the same way as that of the F band, however. Although the F band can be optically bleached without affecting the V_3 band, if the F band is optically bleached during the X-ray irradiation, the V_3 band likewise fails to grow. These facts are thought to be consistent with a model of the V_3 center in which a Cl_3^- molecular ion is located at a cation vacancy. The center could be formed by the X-ray production of an anion vacancy-interstitial pair and the diffusion of a cation vacancy to the interstitial.

12,276 LOW-TEMPERATURE OPTICAL BLEACHING OF F CENTERS IN KCl by A. R. Reinberg and L. I. Grossweiner (Illinois Inst. Tech.); Phys. Rev., Vol. 122, pp. 1734-1741, June 15, 1961

Optical bleaching of F centers in X-rayed and additively

colored KCl has been studied at 77°K with pulse irradiation methods. Constant "F light" incident on the colored crystal establishes a photostationary equilibrium between F and F' centers. The application of a high-intensity light flash of appropriate spectrum displaces the system from equilibrium to either direction. The return to equilibrium is exponential in time, with a rate controlled by the intensity and spectrum of the constant light, but not depending on the F-center concentration or the method of coloration. The results are in agreement with a kinetic model involving only F-to-F' center interconversions. Prior room-temperature optical bleaching inhibits the extent and rate of low-temperature bleaching, probably due to the growth of other bands under the F band. The saturation of the extent of bleaching at high pulse-light intensity and a lower bleaching efficiency for the additively colored crystal indicate that the distribution of F centers in the crystal is significant in low-temperature bleaching.

12,277 THERMAL AND CHEMICAL BLEACHING OF F-CENTERS IN KCl by J. C. Penley and R. S. Witte (U. Notre Dame); Bull. Am. Phys. Soc., Ser. II, Vol. 6, p. 420(A), Nov. 24, 1961

An investigation of the rate of thermal conversion of F centers to colloid centers in additively colored KCl to determine the mechanism of precipitation of the excess potassium was described. The time dependence of the concentration of F centers was found to follow an equation of the form $c(t) = c(t=0) \exp -(t/r)^n$ where n had the values of 2/3, 1, or 3/2. It is believed that the precipitation of the excess potassium is a dislocation induced process in which F centers diffuse to the dislocations where they combine with lattice potassium ions to form colloidal potassium. Crystals heated in the presence of water vapor developed a colorless surface region. Study of the motion of the boundary between this clear region and the colored interior as a function of temperature led to an activation energy of 13.0 ± 1.7 kcal/mole associated with the diffusion of water into the crystal.

12,278 ANISOTROPY OF COLOR CENTERS IN CALCITE by W. F. Kolbe and A. Smakula (MIT); Phys. Rev., Vol. 124, pp. 1754-1757, Dec. 15, 1961

Two absorption bands observed in calcite colored by 3-Mev electrons (10^5 to 10^6 rads) at −190°C at 350 and 290 mμ are discussed. Samples cut parallel to the c axis colored and measured with polarized light ($E_{\perp c}$ and $E_{\parallel c}$) showed that the band at 350 mμ is isotropic while that at 290 mμ is anisotropic. The former is correlated to trapped electrons and the latter to trapped holes. Both bands are stable at −190°C but decay simultaneously at room temperature, accompanied by strong luminescence with a peak at 590 mμ.

12,279 DIFFUSION OF COLOR CENTERS INTO KBr-Tl PHOSPHORS by T. Tamai (Matsushita Electronics); J. Phys. Soc. Japan, Vol. 16, pp. 2463-2466, Dec. 1961

An investigation of the diffusion of color centers into a KBr-Tl phosphor during the coloring process in potassium vapor is reported. Proceeding from the surface to the interior of the crystal, F-centers, complex centers, and Tl neutral centers were observed successively. The boundary between the crystal region containing these centers and the rest of the crystal containing only Tl^+ ion centers was very distinct. The depth of the front surface of diffusing Tl neutral centers was proportional to the square root of the exposure time. Complex centers were composed of a Tl neutral center, a negative ion vacancy and an electron.

Excitation Mechanism for F-Center Electrons - See 12,557

Photochemically Produced Color Centers in KCl and KBr - See 12,544

12,280 STABLE ATOMIC CONFIGURATIONS FOR AN INTERSTITIAL IN COPPER by K. H. Bennemann (U. Illinois); Phys. Rev., Vol. 124, pp. 669-670, Nov. 1, 1961

The stability of various atomic configurations for an interstitial in a model representing Cu is investigated. For the interaction between the lattice ions, a Born-Mayer and a Morse potential are used. Two equilibrium configurations for an interstitial are found. For the two stable positions the formation energies and the changes in volume of the crystal arising from the interstitial are calculated. The calculations show that the crowdion and the "body-centered" interstitial are unstable.

12,281 INTERSTITIAL DEFECTS IN LiH AND NaCl IRRADIATED AT LOW TEMPERATURES by F. E. Pretzel and R. L. Petty (Los Alamos Sci. Lab.); Phys. Rev., Vol. 123, pp. 464-465, July 15, 1961

Expansions of the lattice parameters of both LiH and NaCl exposed to β radiation at 77° and 245°K have been observed using a vacuum X-ray diffractometer stage operated at 77°K. The source of the β radiation was 5.56 per cent LiT contained in a LiH crystal which was ground and mixed with NaCl in the samples. The LiH lattice parameter increased 0.0020 ± 0.0007 A in three samples. This result is consistent with density measurements and with the formation of interstitial He^3 atoms in the LiH lattice. The NaCl lattice parameter increased 0.0061 ± 0.0009 A even though the average β dose for the NaCl was less than 1 per cent of that in the Li(H, T) and tritium β particles with maximum energy cannot produce direct displacements in NaCl. A mechanism is proposed for the production of Cl^- interstitials and vacancies (Frenkel defects) in NaCl which is similar to one proposed by Klick for the production of F and H centers. This mechanism is related to observations of the production of a centers in alkali halides irradiated at low temperatures.

12,282 THE EFFECT OF INTERSTITIAL SOLUTE ATOMS ON THE FATIGUE LIMIT BEHAVIOR OF TITANIUM by H. A. Lipsite and D. Y. Wang (Wright-Patterson AFB); AIME Trans., Vol. 221, pp. 918-923, Oct. 1961

A study of fatigue in high purity titanium and in three high purity alloys of Ti under completely reversed axial tension-compression test conditions is reported. The alloys contain 0.75 atomic per cent of a single interstitial element; C, N, and O respectively. The results corroborate a previously published theory which proposed that strain aging under alternating stress was responsible for the fatigue limit behavior of certain alloys.

DISLOCATIONS

12,283 THEORY OF CONTINUOUS DISLOCATION AND ITS APPLICATION by T. Mura (Northwestern U.); U.S. Gov. Res. Rep., Vol. 36, p. 110(A), July 5, 1961 AD 255 506

A new theory of continuous dislocation is proposed. The stored energy of the continuous dislocation and the kinetic energy are expressed by deformation tensors and their time derivatives as a

natural extension of concepts in the classical theory of dislocations. The slip process in plastic deformation, Frank's network, and the propagation and vibration of dislocations are taken as examples derived from a few fundamental equations which have a correspondence to Maxwell's equations.

12,284 THE PROBLEM OF VISUALIZATION OF DISLOCATIONS IN GERMANIUM BY ETCHING by V. N. Vasilevskaya and E. G. Miselyuk (Acad. Sci., USSR); Soviet Phys.-Solid State, Vol. 3, pp. 313-318, Aug. 1961

The selectivity, durability and plane of action of three different etchants are discussed. The experiment was carried out using Ge monocrystals and the effects of the etchants on the (100), (110) and (111) planes were observed. Two of the etchants are in common use, and the third is one developed by the author. Maximum dislocation density occurred after 10-15 minutes. This observation is used to discuss a result of Auleutner et al. Two of the etchants were found to be more selective in that they showed up dislocations on one or two planes. The etchant due to the author showed up dislocation on all three planes examined. Also the former etchants showed up only edge dislocations while the latter showed up edge, screw and mixed varieties.

12,285 OBSERVATION OF DISLOCATIONS IN GERMANIUM SINGLE CRYSTAL by M. Shoji, S. Tauchi, T. Mitsuishi and M. Tomono (Hitachi); J. Phys. Soc. Japan, Vol. 16, p. 1253 (L), June 1961

The fact that slow etching of Ge produces many more small etch pits than does the CP-4 method is discussed. Dislocation lines in Ge were observed by the method of Bormann, and the density of etch pits were compared with those of X-ray images. Agreement between the density of X-ray images and CP-4 etch pits was found to be good. The small etch pits did not correspond to the usual dislocation lines. Possible sources of these etch pits are suggested.

12,286 NMR STUDY OF DISLOCATION EFFECTS AND ELASTIC AXIAL COMPRESSION EFFECTS IN NaI SINGLE CRYSTALS by H. O. Hooper and P. J. Bray (Brown U.); Bull. Am. Phys. Soc., Ser. II, Vol. 6, p. 234(A), Apr. 24, 1961

Anomalous angular distributions in the intensity of the I^{127} NMR spectra of single crystals of NaI rotated about [110] and [100] type directions perpendicular to the magnetic field were discussed. This intensity anomaly due to the changing amount of first-order quadrupolar broadening of the line has been attributed to oriented dislocations in previously unstrained crystals. The full intensity of the NMR line (i.e., quadrupolar broadening approaches zero) is observed when H_0 is along a [100] type direction. Calculations have been carried out to determine the orientation of screw and edge dislocations that would give rise to such an anomaly. When H_0 is along a [100] type direction, the NaI crystals have been axially compressed in an elastic manner. As the stress was increased, the peak-to-peak height of the derivative curve of the I^{127} line was diminished by as much as 15 per cent, while the integrated intensity was unchanged. Using this compression data, the value of the Sternheimer antishielding parameter for I^{127} in NaI has been estimated.

12,287 DISLOCATIONS AND PLASTIC FLOW IN GERMANIUM by D. Dew-Hughes (U. Cambridge); IBM J. Res. and Dev., Vol. 5, pp. 279-286, Oct. 1961

The determination of dislocation density as a function of plastic strain, and some direct measurements of dislocation velocity for single-crystal Ge specimens tested in tension over a range of temperature and strain rate are described. From these results the plastic behavior of Ge can be explained in terms of dislocation velocity and dislocation multiplication, and is analogous to the interpretation given by Johnson and Gilman for deformation of LiF. Examination of the effects of crystal purity and orientation show that strain-aging effects are absent. Conjectures as to the cause of work hardening are made.

12,288 ANTIMONY EDGE DISLOCATIONS IN InSb by H. C. Gatos, M. C. Finn and M. C. Lavine (Lincoln Lab.); J. Appl. Phys., Vol. 32, pp. 1174-1175(L), June 1961

Two types of edge dislocations produced in InSb by bending wafers 20 mm long by 20 mm thick to a radius of curvature of about 15 cm are discussed. The dislocations produced terminate either in a row of In atoms or a row of Sb atoms which ideally occupy opposite (111) faces. Hall measurements indicate that the Sb dislocations were electron donors whereas the corresponding In dislocations appear to be electron acceptors. A new etchant was developed which is believed to be associated with Sb dislocations selectively. The etchant consists of 30 per cent H_2O_2 + 1 part 48 per cent HF + $8H_2O$ + 0.4 per cent butylthiobutane; the last component is believed responsible for the selectivity of the etchant.

12,289 THE OCCURRENCE OF DISLOCATIONS IN CRYSTALS GROWN FROM THE MELT by S. Howe and C. Elbaum (Brown U.); Phil. Mag., Vol. 6, pp. 1227-1240, Oct. 1961

Dislocations observed in single crystals of Al grown by the Czochralski method at various rates are discussed. X-ray diffraction micrographs were taken of these specimens. The density of dislocations present in an as-grown crystal increases with both increasing diameter and rate of growth. For sufficiently small diameters (below about 0.3 mm) it was possible to grow crystals free of detectable dislocations. These results indicate that the majority of the initial dislocations are produced by the collapse of vacancy discs that are nucleated when a sufficient supersaturation of vacancies is reached in the crystal. Theoretical calculations of the supersaturation of vacancies that arise during crystal growth were made by considering the diffusion of these imperfections in a specimen cooled from the melting temperature. The range of diameters below which the vacancy supersaturation is too small to nucleate a dislocation is of the same order of magnitude as the diameters of crystals that contain no detectable dislocations.

12,290 GENERATION AND DISTRIBUTION OF DISLOCATIONS BY SOLUTE DIFFUSION by S. Prussin (Pacific Semicon.); J. Appl. Phys., Vol. 32, pp. 1876-1881, Oct. 1961

Observations of dislocations in Si wafers which were generated by the stress introduced by solute lattice contraction of boron and phosphorus in Si are reported. Expressions for the density distribution and for the total number of dislocations generated are derived and a mechanism of dislocation generation and distribution during the diffusion process is postulated. The dislocation distribution is shown to be highly dependent upon the nature of the diffusion process, expressions being derived for the conditions of (1) constant surface concentration of solute and (2) diffusion from a finite source. An expression for and means to determine the residual stresses in diffused Si wafers are given.

12,291 GENERATION OF DISLOCATIONS ON ELECTRICAL BREAKDOWN IN IONIC CRYSTALS by M. P. Shaskol'skaya, W. Yen-Wen and K. Shu-Chao (Moscow Steel Inst.); Soviet Phys.-Solid State, Vol. 3, pp. 482-483, Aug. 1961

Preliminary results of an experimental study of the generation of dislocations in alkali-halide crystals on breakdown in a strongly nonuniform field are reported. Crystals split along their cleavage planes were immersed in ether between two electrodes, the voltage was gradually raised to breakdown value, and after breakdown the crystals were etched to show up points of emergence of the dislocations. It was not possible to study the crystal surface at the point of breakdown because of considerable destruction of the crystal lattice. Annealing at comparatively low temperatures and short periods gave the etch figures flat bottoms. This indicates that the dislocations are located mainly in a thin layer near the surface. The substances studied were LiF, KCl, NaCl and AgCl.

12,292 THE PRODUCTION OF DISLOCATIONS BY ELECTRICAL EROSION OF SINGLE CRYSTALS by L. S. Palatnik, A. A. Levchenko and V. M. Kosevich; Doklady AN SSSR, Vol. 138, pp. 96-99, May 1961

An investigation of lattice defects initiated by a spark discharge is reported. Single crystals of Sb, Bi and Zn were used, dislocations being revealed by an etching technique. Dislocations were produced over a wide range and within a thin layer near the surface of the crystal. Their distribution is plotted against the distance from the location of the spark. The number of dislocations per cm^2 is found to be of the order 10^6 even at distances of 1/4 mm; at 1/2 mm their number decreases rapidly.

12,293 ON DISLOCATION FORMATION BY VACANCY CONDENSATION by G. Schoeck and W. A. Tiller (Westinghouse); Phil. Mag., Vol. 5, pp. 43-63, Jan. 1960

The mechanism of dislocation loop formation by vacancy condensation is examined in a quantitative manner. The critical vacancy supersaturation necessary for the growth of the loops and the climb rate of the dislocations are determined. It is shown that the mechanism proposed for lineage formation based upon loop growth is inapplicable. The number of dislocation loops produced by collapsing vacancy discs is calculated as a function of the cooling rate, cooling range and dislocation density existing in the crystal before cooling.

12,294 THE GROWTH OF PRISMATIC DISLOCATION LOOPS DURING ANNEALING by C. A. Johnson and E. R. Parker (U. California); U.S. Gov. Res. Rep., Vol. 35, p. 795(A), June 16, 1961 PB 148 516

Recent observations of the growth of quenched-in dislocation loops during annealing are discussed and a mechanism for the coalescence of loops is proposed. The mechanism depends on short-circuit diffusion around the periphery of prismatic dislocation loops. This mechanism is contrasted with the theory of loop coalescence by vacancy diffusion through the matrix. It is shown that the experimental observations are in better accord with the short-circuit diffusion theory. Interpretation of the experimental observations on the basis of the short-circuit diffusion mechanism leads to a value for the activation energy for diffusion along a dislocation line. For Al this value is calculated to be 0.7 ev.

12,295 SOME ELASTIC PROPERTIES OF AN EDGE DISLOCATION WALL by R. Chang (Atomics Intl.); Bull. Am. Phys. Soc., Ser. II, Vol. 6, p. 522(A), Dec. 27, 1961

Analytical solutions of the dilational strain field of a finite-edge dislocation wall for certain configurations of the dislocation axes were presented. At comparatively large distances from the wall, the contours of equivalue dilation are approximately cylinders of circular cross-section for the isotropic case and of elliptical cross-section for the normally anistropic case. A special case of anisotropy, where the cross-section of equivalue dilation becomes hyperbolic and the dilational strain field becomes long range, was described. At small distances from the wall, small cylindrical regions of dilational strain field of opposite sign to that of the surrounding material are present. The possible importance of such regions as embryos for diffusionless transformation were also discussed.

12,296 OBSERVATIONS ON CHARGED DISLOCATIONS IN IONIC CRYSTALS by J. Vennik, G. Remaut and W. Dekeyser (Lab. Kristall., Belgium); Phil. Mag., Vol. 6, pp. 997-1001, Aug. 1961

Observations of charged dislocations in NaCl and LiF are discussed. These observations differ from those published earlier owing to the fact that the duration of the deformation pulses could be changed. It was found in most of the specimens that the dislocations were negatively charged. A "barrier formation" is described. An electrical effect was obtained in the elastic region of the specimen.

12,297 TENSILE BEHAVIOR OF LITHIUM FLUORIDE by D. B. Hoover and J. Washburn (U. California, Berkeley); U.S. Gov. Res. Rep., Vol. 36, p. S-53(A), Sept. 5, 1961 PB 155 824 $1.60

The tensile behavior of Czochralski-grown LiF bars treated to remove surface dislocation loops is compared with that of similar bars in which mobile surface half loops were introduced. The following conclusions are made: (1) When the number of slip band sources is small, the yield stress is a function of the number of slip bands that are nucleated. (2) When large numbers of sources are present, the yield stress is probably close to the minimum required to move dislocations in the crystal. (3) A slip band on a given (110) (110) system is a more effective barrier to subsequent growth of intersecting bands on the 4 systems that cut through it at 60° than it is to slip on the one other system that cuts through it at 90°.

12,298 EFFECT OF SLIP DISTRIBUTION ON THE FRACTURE BEHAVIOR OF MAGNESIUM OXIDE SINGLE CRYSTALS by R. J. Stokes, T. L. Johnson and C. H. Li (Honeywell Res. Ctr.); U.S. Gov. Res. Rep., Vol. 35, p. 794(A), June 16, 1961 PB 150 558

The tensile deformation of chemically polished MgO crystals is correlated with the distribution of slip at the onset of plastic flow. If two slip bands, generated on orthogonal {100} planes, happen to intersect to nucleate a crack before other slip bands develop nearby, then the crack so formed is unstable and the crystal is completely brittle. If, however, there is a higher density of slip sources, cracks can become stabilized by adjacent slip bands and the crystals continue to deform. Sometimes slip is confined to a single slip band which expands laterally to fill the entire gauge length; these crystals are extremely ductile. The fracture behavior of a given crystal depends critically upon the relative orientation, number, thickness, and spacing between slip bands. The density of slip may be increased artificially when dislocation sources are injected into the crystal surface by sprinkling with carborundum before loading. Such crystals are always ductile in tension. A similar treatment for crystals to be bent leads to a profound change in their fracture behavior.

12,299 FATIGUE OF INDIUM ANTIMONIDE by R. E. Maringer and J. J. Duga (Battelle); Acta Metal., Vol. 9, pp. 617-618(L), June 1961

Fatigue experiments performed on single crystals of InSb are discussed. A straight line relationship between the logarithm of maximum plastic surface strain and the logarithm of cycles to failure, with a slope of −0.5, was observed. The slope agrees with the slopes observed by Coffin for a number of the more common "engineering" metals. During fatigue, surface striations occurred from slip. Cracks occurred on some specimens, particularly those subjected to a relatively large number of cycles. It is suggested that both types of cracks observed are due to dislocation pile-ups. It is pointed out that fracture occurs after a critical number of dislocation intersections has been exceeded.

12,300 THE YIELD STRESS OF IRON ABOVE ROOM TEMPERATURE by D. V. Wilson (U. Birmingham); Acta Metal., Vol. 9, pp. 618-620(L), June 1961

The contribution of temperature dependent (Cottrell) locking of dislocations to yield stress above room temperature is discussed. Experimental evidence obtained on polycrystalline low carbon steel is reviewed and it is pointed out that these data indicate that temperature dependent (Cottrell) locking of dislocations is effective well above room temperature.

12,301 THE EFFECT OF SURFACE TREATMENT ON THE BENDING CHARACTERISTICS OF MgO SINGLE CRYSTALS by L. D. Johnson and I. Cornet (U. California, Berkeley); U. S. Gov. Res. Rep., Vol. 36, p. 83(A), Sept. 5, 1961 AD 258 632 OTS $3.60

The effect of surface treatment on the bending characteristics of MgO single crystals is discussed. As-cleaved specimens of MgO which were chemically polished in phosphoric acid, acetic acid, ammonium acetate, and distilled water exhibited on bending in air a sudden load drop phenomenon. This effect was believed to be associated with the removal of mobile surface dislocation half-loops by the environment. Specimens of MgO which were fatigue strained and then polished in phosphoric acid did not exhibit the load drop effect. Fatigue straining before polishing introduced many mobile dislocations which were not removed by polishing. Specimens of MgO which were alternately deflected 0.02 in. in bending and polished in phosphoric acid exhibited greater deflection than as-cleaved specimens.

12,302 ON THE NATURE OF STRAIN HARDENING IN FACE-CENTERED-CUBIC METALS by P. W. Osborne, S. K. Mitra and J. E. Dorn (U. California); U.S. Gov. Res. Rep., Vol. 36, p. 62(A), Sept. 5, 1961 AD 258 633

The low temperature tensile and creep behaviors of single crystals of Cu are evaluated. This provides an estimate of the separate contributions of short and long range stress fields to strain-hardening. Furthermore, the average force-displacement diagram for a thermally activated intersection of two dislocations has been established. This diagram plus a knowledge of the variation of dislocation spacing and the long-range back stresses with strain permits an accurate prediction of creep rates. The calculated activation energy for intersection under conditions of a constant strain rate increases linearly with the absolute temperature as required by theory.

12,303 PRECIPITATION OF HELIUM ALONG DISLOCATIONS IN ALUMINUM by G. T. Murray (Materials Res.); J. Appl. Phys., Vol. 32, pp. 1045-1048, June 1961

Helium was generated in an Al-0.1 at. per cent Li alloy by transmutation of the Li^6 atoms during neutron irradiation. During subsequent heating of the specimens, the He appeared to precipitate in the form of small "bubbles." On using a dislocation etchant it was found that the regions of largest dislocation density also contained the highest cavity density. In some regions each dislocation etch pit was associated with a cavity; in other regions a series of cavities appeared to delineate the track of a dislocation. It is believed that the He precipitates along the dislocations in the form of continuous or semicontinuous cylindrical cavities.

12,304 SUBSTRUCTURES AND DISLOCATIONS PRODUCED DURING SOLIDIFICATION OF ALUMINUM by H. Biloni (Natl. Atomic Energy Comm.); Can. J. Phys., Vol. 39, pp. 1501-1507, Oct. 1961

The substructure and the dislocation arrangement produced during polycrystalline solidification of 99.99 per cent pure Al, studied by employing the decanting method for the interruption of solidification, are discussed. Etching techniques to reveal individual dislocations and the method of thin epitaxial layers of aluminum oxide to reveal changes in impurity concentration have been employed simultaneously. The development of the structure towards the interior of the solid was studied by successive electrolytic polishings. In this way it was possible to show that the "cell substructure" formed by dislocations originates in areas where "microsegregation" of impurities has occurred. Towards the interior of the solid a dislocation rearrangement into a "macromosaic" substructure which is closely related to the cellular substructure occurs. At the same time a substructure of "macrosegregation" occurs, arising from the original grain boundaries. The results are interpreted in the light of recent theories of solidification.

12,305 THE OBSERVATION OF DISLOCATIONS TO ACCOMMODATE THE MISFIT BETWEEN CRYSTALS WITH DIFFERENT LATTICE PARAMETERS by J. W. Matthews (U. Witwatersrand); Phil. Mag., Vol. 6, pp. 1347-1349, Nov. 1961

An examination, in a transmission electron microscope, of a thin (800 to 1000 A) foil composed of an evaporated single crystal layer of PbS and a layer of PbSe is discussed. The crystals were in parallel orientation and the interface between them was parallel to (001). A square grid of dislocations to take up the misfit between the two lattices was observed. The dislocations were of the edge type and their Burgers vectors were 1/2 a <110>.

12,306 COMPARISON OF STRESSES AND DISLOCATIONS IN A GERMANIUM CRYSTAL by V. I. Nikitenko and V. L. Indenbom (Inst. Cryst. USSR); Soviet Phys.-Cryst., Vol. 6, pp. 341-346, Nov.-Dec. 1961

From birefringence measurements, the stress in a cross-section of a Ge crystal is calculated. From the temperature distribution during crystal growth corresponding to the observed stress field, it is found that the radial temperature gradient during crystal growth is 3.66°C. The stress distribution throughout the grown crystal is also determined. The theoretical dislocation distribution is compared with the experimental dislocation distribution. It is found that the experimental dislocation density exceeds the theoretical prediction and that the distribution of dislocations along the crystal diameter is not linear.

12,307 LARGE DISLOCATION LOOPS IN ANTIMONY TELLURIDE by P. Delavignette and S. Amelinckx; Phil. Mag., Vol. 6, pp. 601-608, May 1961

Large hexagonal loops observed in Sb_2Te_3 grown slowly from the melt are discussed. The observations suggest that these are prismatic loops resulting from deviations of the stoichiometric composition. In particular it is proposed that Te vacancies precipitate in prismatic loops, from which the "geometrical" stacking fault is eliminated, by glide of a partial. An explanation is given for the occurrence of pairs of concentric loops elongated in direction differing by 60°. The equilibrium shape as calculated on the basis of the model agrees reasonably well with the observed shape.

12,308 ACCUMULATIONS OF DISLOCATIONS IN CRYSTALS CONTAINING IMPURITIES by V. N. Rozhanskii and V. L. Indenbom; Soviet Phys.-Doklady, Vol. 6, pp. 101-103, Aug. 1961

A new theoretical attempt at an explanation of some rows of etch-pits observed in α-brass is presented. The dislocations are considered immobile; each dislocation is assumed to attract an atmosphere of impurities, after taking its place in the queue, and is then locked during the addition of its successors. The solution obtained is shown to fit fairly well a micrograph of Bilby and Entwisle and two other micrographs of Cd crystals.

12,309 DYNAMICAL BEHAVIOR OF DISLOCATIONS IN ANISOTROPIC MEDIA by L. J. Teutonico (Republic Aviation); Phys. Rev., Vol. 124, pp. 1039-1045, Nov. 15, 1961

The dynamical behavior of uniformly moving dislocations in anisotropic media, particularly those crystal systems for which the edge and screw components can be considered separately, is discussed. Expressions are obtained for the kinetic and potential energies of both edge and screw dislocations. It is found that screw dislocations behave normally at all velocities up to the limiting velocity. Edge dislocations, however, display an anomalous dynamic behavior. It appears that in general there is a range of velocities for which the shear stress on the slip plane is negative and edge dislocations of like sign attract rather than repel one another. In an isotropic material the upper limit of this velocity range is the velocity of shear sound; the lower limit is the Rayleigh wave velocity which can never be less than 0.69 the velocity of shear sound. In the anisotropic case it is possible for the limiting velocity (for a given orientation) to be less than the corresponding shear wave velocity; also the threshold velocity for the anomalous dynamical behavior can be any velocity from zero up to the shear wave velocity, depending on the elastic constants of the material and the orientation considered. An example of an edge dislocation in a hexagonal material is discussed in some detail.

12,310 ABRUPT-KINK MODEL OF DISLOCATION MOTION by A. D. Brailsford (Ford); Phys. Rev., Vol. 122, pp. 778-786, May 1, 1961

A new model of dislocation motion is presented. The behavior of a dislocation in the presence of an applied stress is described in terms of a redistribution of kinks along its length. The kinks are assumed to be abrupt and kink diffusion is considered to be a thermally activated process. Transport equations which include the effects of generation, diffusion, and collision of kinks are formulated. General results obtained from these equations show that a dislocation does not behave like an extensible string in this model. Particular application to small harmonically-time-dependent stresses leads to a new theory of the Bordoni anelastic peak. The characteristic relaxation time depends on line length as well as the attempt frequency and activation energy for diffusion. As a result, the decrease in the peak height and slight lowering of the peak temperature upon alloying or neutron irradiation are explained. Assuming an exponential distribution of line lengths, the results of the theory are compared with published values of the activation energy. Experiments which might further test the theory are suggested.

12,311 THE FORCE ON A MOVING DISLOCATION by F. R. N. Nabarro; Phil. Mag., Vol. 6, pp. 1261-1266, Oct. 1961

The suggestion that there is a specific "Lorentzian" force on a dislocation moving through a medium which is itself in motion is examined. This suggestion arises from the similarity between the equations of elasticity with anti-plane strain and the equations of electro-dynamics in two dimensions, the screw dislocation being the counterpart of the line charge. The proposed "Lorentzian" force is the analog of the magnetic force on a moving charge. The equations of a linear continuum can be satisfied whether such a force exists or not. A nonlinear model based on that of Peierls is constructed, and an approximate solution of a problem is presented which, if the approximations made are justified, demonstrates that this "Lorentzian" force on a dislocation does not exist.

12,312 VELOCITY OF SLOWLY MOVING DISLOCATION by T. Takeuchi (Natl. Res. Inst.-Metals); J. Phys. Soc. Japan, Vol. 16, pp. 1682-1685, Sept. 1961

The nature of a dislocation line movement when surmounting a Peierls hill is considered. It is assumed that the observed dislocation velocity is the average velocity during the successive jumps, and that the jumping distances are large compared with the atomic spacing. The excitation probabilities for large jumps are calculated by the forces on the dislocation, in which the thermal effects are introduced as a fluctuation of the local shear stress. The dislocation velocity in otherwise perfect crystals of relatively large Peierls stress are obtained as functions of applied stress and temperature.

12,313 "CONSERVATIVE CLIMB" OF A DISLOCATION LOOP DUE TO ITS INTERACTION WITH AN EDGE DISLOCATION by F. Kroupa and P. B. Price; Phil. Mag., Vol. 6, pp. 243-247, Feb. 1961

Observation of a new type of dislocation motion, called "conservative climb", in Zn platelets deformed in tension inside an electron microscope is reported. Circular, prismatic dislocation loops are often forced to climb out of their glide cylinders by their repulsive interaction with edge dislocations. It was observed that the area inside a loop is conserved during its movement, from which it is concluded that the climb occurs, not by self-diffusion, but by the transfer of vacancies around the loop by pipe diffusion. Calculations of the interaction energy, of the total forces on the loop, and of the forces per unit length on the elements of the loop show that conservative climb can be expected to occur when the temperature is not too low and the separation of loop and edge dislocation is small.

12,314 DISLOCATIONS IN VISCO-ELASTIC MATERIALS by J. D. Eshelby (U. Birmingham); Phil. Mag., Vol. 6, pp. 953-963, Aug. 1961

An expression for the force required to move a dislocation steadily through a visco-elastic medium, in particular Zener's standard linear solid, is derived and is applied to the case of a screw dislocation in iron exhibiting the Snoek effect. Schoeck and Seeger's atomic treatment of the same problem contains an error. When this is corrected, the two methods give solutions of the same form.

12,315 FORMATION AND MOTION OF DISLOCATIONS IN NICKEL AND IN Ni-Cr ALLOY by O. I. Mgebryan (Acad. Sci., USSR); U.S. Gov. Res. Rep., Vol. 36, p. 68(A), Aug. 20, 1961 AD 257 672 OTS $1.60

The results of experimental research into the process of formation and the motion of dislocations in Ni-Cr alloy are presented. The research was conducted by a method which permits direct study of the motion of dislocations by utilizing the effects caused by them. This method is based upon the assumption that during the elimination and formation of each dislocation, the lattice undergoes a shear strain equal in magnitude to the Burgers vector, and with a change in dislocation densities it is equal to the magnitude of the total of the Burgers vectors of the eliminated or formed dislocations. The secondary plastic effect during the hardening was also considered for Ni and Ni-Cr alloy with the chemical composition 85.35 per cent Ni, 14.43 per cent Cr, 0.020 per cent Si, 0.020 per cent C, and Mn traces. Samples of a corresponding form prepared from these metals were first annealed in a vacuum to relieve residual stresses.

12,316 ACTIVATION ENERGIES FOR THE MOTION OF DISLOCATIONS IN MgO AND NaCl CRYSTALS FROM STRESS RELAXATION STUDIES by G. G. Bentle and R. Chang (Atomics Intl.); Bull. Am. Phys. Soc., Ser. II, Vol. 6, p. 522(A), Dec. 27, 1961

The kinetics of stress relaxation at constant strain of MgO and NaCl crystals after slight straining by compression to initiate yielding, measured over wide temperature ranges, were discussed. The stress relaxation data yield the following activation energies: 1.1-1.2 ev for MgO (700°-1500°C) and 0.8-0.9 ev for NaCl (300°-550°C) independent of the temperature of measurement. Possible interpretation of the results in terms of thermally activated motion of jogged dislocations under diminishing stress was presented.

12,317 POLYGONIZATION IN BENT ZINC CRYSTALS by P. P. Sinha and P. A. Beck (U. Illinois); J. Appl. Phys., Vol. 32, pp. 1222-1226, July 1961

Polygonization in high-purity Zn crystals, that were grown from the melt by the soft mold technique and bent in such a way that $[0\bar{1}10]$ was parallel to the bending axis and the $[2\bar{1}10]$ slip direction enclosed approximately 45° with the bending radius, is discussed. A dislocation etching technique which reveals the edge dislocations introduced on bending, without the necessity of decoration, was developed. It was found that crystals bent either at room temperature or at liquid nitrogen temperature had approximately two-thirds of the edge dislocations arranged in low-angle tilt boundary segments. The fact that no observable change occurred in the dislocation structure on annealing up to 225°C for 5000 min suggests that the observed low-angle boundaries were formed directly on bending rather than by a thermally activated polygonization process, which might have been thought to take place at room temperature in the interval between bending and etching.

12,318 OBSERVATIONS ON THE POLYGONIZATION OF BENT LiF CRYSTALS BY THE BERG-BARRETT METHOD by M. Yoshimatsu (Rigaku Denki); J. Phys. Soc. Japan, Vol. 16, pp. 2246-2253, Nov. 1961

Polygonization observed in weakly bent LiF crystals successively annealed at various temperatures from 400°-800°C is discussed. Slip lines disappear at about 450°C and appear again at about 500°C. At higher temperatures than 500°C, edge dislocations move to form polygon walls. The complete polygon walls are produced at 660°C, and coarsening of polygon domains occurs above this temperature. The coarsening proceeds through either of two processes: coalescence of two branches of the Y-shaped polygon walls and absorption of a polygon wall by another parallel polygon wall. The formation of L-shaped polygon domains is also discussed.

12,319 CROSS SLIP AND CROSS CLIMB OF DISLOCATIONS INDUCED BY A LOCKED DISLOCATION by J. C. M. Li (U. S. Steel); J. Appl. Phys., Vol. 32, pp. 593-599, Apr. 1961

The nature of double cross slip of screw dislocations as induced by a locked parallel screw dislocation, that of edge dislocations as induced by a locked edge dislocation through climb, and that of the cross climb of edge dislocations as induced by another edge dislocation through slip are studied in the light of the interaction of the mutual stress fields of the dislocations. Some quantitative calculations of the multiplication of a single loop and of the growth of slip bands in LiF are given. A mechanism for linear hardening at low stresses is suggested.

12,320 ELASTIC SELF- AND INTERACTION ENERGIES OF DISLOCATION JOGS by F. Kroupa and L. M. Brown (Cavendish Lab.); Phil. Mag., Vol. 6, pp. 1267-1270, Oct. 1961

An elastic calculation which shows that there is an interaction between two jogs or kinks on an infinite straight dislocation line is discussed. For jogs sufficiently far apart, the interaction potential varies as the reciprocal of the distance between them and as the product of their lengths. Formulae are also obtained for the self-energies of jogs.

12,321 INTERACTION BETWEEN THE MAGNETIC (DOMAIN) AND DISLOCATION STRUCTURE IN FERROMAGNETS [in Russian] by I. Ia. Dekhtiar and E. G. Madatova (Kiev Polytech. Inst.); Izv. VUZ Fiz., No. 1, pp. 63-70, 1961

The interaction of dislocation-type defects in the crystalline lattice with the domain structure is analyzed. The work was done in conformance with modern theories of coercive force and under the assumption that such dislocation-type defects are formed in a metal under high-temperature tempering. A computation of the dependence of the coercive force on the time of low-temperature annealing is in good agreement with the results of experiment. A computation made under the assumption that defects having the shape of spherical inclusions are formed during the high-temperature tempering is not verified by experiment.

Effect of Dislocations on the Superconductive Transition Temperature of Al - See 12,493

12,322 THE OBSERVATION OF DISLOCATIONS IN MICA

by E. C. H. Silk and R. S. Barnes (AERE); Acta Metal., Vol. 9, pp. 558-562, June 1961

Dislocations observed in the cleavage planes of thin cleaved fragments of mica upon examination in an electron microscope are discussed. These dislocations, which are formed by slip, interact simply. The super position of loose sheets of mica produced moiré patterns which revealed those dislocations which were perpendicular to the cleavage plane.

Dislocations in Sb Single Crystals - See 12,411

Dislocation Arrays in Si P-N Junctions - See 12,372

Defects in Silver - See 12,416

GRAIN BOUNDARIES AND OTHER STRUCTURES

12,323 GRAIN BOUNDARY COHESION AND SOLUTE-DISLOCATION INTERACTIONS DURING STRAIN AGING by J. O. Brittain (Northwestern U.); U.S. Gov. Res. Rep., Vol.36, p. S-42(A), Aug. 20, 1961 PB 154 982

The magnitude of the relative displacement of two crystals which is dependent upon the matrix slip and in particular, the movement of dislocations in the grain boundary, is discussed. Obstacles that impede the movement of dislocations into the grain boundary cause a decrease in the magnitude of the grain boundary shear. A theory for the 250°C internal friction peaks observed in cold worked and martensitic steels is developed. This phenomena is described as a process involving the growth and solution of a carbide precipitate as a consequence of an oscillating dislocation.

12,324 THE EFFECT OF STRESS ON GRAIN BOUNDARY SLIDING IN CREEP by N. R. Adsit and J. O. Brittain (Northwestern U.); U.S. Gov. Res. Rep., Vol. 36, p. S-42(A), Aug. 20, 1961 PB 155 041 $1.60

A number of zinc bicrystal specimens tested with the boundary loaded in simple shear are discussed. Creep tests were run in a vacuum at 200°C and under an argon atmosphere at 350°C. The maximum amount of grain boundary sliding at a given time was proportional to the resolved shear stress on the slip plane. Curves of grain boundary sliding vs time were found to be cyclic but with no regular periodicity. The magnitude of the grain boundary sliding was not proportional to the grain boundary orientation. A model that involves ledges in the grain boundary and micromigration of these ledges is proposed.

Diffusion along Grain Boundaries - See 12,333 and 12,351

12,325 A DISLOCATION MODEL OF A TWIN by A. M. Kosevich and L. A. Pastur; Soviet Phys.-Solid State, Vol. 3, pp. 935-938, Oct. 1961

A theoretical discussion of the equilibrium of a number of continuously distributed twinning dislocations in an isotropic medium is presented. An integral equation governing the equilibrium density of dislocations is derived and investigated; a solution of the equation is obtained in the particular case of pure screw dislocations. The possibility of determining experimentally the forces resisting motion of dislocations in the crystal is discussed.

12,326 GROWTH TWINS IN INDIUM ANTIMONIDE by R. K. Mueller and R. L. Jacobson (Genl. Mills); J. Appl. Phys., Vol. 32, pp. 550-551 (L), Mar. 1961

Observations concerning the preferential occurrence of twin boundaries in InSb grown in opposite directions from a series of differently oriented seeds are presented. The crystals studied were grown in a horizontal zone-melting furnace parallel to the <110>, <111>, and <211> axes. Coherent twin boundaries parallel to {111} planes occurred in all ingots. These boundaries were generally found to initiate at the surface of the ingot and tended to extend over the entire {111} twin plane, terminating either at the external surface or on intersection with another boundary. In the latter case, incoherent boundaries emerge from the junction. The frequency of occurrence of the growth twins was found to be insensitive to the rate of growth and to the impurity concentration. The melt surface generally appeared highly reflecting, indicating that a surface oxide layer was rather thin. The low etch-pit density observed suggests that mechanical stresses were not dominant.

12,327 TWINNING IN GRAPHITE by E. J. Freise and A. Kelley (U. Cambridge); Proc. Roy. Soc., Vol. 264, pp. 269-276, Nov. 7, 1961

A detailed investigation of twins in graphite crystals is discussed. The twins are regions misoriented from the crystal by a rotation of 20° 48' about a direction in the basal plane. The twin boundaries are simple tilt boundaries of a particular angle. Bend planes of varying angle are also observed in graphite crystals. The dislocation structure of the twin boundary is deduced and the effect of twins on the mechanical properties of graphite crystals is considered.

12,328 TWINNING IN A CATION-DEFICIENT SPINEL STRUCTURE by J. Goodyear and G. A. Steigman (U. Hull); Proc. Phys. Soc., Vol. 78, pp. 491-495, Oct. 1, 1961

Crystals of β-In_2S_3 have been studied under the polarizing microscope and by X-ray diffraction. Optical examination has shown that the crystals are twinned, and the relative orientations of the twin components have been determined by rotation and oscillation X-ray photographs. The diffraction data have also confirmed the body-centered tetragonal cell proposed by Rooymans. Assuming that the material has a spinel structure, deficient in cations, it follows that twinning takes place when a redistribution in the tetrahedrally occupied sites occurs.

12,329 DIRECT MEASUREMENT OF STACKING-FAULT ENERGIES FROM OBSERVATIONS OF DISLOCATION NODES by A. Howie (Cavendish Lab.) and P. R. Swann (U. Cambridge); Phil. Mag., Vol. 6, pp. 1215-1226, Oct. 1961

Stacking-fault energies determined for a number of Cu and Ag base Al and Zn solid solution alloys and for a number of Ni-Co alloys from measurements of the radius of curvature of extended dislocation nodes observed by transmission electron microscopy are given. Rough estimates of about 40, 25, and 150 erg cm^{-2}, respectively, can be made of the stacking fault energies of Cu, Ag, and Ni. The accuracy of the measurement and the possibility of segregation of solute atoms to stacking faults are discussed.

12,330 CHARACTERISTICS OF THE SIMILARITY BETWEEN THE PLASTIC PROPERTIES OF IONIC AND METAL CRYSTALS by M. Bocek and K. Vacek (Karlsuniversität, Prague); Phys.

Status Solidi, Vol. 1, No. 1, pp. 135-146, 1961

The solidification processes of Zn and Ni-Co monocrystals are compared with that of LiF crystals for the case of relatively small slip. The principal characteristic of the similarities found appears to reside in the generation of atomic imperfections by moving dislocations during the initial stages of plastic deformation. Similar investigations for AgBr, AgCl, and NaCl crystals lead to analogous conclusions.

CHEMICAL IMPURITIES

12,331 ULTRAMICROANALYSIS by J. S. Pelle (Lockheed); Electronic Ind., Vol. 20, pp. 109-111, Dec. 1961

A discussion of how to handle and identify very low concentrations of impurities commonly encountered in most transistors, which are thus limited by the surface state effects caused by unknown adsorbates and trace contaminants, is given. The following techniques and methods are examined: Feigl color spot analysis, crystallographic microanalysis, mass spectrograph, microvolumetric analysis, radioactivity analysis, gas discharge spectrum analysis, surface chemical reactions on water electron reflection diffraction, and chromatographic methods. All the systems except two have been eliminated as either too costly in time and equipment or too specialized and limited. The two remaining methods — gas discharge, and crystallographic microanalysis — are discussed in detail. Two cases of microdetection are illustrated. The practical detection limit of microcrystallographic analysis seems to be 10^{-12} grams.

12,332 ANALYSIS OF IMPURITIES IN SEMICONDUCTORS BY MEANS OF SPECTROSCOPY AND PARAMAGNETIC RESONANCE by M. Balkanski (U. Paris); 1961 Conf. Ultrapurification Semicon. Matl., Macmillan Co., 1962, pp. 382-396

Analytical techniques allowing characterization of the nature of an impurity from the position of the absorption band due to transitions between ground and excited states are discussed. Quantitative analysis by experimental definition of the spectral position of different absorption bands is considered. The absorption coefficient for a given peak corresponding to one of the most intense transitions could be used as a direct measure of the concentration of the considered impurity. The effective concentration range of this method is 10^{14} - 10^{18} atoms/cm^3. Where only one impurity is present, a measure of the free carrier concentration when the impurity is ionized gives the concentration of this impurity. In polar semiconductors, reflectivity measurements give with exactitude the carrier concentration and hence the impurity concentration. When the effective mass is known, Faraday rotation measurements give the carrier concentration and hence the impurity concentration. Another method for finding the chemical nature of the impurity is by paramagnetic resonance, the number of resonance peaks being characteristic of the nuclear spin of the impurity and hence of its nature. The concentration of a given impurity is given by the amplitude of the resonance peaks and the appearance of complementary peaks and their shape. The spin-lattice relaxation times of the nuclear spins (Si^{29}, for example) also depend upon the concentration. The range of sensitivity of this method is between 10^{15} and 10^{18} atoms/cm^3. Combined measurements of Hall effect, infrared spectra, and magnetic resonance allow the establishment of calibration curves of a given effect as a function of the concentration. Such curves, established for different impurities, facilitate the rapid identification and computation of the concentration of the impurity.

12,333 STUDY OF THE STRUCTURE OF METALS BY THE METHOD OF RADIOACTIVE ISOTOPES (SELECTED CHAPTERS) by S. Z. Bokshteyn, S. T. Kishkin and L. M. Moroz (Acad. Sci., USSR); U.S. Gov. Res. Rep., Vol. 36, p. 69(A), Aug. 20, 1961 AD 257 700 OTS $11.00

A method developed for qualitative and quantitative investigations of the dispersion of elements in alloys and the diffusion of the components in the volume and along the grain boundaries is described. The method takes into consideration the radioactive radiation and specific application of radioisotopes. The accepted method of investigation included qualitative autoradiography, quantitative autoradiography and the study of movement along the grain boundaries.

12,334 NEUTRON ACTIVATION STUDY OF GALLIUM ARSENIDE CONTAMINATION BY QUARTZ by W. Kern (RCA); J. Electrochem. Soc., Vol. 108, p. 263C(A), Dec. 1961

GaAs crystals synthesized by the horizontal Bridgman method using neutron-activated boats of natural and synthetic fused quartz are discussed. Instrumental radiochemical techniques were applied to determine the Si concentrations and to identify other transferred trace elements. All crystals were found completely enveloped in an impurity-enriched surface layer with Si concentrations up to 0.2 per cent. Bulk concentrations of Si ranged from 1×10^{17} to 3×10^{18} cm^{-3}. Evidence of several types of transfer mechanisms was obtained. Other transferred impurities include Cu, Ga, Sb, and Au at concentrations below 10^{16} atoms cm^{-3}; these impurities were decreased effectively by use of high-purity synthetic quartz.

12,335 NEW DETERMINATION METHOD OF TRACES OF CARBON IN SOME ELEMENTS - APPLICATION TO SILICON by L. Ducret and C. Cornet (Ctr. Natl. d'Etudes Telecommun.); 1961 Conf. Ultrapurification Semicon. Matl., Macmillan Co., 1962, pp. 461-465

A carbon trace method which allows the determination of carbon impurities in Si (in ppm) is described. First a mixture of finely pulverized Si and pure sulphur is put into a quartz "gooseneck" tube. The tube is sealed in vacuum and heated between 1000° and 1100°C for one hour. After cooling, the "gooseneck" is broken in a container with benzene. The solvent goes up in the tube and dissolves the carbon sulphide which has been formed. After addition of the diethylamine, the benzene is shaken with an aqueous solution of cupric ions. The colorimetry of copper diethyldithiocarbamate is realized at 435 mμ. A standard solution of sulphide carbon is used for calibration. The analysis of a Si single crystal doped by a known quantity of SiC allows the verification of this determination. The results obtained show that the carbon content in "pure" Si is very high; it varies between 500 and 2000 ppm. The method may be applied to other elements, e.g., to uranium.

12,336 FLOATING-ZONE REFINING OF GALLIUM ARSENIDE by F. A. Cunnell (Services Electronics Res. Lab., Baldock); 1961 Conf. Ultrapurification Semicon. Matl., Macmillan Co., 1962, pp. 513-520

The construction and operation of an equipment for the floating-zone refining of GaAs are described. An important feature of this equipment is a quartz work tube which confines the As vapor and yet is demountable, thereby allowing simple

loading and unloading of the semiconductor rods. The work tube is closed at its upper end by a quartz rod capable of sliding freely in a closely-fitting section of the tube. The clearance between rod and tube is very small and as a result the rate of loss of As from the work tube is trivial. This arrangement also permits a mechanical adjustment in the relative positions of the two chucks that hold the ends of the semiconductor rod. The electrical properties of material processed in this equipment are discussed.

12,337 OBSERVATION CONCERNING ZONE REFINING AND THERMAL TREATMENT OF MOLYBDENUM FROM LOW TEMPERATURE RESISTANCE MEASUREMENT by E. Buehler and J.E. Kunzler (Bell Labs.); AIME Trans., Vol. 221, pp. 957-961, Oct. 1961

Resistance ratio ($R_{4.2°K}/R_{273°K}$) measurements on high purity molybdenum after heat treatment and zone refining are presented. Pronounced effects associated with recrystallization are observed at 1200°C and with melting. Melting alone is found to result in a substantial purification by the evaporation of impurities such as Fe. Zone refining is found to be reasonably effective with four passes producing a three-fold decrease in resistance ratio and a minimum ratio of 0.0003. With the aid of low temperature measurements, it has been shown that the buildup of a deposit of the material being zone refined on the radio frequency coil used for heating can lead to contamination of the sample.

12,338 THERMAL BEHAVIOR IN VACUUM ZONE REFINING by D.K. Donald (Ford); Rev. Sci. Instr., Vol. 32, pp. 811-813, July 1961

The temperature distribution and the total radiated power for a bar undergoing zone refining in vacuum are computed using a one-dimensional analysis. Radiated power experiments were performed on Al, Ge, Gd, Si, Ni, Fe, Pt, Pd, V, Mo, Ta, and W using an electron-bombardment zone-refining furnace operated with space-charge limited current. The experiments agreed well with the prediction $P = 4\pi(e\sigma k/5)^{1/2}R^{3/2}T^{5/2}$ for a very thin bar with an infinitesimal zone length.

12,339 EVAPORATION OF SOLUTES IN FLOATING ZONE REFINING OF SEMICONDUCTORS by J. R. Gould (GE); AIME Trans., Vol. 221, pp. 1154-1158, Dec. 1961

A mathematical treatment of multiple-pass floating zone refining of semiconductors, including the evaporation of solutes from the melt at reduced pressure, is presented. Vapor pressures and evaporation rate constants for P, As, and Sb in Ge have been determined from floating-zone experiments conducted at 10^{-5} mm Hg. The rate sensitivity of As in Ge has been examined over the range of 1 to 10 in/hr growth rate. The equilibrium value of the segregation coefficient of As in Ge, as determined by an extrapolation of these data, was found to be 0.09.

12,340 THERMOELECTRIC MATERIALS AND DEVICE RESEARCH by B. R. Gossick and H. B. Whitehurst (Arizona State U.); U.S. Gov. Res. Rep., Vol. 35, pp. 548-549(A), May 16, 1961 PB 153 233

Methods developed for purification of precipitated titanium dioxide are described. The method of preparing high melting point metals in colloidal form is also described, together with the procedures which were used to mix these particles into a matrix of titanium dioxide. Theoretical consideration of the principles involved in the electrical behavior of two phase systems is reviewed. The work being done on the systems for evaluation of the new materials is reported together with the experiments which were done to establish macroscopic metal to rutile junctions.

Nomograph for Doping Ge and Si Crystals - See 12,376

Impurities Introduced during the Growth of GaAs - See 12,379

12,341 STATISTICAL DYNAMICS OF CRYSTALLINE DIFFUSION. Part II. VACANCY MECHANISM by R. Kikuchi (Hughes Aircraft); J. Phys. Chem. Solids, Vol. 20, pp. 17-34, June 1961

The method of treating diffusion of atoms in crystals developed in the first paper of this series is applied to the vacancy mechanism of atomic migration in substitutional alloys. The method is used on a body centered cubic binary system (including vacancies) with the chemical potential gradient along a [100] direction. The system is isothermal and a flow of atoms is maintained by two particle reservoirs of different chemical potentials placed at the two ends of the system. First, the path probability G for change of state during a short time interval is written in terms of the path parameters by using the pair approximation of the cluster-variation method and following the recipe previously proposed by the author. The most probable change of state is then derived by maximizing G with respect to the path parameters. The relations between the atomic fluxes and the chemical potential gradients are derived for the stationary state. Onsager's reciprocal relation holds. The limiting case for no chemical potential gradient becomes identical with the state derived from the equilibrium theory.

12,342 STATISTICAL DYNAMICS OF CRYSTALLINE DIFFUSION. Part III. SELF-DIFFUSION IN AN ORDER-DISORDER SYSTEM by R. Kikuchi (Hughes Res. Labs.); J. Phys. Chem. Solids, Vol. 20, pp. 35-40, June 1961

The self-diffusion coefficient in a β-brass type order-disorder alloy is derived theoretically using the path probability method of irreversible cooperative phenomena and the cluster-variation technique, assuming the vacancy mechanism of atomic migration. The diffusion coefficient is expressed in terms of the probability for a unit jump of an atom into its adjacent vacancy, the near-neighbor interaction potentials between atoms. It is shown that at the Curie point the diffusion coefficient decreases more rapidly on the ordered side than the disordered side; this result agrees with experiment qualitatively.

12,343 ANALYTIC SOLUTION OF THE DOUBLE-DIFFUSION PROBLEM by K.C. Nomura (Honeywell); J. Appl. Phys., Vol. 32, pp. 1167-1168(L), June 1961

By imposing the appropriate boundary conditions and employing Green's functions on the diffusion equation, an analytic solution to the double-diffusion problem is obtained. The complete solution is a superposition of two independent diffusion expressions. This expression may be simply represented by proper choices of surface concentration and diffusion coefficient parameters and hence provides a useful expression not limited as are previously used approximations.

12,344 THE PROBLEM OF DIFFUSION IN AN EVAPORATING SOLID MEDIUM by T. I. Kucher (Phys. Inst. Kiev); Soviet Phys.-Solid State, Vol. 3, pp. 401-404, Aug. 1961

The problem of diffusion in an evaporating solid medium is discussed. A situation of this type occurs in Ge or Si when they

are heated to temperatures near their fusion points. Neglecting the possibility of any diffused material collecting in a thin layer of Si near the evaporating surface the problem may be formulated as follows: diffusion with coefficient D takes place from gaseous phase into a semi-infinite homogeneous solid medium. The concentration C_0 on the separation surface is constant in time. However, this surface is being displaced with velocity v while remaining parallel to its initial position. It is desired to determine the concentration $C(x, t)$ of the diffusion material in the solid medium at distance x from the initial position at time t. An equation is set up and solved. However, the value of C_0 is difficult to determine independently. The solution $C(x, t)$ involves the two unknowns C_0 and D. Therefore two measurements of $C(x, t)$ would suffice to determine the unknowns. Because of the nature of the solutions, an approximation is necessary to solve for C_0 and D. Several such approximations are given. To facilitate practical work, a series of solution curves is given.

12,345 ANELASTIC MEASUREMENT OF DIFFUSION IN α-AgCd ALLOYS by M. A. Quader (Indian Assoc. Cultivation Sci.); Indian J. Phys., Vol. 44, pp. 446-458, Sept. 1961

Measurements of the internal friction peak for three α-AgCd alloys are reported. The peaks are due to changes in local order with the external stress. The measured values of the relaxation time are used to calculate the diffusion coefficient of the AgCd alloys. The calculated values are in good agreement with the directly measured diffusion coefficients of alloys of corresponding compositions.

Diffusion Errors Affecting Junction Depth - See 12,647

Generation and Distribution of Dislocations by Solute Diffusion - See 12,290

Diffusion of As into Thin Ge Slices - See 12,247

12,346 DETAILED ANALYSIS OF THIN PHOSPHORUS-DIFFUSED LAYERS IN P-TYPE SILICON by E. Tannenbaum (Bell Labs.); Solid-State Electronics, Vol. 2, pp. 123-132, Mar. 1961

Detailed concentration profiles of P-diffused layers in p-type Si obtained using a new, accurate technique are discussed. The P distributions were found to be significantly different from those predicted by simple theory in that: (1) under conditions of constant surface concentration, they do not obey the predicted error-function complement, (2) the diffusion coefficient is a constant up to a concentration of about 10^{20} cm^{-3}, but is a strong function of concentration above that value, and the variation is larger than can be accounted for by field-accelered diffusion and (3) at high concentrations, there is a difference between the P concentration determined from resistivity measurements and that determined from radioactive tracer measurements. Electron mobility values in the concentration range above 10^{20} cm^{-3} were obtained from the data. The experimental results suggest that there is a limit to the concentration of electrically active P that can be obtained in Si, and that this limit has been observed.

12,347 EVALUATION OF THE SURFACE CONCENTRATION OF DIFFUSED IMPURITY LAYERS IN SILICON by O. N. Tufte (Honeywell Res. Ctr.); J. Electrochem. Soc., Vol. 108, p. 45C (A), Aug. 1961

The relation between the surface concentration of a diffused layer and the electrical conductivity and Hall coefficient of the layer is discussed. Calculations for a complementary error function impurity distribution in silicon are presented. The results show that the Hall coefficient is very nearly independent of the mobility values used in the calculation. This allows accurate values of the surface concentration to be determined without knowing exactly the variation of the mobility with impurity concentration. An experimental comparison of the surface concentration values obtained by the conductivity and Hall effect methods is made.

12,348 DIFFUSION CONTROL IN GERMANIUM by J. C. Marinace (IBM); U.S. Pat. 3,001,896, Issued Sept. 26, 1961

A technique for reducing the final surface concentration of an impurity diffused into Ge is described. The Ge wafer is first heated in air to form a coating of Ge oxide on its surface. The oxide film should be of a thickness which does not require an excessive diffusion time. A coating consisting of an impurity source is formed on the oxidized surface by hydrolyzing a halide of a doping impurity on the surface. For example, a coating containing Sb can be formed by hydrolyzing $SbCl_5$ to Sb_2O_3 on the surface of the wafer for one minute at 100°C. The diffusion is then performed in an oxidizing atmosphere. The impurity source coating is removed, leaving a semiconductor surface having a resistivity high enough to permit the formation of rectifying contacts which do not have very low reverse breakdown voltages.

12,349 CORRELATION OF ELECTRICAL MEASUREMENTS AND CHEMICAL ANALYSES OF ZINC- AND CADMIUM-DIFFUSED GaAs by J. F. Black (Genl. Tel. Electronics); Detroit Mtg., J. Electrochem. Soc., Vol. 108, p. 178C (A), Aug. 1961

The doping of thin rectangular slices of single-crystal GaAs to degeneracy by indiffusing Zn or Cd at 1100°-1200°C from As-metal vapors in evacuated quartz crystals was described. The gradient of dopant concentration throughout the thickness of the slice was controlled over a wide range. The free hole concentration calculated from Hall effect measurements agreed with the average dopant concentration determined by chemical analysis. Data on measured Hall mobilities were presented and compared with data for melt-doped GaAs.

12,350 THIN COMPOSITIONAL LAYERS IN SILICON by A. Goetzberger and H. Queisser (Shockley); U.S. Gov. Res. Rep., Vol. 36, p. 98(A), Aug. 20, 1961 AD 258 216

Research in three major aspects of thin compositional layers in Si is reported. Part I deals with diffusion, with emphasis on the preparation and the properties of thin diffused layers. The multiple predeposit technique improved uniformity. Box diffusion was found better than open-tube diffusion, with the Pt box superior to a quartz box. Simultaneous oxidation and diffusion of boron and phosphorus yielded higher diffusion constants than those reported by others. Part II discusses the properties of junctions, especially imperfect junctions. Gettering techniques were developed to remove or prevent metal precipitates which caused excess reverse current below avalanche breakdown. A study of light emission from reverse biased p-n junctions revealed 2 types of microplasmas which may be related to certain crystal faults. A theoretical study analyzed the phenomena of secondary ionization, avalanche breakdown and microplasma phenomena in a simplified model. Part III reports on diffusion along grain boundaries. Si bicrystals were grown with one or more small angle grain boundaries. Diffusion of impurities parallel to the dislocations was found to be enhanced

at grain boundaries. A new mathematical treatment of diffusion down dislocations is presented and the experimental results are discussed on its basis. Properties of p-n junctions at grain boundaries are related to possible device applications.

12,351 THE EFFECT OF ARSENIC PRESSURE ON IMPURITY DIFFUSION IN GALLIUM ARSENIDE by L. J. Vieland (RCA); J. Phys. Chem. Solids, Vol. 21, pp. 318-320(L), Dec. 1961

The effect of As pressure on the diffusion of Zn, Mn, S, Sn, and Si in GaAs is discussed. Zn and Mn exhibit pressure-independent behavior at pressures below P_K, the point at which a knee occurs in the junction depth vs As pressure curve of each diffusant. Above P_K, the penetration of Zn and Mn decreases with an increase in As pressure. The decrease in penetration of Zn in the presence of excess As is in qualitative agreement with the radiotracer data of Cunnell and Gooch [see abstract 7572]. The diffusion of S is generally independent of pressure above P_K, and decreases sharply below the knee. The penetration decreases slightly at high pressures. In the pressure independent region, the penetration follows a complementary error function distribution. The activation energy for diffusion $E_a = 1.8 \pm 0.8$ev. When Sn is the diffusant, the junction depth at 1000°C is proportional to the square root of the pressure above P_K; at 1150°C, the diffusion above one atmosphere appears to be independent of pressure. Similar behavior was observed in Si at 1150°C. A sublattice mechanism for diffusion in compound semiconductors is briefly discussed. The observed effects for Zn and S (and probably Mn) do not agree with this mechanism.

12,352 ANISOTROPIC DIFFUSION OF SILVER AND INDIUM TRACERS IN ZINC SINGLE CRYSTALS by J. H. Rosolowski (GE Res. Lab.); Phys. Rev., Vol. 124, pp. 1828-1832, Dec. 15, 1961

The anisotropic diffusion of tracers in zinc single crystals is discussed. The diffusion of Ag-110 was measured over the temperature range from 271° to 413°C by the sectioning technique. Referring the diffusion constants to the direction of the hexagonal symmetry axis of the zinc crystal structure, results are determined. The diffusion of In-114 was measured over the range from 171° to 416°C. The results show that silver diffuses at a rate about one-tenth that of zinc self-diffusion while the indium diffuses at a rate about ten times as great. Also, $D_{\parallel} > D_{\perp}$ for the silver diffusion as it is for zinc self-diffusion, while for the indium diffusion, $D_{\perp} > D_{\parallel}$. These results are interpreted to indicate a vacancy mechanism of tracer migration with the possibility of a strong tracer-vacancy association occurring in the case of the indium.

12,353 MEASUREMENT OF THE SURFACE SELF-DIFFUSION COEFFICIENT OF COPPER BY THE THERMAL GROOVING TECHNIQUE by N. A. Gjostein (Ford); AIME Trans., Vol. 221, pp. 1039-1046, Oct. 1961

The self-diffusion coefficient D_s for a surface near the (100) plane in copper, determined by means of the Mullins theory of thermal grooving, is reported. It was found to obey the Arrhenius relationship, $D_s = D_o e^{-Q_s/RT}$, where $Q_s = 40.8 \pm 2$ kcal per mole and $D_o = 6.5 \times 10^2 \text{cm}^2/\text{sec}$. Suppression of surface diffusion by chemisorbed impurities is not quite satisfactory as an explanation for the large Q_s and D_o. Instead a model is presented which indicates that Q_s, as determined by a mass-transport technique, may involve both the energy needed to form an adsorbed atom from a ledge in the surface and that for the movement of the adsorbed atom.

12,354 SELF-DIFFUSION OF LEAD, THALLIUM AND BISMUTH IN THE SOLID LEAD-THALLIUM SYSTEM by H. A. Resing and N. H. Nachtrieb (U. Chicago); J. Phys. Chem. Solids, Vol. 21, pp. 40-56, Oct. 1961

Results for the self-diffusion of both lead and thallium over the whole range of solid solution for these elements (0 - 87 atomic per cent Tl) for the temperature interval 206°-323°C are given. Data for the trace impurity diffusion of bismuth over the same concentration range are also given for a more limited temperature range. All three elements show the same qualitative dependence of their diffusion coefficient upon alloy composition, namely, a slight maximum at about 35 atomic per cent thallium and a deep minimum at about 75 atomic per cent thallium at all temperatures. The results are compared with the predictions of the corresponding states principle and with theories based upon the Johnson vacancy-solute complex mechanism. A correction applied to the corresponding states principle, based upon lattice parameter deviations from Vegard's Law, leads to agreement with observation. Some evidence for the existence of a superlattice at alloy compositions in the neighborhood of PbTl is inferred from trends in the ratios D_{Tl}/D_{Pb} and D_{Bi}/D_{Pb} with thallium concentration.

12,355 THE EFFECT OF IMPURITY ADSORPTION ON THE SURFACE ENERGY AND SURFACE SELF DIFFUSION IN NICKEL by J. M. Blakely and H. Mykura (U. Glasgow); Acta Metal., Vol. 9, pp. 595-599, June 1961

Striations observed on Ni heated in vacuo at 900°C are discussed. The distribution of striating orientations suggests the presence of point cusps in the plot of surface free energy at (100), (110) and (210) orientations and a line cusp between (410) and (510). Also evidence was found that surface diffusion is fast at (110) and for a range of atomically rough planes between (410) and (210) in addition to the smooth (100) and (111) planes. Both effects are ascribed to impurity adsorption.

12,356 DIFFUSION OF NICKEL IN SILVER by T. Hirone, S. Miura and T. Suzuoka (Tohoku U.); J. Phys. Soc. Japan, Vol. 16, pp. 2456-2459, Dec. 1961

The diffusion coefficient of Ni in single crystals of Ag, measured by the sectioning technique as a function of temperature throughout the temperature range from 750° to 950°C using radioactive isotope Ni^{63} as a tracer, is discussed. The results are expressed as follows:

$$D = (21.9) \exp\left(-\frac{54\,800}{RT}\right) \text{cm}^2/\text{sec}.$$

The value of activation energy, 54.8 kcal/mole, obtained by the present experiment is in good agreement with the result of the screening theory of impurity diffusion.

12,357 DIFFUSION OF ZINC AND TIN IN INDIUM ANTIMONIDE by S. M. Sze and L. Y. Wei (U. Washington); Phys. Rev., Vol. 124, pp. 84-89, Oct. 5, 1961

A radiotracer investigation of the diffusion on Zn and Sn in single crystal and polycrystalline InSb is reported. The temperature dependence of the diffusion coefficients can be represented by: $D(\text{Zn}) = 1.4 \times 10^{-7} \exp(-0.86/kT)\ \text{cm}^2/\text{sec}$ and $D(\text{Sn}) = 5.5 \times 10^{-8} \exp(-0.75/kT)\ \text{cm}^2/\text{sec}$ in single crystal InSb; and $D(\text{Zn}) = 1.1 \times 10^{-6} \exp(-0.85/kT)\ \text{cm}^2/\text{sec}$ in polycrystalline InSb, the activation energies being in

electron volts. From the penetration curves, it appears that in polycrystalline InSb the Zn diffusion is a volume diffusion while the Sn diffusion is mainly a grain boundary diffusion. The different behaviors of Zn and Sn in InSb are discussed on the basis of one-type and two-type vacancy mechanisms.

12,358 BIBLIOGRAPHY ON DIFFUSION OF IMPURITY ELEMENTS IN COMPOUND SEMICONDUCTORS by G. L. Pearson (Stanford U.); U.S. Gov. Res. Rep., Vol. 36, p. S-54(A), Sept. 5, 1961 AD 256 958

A study of the literature pertaining to solid state diffusion in compound semiconductors is reported. The resulting bibliography is given and while no claim is made that the listings are exhaustive, it is believed that the more important publications are included.

12,359 DIFFUSION OF TUNGSTEN IN COBALT-BASED ALLOY by I. I. Kovenskii (Inst. of Cermets and Special Alloys); Soviet Phys.-Solid State, Vol. 3, pp. 252-254, Aug. 1961

The diffusion coefficient of tungsten in a cobalt-based alloy is determined. The alloy samples were in the form of wires on the central portions of which thin layers of radioactive tungsten were deposited. The samples were then subjected to diffusion annealing at a fixed temperature varying with the sample, and at the end, the activity of the tungsten was measured along the length. The activity is proportional to the number of tungsten atoms, so that tungsten concentration could be determined. The procedure was then repeated at another temperature and graphs of the two sets of measurements were plotted on the same scale. Using approximate solutions of the equation in cylindrical coordinates governing the diffusion concentration and information obtained from the graphs, the diffusion coefficient D was calculated for various temperatures from 1100° to 1350°C. The diffusion coefficient was found to satisfy the equation

$$D = 2.88 \exp\left[-\frac{68000}{RT}\right] \text{ cm}^2/\text{sec}.$$

12,360 BORON DIFFUSION IN SILICON by E. L. Williams (Sylvania); J. Electrochem. Soc., Vol. 108, pp. 795-798, Aug. 1961

Investigation by a p-n junction method of the diffusion of boron in silicon over the temperature range of 1050°-1350°C and in silicon material where the n-type impurity density varied over a range 2×10^{13} to 8×10^{19} at./cm^3 is reported. The diffusion coefficient was found to decrease gradually as the purity of the n-type silicon increased. For silicon on the order of 0.1 ohm-cm resistivity $D = 16 \exp(-85 \pm 5 \text{ kcal/RT}) \text{ cm}^2\text{sec}^{-1}$. The effect on the diffusion coefficient of both the bulk impurity density and the boron density in the surface region is discussed.

12,361 THE DIFFUSIVITY OF CARBON IN SILICON by R. C. Newman and J. Wakefield (AEI Res. Lab.); J. Phys. Chem. Solids, Vol. 19, pp. 230-234, May 1961

Radioactive ^{14}C has been diffused into silicon at temperatures in the range 1070°-1400°C. From the resulting distributions of activity, the diffusion coefficient is deduced as:

$$D = 0.33 \exp\left(\frac{-2.92 \pm 0.25 \text{ ev}}{kT}\right) \text{ cm}^2/\text{sec}.$$

The surface concentration increases with increasing temperature, the largest value being about 10^{18} atoms/cm^3 at the highest temperature employed of 1402°C.

Diffusion of Phosphorus in Si - See 12,690

12,362 DIFFUSION OF THALLOUS IONS INTO POTASSIUM BROMIDE SINGLE CRYSTALS by T. Tamai (Matsushita Electronics); J. Phys. Soc. Japan, Vol. 16, pp. 2459-2463, Dec. 1961

The diffusion of thallous ions into KBr single crystals as a function of temperature is discussed. The thallous ions were introduced into the crystal by heating the latter in a vapor of thallium metal. Concentrations of thallous ions were measured by the height of the characteristic absorption band of a thallous ion in a KBr crystal. This height varies linearly with the concentration of thallous ions. The activation energy of diffusion was found to be 1.98 ev.

12,363 MOTION OF THE AMMONIUM ION IN LATTICES OF THE NaCl TYPE by W. Vedder and D. F. Hornig (Princeton U.); J. Chem. Phys., Vol. 35, pp. 1560-1568, Nov. 1961

A discussion of the motion of NH_4^+ in lattices of the NaCl type is presented. The infrared spectrum of NH_4I in the NaCl-type phase gives insufficient information about the motion of the ammonium ions in that phase. Dilute solutions of NH_4^+ in NaCl-type alkali halides provide considerably more detail in the form of a fine structure in most of the absorption bands which becomes visible on sufficient cooling. This fine structure is most certainly correlated with a rotational motion of the NH_4^+ ion. However, both models suggested in the literature —free rotation and rotation of the ion about a $N\text{-}H \cdots X^-$ axis—deviate in many important respects from the experimental results.

12,364 PENETRATION OF SILVER INTO AMORPHOUS AND CRYSTALLINE QUARTZ SUBJECTED TO A CONSTANT ELECTRIC FIELD by I. E. Balygin; Soviet Phys.-Solid State, Vol. 3, pp. 112-119, July 1961

Silver is capable of migrating along the surface of some dielectrics or penetrating them under the effect of an electric field. Experiments performed with amorphous and crystalline quartz to study this phenomenon are described and an exhaustive report on the experimental results is presented in tabular as well as graphical form. It is concluded that silver hardly penetrates amorphous quartz at 300°C and E = 660v/mm while it penetrates crystalline quartz easily at the same temperature with E = 1.7 kv/mm. During a period of about 50 hours almost all the silver which could migrate from the anode did under these conditions. Results under different conditions of temperature and electric field are also presented in detail and analyzed.

12,365 RECOMBINATION KINETICS FOR THERMALLY DISSOCIATED Li-B ION PAIRS IN Si by E. M. Pell and F. S. Ham (GE Res. Labs.); J. Appl. Phys., Vol. 32, pp. 1052-1063, June 1961

The kinetics of a diffusion-limited pairing reaction between oppositely charged impurity ions in a solid, studied by observing the capture of mobile Li^+ ions by B^- ions in Si, are discussed. The kinetics were determined by measuring resistivity vs time after the method of Reiss, Fuller, and Morin [Bell System Tech. J., 35,535(1956)]; as pairing proceeds, the resistivity decreases because of the disappearance of the charged impurity scattering associated with unpaired ions. Measurements were made between 2° and 35°C. The observed kinetics are not of first order, and are best described by a model in which pairing is largely a random process with little correlation between particular Li^+ and B^- ions. Diffusion constants of Li^+

calculated from the kinetics are in accord with previous ion-drift results.

12,366 STUDY OF Li-O INTERACTION IN Si BY ION DRIFT by E. M. Pell (GE Res. Labs.); J. Appl. Phys., Vol. 32, pp. 1048-1051, June 1961

Ion drift in a reverse-biased n-p junction has been used to measure effective drift mobilities of Li^+ between 20°-125°C in Si samples containing oxygen concentrations up to 1.3×10^{18} atoms/cm^3. Previous experiments have indicated that under such conditions, the Li^+ and oxygen will combine to form a complex of the form LiO^+. The ratio of the effective drift mobility of Li^+ in such samples to the known drift mobility of free Li^+, when measured as a function of temperature, can be used to determine the dissociation constant of LiO^+. Thus, at an oxygen concentration of 1.3×10^{18} atoms/cm^3, the diffusion constant at 50°C is reduced from 1.7×10^{-13} cm^2/sec to $(7.6 \pm 2.2) \times 10^{-16}$ cm^2/sec by the Li^+-O interaction. From this and measurements at other temperatures, the dissociation constant of LiO^+ can be calculated, yielding $C = (5.8 \times 10^{15}) \pm 30$ per cent at 50°C with an activation energy of 0.42 ± 0.03 ev, or more generally, $C = (0.5\text{-}8.5) \times 10^{22} \exp -[(0.42 \pm 0.03)\, e/kT]$. At high concentrations the effective drift mobility is found to be inversely proportional to the oxygen concentrations, in accordance with the model. The use of this technique for the measurement of oxygen concentration below 10^{17} atoms/cm^3 is discussed, and some examples of such measurements are given.

12,367 IRON-BORON INTERACTIONS IN SILICON by W. H. Shepherd and J. Turner (Plessy); Detroit Mtg. J. Electrochem. Soc., Vol. 108, p. 179C(A), Aug. 1961

Investigations of time dependent resistivity changes in p-type Si, saturated with Fe and quenched from above 900°C, were described. The changes were due to pairing between Fe and B. At 45°C more than 50 per cent of the B may be paired. Precipitation of the Fe was also studied. Below 200°C the Fe solubility after precipitation is strongly influenced by pairing and electron hole equilibria. Analysis of these data gave the true solubility of Fe at these temperatures.

12,368 STRUCTURE OF DEFECT CLUSTERS IN SOLIDS by J. W. Buttrey (Armour Res. Found.); U.S. Gov. Res. Rep., Vol. 36, p. 75(A), Sept. 5, 1961 AD 258 384

Preliminary results of a small angle scattering study of defect clustering in irradiated single crystals are presented. Si single crystals irradiated to a total of 2×10^{19} nvt fast neutron flux fail to show any small angle scattering. Some small angle X-ray scattering was detected from a lightly irradiated sample of LiF, but preliminary results from a Li-doped Si single crystal are negative, even though it was thought to contain 100 A clusters of pure Li metal. Such clusters should be detectable using small angle X-ray diffraction; no conclusive reasons are apparent why this sample did not show small angle scattering. Scattering intensity calculations are treated in an appendix.

12,369 AN ELECTRON MICROSCOPE EXAMINATION OF SMALL COBALT PARTICLES PRECIPITATED IN A GOLD MATRIX by P. Gaunt (U. Sheffield) and J. Silcox (U. Cambridge); Phil. Mag., Vol. 6, pp. 1343-1345, Nov. 1961

Transmission electron microscope observations made on thin foils of a Au-1.5%Co alloy aged at 565°C after quenching from 880°C are discussed. The observations suggest that most of the ferromagnetic Co precipitate particles are in the form of discs in (100) planes which are arranged in sheets, also on {100} planes. The contribution to the coercivity of the alloy from these particles due to shape anisotropy is small. The high coercivity of the alloy is probably due to some other type of anisotropy.

Coercivity of Au-1.5%Co Alloy - See 12,369

12,370 DETERMINATION OF SMALL STOICHIOMETRIC DEVIATIONS IN OXIDE MONOCRYSTALS by H. B. Sachse (Keystone Carbon); 1961 Conf. Ultrapurification Semicon. Matl., Macmillan, 1962, pp. 423-433

A vacuum procedure for determining the stoichiometric deviations in oxide monocrystals is described. This method suppresses parasitic oxygen during the dissolution process to less than one microatom. The great importance of semiconductor investigations with single crystals made it mandatory to use this method. In MnO-, CoO- and NiO-monocrystals a surplus of one milliatom O/mol oxide could be determined with a reasonable accuracy. In compounds, such as $MgTiO_3$, $BaTiO_3$ and TiO_2 single crystals an oxygen deficiency of 5 milliatoms/mol was detectable.

12,371 MASS SPECTROGRAPHIC EVIDENCE FOR DEVIATIONS FROM STOICHIOMETRY IN GaSb by E. B. Owens and A. J. Strauss (Lincoln Lab.); 1961 Conf. Ultrapurification Semicon. Matl., Macmillan, 1962, pp. 340-348

An analysis of GaSb by a spark source mass spectrograph technique is reported. Impurity isotopes present at concentrations of 1×10^{16} cm^{-3} or greater were examined in order to determine whether the acceptors in GaSb are impurity atoms or lattice defects. The only elements detected besides Ga and Sb were C, O, H, and N, the levels of which were comparable to those obtained in blank runs, so that their concentrations in the GaSb cannot be estimated. It is not very likely that any of these elements would act as an acceptor in GaSb. The analytical results therefore strongly increase the probability that the acceptors are due to deviations from stoichiometry.

STRUCTURE OF SURFACES AND SPECIAL CRYSTAL FORMS

12,372 SLIP PATTERNS ON BORON-DOPED SILICON SURFACES by H. J. Queisser (Shockley); Bull. Am. Phys. Soc., Ser. II, Vol. 6, p. 106(A), Mar. 20, 1961

Etch-revealed traces of (111) slip planes following diffusion of a high concentration of B into a shallow surface layer of p- or n-type Si slices were described. Slip is caused by the heavy deposit of substitutional B atoms which leads to a reduction of the lattice parameter in the shallow surface layer. The dislocation arrays of the slipped regions extend much deeper into the material than one B diffusion length. The high dislocation density thus introduced will affect the behavior of shallow p-n junctions.

12,373 TEMPERATURE DEPENDENCE OF ROLLING TEXTURES IN HIGH-PURITY SILVER by H. Hu and R. S. Cline (U.S. Steel Res. Ctr.); J. Appl. Phys., Vol. 32, pp. 760-763, May 1961

A rolling texture transition from the (110) $[\bar{1}12]$ common Ag type to the (123) $[\bar{4}\bar{1}2]$ Cu type was produced in high-purity

Ag by changing the temperature of deformation. The texture determined at 0°C for a strip rolled at 0°C was a simple (110) [$\bar{1}$12]. Rolling at 200°C produced a texture of the (123) [$\bar{4}\bar{1}$2] type, plus a cube texture component due to partial recrystallization. Results also suggest that the relatively high oxygen content in common Ag is probably not responsible for the formation of the (110) [$\bar{1}$12] texture. The change in texture from one type to the other in high-purity Ag can be obtained by merely varying the rolling temperatures.

12,374 TEXTURAL PROPERTIES OF GERMANIUM FILMS by J. E. Davey (U.S. Naval Res. Lab.); J. Appl. Phys., Vol. 32, pp. 877-880, May 1961

The textural properties of thin Ge films vacuum evaporated onto hot fused-quartz substrates have been investigated in detail over the temperature range from ambient to 650°C. The strongest texture characteristic of these films is the [110], which is obtained at substrate temperatures as low as 175°C, and prevails up to about 350°C. For temperatures between 350° and 575°C, competition for growth occurs and the texture varies principally between being powder, [110] and [111]. Above 575°C the [111] texture becomes dominant.

Field Ion Microscope Analysis of Fe Whisker Structure - See 12,258

CRYSTAL GROWTH

12,375 SHORT NOTE ON CRYSTAL GROWTH PATTERNS [in German] by Z. Gyulai (Inst. Exp. Phys., Budapest); Z. Phys. Chem., Leipzig, Vol. 217, pp. 428-431, Oct. 1961

Helical and linear growth patterns identified by means of chemical etching are discussed. The linear patterns are parallel to [100] directions and appear simultaneously with the helixes. Neither pattern could be reproduced systematically. A cooperation of the two growth mechanism responsible for both types of patterns has been proposed. Kossel's rule for monolayers is also valuable for macroscopic layers.

Growth Twins in InSb - See 12,326

12,376 NOMOGRAPH TECHNIQUE FOR DOPING DETERMINATION IN GERMANIUM AND SILICON CRYSTAL GROWING by N. Hemmat and A. L. MacDonald (Raytheon); Solid State Electronics, Vol. 3, pp. 309-314(L), Nov.-Dec. 1961

Nomographs for the determination of the total weight of impurity required to grow Si and Ge crystals of uniform resistivity by zone leveling are derived. The cases of constant and non-constant drift mobility are considered. In the former case, a separate graph is required for each doping element, while in the latter only one principal nomograph is required. The nomograph technique is illustrated in the horizontal growth of an In-doped Ge crystal with a resistivity of 0.7 Ω-cm. A doping nomograph suitable for use with crystals grown by the Czochralski technique is also presented.

12,377 GROWING HEAVILY COMPENSATED GERMANIUM CRYSTALS OF KNOWN IMPURITY CONCENTRATIONS by L. M. Lambert (Ford); Solid State Electronics, Vol. 3, pp. 316-317(L), Nov.-Dec. 1961

The growth of compensated Ge crystals with a constant concentration of one impurity type and a varying concentration of another is described. Ge containing a high concentration of one of the impurity types is used as a master alloy for the charge in the floating crucible. The compensating impurity is introduced into the reservoir crucible in any of the conventional ways. Prior to crystal growth, the weight of the master alloy corresponding to a given concentration in the final grown crystal for a particular crucible size is determined using the master alloy in the floating crucible and intrinsic Ge in the reservoir crucible. The compensation gradient can be determined from resistivity and Hall measurements since the concentration of the impurity in the floating crucible is constant and known.

12,378 THE TECHNOLOGY OF PULLING SINGLE CRYSTALS. Part I. by H. T. Minden (GE); Semicon. Prod., Vol. 4, pp. 25-28, Nov. 1961

The Czochralski crystal pulling method is discussed with particular attention to the temperature configuration of the system and the technique of seed dipping. A method for increasing the crystal diameter is presented. The causes of twinning and polycrystallinity are indicated, and some of the special problems concerning the growth of compound semiconductor crystals are discussed. The crystal diameter is determined by the circle of intersection between the isotherm and the melt surface, while flat isotherm catastrophe can be avoided by designing the puller so that the freezing isotherm is dish-shaped. If the maximum time rate at which the crystal diameter can be increased is exceeded, spontaneous nucleation and dendritic growth occur. The temperature must be lowered during the growing process to avoid crystal taper. The crystal shape is determined by the pulling rate.

12,379 CRYSTAL GROWTH OF GALLIUM ARSENIDE USING CARBON BOATS by J. R. Knight (Caswell Res. Labs.); Nature, Vol. 190, p. 1001(L), June 10, 1961

The problem of carbon boat induced impurities during the growth of high purity GaAs crystals is discussed. Among the boat materials generally used for the production of GaAs crystals carbon and vitreous silica are the most common. In either case a sealed envelope of vitreous silica is usually employed to prevent the escape of As vapor. The carbon boat facilitates single crystal growth, while the silica boats usually result in polycrystallinity. The crystals produced with carbon boats are more strongly n-type and the impurity is found to be Si. It is suggested that the carbon reduces the silica envelope producing free Si. The Si is then able to dissolve in the molten GaAs. This analysis suggests that carbon should be a satisfactory crucible material under conditions where it is unable to react with reducible oxides such as silica.

12,380 CRYSTAL GROWTH OF III-V COMPOUNDS by W. P. Allred (Bell & Howell Res. Ctr.); 1961 Conf. Ultrapurification Semicon. Matl., Macmillan, 1962, pp. 550-567

Growth of GaAs, InAs, AlSb, GaSb and InSb crystals by the Czochralski technique is discussed. The GaAs and InAs crystals were grown in an As atmosphere within a sealed system using a magnetic type puller. The AlSb was grown in a He atmosphere whereas H_2 was used while InSb and GaSb crystals were being pulled. The impurity types and their sources, such as contamination from the crucible, atmosphere and starting materials of the III-V compounds, are discussed. The effects of

crystallographic orientation and impurity concentration on the effective segregation coefficients are evaluated, and impurity levels are accurately determined by mass spectrographic analysis.

12,381 GROWTH OF SEMICONDUCTING COMPOUNDS FROM NON-STOICHIOMETRIC MELTS by D. T. J. Hurle, O. Jones and J. B. Mullin (RRE); Solid State Electronics, Vol. 3, pp. 317-320(L), Nov.-Dec. 1961

The growth of semiconducting compounds from non-stoichiometric melts is discussed. It is shown that growth in a melt having an excess of one component results in a zone of constitutional supercooling in the melt at the solid-liquid interface. Constitutional supercooling during growth from a non-stoichiometric melt can cause the solid-liquid interface to adopt a cellular form. A cellular structure with faceted {111} surfaces has been observed in an InSb crystal grown under conditions of constitutional supercooling from an In-rich melt. Similar structures have been produced by growing from an Sb-rich melt. It is pointed out that a growth rate which is slow enough to prevent a gradient of constitutional supercooling, and therefore the cellular structure and precipitation of a second phase at the cell boundaries, can be determined.

12,382 IMPROVED ELECTRON GUN FOR ZONE-MELTING BOMBARDMENT by M. Cole, C. Fisher and I. A. Bucklow (Metals Res., Ltd.); Brit. J. Appl. Phys., Vol. 12, pp. 577-578, Oct. 1961

A simple electron focusing device for floating zone electron bombardment furnaces is described. The filament is surrounded by and electrically connected to a water-cooled Cu cage which focuses the electron beam some 3 cm vertically below the filament. The anode is thus largely protected from evaporation from the filament, the molten zone is not obscured and evaporation and sputtering from the zone do not contaminate the filament. The sharpness of the focused beam can be altered by varying the filament diameter and position. Rods of between 3 mm and 12 mm diameter have been successfully zoned.

12,383 CHUCK DESIGN FOR HOLDING A SILICON ROD IN FLOATING ZONE CRYSTAL GROWING by N. Hemmat and A. L. MacDonald (Raytheon); Rev. Sci. Instr., Vol. 32, p. 601(L), May 1961

A chuck design for supporting the Si rod in the tube-type floating zone during the growing operation is discussed. The basic requirements of the design and the schematic sectional drawing of the chuck assembly as well as its position-drawing are presented in detail. The chuck material, stainless steel, is not a source of contamination to the Si. Ta, W, and Mo can also be used.

12,384 A MODIFIED RE COIL TO FACILITATE FLOATING ZONE TECHNIQUES by S. J. Silverman (Bell Labs.); J. Electrochem. Soc., Vol. 108, pp. 585-587, June 1961

A modified RF work coil which provides conditions necessary to grow crystals with larger diameters than those previously reported by the zone process is described. The coil comprises a continuously wound four-turn pancake section in series with two reverse turns above and below it. Observations on the coil's performance are generalized for a broad category of materials. On observing two samples of each material with identical diameters and coupling distances, the operating frequency was not found to be a critical parameter within the frequencies (450 kc and 5 Mc) used in the investigation. A tabulated summary of the zone-geometries for Si, Ge, GaAs, and GaP is given. It is anticipated that eventual modification of the furnace design to incorporate chuck rotation will permit a further increase in diameter.

12,385 PREPARATION OF CRYSTALS OF THE ALLOY SYSTEM Bi-Sb-Se-Te by D. A. Puotinen (MIT); 1961 Conf. Ultrapurification Semicon. Matl., Macmillan, 1962, pp. 585-594

The thermoelectric figure of merit and the preparation of crystals of the quaternary alloy system $Bi_{24}Se_6Sb_{(60+x)}Te_{(150-x)}$ where x varies from −8 to +12, are discussed. The samples were prepared by a modified and carefully controlled Bridgman process. By this technique, large crystals have been obtained over the entire alloy system. Separate direct measurement of α, k, and p on the first material to crystallize indicates that a thermoelectric figure of merit approaching $4 \times 10^{-3}(K°)^{-1}$ may be obtained in this system.

12,386 PREPARATION OF ELECTRONIC GRADE SILICON VIA THE IODIDE PROCESS by J. T. Buford, R. J. Starks et al. (Eagle-Picher); U.S. Gov. Res. Rep., Vol. 36, p. 17(A), July 20, 1961 AD 256 751

The development of a continuous system for the preparation of electronic grade Si via the iodide process is presented. The system includes the processes of synthesis, primary purification by distillation, zone melting, and thermal dissociation of SiI_4. The purification factors obtained in the process, as determined by the base B level of the Si produced, are presented.

12,387 VAPOR-PHASE GROWTH OF SINGLE CRYSTALS OF II-VI COMPOUNDS by W. W. Piper and S. J. Polich (GE Res. Labs.); J. Appl. Phys., Vol. 32, pp. 1278-1279, July 1961

A method of growing doped single crystals of II-VI compounds a few cm^3 in size is described. The crystal is grown from the vapor phase in a closed moving crucible which permits an efficient utilization of the charge and flexibility in the dimensions of the crystal.

Vapor Deposition of Si from $SiHCl_3$ - See 12,687

Preparation of:
Tunnel Junctions by Vapor Deposition - See 12,649
HgTe-CdTe Solid Solutions - See 12,246

12,388 ON THE PREPARATION OF THE NITRIDES OF ALUMINUM AND GALLIUM by A. Addamiano (GE); J. Electrochem. Soc., Vol. 108, p. 1072, Nov. 1961

The preparation and properties of AlN and GaN are discussed. AlN is obtained by firing a fine powder of AlP for 1-2 hr at 1000°-1100°C in a slow stream of dry ammonia. Well crystallized material is obtained only after an overnight firing at 1100°C. The observed stability and properties agree with those reported in the literature. No phase transformation is observed up to 1170°C and the lattice exhibits a low thermal expansion. GaN is obtained by firing a fine powder of GaP or GaAs in a stream of dry ammonia. With GaP, quantitative conversion to GaN occurs in about 2 hr at 1000°-1100°C. With GaAs, quantitative formation of GaN takes place in 1-2 hr at 1000°C. The GaN products, which showed a color variation from white through pale yellow, depending upon starting material and thermal treatment, were always highly

rystalline. GaN was found to be thermally unstable. Attempts at preparing (Ga, Al) N mixed crystals by the heat reatment of mixtures of AlN and GaN powders in sealed uartz containers were unsuccessful. No mixed crystals l(P, N), Ga(P, N), or Ga(As, N) were observed to form uring the preparation.

2,389 A RED ELECTROLUMINESCENT ZnSe PHOSPHOR y W. G. Gelling and J. H. Haanstra (Philips Res. Labs.); hilips Res. Rep., Vol. 16, pp. 371-375, Aug. 1961

he preparation of a red electroluminescent phosphor by firing mixture of ZnSe with traces of Cu and Al in the presence of I_2Se is described. Optimum brightness was found with a Cu ontent of from 3 to 10 x 10^{-4} gram atoms Cu per mole ZnSe nd an Al content of 80 to 100 per cent of the Cu content. he phosphors obtained showed only a feeble emission at room emperature and low excitation frequencies; this effect is asribed to temperature quenching . At higher frequencies 1550 cps) the phosphors show a quantum output equal to the utput of a good green ZnS phosphor under the same excitation onditions. Phosphors in which 5 and 8 atomic per cent of Zn vas displaced by Cd were also prepared; the effects of temperture on the light output is more marked in these mixed phosphors but at higher frequencies the quantum output is equal to hat of the pure ZnSe phosphors.

Dislocations in Al Single Crystals Grown by the Czochralski echnique - See 12,289

2,390 GOLD CRYSTALS ONE ATOM THICK by R. L. Hines Northwestern U.); Bull. Am. Phys. Soc., Ser. II, Vol. 6, . 243(A), Apr. 24, 1961

he thickness and structure of thin films of Au were discussed. Vhen evaporated in a vacuum onto an appropriate singlerystal substrate, the Au forms a single crystal having a defiite orientation with respect to the substrate. If the flux of u atoms is large compared to the flux of residual gas molelles and if a clean substrate surface is exposed at the start of vaporation by cleaving a mica crystal in the vacuum system, nen very thin Au crystals can be made. A film 300 A thick eposited in a vacuum of 10^{-6} mm Hg on a mica surface cleaved utside of the vacuum system shows a fracture pattern characistic of an amorphous film. However, a film 300 A thick rown at a rate of 30 A/sec in a vacuum of 4 x 10^{-7} mm Hg on mica surface freshly cleaved in the vacuum (mica temperare of ~100°C) shows a fracture pattern consisting of straight dges intersecting at angles of 60° and 120°. The thinnest lm obtained to date has a reflection coefficient due to the u of 0.010, indicating a thickness of 7A or only 3 atom yers. The film still shows fracture along lines with hexagoal symmetry.

2,391 FORMATION CONDITIONS AND STRUCTURE OF HIN EPITAXIAL SILVER FILMS ON ROCKSALT by B. W. oope and C. O. Tiller (Virginia Inst. Sci. Res.); J. Appl. ys., Vol. 32, pp. 1331-1336, July 1961

comprehensive experimental investigation relating formation nditions to the structural characteristics of thin, singleystal Ag films vapor deposited onto synthetic NaCl single ystals is reported. The formation conditions studied include eannealing heat treatment of the substrate, postheat treatent of film and substrate, substrate temperature during depocion, and rate of deposition. It is shown that an epitaxial temperature as such does not exist, and that the minimum deposition temperature for the formation of single-crystal films is rate dependent. Crystalline structure, porosity, and stacking fault density of the films are related to the rate of deposition, deposition temperature, and thickness.

12,392 PRODUCTION OF IRON SINGLE CRYSTALS BY THE ZONE MELTING METHOD [in German] by H. Hillmann and A. Mager (Vacuumschmelze); Entwicklungsber. S. and H., Vol. 24, pp. 97-100, June 1961

Experiments showing that Fe single crystals can be grown from the melt are described. Such single crystals are present in the δ-phase immediately after freezing. The results suggest that the orientation of the α-single crystals is predetermined by the orientation of the previously formed δ-single crystals. It is pointed out that the α-γ phase transformation always leads to grain formation. Thus, α-single crystals split up into a polycrystalline aggregate after being in the γ-phase for a short time. It is probable that this occurs at the upward passage of the A_3 point.

12,393 FERROMAGNETIC MATERIAL by B. T. Matthias (Bell Labs.); U.S. Pat. 2,989,480, Issued June 20, 1961

The composition and preparation of a material both ferromagnetic and superconducting at low temperatures (less than about 5°K) are described. The material is composed of cerium, gadolinium, and ruthenium in the proportions $Ce_{1-x}Gd_xRu_2$ where x is between 0.10 and 0.01, inclusive. An optimum formulation is listed. The arc furnace in which the material is processed is shown and described in detail. In operation, temperatures in excess of 3500°C can be generated by the arc. The physical form of the starting material is not critical, and it may consist of the individual metals or solid solutions in suitable percentage composition. Applications requiring combined magnetic and superconducting properties may utilize the product.

Preparation of InSb Films - See 12,589

12,394 MAGNETIC MATERIALS RESEARCH by G. P. Conard, II and E. J. Jablonowski (Lehigh U.); U.S. Gov. Res. Rep., Vol. 36, p. 113(A), July 5, 1961 AD 255 689

The preparation of Co and Co-Fe ferromagnetic thin films by thermal decomposition of acetylacetonates is discussed. A moderate degree of process control has provided films with a range of thickness and composition, and magnetic properties comparable to those of the bulk metal. The problems in utilizing the thermal decomposition method for thin film memory production are improving the reproducibility and reducing the coercivity of the film.

12,395 MODIFIED LITHIUM FERRITE by C. M. van der Burgt and J. F. Gugelot (N. A. Philips); U.S. Pat. 2,986,523, Issued May 30, 1961

The preparation of ferrites with high temperature independent initial permeabilities is discussed. The materials have the composition $Co_x[(Li_{0.5}Fe^{3+}_{0.5})_yZn_{1-y}]_{1-x}Fe_2O_4$, where y varies from 0.3 to 1 and x has a value between about $-0.018y + 0.019$ and $-0.092y + 0.096$. The addition of Co to the ferrite $(Li_{0.5}Fe^{3+}_{0.5})_yZn_{1-y}Fe_2O_4$ described in U. S. Pat. 2,751,353 greatly reduces the temperature dependence of the initial permeability. The preparation of the ferrite is illustrated by a specific example.

12,396 FERRITE COMPOSITION CONTAINING TITANIUM AND NICKEL by J. M. Brownlow (IBM); U.S. Pat. 2,982,732, Issued May 2, 1961

Compositions in the system Fe-Ti-M (where M is Mg or Ni) which produce rectangular hysteresis loop ferrites are plotted and discussed. Squareness ratio values range from 0.70 to 0.86, and magnetostriction is zero over a wide range of compositions. The formula for 16 bodies and the loop squareness ratio of each are listed. A method of preparation is described in detail. These ferrites have the requisites for use as a memory storage element in computer mechanisms.

12,397 THE SOLUBILITY OF NICKEL IN NICKEL FERRITE by R. Parker (Portsmouth Coll. Tech.) and M. S. Smith (U. Coll. N. Wales); J. Phys. Chem. Solids, Vol. 21, pp. 76-80, Oct. 1961

A method for preparing high resistivity nickel ferrites with nickel excess is described. High resistivity materials can be prepared by suppressing Fe^{++} and Ni^{+++} ions in the spinel lattice by suitable heat treatment. Electrical measurements indicate that excess nickel dissolves in the ferrite lattice up to a Ni to Fe ratio of 1.029:2. This result is consistent with available data of saturation magnetic moment.

12,398 MODIFIED NICKEL FERRITE by D. H. Baird, J. J. Dymon and S. Natansohn (Sylvania); U.S. Pat. 2,982,731, Issued May 2, 1961

The addition of predetermined amounts of MnO, Fe_2O_3, and Al_2O_3 to a Ni-ferrite to optimize parameters significant at microwave frequencies is cited. The concentration of each component is represented by: NiO + (a) MnO + (b) Fe_2O_3 + (c) Al_2O_3. Variations in (a), (b), and (c) produce a series of ferrites with low dielectric loss, whose saturation magnitization can be varied from between 100 to 2700 gauss, approximately, with a corresponding range of Curie point from 275° to 575°C. The compositional ranges are listed; with appropriate choice the saturation magnetization may be determined in accordance with the desired operating frequency.

12,399 MANGANESE-ZINC FERRITE by J. M. Brownlow (IBM); U.S. Pat. 2,987,481, Issued June 6, 1961

The preparation of ferrites which demonstrate desirable hysteresis loop squareness and pulse performance is discussed. The approximate composition ranges consist of 38.7 to 43.5 per cent Fe_2O_3, 51.6 to 58.4 per cent MnO, and zero to 8.8 per cent additives, which include oxides of Mg, Cu, Cr, Zn, Li, Al, or Ni. The desired properties are imparted by formation of a second crystalline phase, such as alpha-Fe_2O_3 or Mn_2O_4, in the skin of the ferrite, upon cooling from an initial firing temperature to a subsequent annealing temperature; cooling and annealing take place in oxidizing atmosphere. The temperature and length of time of annealing control the concentration and penetration of the second crystalline phase to optimum values.

12,400 USEFUL TECHNIQUE FOR GROWING LARGE, SINGLE-CRYSTAL YIG by D. Barry and R. W. Roberts (Melabs); J. Appl. Phys., Vol. 32, p. 1405(L), July 1961

A technique for growing large single-crystals of YIG from a powdered charge is described. The charge is melted at 1250°C in a Pt crucible and cooled rapidly to room temperature. By recharging the crucible a larger mass is obtained and a larger crystal is formed from the increased effective melt. The technique is believed to be useful for laboratories with limited facilities.

12,401 ON THE MECHANISM OF DIAMOND FORMATION by M. E. Lipschuta and E. Anders (U. Chicago); Science, Vol. 134, pp. 2095-2099, Dec. 29, 1961

The mechanism of diamond formation is discussed. No evidence of diamond formation or growth was observed in two series of experiments. The first series was an attempt to grow diamonds metastably by allowing iron carbide and iron sulfide melts to decompose spontaneously at atmospheric pressure. In a second series solid iron carbides and nickel carbides were subjected to static pressures above the diamond-graphite equilibrium for extended periods. The mechanism of a direct conversion of graphite to diamond by impact shock is suggested.

12,402 SAPPHIRE WHISKER GROWTH ON A SINGLE-CRYSTAL SUBSTRATE by P. L. Edwards and R. J. Happel, Jr. (U. Nav. Ord. Lab.); Bull. Am. Phys. Soc., Ser. II, Vol. 6, p. 24(A), Feb. 1, 1961

Growth of sapphire whiskers on exposed planes of single crystal of sapphire by heating aluminum filings, located near the crystals, to 1400°C in a stream of wet hydrogen was described. The whiskers grew only in certain directions with respect to structure of the base crystal. Polarized-light examination showed them to be crystallographically coherent with the substrates. The axes of the whiskers were either parallel to the c axis or to one of twelve equally spaced directions in the basal plane. These twelve directions divide into two distinct sets, a $2\bar{1}\bar{1}0$ set and $10\bar{1}0$ set, with each having sixfold symmetry about the c axis, and with the members of one set midway between members of the other. These and the c direction are the Burgers vectors' directions in sapphire; hence it seems plausible that the whiskers grow coherently with the substrate at the sites of emergent screw dislocations. This is in agreement with the work of Webb and Forgeng who have found axial screw dislocations in sapphire whiskers with axes in the c direction.

12,403 SYNTHETIC MICA CRYSTAL GROWTH PROGRAM by J. G. Froemel, E. C. Worden et al. (Synthetic Mica); U. S. Gov. Res. Rep., Vol. 35, p. 798(A), June 16, 1961 PB 155 154

The installation and testing of a laboratory crystal grower designed specifically for synthetic mica work are described. Studies of the growth of mica from high-temperature solutions are included along with solubility and melting data. A series of plantscale experimental melts is described including the use of the central heat-sink, controlled cooling schedules and precise batch control. The second "progressive" melt in which large rectangular electrodes are utilized for thermal gradient control is also mentioned.

12,404 GROWTH OF SINGLE-CRYSTAL CALCIUM FLUORIDE WITH RARE-EARTH IMPURITIES by H. Guggenheim (Bell Labs.); J. Appl. Phys., Vol. 32, pp. 1337-1338, July 1961

The preparation of large single crystals of CaF_2 by the zone melting and the pulling techniques is reported. Many crystals were doped with rare-earth elements. The ingots showed high optical perfection; they could be used in optical maser studies. The annealing of such crystals is discussed.

12,405 INVESTIGATION TO ESTABLISH HOW IMPURITY ATOMS AFFECT CRYSTAL NUCLEATION by G. W. Sears

(GE); U.S. Gov. Res. Rep., Vol. 36, p. 105(A), July 5, 1961 AD 255 093

The theory of preferential etching at dislocations is reviewed and compared to empirical observations on the dissolution of lithium fluoride. It is shown that ferric fluoride is also a growth poison for lithium fluoride from aqueous solution. Ferric fluoride has the properties characterizing a step poison for the lithium fluoride-water system.

Preparation of:
Lead Zirconate-Titanate - See 12,456
Semiconducting Polymer Carbons - See 12,490

CRYSTAL SURFACES

12,406 THE APPLICATION OF COMPUTER TECHNIQUES TO PREFERRED ORIENTATION STUDIES by J. R. Holland (Wright Air Dev. Ctr.); U.S. Gov. Res. Rep., Vol. 36, pp. 81-82 (A), Sept. 20, 1961 AD 258 594 $1.60

A computer technique for plotting normalized pole figures is described and an illustration of the technique applied to data generated using Schulz reflection X-ray diffraction geometry is presented. The computer method enhances the accuracy of the X-ray data and is far less tedious than the usual manual methods of plotting normalized pole figures. Somewhat modified programs should be capable of utilizing data generated by other diffraction geometries commonly used in quantiative preferred orientation studies; thus the method is more versatile than a specialized, completely automatic pole figure plotter.

12,407 SEMICONDUCTOR WAFERS POLISHED ELECTROCHEMICALLY by M. V. Sullivan (Bell Labs.); J. Electrochem. Soc., Vol. 108, p. 119-C(A), June 1961

A new electrochemical technique for rapid, scratch-free polishing of Ge and Si transistor wafers which results in 50 per cent polishing cost savings and improved surface characteristics is described. The wafers are mounted on a nonconducting support disk which is placed over a rotating polishing disk. As the electrolyte (dilute KOH for Ge, dilute HF for Si) is pumped between the disks it acts as a thin film cushion for the wafers. Individual electrical connection to the wafers and film thickness regulation by electrolyte viscosity variation allow polishing results showing no surface roughness even under 53,000 X electron microscope inspection.

12,408 CHARACTERISTICS OF THE {111} SURFACES OF THE III-V INTERMETALLIC COMPOUNDS. Part II. SURFACE DAMAGE by H. C. Gatos, M. C. Lavine and E. P. Warekois (Lincoln Lab.); J. Electrochem. Soc., Vol. 108, pp. 645-649, July 1961

Application of the dissolution rate technique in determining the depth of surface damage resulting from cold working (abrasion) is reported. The following III-V compounds were employed: GaAs, GaSb, InAs, and InSb. It was shown that the dissolution rates are a function of the actual surface area which in turn depends on the amount of cold work present rather than on the original roughening of the surface. The results obtained by this method agreed excellently with results obtained by etching and X-ray diffraction techniques. For the same cold-working treatment the depth of damage in InSb was found to vary for the various orientations as follows: {100} >B{111} > {110} ≥ A{111}, A and B designating the {111} surfaces terminating with In and Sb atoms, respectively. For the same cold-working treatment of the A{111} or B{111} surfaces of the four compounds studied, the depth of damage varied as follows: InSb > InAs > GaSb > GaAs, i.e., the depth of damage decreased with increasing energy gap.

12,409 PHOTOSENSITIVE ETCHING OF SILICON by J. H. Braun (du Pont); J. Electrochem. Soc., Vol. 108, pp. 588-589, June 1961

The photosensitivity of the etch rate of chemical etchants on Si is evaluated. Resolution seems limited only by the optical system used for projection and is independent of the surface preparation of the Si. P-type Si is less sensitive to illumination than is n-type. Experiments were conducted with n-type and p-type Si of 0.1 to 100 Ω-cm resistivity, using "Dash" etch solution and periods from 5 min to 2 days. Illumination was provided in the 10 to 100 ft-candle tungsten range. Etch rates for illuminated regions are estimated to be 10^3 A/sec, suggesting a simple fast technique for transferring patterns.

12,410 ETCH PITS ON CADMIUM SULPHIDE CRYSTALS by A. J. Eland; Philips Tech. Rev., Vol. 22, No. 8, pp. 266-267(A), 1960/61

Color photographs of the surface of a grown CdS crystal, etched in HCl vapor and observed with a microscope using interference contrast, are presented and discussed. From the disposition of the etch pits it is probable that the crystal processes a high degree of perfection; it apparently consists of several large mosaic blocks, differing in their mutual orientation by only a few seconds of arc.

12,411 ETCH GROOVES ON THE (111) PLANE OF ANTIMONY SINGLE CRYSTALS by V. M. Kosevich (Lenin Khar'kov Polytech. Inst., USSR); Soviet Phys.-Cryst., Vol. 6, pp. 379-381(L), Nov.-Dec. 1961

Etch grooves observed on the (111) planes of Sb single crystals are discussed. Crystals having purities of 99.5 and 99.999 per cent were etched with a CP-4 type etch. The grooves consist of a continuous band of small triangular pits. Regions of high etch pit density have high etch groove densities. Generally, a groove passes through one or more etch pits. In crystals containing ~10^4 dislocations per cm^2, the etch grooves are several mm in length and it is difficult to locate the ends of each groove. In crystals having ~10^3 dislocations per cm^2, short grooves which generally terminate at large dislocation etch pits are observed. In slightly bent crystals, both disordered and ordered, networks of etch grooves are observed on the (111) cleavage plane. The latter extend in the $[1\bar{1}0]$ directions, corresponding to points of emergence of $(11\bar{1})$ slip planes on the (111) plane. The number of etch grooves increases when the crystal is deformed.

Dislocation Etching in:
Sb - See 12,288
Ge - See 12,284 and 12,285
Zn - See 12,317

Etching Behavior of Ta - See 12,248

12,412 THE EFFECT OF SILICON SURFACE TREATMENT ON METALLIC IMPURITY DEPOSITION by G. B. Larrabee (Texas

Instr.); J. Electrochem. Soc., Vol. 108, p. 175C (A), Aug. 1961

The effect of silicon surface treatment on metallic impurity deposition is discussed. Electrochemical studies of various Si surfaces show differences in electrochemical potential which can be explained by the mode of formation of the oxide layer on the surface. Radio-chemical studies substantiate the electrochemical findings and show why the condition of the Si surface has such a pronounced effect on the extent of impurity contamination. Autoradiographic studies of the manner in which the metallic impurities are distributed over the various surfaces give additional evidence to explain this phenomenon.

Effect of Surface Treatment on the Bending Characteristics of MgO Single Crystals - See 12,301

12,413 PURIFICATION METHODS IN THE STUDY OF SEMICONDUCTOR SURFACES by J. A. Dillon, Jr. (Brown U.); 1961 Conf. Ultrapurification Semicon. Matl., Macmillan Co., 1962, pp. 604-613

Methods utilized in the study of the surface properties of semiconducting materials are discussed. In recent years argon-ion bombardment followed by annealing in high vacuum has been developed as an important technique in the preparation of surfaces which are atomically clean. This process possesses certain advantages over other techniques such as high-temperature heating, evaporation, or vacuum cleaving. The method is applicable to both polycrystalline or single-crystal samples and to the various crystal planes of the latter, being particularly useful where stable films are not readily removable by high-temperature heating or in which diffusion of film components might alter the surface electrical properties. However, the experimental conditions must be controlled so that the surface is not etched by the bombardment or contaminated by sputtered material. Preliminary studies using a method such as low-energy electron diffraction are also required to determine both the feasibility and the operating conditions necessary in the application of the technique to a particular material.

12,414 NEW METHOD FOR MEASURING SPUTTERING IN THE REGION NEAR THRESHOLD by D. McKeown (Convair Astron. Div., Genl. Dynamics); Rev. Sci. Instr., Vol. 32, p. 133-136, Jan. 1961

Use of a plated quartz crystal oscillator for extremely sensitive measurement of sputtering is described. The crystal is placed in a molecular beam and sputtering of its plating is measured by the frequency change of the oscillator. The relationship between the frequency change of the oscillator and the change in plating mass of the crystal is given. Sputtering of less than a millimicrogram of plating can be measured. A wide range of material can be used to plate the crystal. A crystal oscillator sputtering gauge has been built using a frequency counter with a digital readout to record the oscillator frequency. The operation of the gauge is illustrated by preliminary measurements on the sputtering rates of gold in an argon beam between 0 and 100 ev. Other uses of the gauge, such as a neutral beam detector, are also discussed.

ENVIRONMENTAL EFFECTS

12,415 ANNEALING OF RESIDUAL STRESS IN SILICON MONOXIDE FILMS by J. Priest, H. L. Caswell (IBM), L. Holland and T. Putner (Edwards High Vacuum); Brit. J. Appl. Phys., Vol. 12, pp. 580-581 (L), Oct. 1961

Experiments on the annealing of residual stresses in SiO films are discussed. Priest and Caswell observed that in films deposited on pure Ni substrates there was no detectable change in the stress after heat treatments (in vacuum or in atmospheres of oxygen and water vapor at pressures of 4×10^{-5} to 1×10^{-4} mm Hg) of up to two hours at temperatures of 200°C to 280°C. At partial pressures of oxygen or water vapor in the mm Hg range, the stress is greatly reduced and even becomes compressive under certain conditions. Holland and Putner have found that internal stresses in SiO films deposited on soda lime glass can be relieved by annealing at 200°C or above. Two stress relief mechanisms are suggested: 1) stress relief is due to a reaction between water from the soda lime glass and the SiO film at elevated temperatures, and 2) stress relief is due to gas desorbed by the SiO film.

12,416 ANNEALING OF QUENCHED SILVER by M. Doyama and J. S. Koehler (U. Illinois); Bull. Am. Phys. Soc., Vol. p. 419 (A), Nov. 24, 1961

The quenching of 99.999 per cent pure silver from temperatures between 450° and 850°C was discussed. A defect migrating with an energy of motion of 0.57 ev is observed to anneal in the range from -50° to +150°C. If the annealing is done below 0°C a second-order process is found. On annealing above 100°C the annealing is nearly first order with the same activation energy. Pulsing a quenched wire to 300°C for 1/10 sec produces a defect which anneals with a migration energy of 0.83 ± 0.07 ev. This is probably the lattice vacancy. The binding energy of the defect which produces vacancies on breakup is 0.35 ± 0.08 ev. The identity of the defect which migrates with energy 0.57 ev was discussed.

Stress Induced Point Defects - See 12,261

12,417 THE BAUSCHINGER EFFECT AND RESIDUAL MICRO STRESSES IN ALPHA BRASS by C. J. Newton (Natl. Bu. Stand.); J. Res. Natl. Bu. Stand., Vol. 65C, pp. 265-270, Oct.-Dec. 1961

The determination of residual axial and random microstresses after deformation in a brass by X-ray diffraction measurement is reported. The a brass samples underwent four 1 per cent plastic deformations, consisting of either tension, compression, compression, tension, or compression, tension, tension, compression. Elastic limits were also measured physically. After one deformation residual axial microstresses and a decrease in the elastic limit in a direction opposite to the deformation were observed. After three deformations as given above, residual axial stress was always tensile, although the elastic limits continued to be directional.

Effects of Deformation by Wire Drawing on the Alloy Cu_3Au - See 12,251

12,418 COMPARISON OF RANGES OF APPLICABILITY OF PREDICTIONS OF CREEP BUCKLING TIME by B. M. Lempriere (Stanford U.); U.S. Gov. Res. Rep., Vol. 35, p. 797 (A), June 16, 1961 PB 150 053

The most rigorous theory of the creep buckling of initially imperfect columns is examined for possible simplifications. It is found that the influence of plasticity on the life of a column can be ignored under certain conditions characterized by the

proportional limit stress, a creep parameter, the applied stress, and the initial curvature. These conditions are conveniently presented in the form of graphs for steady creep as represented by the power and the exponential laws. The simplification possible in the regions so defined permits the application of early theories. For steady creep, these lead to simple formulae. Some published data are examined in terms of the present ideas and give encouraging agreement with the theoretical results, for values of the correction factor ranging from 0.0074 to 1.25.

Dislocations and Plastic Flow in Ge - See 12,287

Effects of Deformation on Cu_3Au - See 12,251

NMR Analysis of Elastic Axial Compression Effects in NaI - See 12,286

12,419 IMAGINARY PART OF X-RAY SCATTERING FACTOR FOR GERMANIUM. COMPARISON OF THEORY AND EXPERIMENT by B. W. Batterman (Bell Labs.); J. Appl. Phys., Vol. 32, pp. 998-1001, June 1961

The imaginary part of the X-ray scattering factor for Ge is calculated from dispersion theory and individual Hartree-Fock electron scattering factors and is compared with Hunter's experimental values measured with anomalously transmitted X-rays. The agreement is quite good and verifies the treatment of anomalous transmission by the dynamic diffraction theory. It is shown that the imaginary part of the scattering factor can be related directly to the form factor of the L electrons in germanium and it is concluded that their charge distribution in the solid is essentially the same as in the free atom.

12,420 EXPANSION OF InSb UPON LOW-TEMPERATURE ELECTRON IRRADIATION by F. L. Vook (Sandia); Bull. Am. Phys. Soc., Ser. II, Vol. 6, p. 420(A), Nov. 24, 1961

Precision measurements of the change in length of high purity, single crystal InSb made upon irradiation and annealing were given. The sample was initially irradiated below 110°K to an integrated flux of 2.0×10^{19} electron/cm^2. The specific length expansion was $\Delta L/L = 1.0 \pm 0.1 \times 10^{-23}$ per 2-Mev electron. The sample was then warmed from 50° to 330°K at 10°K/hr. Between 50° and 170°K the sample expanded further in a reverse annealing. Above 290°K the expansion recovered as for a normal anneal. Further irradiation at <175°K with 1.4 Mev electrons to an integrated flux of 1.8×10^{19} electron/cm^2 gave an expansion rate which was smaller than that for 2.0 Mev electrons by a factor of 4.5. The ratio of the two expansion slopes yields a threshold displacement energy of 30 ev in good agreement with Aukerman's carrier removal data, but in disagreement with Eisen's value of 7 ev. The expansion of InSb is much larger than previous measurements on Ge and Si and is attributed to the partly ionic nature of the bonding.

Irradiation Induced Lattice Expansion - See 12,281

12,421 MECHANICAL AND RADIATION INDUCED FAULTING IN SODIUM AZIDE by D. T. Keating (Brookhaven Natl. Lab.); and S. Krasner (Picatinny Arsenal); J. Phys. Chem. Solids, Vol. 20, pp. 150-161, June 1961

Sodium azide powders subjected to mechanical grinding, gamma irradiation, and pile irradiation have been examined by X-ray diffraction techniques. Faulting and strain are found in the ground samples with no indication of decomposition. Faulting and strain are also found in samples subjected to irradiation accompanied by signs of decomposition such as coloration, lowering of the ignition temperature, and a lattice contraction in the direction of the long dimension of the azide ion. Annealing removes some of the faults and strain both in the ground and irradiated samples, but in the latter cases a significant fraction of these imperfections are stable even at the ignition temperature. The two types of irradiation produce qualitatively similar results, and quantitative differences are ascribed to the more inhomogeneous decomposition induced by pile irradiation. In both cases a return to stoichiometry upon annealing is evidenced by a disappearance of the lattice contraction.

12,422 REACTOR IRRADIATION AND ANNEALING OF PbTe by J. C. Corelli, R. T. Frost and D. M. Amorosi (Knolls Atomic Power Lab.); Bull. Am. Phys. Soc., Ser. II, Vol. 6, p. 18(A), Feb. 1, 1961

Results of irradiating samples of n- and p-type PbTe at 60 ± 20°C to a total integrated flux-time of 0.50×10^{20} cm^{-2} of neutrons having energies greater than 1 Mev were reported. Room temperature resistivity increased by factors of 13 and 600 for the n- and p-type samples while the corresponding Seebeck coefficients increased by factors of 1.8 and 2.3, respectively, as a result of the irradiation. Hall coefficient measurements indicated carrier concentration decreases by factors of 4.7 and ~15 for the n- and p-type samples, respectively. Results for the n-type sample indicate a saturation in the accumulation of damage when compared with results obtained on samples irradiated to lower flux-times. In the isothermal annealing experiments performed on the n-type sample measurements of resistivity, Seebeck and Hall coefficients were made successively. The resistivity and Hall coefficient decayed with similar rates. Recovery rates for this sample were greatest in the temperature range 150°-180°C with no unannealable damage in its properties. Similar annealing results for the p-type sample were given.

12,423 CHARACTERISTICS AND ANNEALING OF NEUTRON IRRADIATED PbTe by J. C. Corelli and D. M. Amorosi (Knolls Atomic Power Lab.); Bull. Am. Phys. Soc., Ser. II, Vol. 6, p. 420(A), Nov. 24, 1961

Measurements of conductivity, Seebeck and Hall coefficient changes of n- and p-type PbTe after reactor irradiation, were reported. Irradiation was carried out at levels of $1\text{-}10 \times 10^{19}$ cm^2 of neutrons with energy greater than 1 Mev and thermal neutron doses of 10^{20}-10^{21}/cm^2. Isothermal annealing experiments indicate simultaneous recovery of conductivity, Hall and Seebeck coefficient in the temperature ranges 100°-170°C and 140°-180°C for p- and n-type materials, respectively. The carrier concentration decrease for both materials (factor 5) accounts for nearly the entire increase in Seebeck coefficients (factor 2). Analysis of the annealing of conductivity (increased by factor 17) for the p-type PbTe data yields an activation energy of 1.3 ± 0.1 ev. For n-type PbTe, analysis of both conductivity (increased by factor 12) and Hall coefficient yields an activation energy of 1.3 ± 0.1 ev, and the depression of the carrier concentration can be attributed to a bombardment-induced trapping level 0.026 ev below the bottom of the conduction band. In both materials there is evidence of a second stage in the annealing process. Subsequent to annealing both materials retain their characteristic intrinsic gaps of ≈0.32 ev and the mobility of n-type PbTe exhibits a $T^{-5/2}$ variation. Small permanent changes due to transmutations, and comparisons with previous irradiations at lower doses were discussed.

SOLID STATE PHYSICS

CRYSTAL PHYSICS

BINDING PROPERTIES

12,424 NUCLEAR QUADRUPOLE RESONANCE IN $TiCl_4$, $ThCl_4$, $NbCl_5$, and $TaCl_5$ by A. H. Reddoch (U. California); J. Chem. Phys., Vol. 35, pp. 1085-1089, Sept. 1961

Nuclear quadrupole resonance studies to investigate the nature of the bonds in several chloride compounds are discussed. Cl^{35} resonance at about 6 Mc was observed in $ThCl_4$. The frequency suggests highly ionic binding which contradicts earlier conclusions from X-ray studies. Some double-bond character may be present in the Th-Cl bond. Nb and Cl resonances have been discovered in $NbCl_5$. The niobium resonances are described by a single set of parameters, the coupling constant $eqQ \approx 78$ Mc, and the asymmetry parameter $\eta = 0.32$. Two $\Delta M = 2$ and one $\Delta M = 3$ transitions were observed. Only a single Cl^{35} resonance was found at about 13 Mc, the frequency suggesting appreciable covalency in the Nb-Cl bond in $NbCl_5$. A single resonance observed in $TaCl_5$ at about 13 Mc is believed to be a Cl^{35} resonance. A fairly simple method is outlined for determining the asymmetry parameter of the electric-field gradient from the observed transition frequencies without solving the secular equations directly.

12,425 CLOSED-SHELL ION-ION INTERACTIONS IN CALCIUM FLUORIDE by J. R. Reitz, R. N. Seitz and R. W. Genberg (Case Inst. Tech.); J. Phys. Chem. Solids, Vol. 19, pp. 73-78, Apr. 1961

The short range ion-ion interactions in CaF_2 are assumed to have the form $\phi_{ij} = A_{ij} \exp(-r/\rho)$. By calculating the electrostatic contribution to the elastic constants of CaF_2 and comparing the results with the experimentally observed constants, it is determined that $\rho = 0.28 \times 10^{-8}$ cm, A_{+-} for $Ca^{++} - F^-$ is 3.09×10^{-9} ergs, and A_{--} for $F^- - F^-$ is 1.04×10^{-9} ergs. These results indicate that the $Ca^{++} - F^-$ interaction is about ten times larger than the $F^- - F^-$ interaction in this crystal. The deviation from the Cauchy relation is investigated by means of a model which allows relative motion between the sublattices making up the crystal; the model proves inadequate, however, and it is concluded that the failure of the Cauchy relation is due to a many-electron interaction between ions which cannot be approximated by a central interaction.

ENERGY BAND STRUCTURE

12,426 ON THE BAND THEORY OF MOLECULAR CRYSTALS by S. Flodmark (Stockholm U.); U.S. Gov. Res. Rep., Vol. 36, pp. 83-84(A), Aug. 5, 1961 AD 257 432

The orbitals of the electrons in a crystal adapted to the translational symmetry of the atomic framework are discussed. In the crystal orbital method presented, the use of these orbitals in the Schrödinger equations gives one secular equation for every wave vector. The basic orbitals in this secular equation are the different atomic orbitals for the atoms in the unit cell.

12,427 THEORETICAL INVESTIGATION OF THE ELECTRONIC ENERGY BANDS FOR THE ZIRCONIUM-OXYGEN CRYSTAL. Part II. SYMMETRY-ADAPTED ORBITALS AND SECULAR ELEMENTS by S. Flodmark and B. Roos (Stockholm U.); U.S. Gov. Res. Rep., Vol. 36, pp. 82-83(A), Sept. 5, 1961 AD 258 611

Explicit formulas for the elements of the split secular equations which yield the electronic energy bands in the close-packed hexagonal Zr-O system are presented. The methods used to split the secular equations in the present report are based on the theoretical development outlined previously. Certain singular idempotent projection matrices, labelled by the diagonal elements of the irreducible representations of the different little groups of the crystal symmetry group, are very useful for the determination of the split secular matrices. These matrices are given for the case where the screw symmetry of the crystal is not considered; they are unique except for similarity transformations. A systematic method of further transforming the singular secular matrices into reduced form and finally into real form is outlined. Some relations for the elements of the secular equations and a discussion of the influence of the screw symmetry are given.

12,428 FUNDAMENTALS OF ZONE THEORY by Yu. M. Butusov and M. V. Kopytina; Soviet Phys.-Solid State, Vol. 3, pp. 288-289, Aug. 1961

In solving the problem of a system of interacting conductivity electrons in a crystal in zone theory, the exact Schrödinger equation is replaced by one in which the interaction potentials between each pair of electrons are considered small, and each electron is considered as located in the periodic field of the crystal lattice and the average field of the other electrons. It has been pointed out that the assumption of the smallness of the interaction potential is not justified, and yet good results are obtained. A model wave function is introduced here relating the actual wave function to that of the model, and an expression is obtained for the actual wave function in terms of the single electron wave functions and the operator. It appears that the actual wave function consists of a part due to the aggregate of single electron states and an additive term involving the operator.

12,429 THE APPLICABILITY OF THE DIFFUSE REFLECTION SPECTRUM METHOD FOR DETERMINING THE FORBIDDEN ZONE WIDTH ΔE_{phot} IN POWDER SPECIMENS by E. E. Godik and B. F. Ormont; Soviet Phys.-Solid State, Vol. 2, pp. 2680-2682, June 1961

The use of the diffuse reflection spectrum method for determining the forbidden zone width ΔE_{phot} from phases in the binary system $(ZnSe)_x - (CdSe)_y$ is investigated. It is concluded that this method gives good reproducibility for specimens of different chemical and phase composition, the results being independent of the experimental conditions and in agreement with the results of other methods. The possibility of developing this method into a new rapid and accurate means of phase analysis with simultaneous determination of the important semiconductor phase characteristics ΔE_{phot} is also discussed.

Energy Gaps of $SnSe_2$ and $GeSe_2$ - See 12,482

12,430 IMAGE OF THE FERMI SURFACE IN THE LATTICE VIBRATIONS OF LEAD by B. N. Brockhouse, K. R. Rao and A. D. B. Woods (Atomic Energy, Canada); Phys. Rev. Lett., Vol. 7, pp. 93-95(L), Aug. 1, 1961

Observation of the Kohn anomalies in a single crystal of lead

reported. The dispersion curve shows a sharp anomaly on oth sides of the Brillouin zone boundary. The construction of ie locus of Kohn anomalies for a spherical Fermi surface is iscussed and it is shown that the Kohn construction becomes ore complicated for a non-spherical Fermi surface. The alculations show that the anomalies should be small. The rength of the effect in lead is believed to be connected with ie strong phonon-electron interaction in this material.

ermi Energy of Bi - See 12,464

nergy Bands at Clean Ge Surfaces - See 12,466

nergy Band Distortion in the Surface Layer of Cu_2O - See 2,569

onductivity Measurements of Surface States - See 12,578

2,431 ON THE BAND STRUCTURE OF CUPROUS OXIDE by .G. Zhilich and V. P. Makarov (Leningrad State U.); oviet Phys.-Solid State, Vol. 3, pp. 429-430, Aug. 1961

he first results of a theoretical calculation of the cuprous xide band structure are reported. The calculation is based n the method of Kohn and Rostoker, in which single-electron loch functions satisfying certain variational problems are ought. The solution can be represented as a linear combina- on of the product of lattice harmonics and the solutions of a ifferential equation. The choice of potential for the varia- onal problem is discussed. The problem is solved numerical- for the case where the Brouillon zone wave vector is zero r the even representations Γ_{25}' and Γ_1 (the center of inver- on was the Cu^+ site). The difference between values of the nergies of these representations finally obtained agrees well ith the width of the forbidden energy gap obtained from opti- l observation. This permits the assumption that the energy vel of Γ_1 corresponds to the bottom of the conduction band hile that of Γ_{25}' corresponds to the top of the valence band. tentative interpretation of the formation of electronic states ay be given in terms of the excitation of the electrons from e oxygen levels.

2,432 SYMMETRY OF ENERGY BANDS IN TlSe TYPE CRYS- ALS by F. M. Gashimzade (Physicotech. Inst., Acad. Sci., SSR); Soviet Phys.-Solid State, Vol. 2, pp. 2700-2704, ne 1961

e symmetry of energy bands in chain structure TlSe is dis- ssed. The characters of the irreducible representations of mple groups and double groups constructed from the D_{4h}^{18} space oup and the compatability relations are tabulated. The struc- re of the energy bands in the vicinity of the extremal points also described.

nergy Band Structure of Rutile - See 12,606

LATTICE POTENTIALS AND VIBRATIONS

2,433 NEW POTENTIAL FUNCTION FOR ALKALI HALIDE OLECULES by Y. P. Varshni (Natl. Res. Counc.) and R. C. ukla (Allahabad U.); J. Chem. Phys., Vol. 35, pp. 582- 7, Aug. 1961

new potential-energy function is suggested for the alkali lide molecules: $U = (-e^2/r) + P \exp(-kr^2)$ where P and K are constants. Values of α_e, $\omega_e x_e$, and the ionic binding energy D_i have been derived for the following three functions: the simple Born-Mayer potential, the Rittner potential, and the potential suggested above. The results obtained with the new function are much better than those obtained with the Born-Mayer potential, but slightly inferior to those obtained with the Rittner potential.

12,434 A NEW DERIVATION OF EXPRESSIONS FOR INTERNAL VIBRATIONAL COORDINATES IN TERMS OF ATOMIC DISPLACEMENTS IN POLYATOMIC MOLECULES by L. A. Gribov; Optics and Spectrosc., Vol. 10, pp. 208-209(L), Mar. 1961

A simple derivation of the relationship between the displacements of the atoms of polyatomic molecules from their equilibrium positions and their internal vibrational coordinates is presented. A formula which provides a possibility of easily finding expressions for all possible nonplanar coordinates in terms of the atomic displacements is obtained and examples illustrating this formula are given.

12,435 LONG-WAVE OPTICAL VIBRATIONS IN SIMPLE IONIC CRYSTALS by T. H. K. Barron (U. Bristol); Phys. Rev., Vol. 123, pp. 1995-1998, Sept. 15, 1961

Some of the difficulties recently pointed out by Rosenstock in the theory of the lattice vibrations of ionic crystals of NaCl or CsCl structure are resolved. Long optical waves in these crystals (but not in crystals with only short-range forces) are seen to be purely longitudinal and transverse. With the electrostatic approximation, the Lyddane-Sachs-Teller equation $(\omega_l/\omega_t)^2 = \epsilon_0/\epsilon_\infty$ holds independently of the boundary conditions for modes in which the phase of the ionic vibrations is effectively constant over distances which are large compared with the lattice spacing; such modes must be either curl-free or divergence-free, with respective frequencies ω_l and ω_t. If both curl and divergence vanish, the frequency is indeterminate unless boundary conditions are specified, so that there is a singularity but no inconsistency as the wave number $k \to 0$. When Coulomb retardation is taken into account, this singularity disappears and the frequency at $k = 0$ is found to be ω_l; the range of validity of the Lyddance-Sachs-Teller equation is then $10^{-4} \geq k^{-1} \geq 10^{-6}$ cm. Reasons for believing that the cyclic boundary condition is valid for the thermodynamic properties of large ionic crystals are given.

Lattice Vibrations in Solid CO - See 12,549

Lattice Wave Dispersion Curves of Diamond - See 12,546

12,436 VALENT HYDROXYL VIBRATIONS IN FERROELECTRIC KH_2PO_4 AND KD_2PO_4 CRYSTALS by A. N. Lazarev and A. S. Zaitseva (Silicate Chem. Inst., Acad. Sci., USSR); Soviet Phys.-Solid State, Vol. 2, pp. 2688-2689, June 1961

The absorption spectra of KH_2PO_4 and KD_2PO_4 at temperatures near 300 and 110°K are studied. The significance of the results associated with valent hydroxyl vibrations is discussed. It is suggested that the transfer of a proton in the ferroelectric crystal KH_2PO_4 from one atom to another is possibly a cooperative process and associated with low-frequency OH---O vibrations.

Determination of Lattice Vibration Spectra from Infrared Absorption Spectra - See 12,545

12,437 SOLID-STATE VIBRATIONAL SPECTRA OF METHYL AND METHYL-d3 CYANIDE by D. E. Milligan and M. E.

Jacox (Mellon Inst.); U.S. Gov. Res. Rep., Vol. 36, p. 75(A), Sept. 5, 1961 AD 258 393

Measurements of the vibrational fundamentals of thin films of CH_3CN and CD_3CN at 77°K made with a high resolution, double beam grating spectrometer are reported. Evidence is presented for 3 absorptions assigned to ν_3, ν_6 and $(\nu_7 + \nu_8)$ in the 1/1300 to 1/1500 cm region of the CH_3CN spectrum. Annealing from an initial glassy state to a crystalline form is observed for these deposits. The multiplet structure of the annealed samples indicates that CH_3CN and CD_3CN crystallize in the orthorhombic, tetragonal, or trigonal system. Contrary to predictions based on quadrupole resonance studies, the crystal does not preserve the threefold symmetry of the molecule about its CN triple bond. Although assignment to a crystal class must remain indefinite, the simplest possibility has point symmetry C_{2v}.

ELECTRONIC PROPERTIES

12,438 ELECTRON DENSITY DISTRIBUTION IN ZnO CRYSTALS by G. P. Mohanty (A. O. Smith) and L. V. Azároff (Illinois Inst. Tech.); J. Chem. Phys., Vol. 35, pp. 1268-1270, Oct. 1961

Electron density distributions for two ZnO crystals that had been heated in Zn vapor and for an undoped crystal, determined by X-ray diffraction techniques, are discussed. The doped crystals contain $15\text{-}60 \times 10^{19}$ atoms/cm^3 in the octahedral interstices. The incorporation of this large number of interstitial Zn atoms increases the axial ratio of the hexagonal unit cell from 1.6019 to 1.6025. The density of the interstitials is approximately 1000 times greater than that calculated from the electrical conductivity of these crystals so that it must be concluded that most of the interstitial Zn atoms are electrically neutral. The presence of these interstitials explains why the time required to reach saturation for electrical conductivity is much greater in virgin crystals than in previously doped ones.

12,439 POSITRON LIFETIMES AGAINST ANNIHILATION IN METALS AND ALKALI HALIDES by B. L. Pollak (U. Washington); U.S. Gov. Res. Rep., Vol. 36, p. 97(A), Sept. 20, 1961 AD 259 383

The positron lifetimes against annihilation in three metals (Cu, Ag, Mg) and ten alkali halide crystals (LiF, NaF, NaCl, NaBr, NaI, KCl, KBr, KI, CsBr, CsI) are reported. The lifetimes obtained are in qualitative agreement with the simple theory discussed. A general introduction to the use of the phenomenon of positron-electron annihilation as a tool to explore the electronic structure of solids is presented. A summary of the work (experimental and theoretical) which is pertinent to the subject of this thesis is included. Suggestions for further work on the alkali halides are made.

ELECTRICAL PROPERTIES

GENERAL

12,440 PHYSICS OF THIN RESISTIVE FILMS by E. R. Olson and G. L. Vajda (Halex); U.S. Gov. Res. Rep., Vol. 36, p. S-55(A), Aug. 5, 1961 PB 156 302

Information on the relationships between electrical behavior and process parameters for nichrome, nichrome-silicon and nichrome-silicon oxide films is presented. The results of other investigators are correlated with present results in regard to the effect of process parameters on film properties. Preliminary data on the relationships between structure, stress and electrical properties are given.

12,441 SEMICONDUCTIVE PROPERTIES OF CdS. FORMING, ELECTRON ACTIVATION ENERGY, HALL EFFECT by A. Luyckx, J. Vandewauwer and P. Coopmans (Louvain U., Belgium); U.S. Gov. Res. Rep., Vol. 36, p. 82(A), Aug. 5, 1961 AD 257 345

Measurements and calculations to determine the Hall effect, number of electron carriers, mobility and energy of activation of electrons for extrinsic and intrinsic conduction for several CdS single crystals activated with In, Ga, and Ag are reported. Accurate measurements became possible only after forming at high frequency; comparisons were made between samples formed at high frequencies and in argon at 850°C. Hall effect measurements were reproducible and gave straight lines with variation of magnetic field or current. The extrinsic conduction formula and activation energies for CdS, Ag, and In are given.

DIELECTRIC PROPERTIES

12,442 THE PROBLEM OF INORGANIC ELECTRETS by A. N. Gubkin and G. I. Shanavi (Lebedev Phys. Inst., Moscow); Soviet Phys.-Solid State, Vol. 3, pp. 215-220, July 1961

Studies on electrets of organic (wax) and polycrystalline inorganic (ceramic) dielectrics are reviewed. The electrets are grouped according to their preparation: (1) thermoelectrets, prepared by heating and cooling in an electric field; (2) photoelectrets, prepared in illumination but not heated; and (3) certain ceramic and phosphor electrets prepared in an electric field. The field within the electret, E_i, is derived for the organic short circuited case and the inorganic partially short circuited case. Methods of charging and the measurements of surface charge are discussed in detail. The phenomenological theory is verified quantitatively for various electrets.

12,443 CENTERING OF CHARGES IN CRYSTALLINE IONIC STRUCTURES [in French] by J. D. H. Donnay and G. Donnay (Johns Hopkins U. and Carnegie Inst. Tech.); Compte Rendus, Vol. 253, pp. 291-292, July 10, 1961

The concept of charge centers is generalized to include several ions of the same sign. The twice generalized Bravais law is applied to the crystal morphology of the barite $BaSO_4$ and an example of the charge center structure of barites is provided by sample yz, zx, and xy projections of a $BaSO_4$ crystal. It is shown that neighboring ionic charge centers function as homologous points of the bond structure, independently of their sign. By introduction of the concept of a compensatory quadrupole, a single central charge is substituted for the two like charges of an ion pair. Considerations of the four possible quadrupole and charge interactions support the legitimacy of this substitution.

12,444 CHARGE DISTRIBUTION AND ELECTRIC FIELD GRADIENTS IN IONIC CRYSTALS by G. G. Belfor, R. A. Bernhein and H. S. Gutowsky (U. Illinois); J. Chem. Phys.,

Vol. 35, pp. 1032-1038, Spet. 1961

A method whereby the point-charge model often used for the calculation of electric field gradients in ionic crystals can be verified is presented. The asymmetry parameter of the electric field gradient at a nucleus and the Eulerian angles describing the orientation of the field gradient's principal axes with respect to the crystallographic axes are linear functions of the point charges assigned to each set of atoms in the lattice. If the unit cell is of low symmetry and if there are more than one set of nuclei for which quadrupole interaction data can be observed, the number of observables and equations may equal or exceed the number of unknown charges, thereby enabling the charge distribution to be determined and its internal consistency checked. An application of the method is given employing spodumene as an example.

12,445 PERMITTIVITY OF BARIUM TITANATE DURING SWITCHING by A. Misarova and V. Janousek (Czech. Acad. Sci.); Czech. J. Phys., Vol. 11B, pp. 465-466(L), 1961

Measurements of the complex permittivity ϵ^* of $BaTiO_3$ during switching in the frequency range 5-200 kc are reported. A sinusoidal switching field 7-25 kv/cm in amplitude and 25-50 cps in frequency was used, and it was found that ϵ^* does not depend on the amplitude and frequency of the switching field. The dependence of ϵ^* on the frequency of measuring voltage for constant switching current is discussed. At low frequencies, the increase of ϵ^* does not agree with Debye equation, although agreement is obtained at high frequencies.

12,446 A STUDY OF THE TRANSIENT BEHAVIOR AND THE SWITCHING EFFECT IN ANTIMONY TRISULFIDE by J. R. Davis, Jr. (Kentucky Res. Found.); U.S. Gov. Res. Rep., Vol. 36, p. S-56(A), Aug. 5, 1961 PB 155 127

Precise methods of measuring the important time and electric field dependent characteristics associated with the "switching effect" in stibnite are described. Temperature dependent properties, pre-breakdown pulses and delayed breakdown behavior have been examined. Stoichiometric stibnite, Sb_2S_3, undergoes dielectric breakdown when subjected to an electric field of about 10^6 v/cm which is of the same order as required to break down most dielectrics. However, it was discovered that stibnite containing 1 per cent or more excess antimony undergoes breakdown with much smaller applied fields, about 3000 v/cm and with removal of the field the sample resistance is found to be about four orders of magnitude smaller. In the case of stibnite there is no evidence of decomposition. It was also found that original high resistance of the samples could be restored by heating.

12,447 SOLUTION OF THE PROBLEM OF THERMAL BREAKDOWN IN INHOMOGENEOUS DIELECTRICS by S. N. Koitov and A. N. Tsikin (M. I. Kalinin Polytech. Inst.); Soviet Phys.-Solid State, Vol. 2, pp. 2655-2663, June 1961

Solutions to direct current thermal breakdown in inhomogeneous dielectrics are derived. Two cases are considered where the resistivity is a function of both temperature T and coordinate Z. The method used is sufficiently general and can be used for solving various problems of the theory of direct current thermal breakdown in one-dimensional cases.

Generation of Dislocations in Ionic Crystals on Breakdown - See 12,291

12,448 DIELECTRICS FOR SATELLITES AND SPACE VEHICLES by L. J. Frisco (Johns Hopkins U.); U.S. Gov. Res. Rep., Vol. 36, p. 45(A), Aug. 5, 1961 AD 256 900 OTS $8.10

A study of the effects of simulated high altitude environment on the electrical properties of insulating materials is reported. High vacuum breakdown and flashover measurements in the 10^{-6} mm Hg range at dc, 60 cps, 2 Mc and 18 Mc indicate that electrode surface roughness is the controlling factor. Dielectric properties of the specimen material do not influence flashover voltage. X-ray and ultraviolet radiation have no effect on flashover voltage. Significant changes in low-frequency loss properties and dc conductivity were observed during and after vacuum irradiation with 50 kv X-rays. Ultraviolet radiation produced no immediate effects on loss properties.

12,449 EFFECTS OF RADIATION ON FERROELECTRIC AND FERRIMAGNETIC MATERIALS. Part I. FERROELECTRIC MATERIALS by L. G. Wright, C. A. Rosen and S. I. Taimuty (Stanford Res. Inst.); U.S. Gov. Res. Rep., Vol. 36, p. 55(A), Aug. 20, 1961 AD 257 823

The effects of reactor radiation and Co-60 γ radiation on the dielectric properties of 4 ceramic ferroelectric materials ($BaTiO_3$, 96 per cent $BaTiO_3$ + 4 per cent $PbTiO_3$, 95 per cent $BaTiO_3$ + 5 per cent $CaTiO_3$, and 56 per cent $PbZrO_3$ + 44 per cent $PbTiO_3$) are described. Complex permittivity and large-signal hysteresis properties were measured before and after irradiation, after room temperature aging, and after 500°C heat treatment. The effects on the dielectric constant were small after fast-neutron exposures below 10^{18} n/cm^2. After 10^{18} n/cm^2, decreases in the values of the dielectric constants were observed with the passage of time. The total hysteresis loss at constant maximum electric displacement increased, and the changes in the hysteresis loops were large only in the samples exposed to 10^{18} n/cm^2. The changes in the γ-irradiated samples were similar to but smaller than those in the neutron-irradiated samples.

12,450 THE INFLUENCE OF IRRADIATION OF ALKALI HALIDE CRYSTALS BY THERMAL NEUTRONS ON DIELECTRIC PROPERTIES by V. V. Krasnopevtsev (Lebedev Phys. Inst., Moscow); Soviet Phys.-Solid State, Vol. 3, pp. 156-157, July 1961

Both the dielectric properties and optical absorption (in the visible part of the spectrum) of single crystals of KBr and NaCl after irradiation by thermal neutrons are investigated. Measurements are reported at constant voltage (dielectric loss tangent, $\tan\delta$ and dielectric constant ϵ) and cover the acoustic frequency region under temperature conditions from 20 to 250°C. Plots of the experimental data are given. In general the results for irradiated NaCl agree with those for KBr. The existence of a maximum in the temperature dependence of $\tan\delta$ for irradiated KBr crystals was explained by the fact that the M-centers formed in the lattice under the action of neutron irradiation during the process of annealing at a temperature of about 110°-130°C begin to collapse, decomposing into F-centers and vacancy pairs; this does not make any contribution to ionic electrical conductivity but does cause a sudden increase in $\tan\delta$.

12,451 DIELECTRIC LOSSES OF NaCl CRYSTALS WITH Ca ADMIXTURE IRRADIATED WITH X-RAYS by M. Kaderka (Czech. Acad. Sci.); Czech. J. Phys., Vol. 11B, pp. 456-457(L), 1961

Measurements of dielectric losses of both colored and uncolored

NaCl crystals containing 0.5 mol per cent $CaCl_2$ are reported. The results show that the maxima of the dielectric losses disappear at temperatures 81°, 91° and 96°C and corresponding frequencies 2500, 4000 and 5000 cps. This can be explained on the basis of models of Z centers.

12,452 DIELECTRIC DISPERSION IN LITHIUM FLUORIDE CRYSTALS [in French] by H. Curien and C. Petitjean (U. Paris); Comptes Rendus, Vol. 253, pp. 254-256, July 10, 1961

Measurements of dielectric losses in LiF monocrystals quenched from 300°C are reported. Crystals tempered and slowly cooled after initial quenching do not exhibit these losses. The quenching creates a dielectric relaxation domain in the crystals which enables Mg ions, and divalent impurity ions generally, to form bipolar complexes. Unquenched or tempered specimens thus contain primarily inhibited divalent impurity ions, i.e., those that do not form complexes. It is concluded that the divalent impurity ions which form bipolar complexes with lithium ion gaps cause the dielectric relaxation which leads to the dielectric losses found. The dielectric absorption data of quenched specimens agree with those obtained earlier by Dryden and Rao.

12,453 CONTACT FERROELECTRIC EFFECT APPLIED TO PLASTIC FLOW by B. S. Satyanarayana (Inst. Armanent Studies, India); Brit. J. Appl. Phys., Vol. 12, pp. 563-565, Oct. 1961

Investigations of the ferroelectric effect of MnO_2 are discussed. It was found that a phenomenon, dependent on the efficiency of contact of the oxide surface with the electrodes, exists. The apparent changes in the ferroelectric hysteresis loops with pressure on the electrodes are traced experimentally. The apparent contact variation of the ferroelectric effect in MnO_2 is applied to a comparison of the plastic flow in indentations in metals.

12,454 DIELECTRIC RELAXATION AND COUPLING BETWEEN DIPOLES; FERRO- OR ANTIFERROELECTRIC TRANSITION [in French] by J. Lajzerowicz (U. Grenoble); Comptes Rendus, Vol. 253, pp. 234-236, July 10, 1961

By taking into account the influence of nearest-neighbor interactions in computing the transition probabilities of a dipole, a nonlinear evolution relation is derived. For zero-field situations, the relation indicates possibilities for ferro- or antiferroelectric states. It is found that the logarithm of the relaxation time is not a linear function of T^{-1}. The derivation proceeds from considering a one-dimensional crystal made up of dipoles having two equilibrium positions, the shape of the double potential wells depending on the orientation of the nearest-neighbor dipoles. Analogous to the Bragg-William approximation, small-distance order is completely neglected in the calculations. A static treatment leads to a classification of occurrence of paraelectric, ferroelectric, or antiferroelectric behavior. Finally, a dynamical study yields polarization as a function of time and an expression for the relaxation time involving the initial polarization.

Lognormal Distribution of Magnetic Relaxation Process - See 12,614

12,455 THE FERROELECTRIC PROPERTIES OF STRONTIUM-BISMUTH TITANATE by A. N. Gubkin (Lebedev Phys. Inst., Moscow); Soviet Phys.-Solid State, Vol. 2, pp. 2732-2737, June 1961

The possibility that strontium-bismuth titanate (SBT) has certain ferroelectric properties is reported. It is demonstrated experimentally that in strong fields SBT has a residual polarization and a piezoeffect. The nonlinear properties of SBT have been investigated at high temperatures. A dependence of permittivity ϵ and the tangent of the loss angle $\tan\delta$ on the intensity of an alternating electric field has been observed. Hysteresis has also been investigated at high temperatures. The curves for the dependence of the polarization on field intensity have been found to have shapes similar to the hysteresis loop for ferroelectrics obtained at low field intensities.

12,456 LEAD ZIRCONATE-TITANATE PIEZOELECTRIC CERAMICS by A. E. Crawford (Brush Crystal, England); Brit. J. Appl. Phys., Vol. 12, pp. 529-534, Oct. 1961

The preparation and properties of lead zirconate-titanate piezoelectric ceramics are discussed. These materials have Curie points between 300° and 400°C and exhibit larger piezoelectric effects than $BaTiO_3$. The improvement of the piezoelectric and electrical properties of the basic lead zirconate-titanate solid solution by the addition of small quantities of the oxides of trivalent or pentavalent elements such as La, Nd, or Nb is described. The properties of three commercial ceramics are presented.

12,457 PIEZOELECTRIC GENERATION OF AN ELECTRICAL IMPULSE by M. Redwood (U. London); J. Acoust. Soc. Am., Vol. 33, pp. 1386-1390, Oct. 1961

The problem of a resistance loaded, steady-state stressed piezoelectric ceramic which is suddenly unstressed is examined theoretically. General equations describing the subsequent current and energy dissipation in the resistor are developed and examined in detail for a specific transducer of lead zirconate-titanate ceramic. The general equation for current consists of a series of time-delayed functions, signifying physically that a mechanical wave propagates through the transducer with successive reflections at the end faces, releasing strain energy originally stored in the material; this energy is then dissipated in electrical form in the resistance. The initial current has two components, an exponential function representing the discharge of energy stored in electrical form in the transducer capacitance and a step function representing the release of energy stored in mechanical form. The effect of the magnitude of R on the two components of the current is considered.

12,458 EFFECTS OF HIGH STATIC STRESS ON THE PIEZOELECTRIC PROPERTIES OF TRANSDUCER MATERIALS by H. H. A. Krueger and D. Berlincourt (Clevite); J. Acoust. Soc. Am., Vol. 33, pp. 1339-1344, Oct. 1961

An investigation of the effects of static compressive stress on the piezoelectric properties of two commercial lead titanate zirconate compositions, PZT-4 and PZT-5, and of two barium titanate compositions, commercial Ceramic B (a barium calcium titanate) and BaPb-Ti (12 per cent by wt.), is discussed. The permanent effects of stress exposure, determined at zero stress after exposure to a given stress, were found to be more severe with stress parallel to the polar axis than with perpendicular stress. Under maintained stress, however, the effects of perpendicular stress are more severe. PZT-4 and BaPb12Ti, generally better suited for use as radiating transducers, show effects dependent on exposure time but independent of the number of stress cycles. Ceramic B and PZT-5 show effects

dependent upon the number of stress cycles and less dependent upon the total period of stress exposure. Of the compositions rested, PZT-4 and BaPb12Ti were least affected by high static stress, suffering relatively little from exposure to stress as high as 15,000 psi. Of these two compositions, PZT-4 has markedly higher coupling ($k_{33} \sim 0.64$ compared to 0.365) and therefore offers higher transducer bandwidth.

12,459 PIEZOELECTRICITY OF QUARTZ FOR FINITE STRAIN by S. Machlup (Clevite and Western Res. U.) and M. E. Christopher (Clevite); J. Appl. Phys., Vol. 32, pp. 1387-1391, July 1961

The principal piezoelectric coefficient of a quartz is calculated on the basis of a hard-sphere, rigid-ion model. The results, obtained by purely geometrical reasoning (including an ad hoc geometrical constraint), fits the measured value of e_{11} with an "effective ionic charge" of one-sixth the free ionic charge. Extension of the calculation to finite compressive strain yields a maximum possible polarization of a quartz of 3.4 $\mu coul/cm^2$ at a 34 per cent strain. (Compare with $e_{11} = 16.7\ \mu coul/cm^2$ per unit strain.) For higher strains the polarization drops off rapidly, but the model becomes inconsistent for strains greater than 43 per cent. A test for more general validity of the model, made by obtaining directly the ratio of the two independent piezoelectric coefficients, e_{14}/e_{11}, yields seven times the measured ratio.

CARRIER PROPERTIES

12,460 APPLICATION OF IRREVERSIBLE THERMODYNAMICS IN THE THEORY OF RECOMBINATION IN SEMICONDUCTORS by G. Pataki (Hungarian Acad. of Sci.); Acta Phys., Vol. 13, No. 1, pp. 119-121 (L), 1961

An irreversible thermodynamic formulation of recombination, based on the Shockley-Read statistical theory of recombination, is derived. The non-stationary lifetime τ_r is given which renders, in first approximation, the stationary lifetime of Shockley and Read.

12,461 CONTRIBUTION TO THE STATISTICS OF RECOMBINATION OF ELECTRONS AND HOLES IN IMPURITY CENTERS IN SEMICONDUCTORS by Yu. V. Gulyaev (Inst. Radio Tech. and Electronics); Soviet Phys.-Solid State, Vol. 2, pp. 279-280, Aug. 1961

The recombination of current carriers in multiply charged centers in semiconductors is considered. The physical meaning of the introduced coefficients is discussed for the case where several excited states correspond to a given charged state of the trap and an expression for the lifetime of the minority carriers is obtained. In the course of the theory, the assumption is made that the transition of a trap from one state to another, in which there is no change in the number of captured electrons, takes a considerably shorter time than the transition in which the charged state of the trap changes. Thus the Fermi quasi-level for the given charged trap state can be introduced, which permits the necessary simplifications.

12,462 CHARGE CARRIER RECOMBINATION IN n-TYPE SILICON IRRADIATED WITH γ-RAYS by G. N. Galkin and Shevedev Phys. Inst., Moscow); Soviet Phys.-Solid State, Vol. 3, pp. 462-463, Aug. 1961

The recombination properties of n-type Si grown by pulling from quartz crucibles and containing a quantity of oxygen are discussed. Samples were irradiated with γ-rays from a Co^{60} source. An acceptor type recombination level lying 0.16 ev below the conduction band was formed by the γ-rays. The temperature dependence and absolute values of the capture cross sections for electrons and holes were found for this level. The ratio of the capture sections is practically the same for irradiation with γ-rays and with fast electrons. It therefore appears that either type of radiation produces volume recombination in n-type Si at the same acceptor-type level.

12,463 THE DISTRIBUTION OF NONEQUILIBRIUM CARRIERS IN THE SURFACE LAYER OF A SPACE CHARGE SEMICONDUCTOR AT LARGE SURFACE POTENTIALS by Yu. A. Kurskii (Lebedev Phys. Inst., Moscow); Soviet Phys.-Solid State, Vol. 3, pp. 154-155, July 1961

The possible causes for deviations of the Maxwell-Boltzmann distribution function f_{MB} from thermodynamic equilibrium are analyzed. Two mechanisms are indicated: (1) the presence of a strong electric field near the surface; (2) the generation and recombination of excess carriers. The order of magnitude of the deviation due to a strong electric field as well as to illumination is estimated. From the analysis, it is concluded that the deviations from the equilibrium distribution function are so small that they cannot be detected in the customary experiments from the change in the velocity of surface recombination.

12,464 THE EFFECTIVE MASS OF HOLES IN BISMUTH by G. E. Smith (Bell Labs.); J. Phys. Chem. Solids, Vol. 20, pp. 168-169 (L), June 1961

Past data is reinterpreted using a six ellipsoid model for the hole band to determine the Fermi energy (E_F) and the effective mass (m_h) parameters of holes in bismuth. Using Phillips' value of specific heat, $\gamma = 2.1 \times 10^{-5}$ joule/mole deg^2, the effective mass is calculated to be $m_h = 0.18\ m_0$. Using the anomalous skin effect data, $m_h = 0.17\ m_0$. Using cyclotron resonance data, $E_h = 4.6 \times 10^{-3}$ ev. Brandt's measurements of the de Haas-van Alphen effect at 0.07°K shows $m_h = 0.12\ m_0$; however there exists a factor of four discrepancy in the Fermi energy. This can be explained by postulating the existence of two hole bands.

12,465 ELECTRON MOBILITY IN INDIUM ARSENIDE by R. P. Chasmar (Assoc. Elect. Ind. Res. Labs.); J. Phys. Chem. Solids, Vol. 20, pp. 164-166 (L), June 1961

Results confirming the analytical observation that few acceptor type impurities exist in InAs are presented. The room temperature electron mobility ranges from 22 to 25×10^3 cm^2/volt-sec with a wider spread at 77°K. The room temperature value is in excellent agreement with theoretical calculations obtained by considering polar scattering to be the prime mechanism in limiting the rate of electron transport. Theoretical estimates of the temperature dependence of mobility using 0.03 for the effective electron mass ratio (m^*/m) show fair agreement with empirical data.

12,466 GALVANOMAGNETIC PROPERTIES OF CARRIERS ASSOCIATED WITH THE CLEANED GERMANIUM SURFACE by R. A. Missman, Jr. (U. Illinois); U.S. Gov. Res. Rep., Vol. 36, p. 95 (A), Aug. 20, 1961 AD 258 093

Measurements of the galvanomagnetic properties of the carriers

associated with the clean Ge surface are discussed. The carriers associated with the (100) surface have a p-type Hall contribution from 90° to 300°K. The mobility of these carriers ranges between 500 and 1200 cm^2/v-sec and for a given specimen remains constant over this temperature range. The number of these carriers is about $10^{12}/cm^2$ and is essentially constant with temperature indicating that they are degenerate. There is no evidence for the presence of n-type carriers but their presence cannot be definitely ruled out. If they are present on the (100) surface, their mobility is much smaller than that of the holes. The energy bands appear to be bent upward such that the valence band crosses the Fermi level at the surface. The bending is caused by the presence of relatively immobile electrons distributed randomly over the surface with a density of 1/1000 surface atoms. The same number of holes moves near the surface in the Coulomb fields of these electrons and gives most of the surface conductance. One specimen having a (111) surface was measured and the results showed that there may be both positive and negative carriers with high mobilities present at the surface.

12,467 GALVANOMAGNETIC EFFECTS IN Bi_2Te_3 WITH ANISOTROPIC SCATTERING by I. Ya. Korenblit (Inst. Semicon., Acad. Sci., USSR); Soviet Phys.-Solid State, Vol. 2, pp. 2738-2746, June 1961

The kinetics of scattering in Bi_2Te_3 and the galvanomagnetic coefficients based on the scattering mechanism are derived. The collision term for scattering is obtained in the case where scattering is described by a relaxation time tensor whose components do not depend on the direction of the electron wave vector. By neglecting intervalley transitions, the kinetic equation is solved by the method of successive approximations for weak electric and magnetic films.

12,468 ELECTRON TRANSPORT IN A SEMICONDUCTOR by H. L. Frisch (Bell Labs.) and J. L. Lebowitz (Yeshiva U.); U.S. Gov. Res. Rep., Vol. 36, p. S-57(A), Aug. 20, 1961 PB 155 287

The linear transport properties of electrons in a solid when both phonon and impurity scattering are important are investigated. The problem is treated for the case where Maxwellian statistics apply and the electrons are described by a classical distribution function in position and velocity, $f(r,v)$, satisfying a space dependent equation in which the phonon scattering only is described by a linear Boltzmann type collision term. This equation is solved formally in the presence of a weak external electric field in a form convenient for perturbation expansions in the relative strength of the different scattering mechanisms, some of which are carried out explicitly. When the kernel describing collision with phonons is randomizing, the change in mobility due to the presence of impurities is always negative.

12,469 EVALUATION OF THE ROLE OF MULTIPHONONIC PROCESSES IN THE SCATTERING OF CONDUCTION ELECTRONS IN ATOMIC CRYSTALS by A. I. Ansel'm and I. G. Lang (Polytech. Inst., Leningrad); Soviet Phys.-Solid State, Vol. 3, pp. 223-225(L), July 1961

The contribution of two-phonon processes to the scattering of conduction electrons in atomic crystals for temperatures higher than the Debye temperature is discussed. The density matrix method which takes account of interband transitions of electrons in the intermediate state was used in the study. Transitions in which the number of electron bands changed are not considered. The conditions and criterion necessary to account for the contributions of the two-phonon and multi-phonon processes are derived.

12,470 TRANSITION TO THE HIGH FIELD LIMIT IN THE ZEEMAN SPECTRA OF GERMANIUM DONORS by W. S. Boyle (Bell Labs.) and R. E. Howard (Carnegie Inst. Tech.); J. Phys. Chem. Solids, Vol. 19, pp. 181-188, May 1961

An experimental and theoretical study of the connection between the low field Zeeman spectra and high field photoionization spectrum of donor impurities in Ge is presented. It is shown that at high fields the absorption maxima that occur in the photoionization spectrum correspond to transitions to Landau levels which are bound by a coulomb force to the parent donor impurity. As the magnetic field is decreased some of the lines in the photoionization spectrum remain sharp and pass into Zeeman lines while others have no small field counterpart. These are metastable and become increasingly diffuse with decreasing field.

CONDUCTIVITY (RESISTIVITY)

12,471 THE ELECTRICAL CONDUCTION MECHANISM IN ULTRA-THIN, EVAPORATED METAL FILMS by C. A. Neugebauer and M. B. Webb (GE); U.S. Gov. Res. Rep., Vol. 36, p. 83(A), Aug. 5, 1961 AD 257 421

The electrical conduction mechanism in the film plane of ultrathin, evaporated metal films is discussed. These films consist of a planar array of many small discrete islands. The conduction process consits of, (1) charge carrier creation which is thermally activated and involves charge transfer between initially neutral particles, and (2) the drift velocity of these charges in an applied field. Charge transfer between particles occurs by tunneling. The following features are predicted and can be verified experimentally: (1) the conductivity depends exponentially on reciprocal temperature, and it should be independent of field at low fields; (2) deviations from the exponential temperature dependence can be understood in terms of a spectrum of activation energies, while deviations from Ohm's law at high fields can be explained readily in terms of a field dependent activation energy.

12,472 NOTE ON FOUR-POINT RESISTIVITY MEASUREMENTS ON ANISOTROPIC CONDUCTORS by J. D. Wassch (Philips); Philips Res. Rep., Vol. 16, pp. 301-306, Aug. 19

A method for calculating the voltage difference across two probes when a current is passed through two other probes, the four probes being in a square or colinear arrangement on an anisotropic conductor, is described. The Van der Pauw transformation for isotropic media is used. Thick and thin samples (compared to the probe distances) are considered. The square arrangement is appreciably more sensitive to anisotropies than the colinear arrangement. The three principal values of a resistivity tensor can also be calculated from measurements on only the plane perpendicular to a direction corresponding to one of these principal values. The use of conditions for finite dimensions already calculated for isotropic conductors is discussed.

12,473 CONCERNING THE EFFECT OF CURRENT ELECTRODES ON THE RESISTIVITY CHANGE IN A MAGNETIC FIELD by Yu. I. Gorkun (Phys. Inst., Kiev); Soviet Phys.-Solid State, Vol. 3, pp. 173-177, July 1961

he dependence of the resistivity change in a magnetic field n the geometrical size of a specimen and the arrangement of robes is discussed, taking into account the short-circuiting ffect of current electrodes. A brief review of the previous esults and a theoretical explanation of the problem are given. he potentiometric probe method is used to eliminate errors ssociated with the rectifying properties of current contacts. theory is developed to solve this problem without resorting to onformal transformations, and the probe method is considered o find out whether or not distortions are produced during the easurement of $\Delta\rho_H$. The specimen form is that of a right ngle parallelepiped, and the analysis of the expressions ob- ained shows that the probe arrangement and the specimen's eometry have to be chosen with care. However, no qualita- ive comparison was made due to the lack of data on the eometry of specimens and probe arrangement used in the easurements mentioned in previous literature.

ffects of Annealing on the Resistivity of InSb - See 12,499

2,474 THEORY OF Al-Zn ALLOY RESISTIVITY DURING RE-PRECIPITATION by M. Asdente (Lab. CISE and Inst. is. del Politec., Milan); Acta Metal., Vol. 9, pp. 587-89, June 1961

he electrical resistivity of Guinier-Preston zones in Al-Zn is alculated as a function of zone radius for three different Zn oncentrations within the zone. The problem is solved in the ree electron approximation by the partial wave method. The esistivity per Zn atom was found to decrease continuously for one radii from about 2A to 25A. The usual hypotheses of one formation and growth are therefore insufficient to explain he experimentally observed resistivity maximum. The present alculations indicate that a slightly different hypothesis of the arly stages of zone growth will yield a resistivity maximum.

2,475 RESISTIVITY CHANGES DUE TO FORMATION OF . P. ZONES (CLUSTERS RICH IN SOLUTE) by H. Herman nd J. B. Cohen (Northwestern U.); Nature, Vol. 191, pp. 5-64(L), July 1, 1961

n anomalous increase in resistivity has been observed during e formation of Guinier-Preston zones in several Al alloys. n theoretical grounds a maximum should occur for resistivity ange during zone formation. The research reported sought determine whether a zone of definite size is associated with 's maximum during aging. An alloy of Al-5.3 atomic per ent Zn was studied using both resistance measurements and mall-angle scattering. It was found that the resistance maxi- a were associated with zones of average size 10 A in diam. his compares favorably with the 7 A predicted by theory. The esults, therefore, confirm the relation between resistance aximum and zone size.

esistance Anomalies in Fe-Al Solid Solutions - See 12,249

2,476 THE TEMPERATURE DEPENDENCE OF THE CONDUC- IVITY OF LEAD SULFIDE LAYERS AT 10^{10} CPS by V. G. bfeichev and L. N. Kurbatov; Soviet Phys.-Solid State, ol. 3, pp. 436-438, Aug. 1961

n examination at 10^{10} cps of the temperature dependence of e electrical conductivity of photosensitive PbS layers pre- red by vacuum deposition and subsequent activation is ported. The measurement methods employed are much the me as those used in an earlier paper of the authors. Meas- urements were carried out on seven layers. The conductivity of these layers in the microwave region was found to depend much less on temperature than the dc conductivity. The microwave permittivity was practically independent of temperature. On the basis of previous work, an expression for the temperature coefficient of microwave conductivity is obtained in terms of the conductivities of the high resistance regions and of the grains, and of the permittivity of the semiconductor layer and the microwave wavelength. These theoretical values agree with the experimental conclusions.

12,477 DEVIATIONS FROM MATTHIESSEN'S RULE FOR PLATINUM by P. G. Klemens and G. C. Lowenthal (CSIRO); Austl. J. Phys., Vol. 14, pp. 352-358, Sept. 1961

The resistivity-temperature relationships (to liquid He temperatures) of 17 Pt resistors are analyzed. The analysis shows that deviations from Matthiessen's rule can be classed roughly into three groups. One of them follows the pattern predicted by Sondheimer and Wilson's theory. The other two cannot be fully explained in this way, and may be due to the sensitivity of the electronic band structure of transition metals to small concentrations of impurities. The behavior of a resistor thus depends on the nature as well as the total amount of impurities and imperfections. In low temperature Pt resistance thermometry the resistors should be selected with regard to the type of residual impurity as well as total impurity content.

12,478 ELECTRICAL CONDUCTIVITY OF GERMANIUM WITH LITHIUM IMPURITY AT LOW TEMPERATURES by I. A. Kurova and N. D. Tyapkina (Phys. Inst., Moscow U.); Soviet Phys.-Solid State, Vol. 2, pp. 2761-2764, June 1961

Measurements of specific resistance and Hall constant as a function of temperature for Li-doped Ge are reported. Samples with Li concentrations ranging from 2.3×10^{14} to 2.9×10^{15} atoms/cm^3 were used in the experiments. Anomalies in the specific resistance vs inverse temperature and the Hall constant vs inverse temperature characteristics were observed for the higher doped samples; samples having 2.3 and 3.9×10^{14} atoms/cm^3 concentrations followed the regular exponential law.

12,479 THERMAL EFFECTS IN THE STUDY OF THE ELECTRICAL CONDUCTIVITY OF GERMANIUM IN LIQUID HELIUM by E. I. Zavaritskaya (Lebedev Phys. Inst., Moscow); Soviet Phys.-Solid State, Vol. 2, pp. 2673-2675, June 1961

Measurements of the I-V characteristics of various Ge specimens at liquid He temperatures are reported. A rapid increase in current that takes place at $V = V_{br}$ (low temperature breakdown point) may be non-reversible. It is concluded that the irreversible branch of the I-V curve is associated with an abrupt temperature change caused by a disturbance in the thermal contact between the specimen and the He bath.

12,480 ELECTRICAL CONDUCTIVITY AND THERMODYNAMIC EQUILIBRIUM IN NICKEL OXIDE by S. P. Mitoff (GE); J. Chem. Phys., Vol. 35, pp. 882-889, Sept. 1961

Electrical conductivity of nickel oxide measured at temperatures between 600° and 1350°C and partial pressures of oxygen between 1 and 10^{-4} atm is reported. The slope of log conductivity vs reciprocal temperature plot increases for high temperatures. The temperature at which the change in slope occurs is dependent on the rate of heating or cooling of the crystal. Nickel oxide is a p-type semiconductor in which the conductivity is proportional to the concentration of Ni^{3+} ions in the lattice. The analysis of the conduction mechanism and the

conduction data may be self-consistently correlated with nickel diffusion, nickel vacancy diffusion, and weight changes resulting from equilibration with different oxygen partial pressures. The following constants may be determined from these correlations: heat of formation of nickel vacancies, activation energy for nickel vacancy migration, activation energy for electron hole migration, and concentrations of nickel vacancies and Ni^{+3} ions as a function of temperature and oxygen pressure. Combined results give the following for the concentration of nickel vacancies: $0.11\ (P_{O_2})^{1/6}\ \exp(-17\,800/RT)$ vacancies per ion pair.

Temperature Dependence of Conductivity of Rutile - See 12,606

12,481 ELECTRICAL PROPERTIES OF TlSe by R. Mori (Oki Elect. Ind.) and K. Hashimoto (Hyusyu U.); J. Phys. Soc. Japan, Vol. 16, pp. 1797-1798(L), Sept. 1961

Measurements of the electrical resistivity and Hall coefficient of TlSe single crystals between 100° and 450°K are reported. The Hall coefficients of all the samples were found to be positive. The Hall coefficient and resistivity exhibited temperature dependences characteristic of semiconductors. Anomalous peaks in the Hall coefficient, however, were observed in some samples at about 250°K. It was found that TlSe exhibits at least two activation energies, about 0.6 ev and 1.3 ev.

12,482 SEMICONDUCTING PROPERTIES OF $SnSe_2$ AND $GeSe_2$ by S. Asanabe (Nippon Elect.); J. Phys. Soc. Japan, Vol. 16, p. 1789(L), Sept. 1961

Electrical and optical measurements made on the compounds $SnSe_2$ and $GeSe_2$ are given. Resistivity and Hall coefficient measurements were made on $SnSe_2$ in the temperature range 100° to 800°K. Both the resistivity and Hall coefficient were found to fall abruptly at about 700°K, as is characteristic in ordinary semiconductors. From the temperature dependence of the resistivity in this temperature range, the energy gap is estimated to be about 1.0 ev. Irreversible changes were observed for the resistivity and Hall coefficient measurements made on crystals quenched from 430°C. The changes are attributed to variations in carrier concentrations. From high temperature resistivity measurements in $GeSe_2$, the energy gap was estimated to be 2.3 ev. This agrees with the value of 2.35 ev determined from optical absorption measurements at room temperature.

12,483 THE ELECTRICAL RESISTIVITY OF Mn_3ZnC BETWEEN 4.2° AND 630°K by M. L. Swanson (Atomic Energy of Canada) and S. A. Friedberg (U. Toronto); Can. J. Phys., Vol. 39, pp. 1429-1432, Oct. 1961; U.S. Gov. Res. Rep., Vol. 36, p. 81(A), Aug. 5, 1961 AD 257 317

Measurements of the electrical resistivity of an alloy having approximately the composition Mn_3ZnC between 4.2° and 630°K are reported. From a high residual value, the resistivity increases with temperature in a complicated way up to 550°K, becoming temperature independent above that point. Two anomalous regions are evident, corresponding to the magnetic transitions occurring in this substance at ~240° and ~450°K. The general features of the results are interpreted on the basis of a spin-disorder scattering picture.

12,484 BASIC AND APPLIED RESEARCH ON SEMICONDUCTORS by E. K. Weise (Illinois U.); U.S. Gov. Res. Rep., Vol. 36, p. S-55(A), Aug. 20, 1961 PB 155 529

Measurements of the electrical conductivity of Mg-, Ca-, Sr-, and Ba-titanates as functions of composition and temperature are given. A weighing method was used for the measurement of donor concentration. Its sensitivity was determined by the available analytical balance and in order to overcome this limitation an independent magnetic method was tried; this method seemed to lead to a sensitivity higher than with the weighing method by one to two orders of magnitude.

12,485 ON THE ELECTRICAL CONDUCTIVITY OF Mn-Zn FERRITES by K. Záveta (Czech. Acad. Sci., Prague); Czech. J. Phys., No. 5, Vol. 11B, pp. 376-378(L), 1961

The temperature dependence of the resistivity of Mn-Zn ferrite is plotted as $\log \rho = f(1/T)$. Certain anomalies appeared in the vicinity of the Curie point in some cases; in others, the plot remained linear over the entire range of temperatures. The temperature range included the respective Curie points and terminated some 10°C above. The anomaly could be described either as a break of the linear plot $\log \rho(1/T)$, i.e., as a change in the activation energy ε from the formula $\rho = \rho_0 \exp(\varepsilon/kT)$, or sometimes as a parallel shift of this linear plot without any change of ε. An analysis of test results shows that the anomalies were present in samples having lowest ρ_0 while high ρ_0 gave smooth dependences.

12,486 THE ELECTRICAL CONDUCTIVITY OF COBALT-MANGANESE SPINELS WITH ADMIXTURES OF LITHIUM, TITANIUM AND COPPER OXIDES by M. Ya. Kushnerev, V. R. Linde and S. Z. Roginskii (Inst. Phys. Chem.); Soviet Phys.-Solid State, Vol. 3, pp. 281-287, Aug. 1961

The structure transformations and temperature dependence of the electrical conductivity of normal ($CoMn_2O_4$) and inverse ($MnCo_2O_4$) cobalt-manganese spinels are discussed. Studies were made as a function of the amount of Li, Ti and Cu admixtures. Powdered spinels with the admixtures were made and diffraction patterns were obtained with a Debye camera. The powders were ground into tablets and wire probes were inserted and used to measure resistance in the temperature range 100° - 600°C. A sample was placed in a quartz cell, argon was introduced, and measurements were made after the establishment of constant temperature and resistance. The resistances were used to establish a detailed mechanism of conduction for the spinels considered. The mechanism was found to be different from that proposed by Verwey. The experiment show that the valence state and nature of the cations, rather than the crystal structure, govern the electrical properties of spinels.

12,487 ELECTRICAL CONDUCTIVITY OF SYNTHETIC CRYSTALLINE ZEOLITES by D. C. Freeman, Jr. and D. N. Stamires (Linde Co.); J. Chem. Phys., Vol. 35, pp. 799-806, Sept. 1961

Measurements of the electrical conductivity of anhydrous Linde zeolite types A, X, and Y in various cationic forms between 20° and 400°C are reported. The conductivity is ohmic, essentially noncapacitive, and appears to be strictly ionic with unusually low activation energy. From the effect of zeolite channel size, type of cation and cation density on ΔH, ΔG, and ΔS for the conduction process, some conclusions as to the zeolite internal structure and surface energy have been obtained. The heterogeneity of the internal surface energy

ound by the measurement of adsorption heats is discussed in
e light of these conclusions.

2,488 INVESTIGATION OF THE ELECTRICAL CONDUCIVITY OF RUBIDIUM BORON GLASSES by B. I. Markin; oviet Phys.-Solid State, Vol. 3, pp. 328-331, Aug. 1961

he electrical conductivity of rubidium boron glasses of varius compositions is discussed. Measurements were compared ith those for other boron alkali glass systems. Samples were repared from triply recrystallized boric acid and "pure" grade ubidium nitrate. The compositions of two of the samples from given melt were analyzed and their density was calculated. lectrical conductivity measurements were made with an elecometer using rubidium amalgum electrodes. It was found that he conductivity of the glasses rises by a factor of about 100 n increase of the atomic concentration of rubidium to 0.006 -atom/ml. Increasing the concentration by a factor of 3 ises conductivity by a factor of $\sim 10^6$. The equivalent elecical conductivity of the glasses also exhibits minima in its omposition dependence. These are shifted towards higher ubidium concentrations with temperature increase. In general quivalent conductivity minima of two-component boron lkali glass systems exhibit similar behavior on increase of the obile cation radius.

onductivity of Evaporated Anthracene Films - See 12,579

2,489 CARRIER BEHAVIOR IN NICKEL-DOPED POLYMER ARBONS by H. A. Pohl and J. P. Laherrere (Princeton U.); .S. Gov. Res. Rep., Vol. 36, p. S-58(A), Aug. 5, 1961 3 156 278

he conductivity and Hall coefficients of a series of variously eat-treated and Ni-doped polymer carbons prepared from eriously loaded ion exchange resins by pyrolysis are discussed. is observed that the Hall mobility increases with impurity ddition in these condensed molecular solids. A theoretical terpretation of the conduction in such inhomogeneous molecr solids is suggested. An alternate interpretation based upon barrier layer model is also considered.

:,490 SEMI-CONDUCTION IN NICKEL-DOPED POLYMER RBONS by H. A. Pohl and J. J. Hoglen (Princeton U.); S. Gov. Res. Rep., Vol. 36, p. S-58(A), Aug. 5, 1961 156 279

tudy of the preparation and the electrical character of semiductors made of Ni-doped polymer carbon is presented. ese materials were made from variously Ni-loaded ion exange resins which were then pyrolyzed to temperatures rangg from 700° to 1200°C and in yields of about 13 per cent, sed on dry resin. The electrical conductivity and its temperure coefficient and the Hall coefficient were studied, and e pyrolysis and conduction mechanism were examined. Nickel ntents up to 12 atomic per cent were studied.

SUPERCONDUCTIVITY

,491 LIFETIME EFFECTS IN CONDENSED FERMION SYSMS by A. Bardasis and J. R. Schrieffer (U. Illinois); Phys. . Lett., Vol. 7, pp. 79-81 (L), Aug. 1, 1961

e importance of lifetime effects in the superconducting state for obtaining the excitation spectrum of a system is discussed. A Green's function theory of superconductivity including finite-lifetime effects for a particular type of damping is formulated and compared with Bardeen, Cooper and Schrieffer's theory for three different cases. It is shown that for He^3, damping effects are important in determining the energy gap and transition temperature to a possible superfluid state.

12,492 SUPERCONDUCTIVITY IN THE NEIGHBORHOOD OF METALLIC CONTACTS by L. N. Cooper (Brown U.); Phys. Rev. Lett., Vol. 6, pp. 689-690 (L), June 15, 1961

A simple microscopic theory of superconductivity in metal-to-metal contact neighborhoods, based on a modification of the parameter $[N(0)V]$ which occurs in the Bardeen-Cooper-Schrieffer expression for the energy gap, $\epsilon_0 = 2(\hbar w)_{av} \exp[-1/N(0)V]$, is developed. Due to electron-electron interaction there is a nonzero matrix element $V_{k'k}$ for scattering from a two-electron state labelled by k to one labelled by k'. This matrix element, summed over all k in the interaction region, yields $[N(0)V]_{av}$ which determines the energy gap and the transition temperature. This average will be decreased if the electron normalization volume is increased while the electron-electron interaction acts over only a part of the volume. This should result in a decrease of the transition temperature of a superconductor in contact with a normal metal. The refraction-producing, differing Fermi momenta in the two metals must be considered, as well as the usually formed chemisorbed oxygen layer between the two metals which creates a potential barrier of several tenths ev for a distance of several angstroms.

12,493 EFFECTS OF PLASTIC DEFORMATION ON SUPERCONDUCTIVE PROPERTIES OF METALS by B. Serin (Rutgers U.); U.S. Gov. Res. Rep., Vol. 36, p. 80(A), Aug. 5, 1961 AD 257 195

An investigation of the effects of dislocations on the superconductive transition temperature of Al is reported. The dislocations were generated in the specimens by cold work, fatigue and tensile stress. Isochronal annealing studies were made of cold rolled Al specimens. Results show that the changes in transition temperature (T_c) and residual resistance produced by deformation are small between 0° and 200°C, partially anneal out rapidly in the 200° to 300°C range and anneal to completion more slowly in the 300° to 600°C range. This result makes it unambiguously clear that the effects can be ascribed only to dislocations. Preliminary measurements on specimens deformed by fatigue have indicated that the transition temperature may be increased slightly. Specimens deformed in tension by 1 and 2 per cent showed no change in T_c.

12,494 SOME THERMAL AND MAGNETIC PROPERTIES OF TANTALUM, NIOBIUM AND VANADIUM AT HELIUM TEMPERATURES by A. Calverley (Services Electronics Res. Lab.), K. Mendelssohn and P. M. Rowell (Clarendon Lab.); Cryogenics, Vol. 2, pp. 26-33, Sept. 1961

Measurements of thermal conductivity and of critical field (field at which superconductivity is destroyed) are reported graphically for Ta, Nb, and V. The preparation and purity of the specimens and the measuring techniques employed are briefly discussed. Measurements of thermal conductivity of superconductors in the normal and superconducting state can be used to indicate the chemical purity and the physical state of the lattice of a metal crystal. The method has recently been applied to the effects of radiation damage.

12,495 SUPERCONDUCTING VANADIUM THIN FILMS by C. T. Thompson and J. F. Gerber (Burroughs); Solid State Electronics, Vol. 2, pp. 259-260(L), May 1961

Superconducting vanadium thin films are discussed. The different results in the resistance versus temperature behavior of two specimens studied has been explained as due to a different content of gaseous impurity.

12,496 SUPERCONDUCTIVITY AT HIGH MAGNETIC FIELD AND CURRENT DENSITIES IN SOME Nb-Zr ALLOYS by T. G. Berlincourt, R. R. Hake and D. H. Leslie (NA Aviation); Phys. Rev. Lett., Vol. 6, pp. 671-674(L), June 15, 1961

Experiments showing that cold-worked Nb-rich Nb-Zr alloys display zero electrical resistance at current densities as high as 10^5 amp/cm^2 at 30 kgauss and at 4.2°K are reported. The measurements reveal the following high-field superconducting effects in these alloys: (1) a marked dependence of the magnitude of the maximum zero-resistance current upon the direction of the externally applied magnetic field relative to the rolled surface of the specimen, and (2) an anomalous increase of the maximum zero-resistance current with increase of magnetic field strength over certain field regions in certain alloy specimens. Micrographic examination of the various source material indicated that all the samples were predominantly bcc. The "critical current density," J_c, is defined; it was found to depend markedly upon the direction of the transverse magnetic field relative to the rolled face of the specimen. The observation of large high-field critical currents in flexible Nb-25 atomic per cent wire suggests the use of such wire for superconducting solenoids possibly well in excess of 30 kgauss.

Specific Heat of Ti-Mo Superconductors - See 12,597

Superconducting Magnets - See 12,731

Frequency Mixing with Superconducting Elements - See 12,732

BREAKDOWN

12,497 BREAKDOWN IN NONPOLAR SEMICONDUCTORS by H. Frohlich; Soviet Phys.-Solid State, Vol. 3, pp. 491-492(L), Aug. 1961

An objection is raised to an assertion of Gordeev (See abstract 7315) that a theory of breakdown in nonpolar substances formulated by the author (Proc. Phys. Soc., Vol. B69, p. 21, 1956) contained an error. Gordeev's assumption that the electron mean free path is independent of the electron energy even at breakdown is questioned. It is stated that the electron mean free path rises with increases in electron energy in this energy region.

Thermal dc Breakdown in Dielectrics - See 12,447

MAGNETOELECTRIC (GALVANOMAGNETIC) PROPERTIES

12,498 A DEVICE FOR INVESTIGATING THE MAGNETOELECTRIC EFFECTS UNDER HYDROSTATIC PRESSURE by A. A. Averkin and V. N. Bogolomov (Acad. Sci., USSR); Soviet Phys.-Solid State, Vol. 3, pp. 460-461, Aug. 1961

A device for investigating the influence of hydrostatic pressure on magnetoelectric effects is described. A magnetic field is produced inside a pressure cell which is made of a ferromagnetic material. (This contrasts with the usual nonferromagnetic cells.) The cell avoids cumbersome external magnetic systems and allows the use of alternating magnetic fields with the advantages of greater convenience and sensitivity.

12,499 THE EFFECT OF ANNEALING ON THE ELECTRICAL AND MAGNETOELECTRIC PROPERTIES OF INDIUM ANTIMONIDE by V. E. Il'in and I. E. Gorbacheva (S. I. Vavilov State Opt. Inst.); Soviet Phys.-Solid State, Vol. 3, pp. 392-399, Aug. 1961

A study of the effects of annealing on the electrical and magnetoelectric properties of n- and p-type polycrystalline InSb is discussed. The sample was heated to a selected temperature between 300° and 500°C, was kept at this temperature for 60 hrs and was then slowly cooled to room temperature. The samples were etched in SR-4 after annealing. Measurements were carried out using a compensation method and pressure contacts. Temperature dependence of the Hall constant R and the electrical conductivity σ were studied between 90° and 400°K. The dependence of R, σ and the magnetoresistance $\Delta\rho_H/\rho_0$ on the magnetic field intensity H were studied at room temperature and at the temperature of liquid oxygen. The effect of H on R (1/T), σ (1/T) and $\Delta\rho_H/\rho_0$ (1/T) was also investigated. The possible effects of annealing for long periods on crystals are considered. Resultant calculations of the activation energies agree fairly well with experimental values. The reasoning indicates that annealing of n-type InSb at about 500°C converts the material to p-type. Serious difficulties are met in the interpretation of some of the results obtained, however.

Galvanomagnetic:
- Effects in Bi_2Te_3 - See 12,467
- Properties of Carriers Associated with Clean Ge Surfaces - See 12,466

Temperature:
- Variation of the Hall Coefficient of Li-Doped Ge - See 12,478
- Dependence of the Hall Coefficients of $SnSe_2$ and $GeSe_2$ - See 12,482

Hall:
- Coefficient of TlSe - See 12,481
- Coefficients of Ni-Doped Polymer Carbons - See 12,489 and 12,490

OTHER ELECTRICAL PROPERTIES

12,500 ON THE THERMIONIC PROPERTIES OF ZrC, UC AND A ZrC·UC MIXTURE by W. E. Danforth and A. J. Williams, III (Franklin Inst.); J. Appl. Phys., Vol. 32, pp. 1181-1182(L), June 1961

Measurements taken with a guard-ring anode on specimens of fused ZrC and hot pressed $ZrCo_{0.8} \cdot UC_{0.2}$ after heating by electron bombardment are reported. Empirical Richardson constants were obtained. The values of A and ϕ for ZrC are in agreement with those of Pidd et al., but the latter's high values for ZrC·UC were not repeated. Explanations for those high values are briefly discussed.

OTHER ELECTRICAL PROPERTIES (Cont'd)

Work Function of CdTe and CdS - See 12,585

ot Electron Emission from Si Junctions Parallel to the Surface- ee 12,645

2,501 THE ROLE OF THE DIELECTRIC WHEN INVESTIGATING THE EFFECT OF FIELD IN SEMICONDUCTORS by V. E. rimachenko and O. V. Snitko (Acad. Sci. Phys. Inst., krSSR); Soviet Phys.-Solid State, Vol. 3, pp. 9-12, July 961

xperiments on the measurement of field effect and capacitor hoto-EMF, with and without mica, in a vacuum and in air f varying humidity, are reported. The study of the field effect, the influence of an electric field on the capacitor photo-MF and the relaxation of the field effect showed an absence f charge transfer from the semiconductor to the dielectric in vacuum in dry air up to fields of 10^5v/cm. However, to easure the field effect in moist atmosphere, the use of a roper time-variable external field is suggested.

2,502 DISTRIBUTION OF SPACE CHARGE IN HOMOGENEOUS METAL OXIDE FILMS by J. N. Butler (U. Brit. Columia); J. Chem. Phys., Vol. 35, pp. 636-643, Aug. 1961

oisson's equation for a homogeneous semiconducting oxide lm on a metal or semiconductor substrate is solved exactly. ne potential drop from the interior of the substrate to the exrnal surface of the oxide is given as a function of the thickss of the oxide, and the distribution of potential within the yer is described. The form of the functions is shown for an bitrary choice of constants. The potential drop across the ide film is calculated as a function of thickness for Cu_2O on at 1000°C.

nneling in Degenerate Junctions - See 12,640

MAGNETIC PROPERTIES

GENERAL

,503 A NEW MAGNETIC METHOD FOR MEASURING ABDLUTE MAGNETIC SUSCEPTIBILITIES by P. K. Ghosh (I. A. S., Jadavpur); Indian J. Phys., Vol. 44, pp. 319-320 (L), ne 1961

method of measuring magnetic susceptibilities, utilizing a rrent carrying coil that is placed in a magnetic field with its ment parallel to the field direction, is described. By plac- the sample inside the coil and adjusting the current in a irie balance type set-up, the moment of the coil may be ide equal and opposite to the moment induced in the sample d the system will experience no translatory force. An equain for the mass susceptibility of the sample is cited and the vantages of the method are listed.

,504 AN APPARATUS FOR THE MEASUREMENT OF MAGTIZATION IN DILUTE ALLOYS AT LOW TEMPERATURES O. S. Lutes and J. L. Schmit (Honeywell Res. Ctr.); U.S. v. Res. Rep., Vol. 36, p. S-48(A), Sept. 5, 1961 150 643

apparatus for measuring the magnetic moment of metallic mples under isothermal conditions at temperatures extending ow 1°K is described. The report covers He^3 refrigeration, magnetic measurement, and thermometry.

12,505 MINIATURE COILS FOR HIGH MAGNETIC FIELD RESEARCH by R. W. DeBlois (GE Res. Lab.); Rev. Sci. Instr., Vol. 32, pp. 816-818, July 1961

Millimeter-diameter coils which are supplied by energy storage units of only several joules capacity and which can produce pulsed magnetic fields greater than 100 koe and of microsecond duration are described. Demonstrative experiments which show the magnetic-state transitions of a 20-μg specimen of MnAs near 90 koe, the shift in transition temperature when the specimen and coil are subjected to hydrostatic pressures up to 850 atm, and the reversal of magnetization of a 0.5-μg iron cube from which all reverse nuclei were presumably driven are discussed.

12,506 INTERNAL MAGNETIC FIELD IN RARE EARTH METALS by J. Kondo (U. Tokyo); J. Phys. Soc. Japan, Vol. 16, pp. 1690-1691, Sept. 1961

The effective magnetic field at nuclei in the rare earth metals Pr, Nd, Tb, Dy, Ho, Er, Tm, and Yb are calculated. The contribution from the orbital angular momentum of 4 f electrons was found to amount to several thousand koe.

Analysis of Inverse Magnetostriction - See 12,738

FERRO- AND FERRIMAGNETISM

12,507 MAGNETISM IN TRANSITION METAL ALLOYS by W. M. Lomer (Atomic Energy Res. Estab.); Brit. J. Appl. Phys., Vol. 12, pp. 535-536, Oct. 1961

The magnetic behavior of transition metal alloys is discussed. The validity of the idea of a local atomic spin is emphasized and it is pointed out that the collapse of this model is associated with the lifetimes of the spins. When the lifetime becomes very short, the model is entirely inappropriate. It appears, however, to apply to the metals Cr, Mn, Fe, Co, Ni, and to their alloys with many simple metals.

12,508 GROUND STATE OF AN ISING FACE-CENTERED CUBIC LATTICE by A. Danielian (King's Coll., London); Phys. Rev. Lett., Vol. 6, pp. 670-671 (L), June 15, 1961

By simple topological and energy arguments a complete classification of the ground-state configurations of fcc magnetic structure antiferromagnetic compounds is derived. Exact thermodynamic results at T = 0°K are deduced. Assuming only nearest neighbor interaction and +, -spin states, it is shown that every tetrahedron in the lattice must be in the same ground state w. Considering the fcc lattice as built up of layers of triangular lattices, it is proved that the ground configurational state of the whole fcc system is determined by the ground configurational state of any one of its triangular layers. Because each tetrahedron ground state must be w, it follows that there are only four basic types of clusters, each having central spin with its twelve nearest neighbors. It is concluded that the degeneracy of the ground state of the fcc system is $\exp(AN^{1/3}\ln 2)$, and that in the limit $N = \infty$ the entropy per spin tends to zero as $T \to 0$°K. Since all triangular layers have identical configurations and all possible configurations have zero moment, it follows that the susceptibility is zero at T = 0°K.

12,509 SOLUTIONS TO THE TWO DIMENSIONAL SPIN WAVE HAMILTONIAN by D. I. Paul (U. California, Los

Angeles); U.S. Gov. Res. Rep., Vol. 36, p. 88(A), Aug. 5, 1961 AD 257 569

Some exact solutions for the Dirac spin wave Hamiltonian of a two dimensional periodic rectangular array of N atoms are derived. Each atom in its isolated state is considered to have an outer electron which is in an s state, all other electrons being in closed shells. It is shown that if the number of spin waves is not greater than the number of atoms in either of the two lattice directions, exact solutions exist in which the spin waves are independent of one another except to the extent that they obey the Pauli exclusion principle. Thus, the energy eigenvalues for these particular solutions are rigorously additive and are the same as those obtained by Bloch although the number of allowed eigenstates is more restricted.

12,510 SHEAR-COMPENSATED HYSTERESIGRAPH FOR THIN MAGNETIC FILMS by M. J. Schindler (RCA); Rev. Sci. Instr., Vol. 32, pp. 862-864(L), July 1961

Accurate determination of intrinsic material characteristics from 3/4 in diam plated disks (made possible by the addition of a shear-compensating circuit to a hysteresigraph) is discussed, and the circuit diagram and its functioning are shown. By adjusting a compensating resistor, full compensation can be reached. This system is most applicable where a large number of measurements have to be made on samples of identical size and shape, but is hardly applicable for thin films which are attached to rather thick substrates.

12,511 THE IRREVERSIBLE CHANGE OF MAGNETIZATION PRODUCED IN A 'SQUARE LOOP' FERRITE BY PULSED MAGNETIC FIELDS by J. E. Knowles (Mullard Res. Labs.); Proc. Phys. Soc., Vol. 77, pp. 576-586, Mar. 1961

An examination of a core of square loop ferrite under pulse magnetization conditions is discussed. Starting from remanence the irreversible change of magnetization produced by a series of very short pulses was measured by a ballistic galvanometer method. The results are interpreted on the basis of a domain wall model, which enables an estimate to be made of the ratio of the time spent by the walls in reversible motion to the time spent in irreversible motion. From this ratio the average number of times that the domain wall energy passes through a maximum during the course of a magnetization reversal is derived. The result, twenty five, agrees well with that obtained by an independent method due to Néel.

12,512 LOCKED ROTATION IN THIN FERROMAGNETIC FILMS [in German] by E. Feldkeller (Siemens-Halske); Elektron. Rechenanl., Vol. 3, pp. 167-175, Aug. 1961

The processes of magnetization of thin anisotropic magnetic films are described. If the magnetization of anisotropic thin films is reversed by rotation, different processes may build up Néel walls, dividing the films into narrow domains. Rotation in the domains is locked by stray fields of the Néel walls. Thus the hysteresis loops which could not be derived from the single domain theory can now be understood. Creation and motion of Bloch lines in the Néel walls counteract the forces that produce the locked state, allowing a complete reversal of the magnetization. All of these processes are shown in electron micrographs. It is assumed that the long switching times of incoherent rotation are also based on the stray fields of Néel walls.

12,513 STUDY OF THE MAGNETIZATION OF THIN, EVAPORATED NICKEL FILMS IN A CHANGING ENVIRONMENT by C. A. Neugebauer (GE); U.S. Gov. Res. Rep., Vol. 36, p. 74(A), Sept. 5, 1961 AD 258 376

Measurements of the magnetization of Ni films in the thickness range from a few to several hundred angstroms, first under ultrahigh vacuum conditions and then after exposure to an O_2 or H_2 atmosphere at various pressures, are reported. Oxidation of the films to a depth of 10 to 15 A takes place in a short time even at oxygen pressures in the 10^{-8} mm range. Exposure to H_2 of initially clean films resulted only in reversible change of the transverse anisotropy constant. Unusually large increases in the transverse anisotropy of Ni films result when a Ni-vacuum interface is changed to a Ni-Cu interface.

12,514 THE EFFECT OF MAGNETIC ANISOTROPY IN COBALT FERROMAGNETIC THIN FILMS by A. Corciovei (Inst. Atom. Phys., Bucharest); J. Phys. Chem. Solids, Vol. 20, pp. 162-164(L), June 1961

A theoretical study of ferromagnetic thin films, taking into account an anisotropy term in the Hamiltonian, is presented. Results were obtained for the Curie temperature, T_c, using cobalt thin films a few monatomic layers thick. The Curie temperature as a function of thickness of the thin film is plotted for different values of the coefficient. The results predict that the Curie temperature must be lower for very thin films than for the bulk material and suggests the possibility that the degree of anisotropy may not be negligible.

12,515 THE SPIN-WAVE RESONANCE AND SATURATION MAGNETIZATION OF THIN COBALT FILMS by Z. Frait and M. Ondris (Czech. Acad. Sci.); Czech. J. Phys., Vol. 11B pp. 463-465(L), 1961

An investigation of the phenomenon of multiple resonance in thin Co films deposited on heated slides is reported. The magnetic field is in a direction normal to the film. The resonance spectrum looks simpler than for films deposited on unheated slides. The multiple resonance indicates the production of spin-wave resonance with an exchange constant approximately equal to 1.3×10^{-6} erg cm^{-1} (± 8 per cent). The result of the saturation magnetization, calculated from the resonance measurements, confirms the postulate that the resonance condition can be influenced by stress existing in the thin films.

12,516 DYNAMICS OF POWDERED FIGURES ON SINGLE CRYSTALS OF MAGNESIUM-MANGANOUS FERRITES by A. I. Drokin, V. D. Dylgerov and Yu. M. Zolotareva (Inst. Phy Siberian Sect.); Soviet Phys.-Solid State, Vol. 3, pp. 405-408, Aug. 1961

The behavior of domain structure in single crystals of magnesium-manganous ferrites which have a spontaneous octangular hysteresis loop is discussed. Crystal platelets were magnetized and the magnetization revised with the aid of a speci electromagnet. Powdered figures were observed and photographed at various stages. Two sets were obtained, one with the magnetization in the [011] direction and the other with the field perpendicular to it. On the basis of these results, the following conclusions were drawn: (1) In the case of magnetization along the [011] direction, no displacement of the boundary between the domains is observed. During the reversal of magnetization, rotation processes take place with preservation of domain structure. (2) In fields close to the value of the coercive force, the magnetization vectors undergo an abrupt turning. (3) In the case of magnetization perpendic

the [011] direction, boundary displacement processes are bserved, and also processes involving the rotation of the in-ensity of magnetization vector. (4) The mechanism of the eversal of magnetization process in ferrites with rectangular ysteresis loop differs from that in other metals in that the enesis and growth of nuclei with inverse magnetization are ot observed on changing field direction.

islocation-Domain Structure Interactions in Ferromagnets - ee 12,321

2,517 RESEARCH IN FERROMAGNETICS WITH APPLICA-IONS TO NEW STORAGE DEVICES by H. W. Fuller and D. Sullivan (LFE); U.S. Gov. Res. Rep., Vol. 36, pp. S-38-9(A), Aug. 5, 1961 PB 154 240

lethods of experimentally studying the interaction between agnetic domain walls in adjacent thin films are described. he interaction energy between two walls in adjacent films is alculated using a simplified model for a domain wall consist-g of a linear dipole. A calculation of the interaction be-veen one symmetrical and one asymmetrical wall is also made nd two important special cases are considered. The force nction h'f(u) describing the equilibrium positions of magneto-atically interacting domain walls is plotted for various cases unequal wall widths and adjacent film separations. Some pects of a technique for measuring the external fields of alls in thin films using powder patterns are discussed in light Kittel's calculation concerning particle collection. Ob-rvations of particle collection on walls in a film overcoated th a non-magnetic layer are described. The principle of a ll-stepping device that may yield a new class of two-film orage devices is described. The magnetostatic interaction tween a wall in one film and a parallel line imperfection in adjacent film is considered. The magnetization distribution striking spiral-wall configurations is deduced and a hypoth-is for the mechanism of their formation is advanced.

,518 FARADAY EFFECT ANOMALIES OCCURRING AT SONANCE IN THE 10,000 MEGAHERTZ BAND OF VARI-S FERRITES [in French] by M. C. Vigneron (Bordeaux U.); mptes Rendus, Vol. 253, pp. 251-253, July 10, 1961

Faraday effect in Ferroxcube 4D, Ni-Zn and Ni ferrite ndrical sticks has been studied in the 3 cm band with a rtz polarimeter. The effects are quite similar to the opti-Faraday effect in the absorption region of paramagnetic ions. The anomalies consist of a variation of the magnetic tatory power Θ and a coupled elliptic variation. Curves wing the variation of Θ vs gauss for specimens of the three rites having diameters of 3.9 mm, 2.9 mm and 2 mm present results in graphical form.

519 HIGHER APPROXIMATIONS IN THE THEORY OF ROMAGNETIC RESONANCE by S. V. Tyablikov and Pu rch'o (V. A. Steklov Math. Inst., Moscow); Soviet Phys.-id State, Vol. 3, pp. 102-104, July 1961

ethod of calculating the Kubo expansion based on the con-eration of many-timed temperature retarded Green functions iven. Commutation functions, rather than the many-timed en functions, are found more appropriate for constructing equations of the problem. There is a fair agreement of the ression obtained with the classical results.

12,520 SOME EXPERIMENTAL RESULTS ON RELAXATION PHENOMENA IN Mn-Zn FERRITES [in French] by A. Braginski, A. Marais and T. Merceron (Lab. Magn. Phys. Solide, Bellevue); Comptes Rendus, Vol. 253, pp. 239-241, July 10, 1961

Several magnetic relaxation phenomena observed in Fe-rich Mn-Zn ferrites in the range -200° to +250°C are reported. The results are compared with those of an earlier experiment on Fe-rich Ni-Zn ferrites. The specimens were heat-treated at 1250°C for four hours in a CO_2 atmosphere containing 0.5 per cent O_2 and were studied by means of breakdown of the initial permeability μ. The specimens showed increased oxidation and a greater number of gaps corresponding to higher Fe content. Graphs showing $\Delta\mu/\mu$ vs °C for the Ni-Zn and Mn-Zn systems are included. Both systems exhibit a maximum of the curve $\Delta\mu/\mu$ vs °C near −196°C, at a temperature decreasing with increasing Fe content. This relaxation is due to the electronic exchange $Fe^{2+} \rightleftharpoons Fe^{3+}$. A second relaxation occurring at room temperature is found to be independent of the Fe content, and is quite similar to the same phenomenon in Ni-Zn ferrites. At a temperature between 100° and 200°C a third relaxation phenomenon occurs. The maximum of the curve here increases sharply with increasing Fe content. A superposition effect at this temperature, due to an inobservable relaxation above the Curie point, is postulated.

12,521 ON PROPERTIES OF MIXED YTTRIUM-HOLMIUM GARNETS [in French] by A. Vassiliev, J. Nicolas and M. Hildebrandt (Genl. Teleg. Puteaux); Comptes Rendus, Vol. 253, pp. 242-244, July 10, 1961

Measurements of the magnetic saturation moments of garnets corresponding to the formula $3[(1-x)Y_2O_3, xH_2O_3] \cdot 5Fe_2O_3$ as a function of temperature are reported. Specimens for which $x = 0, 0.1, \ldots, 0.9, 1$, respectively, were prepared by heat treatment at 1350°C for three hours. The Curie points and the compensation points of these garnets are obtained from the curve $\mu\beta$ vs °K and are tabulated. The values of the effective gyromagnetic factor, the resonance linewidth measured at room temperature and 9535 Mc, and the precision of measurement are given in a second table.

Lognormal Distribution of Dielectric Relaxation Process - See 12,614

Ferrimagnetic Structure of Fe_7Se_8 - See 12,255

Magnetic Properties of a Modified Ni Ferrite - See 12,398

12,522 MAGNETIC ANISOTROPY OF HEUSLER SINGLE CRYSTAL by K. Aoyagi and M. Sugihara (Nippon Tel. and Tel.); J. Phys. Soc. Japan, Vol. 16, p. 1027(L), May 1961

Anisotropy measurements on a Cu_2MnAl single crystal ingot, performed in the temperature range between liquid nitrogen and 80°C after rapid cooling from 750°C, are reported. Measurements were also performed at liquid nitrogen and room temperature on the crystal subjected to 110°C heat exposure for 1000 hours. A magnetic field of 8200 oe was applied parallel with the (100) surface and the cubic anisotropy constants, K_1, were determined by Fourier analysis of the measured torque curves. K_1 was -3.7×10^3 ergs/cm^3 and -1.5×10^3 ergs/cm^3 at liquid nitrogen and room temperature, respectively, in the state cooled rapidly from 750°C. Measurements on K_1 with aging at 110°C showed no change at either temperature during 1000 hours.

12,523 THE MAGNETIC SUSCEPTIBILITY OF SOLID SOLUTIONS OF SEMI-CONDUCTING COMPOUNDS OF $A^{III}B^{V}$ by M. Matyas (Czech. Acad. Sci.); Czech. J. Phys., Vol. 11B, pp. 461-463(L), 1961

Gouy method measurements of the molar susceptibility X_{mol} of polycrystalline samples of InSb-GaSb are reported. The results show that X_{mol} is not a linear function of the composition of the solid solution if the element A in the compound $A^{III}B^{V}$ is replaced by another element from Group III of the periodic system. This agrees well with the empirical formula obtained by Matyas according to which X_{mol} is a quadratic function of the composition.

12,524 MAGNETIC SUSCEPTIBILITY OF MATERIALS COMMONLY USED IN THE CONSTRUCTION OF CRYOGENIC APPARATUS by G. L. Salinger and J. C. Wheatley (U. Illinois); Rev. Sci. Instr., Vol. 32, pp. 872-874(L), July 1961

Measurements of the magnetic susceptibility of some weakly magnetic materials in the 1.6 - 4.2°K temperature range are reported. The results are given in the form $X/\rho = B + (C/T)$ where X is the magnetic susceptibility and ρ is the density. The materials are divided into several classes and are tabulated with respect to use, values of C and B, and supplier.

12,525 THE MAGNETIC SUSCEPTIBILITIES OF CRYSTALLINE STABLE FREE RADICALS IN THE 77°-293°K TEMPERATURE RANGE by W. Duffy, Jr. (Santa Clara U.); U.S. Gov. Res. Rep., Vol. 36, p. 84(A), Sept. 5, 1961 AD 258 719

Measurements of the powder susceptibilities of crystalline stable free radical samples of Wurster's blue, DPPH and 1, 3-bisdiphenylene-2-phenyllalyl, as a function of temperature from 77°-293°K are reported. All exhibit negative Curie points with values in the range -36°K to -6°K. For Wurster's blue, the Néel temperature is found to be 186°K. The microbalance system constructed for the measurements is described.

12,526 MAGNETIC SUSCEPTIBILITIES OF ERBIUM AND HOLMIUM ETHYLSULPHATES by A. H. Cooke, R. Lazenby and M. J. M. Leask (U. Oxford); U.S. Gov. Res. Rep., Vol. 36, p. S-12(A), Aug. 5, 1961 PB 155 474

Measurements of the magnetic susceptibilities of Er ethylsulphate and Ho ethylsulphate between room temperature and 1.3°K are reported. The results are compared with the values calculated from paramagnetic resonance data and good agreement is obtained. The susceptibility of the erbium salt at low temperatures can be accounted for by a ground doublet having $g_{\parallel} = 1.58 \pm 0.05$ and $g_{\perp} = 8.53 \pm 0.05$, with the lowest excited states some 50 cm^{-1} above the ground doublet. The susceptibility of the holmium salt in the helium range of temperatures can be accounted for by a triplet ground state having $g_{\parallel} = 7.70 \pm 0.05$ and $g_{\perp} = 3.86 \pm 0.05$, split into a doublet and a singlet, the singlet being 5.5 cm^{-1} above the doublet. The Jahn-Teller splitting of the doublet is not more than 0.1 cm^{-1}.

12,527 SPIN ABSORPTION IN CERTAIN PARAMAGNETIC SALTS IN PARALLEL FIELDS by Yu. I. Nyashin (A. M. Gor'kii Permsk State U.); Soviet Phys.-Solid State, Vol. 3, pp. 110-111, July 1961

The experimental dependence of spin absorption on magnetic field is discussed. Formulas suggested by various authors are discussed and compared with experimental results. This comparison for salts of Fe, Mn and Cr is presented graphically, giving values of the isothermal relaxation time of the magnetic moment, T_s, and the constant b/c. These do not differ greatly from the previous known values.

12,528 PARAMAGNETIC RESONANCE IN SEMICONDUCTORS by A. Honig (Syracuse U.); U.S. Gov. Res. Rep., Vol. 36, p. 87(A), Aug. 5, 1961 AD 257 488

An extensively referenced summary of research conducted on electron spin-lattice relaxation in Si, electron spin-spin relaxation in Si, γ-ray anisotropy from dynamically oriented nuclei and combined infrared radiation-spin resonance is presented. The electron spin-spin relaxation work is described in detail. Results from the combined infrared radiation-spin resonance program relate to: (1) trapping lifetimes and transport phenomena; (2) conduction electron-phosphorus impurity atom singlet exchange cross-section in Si; (3) photo-induced electron spin-lattice relaxation mechanisms; (4) compensation dependent electron spin-lattice relaxation mechanism; and (5) a metastable photoexcited paramagnetic state in Si.

12,529 SPLITTING OF PARAMAGNETIC RESONANCE LINES IN INHOMOGENEOUS FIELDS by V. N. Lazukin (Moscow State U.); Soviet Phys.-Solid State, Vol. 3, pp. 297-298, Aug. 1961

The investigation of a chance observation of the splitting of paramagnetic resonance lines at room temperature is reported. Experiments were carried out at 9,400 Mc by means of a balance radio-spectroscope using two types of absorption cell. In the case where the constant magnetic field H_0 wc homogeneous, while the microwave magnetic field possessed gradient, splitting was not observed but distortion was; where both fields were inhomogeneous splitting was observed and was larger than the expected amount by a factor of 10^2-10^3. Change in the magnitude and gradient of H_0 can vary the number of components in the splitting; in all cases H_0 was very small and the splitting did not exceed 1-3 oe.

Analysis of Impurities by Paramagnetic Resonance - See 12,3

Amplification by Paramagnetic Resonance - See 12,712

12,530 EFFECT OF PRESSURE ON THE SPECTRUM OF RUBY by D. R. Stephens and H. G. Drickamer (U. Illinois); J. Che Phys., Vol. 35, pp. 427-429, Aug. 1961

The effect of pressures of up to 120 kbar, applied both parallel and perpendicular to the c axis, on the spectrum of ruby is discussed. From these data it is possible to calculate the change in crystal field strength Dq in interelectronic repulsion B and in trigonal field distortion ($-\frac{3}{2}$ K). The crystal field increases with increasing pressure, while the interatomi repulsion decreases, indicating covalency. The trigonal distortion is constant to about 60 kbar, and then increases markedly at higher pressures. The fractional change in Dq with pressure follows the R^{-5} law closely to 30 kbar, the upp limit of the p-v data.

12,531 A PARAMAGNETIC SPECIES IN IRRADIATED NaNC by H. Zeldes and R. Livingston (Oak Ridge Natl. Lab.); J. Chem. Phys., Vol. 35, pp. 563-567, Aug. 1961

Single crystals of $NaNO_2$ irradiated with Co^{60} gamma rays at 77°K and studied by the paramagnetic resonance method are discussed. An anisotropic three-line hyperfine spectrum is associated with a single paramagnetic species. The hyperfine

ARAMAGNETISM (Cont'd)

ructure arises from a nitrogen nucleus in the paramagnetic ecies at a position of mm point symmetry. The principal lues of the g tensor and the hyperfine tensor are deduced as ell as the directions of their principal axes. The paramag-tic species is believed to be NO_2.

2,532 EPR STUDIES OF SPIN CORRELATION IN SOME ION ADICAL SALTS by D. B. Chesnust and W. D. Phillips (du ont); J. Chem. Phys., Vol. 35, pp. 1002-1012, Sept. 1961

ectron spin resonance studies carried out on a number of n-radical salts based on the strong π-acceptor, tetracya-oguinodimethane (TCNQ) are discussed. Spin correlation xists between the magnetic electrons in these salts, giving se to a ground triplet state and a thermally accessible trip-t state. Typical singlet-triplet separations (J) derived from he observed temperature dependences of EPR signal intensi-es and detailed analysis employing the appropriate spin amiltonian $H = \beta H \cdot g \cdot S + DS_z^2 + E(S_x^2 - S_y^2)$ are given. The nportance of paramagnetic impurities in studies of the mag-etic properties of organic solids is emphasized. Examples re given which illustrate how a per cent or so of doublet-ate impurity species can dominate resonances near g = 2.002 molecular solids obeying singlet-triplet statistics.

2,533 HYPERFINE STRUCTURE AND g-TENSOR ANISOT-OPY OF THE PARAMAGNETIC RESONANCES OF MANGA-IESE IN Ti O_2 by H. G. Andresen (USASRDL); J. Chem. nys., Vol. 35, pp. 1090-1096, Sept. 1961

leasurements of Mn-doped TiO_2 single crystal rutile struc-ures at room temperature and at X band frequencies are eported. The anisotropy of the g-tensor and that of the A ensor were evaluated using resonance data measured at orien-tions of the magnetic field parallel to the three magnetic xes of the rutile crystal. The hyperfine structure patterns of he manganese resonances are discussed qualitatively for arious crystal orientations; two property selected $|\Delta m_I| = 1$ ransitions were employed to estimate the upper limit of the uadrupole-term parameters of the spin Hamiltonian. Para-agnetic resonances of manganese in rutile were also investi-ated at liquid nitrogen temperature. Additional strong reso-nces were observed. Though it is likely that these esonances can be attributed to manganese atoms of a different alence state, the data at X band frequencies are insufficient o determine the origin of these resonances unambiguously.

2,534 NUCLEAR RELAXATION AND DYNAMIC POLARI-ATION IN SOLIDS by P. L. Scott (U. California, Berkeley); .S. Gov. Res. Rep., Vol. 36, p. S-51 (A), Aug. 5, 1961 3 152 382

eoretical mechanisms for relaxation and dynamic polariza-on of nuclei in a solid containing a small percentage of arama netic impurities are discussed. Spatial diffusion of uclear polarization is taken into account, and its effects on oth the transient and steady state behavior of the average uclear polarization are worked out in detail for a simple odel.

2,535 F^{19} NUCLEAR MAGNETIC RESONANCE IN POLY-RYSTALLINE MgF_2 by S. K. Ghosh, J. Lahiri and S. K. inha (Saha Inst. Nuclear Phys.); Indian J. Phys., Vol. 44, p. 236-239, May 1961

e F^{19} nuclear magnetic resonance line in polycrystalline MgF_2 is discussed. The second moment of the recorded line-shape is compared with that computed from the known lattice structure of MgF_2 crystal as given by X-ray diffraction studies. The agreement is satisfactory.

12,536 NUCLEAR MAGNETIC RESONANCE STUDIES OF B" IN CRYSTALLINE BORATES by P. J. Bray, J. O. Edwards, J. G. O'Keefe, V. F. Ross and I. Tatsuzaki (Brown U.); J. Chem. Phys., Vol. 35, pp. 435-442, Aug. 1961

The coordination state of the boron atom is correlated with the properties of the nuclear magnetic resonance (NMR) signals arising from the boron nuclei. Characteristic resonance line shapes occur when the NMR transitions are perturbed by interactions between the B" nuclear electrical quadrupole moment and the electrical field gradient at the boron site. In polycrystalline borates, boron in trigonal and tetrahedral coordination may be resolved by analysis of first and second-order quadrupole effects on the NMR transitions. The B" quadrupole coupling constants have been measured for the simple trigonal BO_3 and tetrahedral BO_4 groups. The analysis has been extended to include polyborate structures having both trigonal and tetrahedral boron atoms. Results of the NMR study of simple, known bonding configurations are discussed and correlated with measurements of alkali-borate glasses and of miscellaneous borate and mineral compounds.

DIAMAGNETISM

12,537 MAGNETIC SUSCEPTIBILITY OF MERCURIC OXIDE AT VARIOUS TEMPERATURES by H. Mikhail (Cairo U.), Z. Hanafy and T. M. Salem (Dukki, Cairo); J. Chem. Phys., Vol. 35, pp. 1185-1188, Oct. 1961

The magnetic susceptibility of both the red and the yellow oxides of Hg is discussed. The red form has a mass susceptibility of $(-0.2217 \pm 0.0002) \times 10^{-6}$ emu/g, while the yellow one has a slightly lower mass susceptibility of $(-0.2165 \pm 0.0002) \times 10^{-6}$ emu/g at room temperature (25°C). The temperature variation of their mass susceptibility between 25° and 300°C was also investigated. The general shape of the curve for the two oxides is essentially the same, namely, an increase in diamagnetism with rise in temperature followed by a mild drop and subsequently a sharp rise. The position of the peak occurs at about 50°C for the red oxide and about 114°C for the yellow oxide. A tentative explanation of their behavior is given, based upon impurity ionization.

OPTICAL PROPERTIES

GENERAL

12,538 OPTICAL PRINCIPLE OF REVERSIBILITY AND ITS APPLICATION IN THE THEORY OF THIN-LAYER COATINGS by P. G. Kard; Optics and Spectrosc., Vol. 11, pp. 125-127, Aug. 1961

The optical principle of reversibility is generalized to include the presence of absorbing media. Reversibility is applied to the derivation of basic relationships in the theory of thin optical coatings. In comparison with the method that takes the boundary conditions into consideration explicitly, the reversibility method is simpler and may be considered as more general.

Spectroscopic Analysis of Impurities - See 12,332

12,539 REABSORPTION IN CRYSTALS OF A FINITE THICKNESS by V. M. Agranovich and Yu. V. Konobeev; Optics and Spectrosc., Vol. 11, pp. 199-206, Sept. 1961

Results derived from a theory of the reabsorption of light in crystals of finite thickness are presented. Calculated values are listed for the stationary case, making it possible to determine the shape of the luminescence spectrum and the quantum yield for phosphors of arbitrary thickness. Accurate, new exact equations have been obtained for the nonstationary case (luminescence decay), from which formulas are derived for the average time of luminescence decay. Various asymptotic cases are studied in detail. The results obtained for nonstationary processes can be used in the theory of radiant energy transfer in planetary atmospheres and in the theory of neutron moderation.

Effects of Irradiation on Absorption in KBr and NaCl - See 12,450

12,540 ELECTRIC-FIELD-INDUCED MODULATION OF THE ABSORPTION DUE TO INTERBAND TRANSITIONS OF FREE HOLES IN GERMANIUM by M. A. C. S. Brown and E. G. S. Paige (Roy. Radar Estab.); Phys. Rev. Lett., Vol. 7, pp. 84-86 (L), Aug. 1, 1961

Observation of the change in absorption due to a change in distribution produced by a high electric field is reported. For the purpose of comparison, the distribution function is changed in a known way by raising the lattice temperature a small amount δT. The change in absorption can then be calculated from Kane's theory. Measurements have been made at various lattice temperatures between 90° and 320°K on a p-type Ge sample containing $4.4 \times 10^{15}\,cm^{-3}$ free carriers. At 93°K, a comparison between the field effect and the δT effect shows that in electric fields up to $350\,v\,cm^{-1}$, the distribution remains Maxwellian. At 293°K, there is a marked difference between the field effect and the δT effect. It is pointed out that the theoretical response time of the modulation is the energy relaxation time of the free holes. Since substantial depths of modulation can be achieved at 93°K, the field effect could form the basis of a modulator capable of modulating a high frequency light beam.

12,541 THE EFFECT OF AN INVERSE MAGNETIC FIELD UPON THE EXCITON ABSORPTION SPECTRUM OF CdS CRYSTALS by E. F. Gross, B. P. Zakharchenya and O. V. Konstantinov (A.F. Ioffe Inst. of Phys. and Tech., Leningrad); Soviet Phys.-Solid State, Vol. 3, pp. 221-223 (L), July 1961

The action of a magnetic field upon the CdS absorption spectrum is discussed. Single CdS crystal samples approximately 1-3μ wide with their optical axes within the plane of the crystal plate were used. They were cooled to 1.3°K and apparatus of high resolving power and high dispersive power from 4 to 1.5 A/mm was employed. In the absence of the magnetic field, a group of absorption lines of varying polarization and high intensity were seen in the absorption spectrum of thin single crystals. When E was approximately parallel to the optical axis of the crystal the lines (λ4853, λ4813, and λ4806) ascribed to the exciton absorption of the crystal narrow and weaken in intensity. During changes in the direction of the magnetic field, there was a shift of the components of the high intensity doublet in the high energy direction by $\Delta\lambda = 0.4$ A and their intensity changed. Onsager's principle for the conductivity tensor was used to explain the observed changes in th spectrum for an inverse magnetic field.

12,542 EXCITON STRUCTURE AND ZEEMAN EFFECTS IN CADMIUM SELENIDE by J. O. Dimmock and R. G. Wheeler (Yale U.); U.S. Gov. Res. Rep., Vol. 36, p. 96 (A), Aug. 20, 1961 AD 258 198

The exciton spectra in wurtzite CdSe are discussed. The identification and interpretation of the spectra involved measurements of the magneto-optical effects. A qualitative understanding of the band symmetries at K = 0, 0, 0 in crystals of C_{6v}^4 symmetry was obtained. A quantitative comparison with an exciton mass theory which permits evaluation of the electron and hole mass and g value parameters was outlined.

12,543 PHOTON ABSORPTION BY VALENCE ELECTRONS IN ALUMINUM by D. H. Tomboulian (Cornell U.); U.S. Gov Res. Rep., Vol. 36, pp. S-50-S-51 (A), Sept. 5, 1961 PB 155 514

Photon absorption by valence electrons, which are also involved in the characteristic energy loss mechanism, is discussed. Measurements dealing with the absorption spectra of Al over an incident photon energy range extending from 15 to 50 ev are reported.

Absorption in KH_2PO_4 and KD_2PO_4 - See 12,436

12,544 PHOTOCHEMICALLY PRODUCED COLOR CENTERS IN KCl AND KBr by J. Cape (U. Illinois); U.S. Gov. Res. Rep., Vol. 36, p. S-51 (A), Sept. 5, 1961 PB 150 232

The effects of X-ray and unfiltered quartz-mercury arc radiation at 15°K on the optical absorption spectra of KCl and KBr crystals are compared and changes in the absorption spectra at various annealing temperatures are discussed. It is concluded that the H centers bleach thermally by diffusing to and combining with other color centers. Recombination with F and a centers annihilates the H centers and leads to the formation of V_K centers, while recombination with a third center (possibly a positive ion vacancy) results in the formation of V_1 centers. U, U_1, U_2, O^-, and a centers are produced by the uv irradiation as well as F and H centers. The F center concentration is much smaller in proportion to the H center concentration compared with X-irradiated KCl and KBr. The photo-produced F centers may be bleached optically at 15°K.

Color Centers - See 12,273-12,279

12,545 SOME ASPECTS OF THE INFRA-RED ABSORPTION SPECTRA OF SEMICONDUCTORS by D. H. Parkinson (Roy. Radar Estab.); Contemp. Phys., Vol. 3, pp. 58-74, Oct. 196

The two chief features in the infrared absorption spectrum of a semiconductor — the intrinsic edge and lattice bands — are discussed. Measurements of the absorption spectra near the intrinsic edge in Ge and Si show that indirect transitions take place and that 'excitons' are formed. The intrinsic energy gap can be determined accurately by these measurements. The lattice bands yield the main features of the lattice vibration spectrum.

12,546 TWO-PHONON INFRA-RED LATTICE ABSORPTION IN DIAMOND by J. R. Hardy and S. D. Smith (U. Reading); Phil. Mag., Vol. 6, pp. 1163-1172, Sept. 1961

A grating spectrometer investigation of the specimen-independent infrared absorption spectrum of diamond in the 2μ to 6μ

gion is discussed. The results are analyzed in terms of ulti-phonon processes. In particular, the two phonon ab-rption is examined in detail in an attempt to deduce onon energies for the various branches of the frequency ectrum at symmetry points in the reduced zone. Sets of ttice wave dispersion curves have been constructed from ese results which are very unlike those for Si and Ge.

2,547 THE INFRARED ABSORPTION SPECTRUM OF SILVER XIDE by E. F. Gross and F. I. Kreingold; Optics and Spec-osc., Vol. 10, p. 211(L), Mar. 1961

he infrared absorption spectrum of Ag_2O in the 410 to 1500 m^{-1} region is discussed. Measurements were made using KS-6 and IKS-14 infrared spectrometers. Three absorption ands with considerably narrower band width than the orresponding bands in Cu_2O are present. The various absorp-ion bands are displaced to different extents as a result of the ransition from one material to the other. The results are xplained by assuming that there are nonpolar bonds in both Ag_2O and Cu_2O, but that the fraction of bonds with homeo-olar components is larger in Ag_2O.

2,548 INFRARED ABSORPTION SPECTRA OF SYNTHETIC LUMINATES OF THE ALKALI AND ALKALINE EARTH ETALS by V. A. Kolesova; Optics and Spectrosc., Vol. 10, p. 209-210(L), Mar. 1961

he infrared absorption spectra of synthetic aluminates $LiAlO_2$, AlO_2, $RbAlO_2$, $CaAl_2O_4$, $BaAl_2O_4$ and of $NaAlO_2$ are de-cribed. A VIKS-M3 vacuum spectrometer with a NaCl prism nd an ISP-14b spectrometer with a KBr prism were used to btain the spectra. It is concluded that the difference in the osition of analogous bands in the spectra of aluminates and licates with the same degree of polymerization of their ionic frameworks results from difference in the force con-rants between the Si-O bond and the Al-O bond.

2,549 INFRARED SPECTRUM OF SOLID CARBON MONOX-DE by G. E. Ewing and G. C. Pimentel (U. California); . Chem. Phys., Vol. 35, pp. 925-930, Sept. 1961

he infrared spectrum of solid carbon monoxide is considered the fundamental and overtone regions at 20°K. Sharp atures (bandwidths about one cm^{-1}) are assigned to vibra-onal modes of the various isotopic species: $C^{12}O^{16}$, 2138.1 m^{-1}; $C^{12}O^{17}$, 2112.3 cm^{-1}; $C^{13}O^{16}$, 2092.2 cm^{-1}; and $C^{12}O^{18}$, 088.4 cm^{-1}. These frequencies are examined with the aid of existing theories of frequency shifts in condensed phases. A road absorption (bandwidth about 40 cm^{-1}) centered at 2208 m^{-1} is assigned to combinations of the fundamental mode with attice modes. Calculations suggest that the lattice modes in-olved probably include translations as well as vibrations.

2,550 INFRARED SPECTRA OF CARBON MONOXIDE AS A OLID AND IN SOLID MATRICES by A. G. Maki (Natl. Bu. tand.); J. Chem. Phys., Vol. 35, pp. 931-935, Sept. 1961

he fundamental infrared absorption frequency of several iso-opes of CO in solid carbon monoxide and in solid matrices $_2$, Ar, and CH_4 is discussed. The overtone in solid carbon onoxide has been measured. Frequency shifts due to isotopic ubstitution in the solid state follow formulas developed for he gas phase only when the molecules of the same isotopic pecies are not adjacent to each other (i.e., only in dilute olutions).

12,551 STUDIES OF THE OPTICAL AND INFRARED ABSORPTION SPECTRA OF RUTILE SINGLE CRYSTALS by B. H. Soffer (MIT); J. Chem. Phys., Vol. 35, pp. 940-945, Sept. 1961

The optical absorption of single crystals of synthetic rutile in the spectral range 1200 to 25,000 cm^{-1} from room temperature to 1000°C is discussed. The electronic absorption exhibits dichroic behavior. For a decadic absorption a^1 of 400 cm^{-1}, the shift is -7.1×10^{-4} ev/°K, while at 1 cm^{-1} it is -9.5×10^{-4} ev/°K. The broad band in the region of 6850 cm^{-1} which occurs in reduced rutile does not appear in fully oxidized rutile. At high temperatures an additional wavelength-independent absorption appears which can be correlated in good agreement with dc conductivity by applying the Drude-Zener theory of free carrier absorption. New bands in the 3300 cm^{-1} region stem from O-H valence vibrations. The main bands have peaks at 3277 and 3322 cm^{-1} and half-widths of 28 and 13 cm^{-1}. A satellite structure of combination and difference bands exists. Deuterium substitution produces an absorption band at 2442 cm^{-1}. The entire structure has a marked dependence of the absorption on the polarization direction of the light.

12,552 OPTICAL ABSORPTION OF SOME OXIDES IN THE SCHUMANN ULTRA-VIOLET REGION by W. P. Doyle (U. Coll., London) and F. J. P. Clarke (Atomic Energy Res. Estab.); Brit. J. Appl. Phys., Vol. 12, pp. 574-576, Oct. 1961

Measurements of the optical absorption of thin films of SnO, SnO_2, PbO, AsO_3, SbO_3, BiO_3, BeO, ZrO_2, TaO_5, in the energy range 4 to 10.5 ev, are given. The experimental procedure is outlined. Because the thickness of the films was not determined, accurate values of absorption coefficients could not be obtained. It is suggested, however, that in the regions of maximum absorption the absorption coefficient is about 10^5 cm^{-1}.

12,553 ABSORPTION AND FLUORESCENCE SPECTRA WITH MAGNETIC PROPERTIES OF $ErCl_3$ by G. H. Dieke and S. Singh (Johns Hopkins U.); J. Chem. Phys., Vol. 35, pp. 555-563, Aug. 1961

The absorption and fluorescence spectra of $ErCl_3$ diluted by $LaCl_3$, along with the Zeeman effects of many lines, are given. All expected electronic levels to 30,000 cm^{-1} above the ground state have been found, and their interpretation fits into the theoretically expected scheme. Examples are also given of the absorption and fluorescence spectrum of pure $ErCl_3$ which show that the pure salt has a structure quite different from that of $LaCl_3$.

12,554 THE LOW TEMPERATURE LUMINESCENCE AND ABSORPTION OF BiI_3 CRYSTALS by R. I. Shekhmamet'ev (Leningrad State U.); Soviet Phys.-Solid State, Vol. 3, pp. 426-428, Aug. 1961

The low temperature absorption and luminescence of monocrystalline and sublimated fine-grained BiI_3 are discussed. The absorption at 77°K was dependent on thickness. For thick layers an absorption band near 639 mμ and absorption steps were observed; in thinner layers absorption bands at 579 mμ and 639 mμ were observed (the 639 band being the weaker). Studies of the diffuse reflection spectra also made it possible to compare the structure in the absorption edge region. On excitation with ultraviolet light, a fine-grained layer of BiI_3, cooled to 77°K, luminesced in the absorption edge region. This luminescence consisted of several bands. Crystals prepared

directly from BiI_3 powder did not exhibit luminescence. The study shows once more that the edge luminescence is related to the structure of the fundamental absorption edge.

RADIATION AND LUMINESCENCE

12,555 BAND-SPLITTING IN THE SPECTRA OF CUBIC CRYSTALS SUBJECTED TO ORIENTED DEFORMATION by A. A. Kaplyanski (Acad. Sci., USSR); Optics and Spectrosc., Vol. 10, pp. 83-87, Feb. 1961

An investigation of the amount of splitting of the spectral bands associated with anisotropic centers in cubic crystals subjected to deformation along certain crystallographic directions is analyzed. It is shown that the amount of splitting is determined by two or three independent parameters which characterize the interaction of the centers with the lattice. The possibility of a similar splitting in the exciton and band state spectra of crystals subjected to oriented deformation is discussed.

12,556 ANALYSIS OF POLARIZED CRYSTAL SPECTRA. THE SPECTRUM OF COBALT (III) ACETYLACETONATE by T. S. Piper (U. Illinois); J. Chem. Phys., Vol. 35, pp. 1240-1242, Oct. 1961

Broad bands observed in the polarized electronic spectra of transition metal ions in crystals are analyzed. The band of cobalt (III) acetylacetonate due to the transition $^1T_1 \leftarrow {}^1A_1$ is found to be split by the trigonal field into components at 16,200 cm^{-1} ($^1A_2$) and at 17,000 cm^{-1} (^1E). The spectra indicate that the trigonal field of the free molecule is not appreciably distorted in the monoclinic crystal.

12,557 AN EXCITATION MECHANISM FOR F-CENTER AND EXCITON ELECTRONS IN A MOLECULAR SHELL MODEL by A. A. Tsertsvadeze (I. V. Stalin Tbilisi State U.); Soviet Phys.-Solid State, Vol. 3, pp. 370-376, Aug. 1961

The problem of the energy variation of an F-center electron in the ground state during its transition to the metal ions located in the next coordination sphere surrounding the vacancy is examined, taking into account polarization of the surrounding ions by the electron and hole. Subsequent comparison between the calculated results and experimental data is made. The case of the F-center electron is examined first, and the results are used to calculate the excitation energy of the exciton electron. Calculated and experimental results of the energy are in good agreement for LiCl, LiBr and KI crystals, but those for NaCl and KCl exhibit a pronounced discrepancy. If account is only taken of the coulomb interaction between the electron and hole, the picture is reversed. The numerical results are based on the assumption that the F-center electrons are fast and result in only inertialess polarization of the lattice ions. If the exciton is considered to move slowly and results in polarization with inertia, calculations show that the effect on calculated values is small.

12,558 STUDY OF THE EMISSIVE POWER OF CERTAIN HIGH-MELTING COMPOUNDS IN THE INFRARED REGION by G. V. Samsonov and V. V. Pen'kovski; Optics and Spectrosc., Vol. 11, pp. 219-222, Sept. 1961

The infrared emissive power of certain high-melting point compounds is discussed. It is shown that, in the region from 4 to 14μ, the intensity of the radiation from a Globar and from silicon carbide-molybdenum silicide and silicon carbide-silicon nitride-molybdenum silicide composites is the same. The position of the maxima in the emission spectrum of silicon carbide does not change on the addition of molybdenum silicide (3-14 mole per cent), but the addition of 6 mole per cent silicon nitride to silicon carbide leads to a shift of the maxima toward shorter wavelengths.

12,559 THE EFFECT OF SMALL AMOUNTS OF GALLIUM IMPURITIES ON THE POSITIONS OF $L_{\alpha 1,2}$ AND $L_{\beta 6}$ EMISSION LINES OF GERMANIUM by M. I. Korsunskii, L. B. Litvinova and G. P. Borovikov (V. I. Lenin Polytech. Inst., Kharkov); Soviet Phys.-Solid State, Vol. 3, pp. 205-207, July 1961

A study of the nature of changes occurring in the L-series X-ray emission spectrum of Ge produced by small amounts of Ga is presented. Analysis of $L_{\alpha 1,2} - L_{\beta 6}$ lines region into dispersion components shows that Ga impurities displace the $L_{\beta 6}$ line toward long wavelengths with respect to the $L_{\alpha 1,2}$ line, in contrast to Sb which displaces this line toward short wavelengths. The magnitude of the displacement $\Delta E_{\beta 6-\alpha 1,2}$ is proportional to the cube root of the impurity concentration. It is found that the maximum amounts of Ga and Sb which can be dissolved in Ge produce practically the same change (of the order of 2 ev) in the energy difference between $L_{\beta 6}$ and $L_{\alpha 1,2}$ lines.

12,560 ASYMMETRY OF THE $K_{\alpha 1,2}$ LINES OF ZINC IN ITS SEMICONDUCTING COMPOUNDS WITH ANTIMONY by I. I. Kapshukov and Ya. A. Ugai (Voronezh State U.); Soviet Phys.-Solid State, Vol. 3, pp. 73-74, July 1961

The form of the $K_{\alpha 1,2}$ spectral lines of Zn in its semiconducting compounds with Sb (ZnSb, Zn_3Sb_2, and Zn_4Sb_3) and the shape of the K_α lines of pure metallic Cu and Zn, ZnO and ZnS are discussed. The experimental data are in good agreement with the values of the asymmetry index in Cu, Zn, ZnO and ZnS found in the literature. An explanation of the change of asymmetry index of the $K_{\alpha 1,2}$ lines of Zn in its compounds is given. A relatively small variation of the breadth of the $K_{\alpha 1,2}$ lines was noted in the Zn compounds investigated. However, no regularity of change of this characteristic as a function of type of chemical compound was observed.

12,561 NOTES ON THE CONCEPTS OF "YIELD", "MEAN LIFETIME", AND "DECAY LAW" AND THEIR USE IN LUMINESCENCE by V. L. Levshin; Optics and Spectrosc., Vol. 11, pp. 195-199, Sept. 1961

The concepts of "yield", "lifetime", and "decay law" of luminescence are analyzed and the difficulties which arise during their use in complex cases of luminescence are pointed out. Attention is given to the difference of physical meaning of the yield concept for short- and long-duration luminescence. A definition of luminescent yield suitable for stationary luminescent processes of both short and long duration is proposed. The use of the yield concept for nonstationary processes is considered and formulas corresponding to various cases are presented for calculating the yield of nonstationary processes. The need for studying the characteristics of partial processes is pointed out.

12,562 SHOCK-INDUCED LUMINESCENCE by M. Solow, R. C. Wiley and N. L. Coleburn (U.S. Naval Ord. Lab.);

S. Gov. Res. Rep., Vol. 36, p. S-57(A), Aug. 5, 1961
171 817

ock-induced luminescence of the oxide layer on the surface an Al sphere is discussed. When a 270 kbar shock wave ierges from an illuminated Al surface in a vacuum, blue ght is emitted; this phenomenon is affected significantly by face conditions. A chemically-formed Al oxide surface yer on the metal luminesces brightly for at least 0.64 μsec. ormally oxidized Al surfaces luminesce less brightly for a ch shorter time (~0.01 μsec). Shocked gold does not lu- nesce showing the effect of non-oxidized material on the enomenon. The luminescence from Al is attributed to ectrons, dragged by the shock (acoustoelectric effect). The ectrons reach the Al oxide layer and falling into the ionized centers, emit blue light.

2,563 ON THE ELECTROLUMINESCENCE EXCITATION ROCESS IN ZINC SULFIDE by A. N. Georgobiani; Optics nd Spectrosc., Vol. 11, pp. 231-232, Sept. 1961

he electroluminescence excitation process in ZnS is dis- ussed. Both impact ionization and direct field-induced nization can occur in varying degrees. If the excitation gion of the crystal is too small to develop an avalanche, ut the field in this region is still quite high, then field- duced excitation (zener effect) occurs. On the other hand conditions are favorable for an avalanche to develop (both he field and the region in which it is distributed are large hough), then impact ionization will predominate over field- duced ionization. A tunneling transition which can be nnected with direct field-induced ionization of the crystal ttice and of the luminescence centers is also discussed.

2,564 ON THE THEORY OF ELECTROLUMINESCENCE TERIORATION by P. M. Jaffe (Westinghouse); J. Electro- hem. Soc., Vol. 108, pp. 711-712, July 1961

he maintenance curve for a green electroluminescent ZnS: u,Cl powder phosphor is shown. The glow curves (relative ntensity vs T) taken after 0, 96, 600, and 1000 hrs of opera- ion are also shown and discussed. All the curves have in ommon a pronounced glow peak located around -145°C. It postulated that under the influence of the applied electric eld, the donor is induced to diffuse away from its equilibrium osition near the acceptor. This postulated diffusion of the nor with the resultant trap formation causes the initial rapid ecrease in light output.

2,565 CERTAIN REGULARITIES IN THE ELECTROLUMINES- ENCE OF ZnS:Cu:Al PHOSPHORS WITH HIGH COPPER ONTENT by A. M. Bonch-Bruevich; Optics and Spectrosc., ol. 11, pp. 114-117, Aug. 1961

he kinetics of the decrease in intensity of the green and blue uminescence pulses which accompany the turning on and off f the voltage applied to ZnS:Cu:Al phosphors are described. he steady state luminescence characteristics (the amplitudes f the luminescence pulses and the light sum emitted under the ction of a pulsed voltage) are also discussed. Essential dif- erences exist between the green and blue luminescence bands ith regard to a number of the regularities observed.

lectroluminescence from GaP Point Contact Diodes - See 2,632

12,566 ELECTRO-X-RAY LUMINESCENCE OF KBr CRYSTALS by A. S. Andrianov and M. L. Kats; Optics and Spectrosc., Vol. 11, pp. 228-229, Sept. 1961

A discussion of the luminescence of KBr crystals which appears under the simultaneous action of X-rays and an electric field is presented. No electroluminescence is observed when the substance is subjected to the electric field alone even if the intensity of the field is increased up to breakdown values. Luminescence is observed when the crystals are subjected to X-irradiation alone but the intensity of the luminescence increases considerably with the additional application of the electric field. The amplification effect which occurs under the action of the field can be attributed to the delocalization of electrons or holes from trap levels by the field.

12,567 EFFICIENCIES OF PHOSPHORS FOR SHORT WAVE ULTRA-VIOLET EXCITATION by A. Bril and W. Hoekstra (Philips); Philips Res. Rep., Vol. 16, pp. 356-370, Aug. 1961

A direct method of measuring the absolute value of the efficiency of phosphors irradiated by short-wave ultraviolet excitation is described. The specimens were excited with the aid of a high-pressure mercury lamp from which the wavelength region 250-270 mμ was isolated with filters, thus providing a high excitation density in a narrow wavelength region; a fast thermopile was used as a detector to obtain an essentially constant spectral power response over the entire wavelength region. The absolute measurements are tabulated and the sources of errors are analyzed. It is shown that the efficiencies of other phosphors may easily be measured using a standard phosphor (e.g., $MgWO_4$).

12,568 RESEARCH AND DEVELOPMENT FOR THE STUDY OF THE STORAGE OF ELECTRICAL ENERGY WITH THE HELP OF PERSISTENT INTERNAL POLARIZATION OF PHOSPHORS by H. Kallmann and J. Rennert (New York U.); U.S. Gov. Res. Rep., Vol. 36, p. S-53(A), Sept. 5, 1961 PB 152 745

Low temperature apparatus and measuring equipment for electrical energy storage in phosphor material is described. This apparatus is to be used for measurement of electrical energy storage by persistent internal polarization of phosphor layers at low temperatures. The components are a vacuum tight sample chamber with provisions for thermostating the sample down to liquid nitrogen temperature and circuitry including an electrometer and recorder for measuring and recording the electrical energy stored in the phosphor layers as well as thermocouple leads to measure sample temperature. The details of phosphor sample preparation by sedimentation techniques are described.

12,569 INFRARED LUMINESCENCE OF THE SURFACE LAYER OF COPPER OXIDE by Yu. V. Vorob'ev and Yu. I. Karkhanin (T. G. Shevchenko State U., Kiev); Soviet Phys.-Solid State, Vol. 3, pp. 150-153, July 1961

The dependence of the luminescent intensity of Cu_2O upon the external potential applied to the copper oxide-electrolytic system is discussed. The experimental procedure and results are presented. The capacitance and resistivity of the double layer at the copper oxide electrolyte boundary have been measured; the character of the energy band distortion (shift) at the surface of the sample is determined by the sign and magnitude of the capacitive photoeffect. It is concluded that the boundaries of the energy bands at the surface of the semiconductor are shifted in the forbidden direction by an amount that is practically equal to the magnitude of the external

applied potential; and that the influence of the external potential upon the extinguishing of the luminescence of Cu_2O in electrolytic solution can be explained both qualitatively and quantitatively by the formation of a forbidden energy band (an energy barrier) at the surface of the semiconductor.

12,570 LUMINESCENCE OF PURE AND DOPED CRYSTALS OF AgCl AT LOW TEMPERATURES [in French] by K. Vacek and J. Ringeissen (U. Strasbourg); J. Phys. Radium, Vol. 22, pp. 519-520, Aug.-Sept. 1961

Measurements of the luminescence of AgCl, AgCl + 0.01 mole per cent $CdCl_2$, and AgCl + 0.5 mole per cent TlCl crystals at liquid nitrogen and helium temperatures are given. A displacement of the emission band at about 4800 A was observed at 77°K as a function of the doped ion. The emission in the red region of the luminescence spectrum disappears at 4°K and the fundamental emission band is displaced towards lower energies when the temperature decreases.

12,571 LUMINESCENCE IN KI:Tl by J. E. Alderson and S. E. Williams (U. Western Australia); Austl. J. Phys., Vol. 14, pp. 368-380, Sept. 1961

The luminescence phenomena of single crystals of KI:Tl containing various concentrations of Tl at temperatures between −140° and 45°C are discussed. The relative luminescence efficiencies in the Tl absorption bands and the host crystal fundamental absorption edge show that energy is transferred from host crystal to impurity center to produce luminescence at room temperatures. Luminescence production shows a slow build-up which has been analyzed in detail for irradiation at 1608 and 1216 A. Thermal escape from traps followed by radiationless de-excitation has been observed by investigating the changes of the instantaneous component of luminescence production with varying intervals of darkness. An explanation is proposed in terms of the migration of holes from shallower to deeper traps near luminescence centers followed by recombination with free electrons.

12,572 INTERFERENCE OF LUMINESCENT EMISSION FROM AN EVAPORATED PHOSPHOR by N. A. Vlasenko, V. K. Miloslavski and I. N. Shklyarevskii; Optics and Spectrosc., Vol. 11, pp. 216-219, Sept. 1961

The interference of luminescent emission from a thin layer of evaporated ZnS:Mn phosphor excited by monochromatic ultraviolet radiation is discussed and the experimentally observed peculiarities of this effect which distinguish it from the usual interference in the same nonexcited evaporated phosphor illuminated by an external source of light are described. The interference pattern of the luminescent emission is calculated on the assumption that no coherence exists between the elementary radiators.

12,573 THE YELLOW LUMINESCENCE OF ZINC OXIDE by Ya. M. Zelinin and A. P. Zhukovskii; Optics and Spectrosc., Vol. 11, pp. 212-215, Sept. 1961

The different hypotheses concerning the centers responsible for the yellow luminescence band of ZnO are discussed. The conclusion reached is that an excess of oxygen and some kind of structural defects are necessary for the development of yellow luminescence. A brief description of sample preparation and of experimental details is given.

12,574 INVESTIGATION OF DETAILS OF THE LUMINESCENCE MECHANISM OF NaCl-Ni PHOSPHORS [in Russian] by I. A. Parfianovich and E. I. Shuraleva (Irkutsk U.); Izv. VUZ Fiz., No. 1, pp. 94-97, 1961

Investigations of NaCl-Ni phosphors during excitation, including observations of their luminescent properties under the effe of X-rays, are discussed. The studies were aimed at resolving the question of the nature of the fluorescent centers and the recombination of free electrons with these centers which lead to the emission of light quanta characteristic for an activator. Data on the details of the persistence mechanism of these phosphors are collected and discussed.

Luminescence of BiI_3 - See 12,554

Fluorescence in $ErCl_3$-$LaCl_3$ - See 12,553

12,575 SOME CONCENTRATION EFFECTS IN PLASTIC SCINTILLATORS by L. S. Kukushkin and L. L. Nagornaya; Optics and Spectrosc., Vol. 11, pp. 206-208, Sept. 1961

Qualitative calculations which make it possible to describe concentration effects on a number of the optical characteristics of plastic scintillators are given. The behavior of the luminescence spectra of plastic scintillators based on polystyrene with different concentrations of luminescing additives is studied. It is shown that the experimental data are in good agreement with the point of view presented.

PHOTOELECTRONIC PROPERTIES

12,576 INVESTIGATION OF THE KINETICS OF IMPURITY PHOTOCONDUCTION AS A METHOD OF DETERMINATION OF PARAMETERS OF LOCAL LEVELS by S. M. Ryvkin, L. G. Paritskii, R. Yu. Khansevarov and I. D. Yaroshetskii (A. F. Ioffe Inst. Phys. and Tech., Leningrad); Soviet Phys.-Solid State, Vol. 3, pp. 185-194, July 1961

The most important cases of the photocurrent relaxation during excitation in the impurity region are analyzed from the theoretical point of view. The basic laws of the kinetics of impurity photoconduction during excitation of carriers from one type of local centers, the effect of constant irradiation from the impurity region on the kinetics of the process, and the case of relaxation of the impurity photoconductivity in the presence of constant irradiation from the region of intrinsic absorption are discussed. Certain properties of the effect of shortwave-illumination on the relaxation of the impurity photoconductivity when the intrinsic photoconductivity is bipolar and the possible methods of determining the parameters of impurity centers are also discussed. A detailed analysis showed that the experimental investigation of the kinetics of impurity photoconduction is a reliable method of determining a number of important parameters of impurity centers (the photon capture cross section, the free carrier capture cross section of centers and also the energy position of the impurity level in the forbidden band, the concentration of centers and their occupancy

12,577 THERMAL ACTIVATION ENERGIES OF DARK CONDUCTIVITY IN ORGANIC COMPOUNDS by A. T. Vartanyan and L. D. Rozenshtein (Vavilov State Opt. Inst., Leningrad); Soviet Phys.-Solid State, Vol. 3, pp. 520-526, Sept. 1961

Determination of the value of the dark conductivity activation energy for a number of organic dyes and colorless compounds is described. The absorption spectra of solid films of fluorescei

benzophenone, anthranilic acid, phenylanthranilic acid and seven phthalimide compounds were also measured. It is shown that the activation energy values agree with the longwave regions of descent of the spectrum absorption curves of the corresponding materials.

12,578 ENHANCED PHOTOCONDUCTANCE AND SHADOWS ON CADMIUM SULFIDE SINGLE CRYSTALS by Staff (Western Reserve U.); U.S. Gov. Res. Rep., Vol. 36, p. 77 (A), Aug. 5, 1961 AD 257 072

The effect of a capacitive electric field applied normal to the surface on the conductivity of the semiconductor is discussed. The effects of such a capacitive field on the resistance are expected to vary directly with the equare of the resistivity of the material. The discrepancy between the observed and expected change in conductance arising from an applied field is used to study the density and energies of the surface states on semiconductors.

12,579 ELECTRICAL CONDUCTIVITY AND PHOTOCONDUCTIVITY OF THIN ANTHRACENE LAYERS IN VACUUM by C. Gheorghita-Oancea (Polytech. Inst., Bucharest); Brit. J. Appl. Phys., Vol. 12, pp. 579-580 (L), Oct. 1961

Electrical conductivity and photoconductivity measurements performed on thin evaporated layers of anthracene are discussed. In order to eliminate as much as possible the surface phenomena produced by air and water vapor adsorption, cells were prepared inside the vacuum system used for the electrical conductivity and photoconductivity measurements. It was found that the dark and photocurrents increase with increase of pressure.

Photoconductivity of HgTe-CdTe Solid Solutions - See 12,246

12,580 THE EFFECT OF ABSORBED OXYGEN ON THE PHOTO-EMF OF LEAD SULFIDE LAYERS by R. Ya. Berlaga and T. V. Bykova (Leningrad State U.); Soviet Phys.-Solid State, Vol. 2, pp. 2705-2706, June 1961

The effects of absorbed oxygen and of temperature on the photovoltage of PbS layers are described. It is found that the air absorbed by the layer has a reversible effect on the magnitude of the photo-EMF in the temperature range from 20° to 200°C and the resistance of the layers also varies during the process of absorption and desorption of oxygen.

Photo-EMF in Semiconductors - See 12,501

12,581 THE FUNDAMENTAL PHOTOELECTRIC EFFECT OF SEMICONDUCTORS AND OF Cs_3Sb [in French] by A. Meessen (U. Louvain); J. Phys. Radium, Vol. 22, pp. 472-480, Aug.-Sept. 1961

A theory of the fundamental photoelectric effect in semiconductors for both direct and indirect transitions from the valence band to the conduction band is proposed. The numerous experimental results for Cs_3Sb permit separation of the fundamental photoelectric effect from secondary effects and suggest new lines for other experimental research. The photoelectric emission depth becomes smaller near the photoelectric threshold of electron scattering by impurity centers.

12,582 THE LIMITED APPLICABILITY OF THE CONCEPT OF UNIVERSAL SPEED OF SURFACE RECOMBINATION DURING THE INVESTIGATION OF KINETICS OF PHOTOELECTRICAL PROCESSES by V. A. Romanov (Phys. Inst., Kiev); Soviet Phys.-Solid State, Vol. 3, pp. 23-25, July 1961

The applicability of a simplified theory of photoelectric kinetics that involves the exclusion of the speed of surface recombination is considered. Only limited applicability of this theory could be experimentally verified from relationships found between η_b and the external field in Ge specimens.

12,583 PHOTOELECTRIC COLORING OF LEAD OXIDE by M. S. Kosman and V. A. Izvozchikov (A. I. Hertz State Pedag. Inst., Leningrad); Soviet Phys.-Solid State, Vol. 3, pp. 85-87, July 1961

Photoelectric coloring (blue for red PbO and green for yellow PbO) of polycrystalline lead oxide is discussed. More than 100 samples were investigated and the experimental results are described in detail. Three factors (illumination of the polycrystal in the region of relatively high photosensitivity, a strong electric field and moisture) were found to be responsible for the coloring of PbO.

12,584 OPTICAL PROPERTIES AND PHOTOELECTRON EMISSION OF AMORPHOUS AND CRYSTALLINE GERMANIUM FILMS by P. G. Borzyak and R. D. Fedorovich (Phys. Inst. Acad. Sci.); Soviet Phys.-Solid State, Vol. 2, pp. 2683-2687, June 1961

The reflection, transmission and emission characteristics of amorphous and crystalline Ge films that were prepared under vacuum are discussed. Measurements were made under vacuum and during exposure to air; differences were noted after the first few seconds of exposure but further changes were not observed. Comparisons of the in vacuo and air characteristics of amorphous and crystalline films are discussed and graphically presented.

12,585 PHOTOELECTRIC EMISSION FROM CADMIUM TELLURIDE by J. J. Schear (Philips) and J. Van Laar (Riijksuniversiteit, Utrecht); Philips Res. Rep., Vol. 16, pp. 323-328, Aug. 1961

Photoelectric emission from both single crystal and evaporated layers of CdTe is discussed. Measurements on a CdTe crystal cleaved along the (110) plane in a high vacuum lead to a value of the work function ϕ equal to 5.90 ± 0.05 ev for a clean surface. The photon current vs photon energy curves show a tail at the long-wavelength end which is thought to be caused by impurities; measurements of crystals broken in air show a more pronounced tail tending to confirm this conclusion. Neglecting the tail effects, it is seen that there is no difference in photoemission from n- and p-type CdTe crystals. Results of measurements of CdTe and CdS crystals cleaved in air show a difference in photoelectric work function ϕ of about 1.0 ev; thus it is concluded that CdS and CdTe have approximately the same electron affinity of 4.5 ev.

12,586 FINE STRUCTURES OF PHOTOPROTONS FROM Si^{28} by K. Shoda, K. Kobayashi, S. Siina, K. Abe and M. Kimura (Tohoku U.); J. Phys. Soc. Japan, Vol. 16, pp. 1031-1032 (L), May 1961

Photoprotons from Si^{28} using 24 Mev bremsstrahlung have been investigated using a target consisting of the powder of natural Si deposited on an Au foil. The results show the energy spectrum of photoprotons from Si to be in close agreement with the calculated curve of the statistical model using the level density $\omega = C \exp [E/2.8]$ Mev^{-1}. The observed fine structures are

explained by a resonating group model which yields similar fine structures. The energy distribution of Si is compared with the cross section calculated from the inverse reaction of Al^{27} (P, γ) by detailed balance. The shapes of the cross sections coincide fairly well, though their energy scales are not the same, possibly because they are not exact inverse reactions.

12,587 THEORY OF TRANSVERSAL PHOTOMAGNETIC EFFECT by A. A. Grinberg (Leningrad Physico-Tech. Inst., USSR); Soviet Phys.-Solid State, Vol. 3, pp. 64-70, July 1961

Taking into account the precise mechanism of the scattering of current carriers, the theory of transversal photomagnetic effects in an anisotropic semiconductor is developed. The physical causes of the change in sign of the transversal effect in an anisotropic semiconductor is developed. The physical causes of the change in sign of the transversal effect in an isotropic semiconductor are also clarified.

ELECTROMAGNETIC PROPERTIES

12,588 THE INFLUENCE OF VARIATION OF THE ELECTRON MEAN FREE PATH ON THE OPTICAL CONSTANTS OF SPHERICAL METALLIC CRYSTALLITES [in French] by J. P. David and P. Dumontet; Comptes Rendus, Vol. 253, pp. 248-250, July 10, 1961

Spherical crystallites having radii of the order of the mean free path in the bulk metal, as well as smaller spheres, are investigated. It is assumed that the spheres contain enough free electrons so that the Boltzmann equation holds. Assuming a uniform electric field and an isotropic electron distribution, while neglecting magnetic effects, the electron distribution function is calculated. The current density in the field direction is then derived from this function. Curves showing the variation of the optical constants ν and χ, derived by using the previous results, are also included. From these curves it is concluded that the optical constants equal those of the bulk metal except for spheres of radius <40°A. It is shown that with infrared radiation of wavelength greater than several microns thin films of granular structure should exhibit pronounced variations of optical constants, while radiation in the visible light range does not affect the optical constants.

12,589 OPTICAL PROPERTIES OF EVAPORATED InSb FILMS by R. F. Potter and G. G. Kretschmer (U.S. Naval Ord. Labs.); J. Opt. Soc. Am., Vol. 51, pp. 693-696 (L), June 1961

Gunther's 3-temperature technique for preparing polycrystalline InSb films in vacuum by evaporating the constituents onto a substrate of controlled temperature is described. A method for measuring the transmittance and refractive index of the films at wavelengths from 2 to 15 μ is then discussed. The very evident dispersion is attributed to the small electron effective mass, which is determined. Two substrates were used: polished slips of glass, and polished single crystal slabs of CdS. The latter were found to be especially appropriate because of the similarity between their coefficient of expansion and that of InSb.

12,590 REFRACTIVE INDEX OF Cu_2O CRYSTALS IN REGION UP TO 10 μ by J. Pasternák (Czech. Acad. Sci., Prague); Czech. J. Phys., No. 5, Vol. 11B, pp. 374-376 (L), 1961

Measurements of the dependence of the refractive index on wavelength using a 12 x 8 mm prism, ground from a sample of Cu_2O, are reported. The results, obtained using a ZMR-2 infrared spectrometer, show that the refractive index decreases only very gradually to $n = 2.5$ for $\lambda \cong 6\mu$ after a sudden fall in the region of the visible spectrum. The value of $\epsilon_0 = n^2 = 6.2$ is close to the static dielectric constant given for stoichiometri Cu_2O, $\epsilon_{st} = 7.6$, which indicates the large part played by the covalent bond in this crystal.

12,591 LIGHT SCATTERING IN CRYSTALLINE POLYMERS by O. N. Trapeznikova, G. E. Novikova and S. V. Minakov; Optics and Spectrosc., Vol. 11, pp. 190-193, Sept. 1961

An investigation of the temperature dependence of the index of refraction of the crystalline and amorphous phases of polychloroprene and a determination of the degree of crystallization are discussed. The temperature dependence of the index of refraction was measured in 11 per cent and 7 per cent crystalline polychloroprene and also in amorphous polychloroprene. The mole refraction and the temperature dependence of the index of refraction of the crystalline phase were calculated. The intensity of the depolarized component of scattered light was shown to have a temperature dependence caused by changes of the relative index of refraction of the crystalline and amorphous phases with temperature. A method for quantitatively determining the relative amounts of the amorphous and crystalline phases in polychloroprene is proposed.

12,592 STUDY OF GERMANIUM BY TRANSPARENCY IN INFRARED LIGHT; DOUBLE REFRACTION OF SILICON AND GERMANIUM by C. Grandjean (Philips); Philips Res. Rep., Vol. 16, pp. 343-355, Aug. 1961

Measurements of the photoelastic constants of Ge and Si by apparatus consisting of a Nipkov disk and a PbS cell are reported. The apparatus allowed low definition examination in linearly or circularly polarized light. Photoelastic constants measured are: $k = 1.97 \pm 0.05$ for Si in [111] direction; $k = 0.026 \pm 0.04$ for Ge in [100] direction. Minimum stresses that can be detected in Ge or Si are also discussed with respect to the above constants.

12,593 THEORY OF LIGHT REFLECTION FROM A THIN ABSORBING FILM DEPOSITED ON A METAL by A. Vasicek (The Univ. Brno); Optics and Spectrosc., Vol. 11, pp. 128-130, Aug. 1961

An expression for light reflection from thin metallic or semiconductor layers is derived. The Stokes principle of reversibility is employed for the derivation of this formula, along with the condition that for zero thickness of the thin metallic layer the reflection is the same as in the case of a pure metallic substrate without any surface layer. The formula is derived for the two simplest cases: for a layer of low absorption (semiconducting layer), in which case it is possible to consider a large number of reflections in a thin layer, and for a strongly absorbing metallic layer, in which case one may, for practical purposes, consider only one reflection of light from a thin metallic layer.

Reflection Spectrum Determination of the Energy Gap of Binary $(ZnSe)_x$-$(CdSe)_y$ - See 12,429

12,594 CONCERNING THE CONNECTION BETWEEN CERTAIN THERMAL FEATURES OF SOLIDS by V. S. Neshpor (Acad. Sci., USSR); U.S. Gov. Res. Rep., Vol. 36, pp. 87-88(A), Aug. 20, 1961 AD 257 677

Quantitative relationships between the thermal features of solids such as the melting point, thermal coefficient of linear expansion, and heat-conductivity coefficient, and the solidity possibilities of solids under conditions of increased temperature are presented. The properties discussed include: the relation between the modulus of normal elasticity and the thermal coefficient of linear expansion; the relation between the Debye characteristic temperature of the solid and the modulus of its normal elasticity; the Debye characteristic temperature and the melting point of a substance; the relation between the melting point and coefficients of linear expansion of cubic and hexagonal metals, metallic compounds, and alkali halide salts; and the relation between the characteristic temperature and the melting point for metals and chemical compounds with a metallic type of connection.

12,595 PHYSICAL PROPERTIES OF HIGH TEMPERATURE MATERIALS. PART VI. ENTHALPY AND HEAT CAPACITY OF MAGNESIUM OXIDE, ZIRCONIUM OXIDE, AND ZIRCONIUM SILICATE FROM 0° TO 900°C by A. C. Victor and T. B. Douglas (Natl. Bu. Stand.); U.S. Gov. Res. Rep., Vol. 36, p. 75(A), Sept. 5, 1961 AD 258 383

Measurements of the heat contents of three refractory substances, MgO, ZrO, and $ZrSiO_3$ are reported. The measurements were made relative to 0°C at 100-degree intervals up to 900°C, using a precise drop calorimetric method. The MgO sample was of high purity but the other samples were of relatively low purity. No attempt was made to correct heat-content and heat-capacity values for impurities. Specific heats were derived from and described by equations in calories per gram-deg C. The specific heats from these equations are compared with values from the literature.

12,596 NUCLEAR CONTRIBUTION TO THE HEAT CAPACITY OF TERBIUM METAL by E. C. Heltemes and C. A. Swenson (Iowa State U.); J. Chem. Phys., Vol. 35, pp. 1264-1265, Oct. 1961

Measurement of the heat capacity of Tb metal between 0.25° and 1.0°K is reported. The high temperature data can be expressed as $C = 28R \times 10^{-3}/T^2$ cal/mole-deg which is in excellent agreement with the paramagnetic resonance experiments of Baker and Bleany on terbium ethyl sulfate. The data are compared with a Shottkey formula for the heat capacity, assuming equal spacing between the nuclear hyperfine levels with an over-all spacing $\Delta = 0.45$°K, corresponding to the high temperature expression above. The agreement is within experimental error except at the very lowest temperatures obtained. The effective field at the nucleus of the terbium atom can be calculated and is found to be $H_{eff} = 4 \times 10^6$ gauss.

12,597 SPECIFIC HEATS OF SOME CUBIC SUPERCONDUCTING TITANIUM-MOLYBDENUM ALLOYS BETWEEN 1.1° AND 4.3°K by R. R. Hake (Atomics Intl., NA Aviation); Phys. Rev., Vol. 123, pp. 1986-1994, Sept. 15, 1961

Measurements of the specific heats of four bcc Ti-Mo alloys between 1.1° and 4.3°K and at atomic fractional Mo concentrations between 0.0625 and 0.0860 are given. The normal state molar specific heats can be represented by the usual expression $C_n = \gamma T + \beta T^3$, where it is assumed that $\gamma \alpha N(E_F)$, the energy density of electronic states at the Fermi energy, and $\beta \alpha \theta_D^{-3}$. For each of the alloys the apparent electronic superconducting state specific heat for $1.3 < (T_c/T) < 2.6$ can be represented as $C_{es}/\gamma T_c = a \exp(-bT_c/T)$ where $a = 10.5$, $b = 1.52$, and the superconducting transition temperature, T_c, is taken as the midpoint of the rather broad (≈ 0.45°K) superconducting transition. The measured values of T_c, θ_D, and γ are all rapidly varying and nearly linear functions of atomic fractional Mo concentration, f. At the mean solute concentration ($f = 0.0742$): $T_c = 2.59$°K, $d\ell n\, T_c/df = 16.7$; $\theta_D = 337$°K, $d\ell n\, \theta_D/df = -6.2$; $\gamma = 5.45$ millijoules/mole $(°K)^2$, $d\ell n\, \gamma/df = d\ell n\, N(E_F)/df = +7.7$. On the basis of the Bardeen-Cooper-Schrieffer theory of superconductivity, the relative variations of T_c, θ_D, and $N(E_F)$ indicate that the electron-electron interaction parameter of that theory, A, is a relatively slowly varying function of solute concentration ($d\ell n\, A/df = -3.0$).

12,598 ATOMIC FORCES AND THERMAL EFFECTS IN SOLIDS by H. B. Rosenstock (U.S. Naval Res. Lab.); J. Chem. Phys., Vol. 35, pp. 420-423, Aug. 1961

The vanishing of an interatomic force constant in a solid which can produce specific heat anomalies similar to the well known "lambda point" phenomena is discussed. The lambda points are often associated with second- or higher-order phase changes. A decrease in the strength of one or more of the atomic force constants is expected to produce an increase in the low-temperature specific heat of the solid. Specific heat anomalies that might appear in a solid if one of the interatomic force constants changes with temperature and approaches zero at some critical temperature are calculated and compared with observed lambda points. An example of the method is given using a monatomic simple cubic lattice with forces between 1st and 4th neighbors.

12,599 HIGH-TEMPERATURE THERMAL CONDUCTIVITY MEASUREMENTS IN SEMICONDUCTORS by R. G. Morris (S. Dakota School of Mines and Tech.); U.S. Gov. Res. Rep., Vol. 36, p. S-58(A), Aug. 5, 1961 PB 171 837

Measurements of the contact and bulk thermal conductivities of semiconductors, including Bi_2Te_3 and Si, at above room temperatures are reported. The method requires the use of a standard of known conductivity. Measurements on p-type polycrystalline Bi_2Te_3 have been made up to temperatures as high as 330°C. A series arrangement is used whereby the sample is sandwiched between two standards. The standards are soldered directly to the heat source and sink. Chromel-alumel thermocouples with butt-welded junctions are used and temperature differences are measured by means of a comparator circuit. The temperature of the sample is monitored continuously on a self-balancing recording potentiometer. The results indicate that the relationship between the heat and the conductivity is usually linear but is affected by radiation or conduction losses or gains.

12,600 THERMAL CONDUCTIVITY IN TWO-PHASE ALLOYS by J. B. Schroeder (Ohio Semicon.); J. Appl. Phys., Vol. 32, pp. 1798-1799(L), Sept. 1961

A theory to account for spuriously high experimental values of the thermal conductivity of a heterogeneous sample is proposed and analyzed. The generation of a Seebeck EMF between adjacent chemically differing grains and consequent heat transfer by the Peltier effect is assumed. The analysis is confined to

the case of a lamellar grain structure which is parallel to the heat current. A simple model indicates that the proposed mechanism cannot account for the high experimental values when the minor phase of the two-phase alloy is present in less than 10 per cent volume.

12,601 THEORY OF HEAT CONDUCTIVITY IN DIELECTRICS AT TEMPERATURES BELOW THE DEBYE-TEMPERATURE by V. M. Agranovich and Yu. V. Konobeev; Soviet Phys.-Solid State, Vol. 3, pp. 71-72, July 1961

A solution of the Boltzmann equation developed by Ziman, using the method of least squares is given. The expression for the coefficient of heat conductivity (χ) obtained explains the behavior of χ in the region of low temperature qualitatively as well as Ziman's formula. A simplified expression for χ, taking into account the scattering of phonons on the impurities (the most important process in these regions) gave a value 2-3 times greater than that calculated by Ziman's formula. However, the calculated value was found to be in better agreement with experimental results.

12,602 CHANGES IN THE THERMAL CONDUCTIVITY OF TIN, BISMUTH AND GALLIUM ON MELTING by B. D. Pashaev (Dagestan State U.); Soviet Phys.-Solid State, Vol. 3, pp. 303-305, Aug. 1961

Measurements of the thermal conductivities of Sn, Bi and Ga made by the plane compensation method of Amirkhanov are reported. A sample was placed in an asbestos-current ring and fixed between a heater and a refrigerator. The heat losses of the main heater were compensated for by auxiliary heaters. The sample temperature and heater power were measured. Total error in the thermal conductivity was under 5 per cent. The conductivity of Sn was found to fall by a factor of 1.82 on melting, corresponding to a rise in the coordination number from 6 to 10. Above the melting point, conductivity continued to fall. The conductivity of Bi fell, then rose just before melting. On melting it doubled, corresponding to an increase in co-ordination number from 3-3 to 7-8; it then continued to rise. The conductivity of Ga was independent of temperature before melting, rose sharply on melting and immediately dropped again; it then continued to rise, having two inflection points. The observations are in accordance with previous work and explanations for the phenomena are given.

12,603 THE EFFECT OF THALLIUM ON THE THERMAL CONDUCTIVITY OF POLYCRYSTALLINE SELENIUM by G. B. Aboullaev, M. I. Aliev and S. A. Akhundova (Azerbaidzhan State U.); Soviet Phys.-Solid State, Vol. 3, pp. 234-235, Aug. 1961

Measurements of the thermal conductivity of Se samples containing from 0.0125 to 1.5 wt per cent Tl are reported. The samples were made by melting high purity Se and Tl_2Se in 10^{-4}mm Hg vacuum, and were annealed before the measurements for an hour at 110° and 210°C. The thermal conductivity was measured using an instrument with a guard ring and a thermocouple at temperatures between 20° and 90°C. The thermal conductivity λ varied linearly with temperature T, $\lambda = \lambda_0 - \alpha T$. λ and α varied with the amount of Tl present, minima occurring at concentrations of about 0.05 per cent. The results may be explained by assuming that the mechanism of the effect of Tl on the conductivity is different at high and low concentrations.

Thermal Conductivity of Group V-b Metal Superconductors - See 12,494

12,604 THERMOELECTRIC MATERIALS by H. E. Wenden, S. R. Ali Zaidi and T. S. Shevlin (Ohio State U.); U.S. Gov. Res. Rep., Vol. 36, p. 100(A), Aug. 20, 1961 AD 258 340

An apparatus using metal tubes which was fabricated for studying the differential Seebeck coefficient of liquid materials is described. Ceramic spacers about 1/2-in long whose outside diameters were the same as the inside diameter of the outer metal tube were placed on the inner stainless tube at 1/2-in intervals. The space between the ceramic spacers was filled with powdered $Na_20.6V_2O_5$(I). Other components included an outer stainless tube, a water cooling coil, a thermocouple for the outside temperature of the outer tube, and a thermocouple for the inside temperature of the inner tube. The composite tube was placed inside a tubular furnace so that only the central part of the tube was heated. A very small EMF was generated for various temperature differences. A similar composite tube, only 1-in long with I in the middle and with the ends sealed by ceramic spacers, was also built. In this case a large EMF was generated for a small temperature difference.

12,605 THERMOELECTRIC POWER OF SINGLE CRYSTALS OF GALLIUM by D. Horner (Roy. Mil. Coll. Sci.); Nature, Vol. 191, pp. 58-59(L), July 1, 1961

The thermoelectric power of single crystals of Ga is discussed. The crystals were grown by passing a freezing plane through the super-cooled melt; three crystals were produced in which the red- and crystallographic-axes coincided to 1° or better. The lower ends of the crystals were placed in alcohol, while the upper ends protruded into a 'Perspex' container filled with a mixture of ice and water. Commercial Cu wire, annealed to cherry red heat, was used as reference material. A Cu lead was welded to the end of the crystal, and Seebeck EMF's with respect to Cu were measured with a Cambridge Vernier potentiometer. One junction was maintained at 0°C while the temperature of the other was successively varied between +30° and -70°C. The crystals were aligned along the (100), (010) and (001) axes respectively. The absolute thermoelectric power (Q^*) of Ga in the three directions was calculated using the known value of the absolute thermoelectric power of Cu, and was expressed in the form $Q^* = A + BT$ where T is the temperature of the variable junction and A and B constants. The ratio of the A coefficients is not as large as those of electrical or thermal conductivity, and some interesting remarks are made about the B coefficients.

12,606 THERMOELECTRIC BEHAVIOR OF RUTILE by K. Sakata (Natl. Res. Inst. Metals); J. Phys. Soc. Japan, Vol. 16, p. 1026(L), May 1961

Measurements of the temperature dependence of conductivity and of the thermo EMF for rutile samples sintered in different oxygen atmospheres are given. Experimental evidence indicates that the value of the forbidden gap energy is 3.0 ev and that the Fermi level approaches the middle of the forbidden gap, 1.55 ev, in the intrinsic region. The conductivity behavior and the corresponding thermo EMF suggest that in highly reduced rutile metallic conduction takes place in the narrow α-band and that intrinsic conduction begins at about 1150°C.

12,607 THE THERMALLY STIMULATED EMF ARISING IN IRRADIATED SOLID HYDROCARBONS IN THE PRESENCE OF A TEMPERATURE GRADIENT by E. L. Frankevich and V. L.

HERMAL PROPERTIES (Cont'd)

al'roze (Inst. Chem. Phys., Moscow); Soviet Phys.-Solid ate, Vol. 3, pp. 131-132, July 1961

hermally stimulated EMF's arising in sample paraffin plates nd in polyethylene irradiated by electrons at low temperatures e discussed. The samples studied, 1 x 3 x 5 mm in size, were laced in a vacuum chamber between two electrodes, one of hich served as a conductor of cold and the other was con- ected to the thread of the electrometer. The magnitude of e EMF between the plates, which is a function of the irradi- ion dose (from 1 to 1000 mrad) and the temperature drop xperimentally <20°K drop), is between 50 and 1000 volts ic] maximum. Isothermal warming of the samples produced EMF. Such an EMF is considered to be associated with the ppearance within the mass of current carriers which are cap- red by some type of "small traps" in the irradiation process d its temperature dependence is due to the inhomogeneity in e current carrier density within the volume. An equivalent ectric circuit for the sample irradiated at low temperature is nstructed; the circuit is represented by a series of capacitors d resistors.

ermal EMF of:
MnO - See 12,693
HgTe - See 12,246

,608 INVESTIGATION OF THE NERNST-ETTINGSHAUSEN HERMOMAGNETIC EFFECTS IN SOLID SOLUTIONS OF THE STEM InSb-AlSb by Ya. Agaev, O. V. Emel'yanenko and N. Nasledov (Leningrad Inst. Phys. and Tech.); Soviet ys.-Solid State, Vol. 3, pp. 141-143, July 1961

easurements of the temperature dependence of the Nernst- ttingshausen coefficient in four different solid solutions of Sb-AlSb are reported. It is concluded that the regular change the coefficient of the transverse N-E effect with composition, hich can be adequately accounted for on a quantitative basis the change in mobility of the current carriers and the width the forbidden zone in the compositions investigated, points the fact that the electron processes which determine the ermomagnetic effect have in general the same character in e solid solutions as in the two components of the system. ther, it is concluded that the negative sign of N-E constant solid solutions in the combined conductivity region is evi- nce of the absence of any appreciable scattering of current riers at the alloy lattice.

,609 THE THERMOMAGNETIC BEHAVIOR OF COBALT RRITE by L. F. Bates and A. J. Pacey (U. Nottingham); oc. Phys. Soc., Vol. 77, pp. 567-575, Mar. 1961

mall heat changes which accompany the magnetization of balt ferrite rods are discussed. One rod had been heat- eated to destroy uniaxial anisotropy and the other was un- eated. A new method of analyzing the results is described. hile its application to these specimens may not have led to nclusive results, it appears to give useful information when plied to materials of less complex magnetic behavior.

,610 THE THERMAL EXPANSION OF THE CRYSTALLINE EDIUM. PART II. THE COEFFICIENT OF EXPANSION [in ench] by J. Laval (Coll. France, Paris); J. Phys. Radium, l. 22, pp. 465-471, Aug.-Sept. 1961

expression for the linear expansion coefficient of a crystal d its derivative with respect to temperature are derived. The expansion coefficient is directly related to the potential energy and to the elementary vibrations of the crystal. It is found that the expansion coefficient increases with temperature, roughly as the specific heat at constant volume. It is annulled at absolute zero and increases with the absolute temperature according to a parabolic law when the temperature approaches the melting point.

12,611 ON THE EVALUATION OF THE COEFFICIENTS OF THERMAL EXPANSION OF CRYSTALS FROM X-RAY DATA by V. T. Deshpande and V. M. Mudholker (Osmania U.); Indian J. Phys., Vol. 44, pp. 434-436, Aug. 1961

The evaluation of the thermal expansion coefficient of $NaClO_3$ by various methods is discussed. The first method used is to obtain the mean value of the derivative da/dt over small intervals of temperature (where "a" is the lattice constant). The second method used is to express "a" as a quadratic function of temperature, then differentiate it with respect to temperature. This procedure is more rigorous but the thermal expansion coefficient may not be a linear function of temperature. Although the linear character can be removed if a cubic function of "t" is used, the calculations involved are rather lengthy. It is concluded that the first method is preferred to calculate the temperature variation of the thermal expansion coefficient.

12,612 ANHARMONICITY AND THE THERMAL EXPANSION OF SOLIDS by G. C. Fletcher (U. Sydney); Austl. J. Phys., Vol. 14, pp. 420-431, Sept. 1961

Using many-particle perturbation theory, the thermal expansion of NaCl is calculated. The lowest order anharmonic terms in the potential energy of the crystal are included in the calculations. The results are disappointing; agreement with experiment is poor except at low and moderate temperatures. One reason for this poor agreement is the poor convergence of a method based on the series expansion of the crystal potential in terms of particle displacements. This point is further illustrated by calculations of specific heat and compressibility.

12,613 THE ANOMALOUS THERMAL EXPANSION OF CHROMIUM by G. K. White (CSIRO); Austl. J. Phys., Vol. 14, pp. 359-367, Sept. 1961

Experimental data on the linear thermal expansion (between 20° and 50°C) of specimens of high-purity Cr which confirm the existence of an anomaly centered at 38°C are discussed. The exact shape of this expansion anomaly between about 37° and 39°C varies markedly from sample to sample, but outside this narrow temperature interval the behavior is more regular and seemingly related to antiferromagnetic ordering. Data on expansion are compared with other recent observations on heat capacity, magnetic susceptibility, and electrical resistivity of high-purity Cr. It is suggested that an electronic term in the expansion coefficient, observed below 20°K to be negative, is sensitive to band structure and may be partly responsible for the change in expansion coefficient.

Thermal Expansion Coefficients of Si - See 12,253

MECHANICAL PROPERTIES

12,614 LOGNORMAL DISTRIBUTION FUNCTION FOR DESCRIBING ANELASTIC AND OTHER RELAXATION PROCESSES. PART II. DATA ANALYSIS AND APPLICATIONS by A. S. Nowick and B. S. Berry (IBM); IBM J. Res. and Dev., Vol. 5,

pp. 312-320, Oct. 1961

Applications of a relaxation process governed by a lognormal distribution of relaxation times is described. The experimental determination of the basic parameters is shown to require a number of corrections to the usual type of dynamical data. General expressions for these corrections are derived, and the data necessary for their use are presented in graphical form. Specific examples of the application of the theory to the analysis of anelastic relaxation phenomena are presented.

12,615 THE ELECTRONIC CONTRIBUTION TO THE ELASTIC PROPERTIES OF GERMANIUM by R. W. Keyes (IBM); IBM J. Res. and Dev., Vol. 5, pp. 266-278, Oct. 1961

Theories of several elastic effects resulting from the contribution of electrons to the strain energy function of Ge show that these effects are appreciably changed by doping with donor and acceptor impurities. The properties considered are: 1) volume, 2) elastic constants of degenerate n-type material, 3) third-order elastic constants of degenerate n-type material, 4) elastic constants of degenerate p-type material, 5) elastic constants of material containing electrons bound to donors, and 6) elastic constants of material containing electrons bound to pairs of donor atoms. The most striking effect is found for degenerate n-type Ge, for which the theory predicts that the coefficient c_{44} can be lowered by 8 per cent with attainable doping levels.

12,616 EXPERIMENTAL EVALUATION OF PULSE ECHO TECHNIQUE by J. A. Corll (Case Inst. Tech.); U.S. Gov. Res. Rep., Vol. 36, pp. 93-94(A), Aug. 20, 1961 AD 258 023

A systematic experimental evaluation of the ultrasonic pulse echo technique for the determination of elastic constants and pressure derivatives, made by inter-comparing the directly measured values of these two quantities which are associated with wave propagation in three directions, is presented. The measurements were made on 3 single crystals of Ag with 10 Mc ultrasonic gear and a pressure range to 9,500 atmospheres. Comparison of the measured values of the elastic constants yielded a maximum discrepancy of 0.3 per cent. A similar comparison of the measured values of the pressure derivatives yielded a maximum discrepancy of 3.5 per cent.

12,617 ELASTIC CONSTANTS OF TiC AND TiB_2 by J. J. Gilman and B. W. Roberts (GE); J. Appl. Phys., Vol. 32, p. 1405(L), July 1961

Possible anisotropy in the elastic constants of TiC and TiB_2 is discussed. Measurements are compared with the microhardness and elastic constants of diamond and sapphire to determine the degree of anisotropy and to correlate elastic properties with hardness. The pulse-echo technique was employed, using velocity measurements of sound waves in the <100> and <111> directions. TiB_2 was found to approach diamond in resistance to dilational strains but has considerably less resistance to shearing strains, reflecting its metallic binding rather than the covalent binding of diamond. TiC is nearly elastically isotropic and the relation $C_{12} = C_{44}$ is approximately obeyed while $2C_{44}/(C_{11}-C_{12}) = 0.91$.

12,618 CHANGES OF ELASTIC MODULUS ASSOCIATED WITH INTERNAL FRICTION IN SODIUM CHLORIDE by R. W. Whitworth (Imperial Coll.); Phil. Mag., Vol. 6, pp. 1115-1118, Sept. 1961

An extension of previous measurements of the amplitude-dependent internal friction of NaCl at 90 kc and room temperature to study the corresponding changes in Young's modulus is reported. It is concluded that the motion of dislocations giving rise to the amplitude-dependent damping lags in phase behind the stress by about 30° to 60°. Previously described changes damping produced by high amplitude vibration are associated with corresponding changes in the modulus defect.

12,619 PHOTOELASTIC BEHAVIOR OF RUBIDIUM HALIDES by T. S. Narasimhamurty (Michigan State U.); J. Opt. Soc. Am., Vol. 51, pp. 914(L), Aug. 1961

Stress-birefringence measurements on rubidium halides at room temperature and $\lambda = 5893$ are reported. The results confirm Mueller's prediction that $(q_{11}-q_{12})$ should be positive and q_{44} negative. Comparison with the values of q's for potassium halides is discussed. The stress birefringence of rubidium halides is much greater than that of potassium halides, though their behavior is not so widely different with respect to their elastic and optical properties.

12,620 PHOTOELASTIC CONSTANTS OF AMMONIUM DIHYDROGEN PHOSPHATE (ADP) by K. Achyuthan and M. A. Breazeale (Michigan State U.); J. Opt. Soc. Am., Vol. 51, pp. 914(L), Aug. 1961

The ratios of the strain constants in ADP p_{12}/p_{11}, p_{31}/p_{11}, and p_{13}/p_{33}, determined by using Mueller's ultrasonic technique, are reported. A complete set of strain constants p_{ij}'s can be obtained by knowing the ratios of these constants along with the photoelastic constants q_{ij}'s and elastic constants c_{ij}'s. These results combined with Carpenter's data for q_{ij}'s and Bechmann's data for c_{ij}'s provide the desired data p_{ij}'s which are listed. The limit of accuracy of these quantities is discussed.

12,621 THE PHENOMENON OF "PHOTOINELASTICITY" IN AgCl by Yu. Kh. Velikov (Moscow Steel Inst.); Soviet Phys.-Solid State, Vol. 3, p. 400, Aug. 1961

The internal friction of AgCl which has previously been exposed to ultraviolet light was measured by means of torsional vibrations of small amplitude at a frequency of 1 cps. An annealed single crystal specimen was used. In illumination, the internal friction increases and eventually becomes constant; when illumination ceases there is an immediate drop to a lower constant level. This phenomenon is repeated on subsequent exposures. The fall is attributed to the migration of color centers to dislocations and to their reduction at silver atoms, as a result of which the length of the dislocation between points of attachment should decrease. The rise is attributed to ionization of the silver atoms.

12,622 A UNIFIED STATISTICAL THEORY OF STRENGTH OF SOLID BODIES by S. D. Volkov (Acad. Sci., USSR); U. S. Gov. Res. Rep., Vol. 36, p. 86(A), Sept. 5, 1961 AD 258 814

A unified theory of strength which can be used both in the mechanism of fracture and to derive a single set of conditions of strength which will fit all stress states is developed. By applying statistical mechanics to a model of a quasi-isotropic single-phase polycrystal, it can be demonstrated that the modulus of distribution of volumes V of crystallites according to stresses is a function of the external load. This circumstance is utilized to provide a unified explanation of cleavage fracture caused by tension or compression of brittle bodies; the fracture occurs through the action of tensile stresses.

MECHANICAL PROPERTIES (Cont'd)

Tensile Strength of LiF - See 12,297

Yield Stress of Fe - See 12,300

Slip Distribution Effects on Fracture in MgO - See 12,298

Fatigue in:
InSb - See 12,299
Ti and Ti Alloys - See 12,282

Plasticity of Ionic and Metal Crystals - See 12,330

Measurements of Relative Rates of Plastic Flow in Metals by Contact Ferroelectric Effect - See 12,453

Dislocation Strain Hardening in fcc Metals - See 12,302

12,623 MULTIPLE SHOCK WAVE STRUCTURES IN POLYCRYSTALLINE FERROELECTRICS by C. E. Reynolds and G. E. Seay (U. California, Los Alamos); J. Appl. Phys., Vol. 32, p. 401 (L), July 1961

An experiment which confirms the existence of two-wave shock structures, under explosive loading, in three ferroelectric ceramics is described. They are: (1) $Pb(Zr_{0.52}, Ti_{0.48})O_3$ with a 1 wt per cent addition of Nb_2O_5, (2) pure $BaTiO_3$, and (3) 95 per cent $BaTiO_3$ and 5 per cent $CaTiO_3$. An explosive-driven impedance-mismatch attenuator system was used to transmit the shock. The ceramic was coated with a conducting material to short-circuit the electrical charge released. Free-surface velocities were measured by the knife-edge technique, and shock velocities were determined using transit times measured with (a) shock-detecting ferroelectric wafers, and (b) a streak camera.

12,624 TECHNIQUES FOR THE DETERMINATION OF ULTRASONIC ATTENUATION IN FUSED SILICA by R. F. Weeks (Brew); 1961 IRE Intl. Conv. Rec., Part 6, pp. 296-303

The frequency dependence of the intrinsic ultrasonic attenuation in fused silica is discussed. Studies using conventional delay lines are complicated by the difficulty of measuring transducer losses. A second technique makes use of two optical measurements of the integrated acoustic flux within a small polished test sample. This technique is in principle independent of frequency, transducer radiation pattern and the dimensions of the sample. These two techniques are discussed in detail and measurements are presented.

12,625 ULTRASONIC ATTENUATION AND VELOCITY MEASUREMENTS IN QUARTZ by T. Fitzgerald and R. Truell (Brown U.); U.S. Gov. Res. Rep., Vol. 36, p. 78(A), Aug. 1, 1961 AD 257 086

The frequency dependence of the attenuation of compressional waves in X-cut quartz is discussed. The dependence obeys an approximate square law consistant with the dislocation damping theory which predicts a square-law frequency dependence up to a resonant frequency. The behavior of the attenuation as a function of temperature below 100°K is in agreement with that predicted by a phonon-phonon process. Above 40°K the thermal conductivity varies approximately as 1/T while the specific heat increases linearly with the temperature between 40° and 150°K. The temperature dependence of the velocity measured in this experiment indicates that it remains constant at a value of 5.75×10^6 cm/sec to within ± 0.02 per cent. In the region where the attenuation is rapidly changing there is apparently no associated velocity change.

12,626 FUNDAMENTAL STUDIES OF THE PROPERTIES OF NATURAL AND SYNTHETIC QUARTZ CRYSTALS by J. C. King (Bell Labs.); U.S. Gov. Res. Rep., Vol. 36, p. 26(A), Sept. 5, 1961 AD 258 444

Further measurement of acoustic absorption at elevated and low temperatures is discussed. It has been established that contact metal electrodes used in electrolyzing quartz yield incompletely treated material and that in this respect vapor-plated gold electrodes are superior. The turnover point (temperature where $df/dt = 0$, for a curve of frequency vs temperature) has been studied as a function of angle of rotation from the Y-axis. A resonator cut at θ equal to +53 degrees from the Y-axis has a turnover point at 535°C. This has facilitated the measurement of acoustic absorption at elevated temperatures. From preliminary results on these high-angle crystals, it appears feasible to fabricate a high-temperature resonator operating at its turnover point. One specimen of electrolyzed synthetic quartz operating at 5 Mc has yielded a value of Q in excess of 600,000 at 500°C.

12,627 ON THE PROPAGATION OF WAVES IN AN ELECTROMAGNETIC ELASTIC SOLID by J. W. Dunkin and A. C. Eringen (Purdue U.); U.S. Gov. Res. Rep., Vol. 36, p. 32 (A), Aug. 5, 1961 AD 257 476

The coupling of electromagnetic and elastic waves is considered from the standpoint of linear elasticity and a linearized electromagnetic theory. The problem of plane waves traveling through a uniform magnetostatic field is considered and couplings of the waves are studied. An investigation of the same problem for a uniform electrostatic field shows that the usual plane waves propagate without any change in their phase velocities but that the mechanical waves are accompanied by small fluctuating electromagnetic fields. The problem of the vibration of a free infinite elastic plate in a large magnetostatic field is examined under the assumption that the resulting electromagnetic fields are quasi-stationary. Frequency equations are obtained for both symmetric and antisymmetric vibrations and the damping caused by the field for both the first two symmetric and antisymmetric modes is obtained as a linear correction to the usual free plate frequencies.

12,628 QUANTUM EFFECTS IN DIFFUSION: INTERNAL FRICTION DUE TO HYDROGEN AND DEUTERIUM DISSOLVED IN α-IRON by W. R. Heller (IBM); Acta Metal., Vol. 9, pp. 600-613, June 1961

An experimental and theoretical study of internal friction due to hydrogen and deuterium dissolved in α-iron is discussed. A torsion pendulum is employed which can be used in a Collins cryostat at temperatures in the range 4.2°-300°K. A peak of damping is found in the range 105°-120°K (corresponding to that earlier studied by Gensamer and co-workers). An additional peak associated with hydrogen is found at 30°K and, correspondingly, one associated with deuterium is found at 35°K. Magneto-mechanical damping is found at all temperatures, with a peak in the range 4.2°-15°K depending upon the treatment of the metal specimen. The isotope-shifted peaks may be due to atoms dissolved in the undistorted lattice, whose motion must be treated quantum-mechanically to account for the experimental results. Tunneling and localized lattice distortions around the dissolved atom are suggested by the data.

Internal Friction in:
α-AgCd - See 12,345
Steel - See 12,323

SOLID STATE DEVICES

GENERAL

12,629 PUTTING PRESSURE ON ELECTRONIC CIRCUIT COMPONENTS by C.L. Buchanan and M. Flata (U.S. Naval Res. Lab.); ISA J., Vol. 8, pp. 38-42, Nov. 1961

Tests of electronic circuit components under enormous hydrostatic pressures (10,000 psig) are described. Film deposition type resistors are nearly independent of pressure, while standard carbon composition resistors are strongly pressure dependent and may be employed for use as pressure transducers. Capacitors have all worked satisfactorily at pressures to 10,000 psig except those sealed with air entrapped. Changes of magnetic materials were not great except in isolated cases. Some subminiature tubes also performed satisfactorily. Many semiconductor devices failed to withstand the pressures due to the common practice of sealing in a metal case with some inert material. Most types of small transistors however can be potted in plastic resins and made to withstand high pressures. Circuits can be constructed of lightweight materials and encapsulated in filled resins to obtain operating units lighter than water and capable of withstanding high pressures. Such techniques may become necessary in future construction of oceanographic or acoustic instrumentation systems.

12,630 THE EFFECT OF NUCLEAR RADIATION ON ELECTRONIC COMPONENTS by D.J. Hamman, W.E. Chapin et al. (Radiation Effects Info. Ctr.); U.S. Gov. Res. Rep., Vol. 36, p. 79(A), Oct. 5, 1961 AD 260 303

Present knowledge on the effects of nuclear radiation on basic electronic parts is summarized. The results are intended to provide a basis for judging the merits of the parts when they are to be used in circuitry that will be exposed to a radiation environment. Some of the data can be considered as design oriented to the extent that they indicate radiation levels at which the parts can be expected to perform satisfactorily.

RESISTORS

12,631 PROPERTIES OF FLAT NICKEL-CHROMIUM FILM RESISTORS by W.E. Isler (Diamond Ord. Fuze Labs.); U.S. Gov. Res. Rep., Vol. 36, p. 22(A), Dec. 5, 1961 AD 263 388

The preparation and properties of vacuum-deposited resistors with values ranging from 35 to 4700 ohms/sq in are discussed. The resistors were made by first depositing a layer of Ni-Cr alloy on glass substrates and then a protective layer of SiO. Heating at 250°C for 10 min caused the values of the resistors to increase by 95 per cent for the thinnest films and by 0.3 per cent for the thickest. A shelf-life study of the test resistors showed most of them to be stable within ±10 per cent over a period of more than 3000 hr of storage at room temperature; for the same resistors, the change due to storage in air at 70°C for 2900 hr ranged from 4.5 to 27 per cent. It was found that reproducible resistors were more readily obtained when the end contacts or electrodes were deposited over the resistor films than when this procedure was reversed. Power capacities up to 1.7 w/sq cm were measured. Excluding annealing effects, the values at temperature coefficient of resistance varied from 4 to 220 ppm/°C.

Effects of Temperature on Pt Resistors - See 12,477

DIODES

12,632 ELECTROLUMINESCENCE IN GALLIUM PHOSPHIDE SINGLE CRYSTALS by S. Iizima and M. Kikuchi (Electrotech. Lab., Tokyo); J. Phys. Soc. Japan, Vol. 16, pp. 1784-1785 (L), Sept. 1961

Current-voltage characteristics and electroluminescence observed in point contact GaP diodes fabricated from GaP crystals prepared in argon at elevated temperatures are discussed. Good rectification characteristics were obtained. An orange-yellow emission was observed at breakdown, i.e., about 5 to 10 volts. The emission appeared over the whole crystal but is probably due to the internal reflection of the light emitted at the point contact. No electroluminescence was observed with forward bias, probably due to the presence of deathnium levels produced by the large amount of impurities unintentionally introduced into the crystals. The current versus light intensity data suggest that bimolecular radiative recombination is the principal cause of the emission.

12,633 ELECTRICAL TRANSLATOR DEVICE AND METHOD OF MANUFACTURE by D.S. Jenkins (Sylvania); U.S. Pat. 3,002,134, Issued Sept. 26, 1961

The preparation of point contact electrodes for use in point contact diodes is described. A coil is made of the lead wire by winding the wire on a mandrel which has a diameter slightly larger than the diameter of the cat whisker. The coil is placed in a jig with the uncoiled portion of the lead wire extending downwards from the jig. The much narrower cat whisker wire is then threaded through a central hole in a punch which is above and axially aligned with the coil so that it extends into the coil. Pressure is applied to the punch so that the cat whisker and the lead wire are pressed together. The cat whisker is formed into an S-shape and is cut from the wire extending through the punch.

12,634 CONSTRUCTION AND CHARACTERISTICS OF SILVER BONDED DIODES by S. Kita (Nippon Tel. and Tel.); Rev. Elect. Commun. Lab. Japan, Vol. NTT-9, pp. 26-30, Jan.-Feb. 1961

A Ag-bonded diode developed for use in parametric amplifiers is described. The diode was produced by bringing the tip of a Ag whisker containing a small amount of Ga into contact with an n-type Ge wafer, and electrically forming the device. The impedance of the diode was measured with a coaxial type standing wave detector at room temperature and at 100°K. The minimum barrier capacitance was about 0.1 pf, the series resistance 10 ohms, and the cutoff frequency at breakdown voltage 200 Gc.

12,635 NEGATIVE RESISTANCE DIODE HANDLES HIGH POWER by A.P. Schmid, Jr., (Raytheon); Electronics, Vol. 34, pp. 44-46, Aug. 25, 1961

A new semiconductor diode with high power-handling capability is described. The bonded NR diode is an n^+n junction device fabricated by pulse-bonding a doped Au wire to a high-resistivity n-type semiconductor. The input and output circuits

ay be coupled through the diode with some degree of isolation rnished. The device reactance shows strong frequency-dependent effects at low frequencies. In switch operation, a 32 w output pulse has been produced from a 3 μw input pulse. he diode exhibits switching speeds of 3 to 10 nsec and has een switched by 3 nsec pulses. The highest oscillation frequency attained is about 200 Mc. Power output was 0.8 mw.

2,636 GERMANIUM-DOPED GALLIUM ARSENIDE TUNNEL IODES by R. Solomon (Hughes Semicon.), R. Newman, and .R. Kyle (Hughes Res. Lab.); J. Electrochem. Soc., Vol. 08, pp. 716(L), July 1961

he preparation of degenerate p-type GaAs using Ge as the ppant is described. Tunnel diodes fabricated from this material khibit electrical characteristics identical to those fabricated om Zn-doped material.

2,637 APPLICATION OF TUNNELING TO ACTIVE DIODES N. Holonyak, Jr. (GE); U.S. Gov. Res. Rep., Vol. 36, . S-19(A), Sept. 5, 1961 AD 257 423

n all-Ge-doped GaAs tunnel diode and its properties are escribed. The dependence of hump tunnel currents upon minority carrier injection in a variety of tunnel diodes is outned. Some of the measured properties of Mn-doped GaAs e presented. A description is given of a simple means of asking against epitaxial GaAs crystal growth on a GaAs seed. he properties of Mn-doped GaAs tunnel diodes are described.

2,638 APPLICATIONS OF TUNNELING TO ACTIVE DIODES (GE Res. Lab.); U.S. Gov. Res. Rep., Vol. 36, p. -21(A), Sept. 5, 1961 AD 257 387

he characteristics of forward injection failure in GaAs tunnel odes are summarized. A model involving rapidly diffusing purities and junction traps is proposed as the failure mechasm. The diffusion and solubility of Cu in heavily doped GaAs ave been examined. This impurity has been found to diffuse pidly at low temperatures in p-type GaAs and is suspected of ing an important contributor to the failure process. Drift periments have shown that the rapidly diffusing species is charged in p-type material, contrary to expectations. The fectiveness of various procedures for removing Cu from the face or volume of GaAs specimens has been studied. The pendence of tunneling upon uniaxial strain in Ge has also en studied and a theoretical model which qualitatively acounts for the data is presented. As and Sb doped junctions have quite differently and it is expected that further study of ese differences will provide and understanding of the phononisisted and unassisted components of tunneling in these materials. The results of some measurements on n-type CdS crystals e reported.

2,639 INDIUM ANTIMONIDE TUNNEL DIODES IN HIGH AGNETIC FIELDS by P.N. Butcher, J.A. Hulbert, and K.F. ulme (Roy. Radar Estab.); J. Phys. Chem. Solids, Vol. 21, o. 320-324(L), Dec. 1961

theoretical expression for the magnetic field dependence of urrent in tunnel diodes is derived. The derivation is based on theory of tunneling through a parabolic potential barrier hich contains no disposable parameters. The theoretical reults are compared with the magnetic field dependence at 77°K the peak current in three InSb tunnel diodes having different nor concentrations. The theoretical results are also compared with the magnetic field dependence of the tunnel current in one diode at three different reverse voltages. The theory has also been used to analyze data on the peak current densities at zero magnetic field for a large number of diodes with various doping concentrations. The theory is in good agreement with the experimental results obtained with forward bias, reverse bias, and with zero magnetic field.

12,640 TOWARD THE THEORY OF THE DEGENERATE P-N JUNCTION by I.I. Ivanchik (Lebedev Phys. Inst., Moscow); Soviet Phys.-Solid State, Vol. 3, pp. 75-84, July 1961

Tunneling theory for degenerate p-n junctions is discussed in detail. Formulations of current flow in the limiting cases of long or short electron free paths are derived after an extensive investigation of the potential structure and band transition probability. Formulas derived are compared with experimental results obtained from a study of current in a Ge junction having an impurity concentration of 2×10^{19} cm^{-3}.

12,641 METHOD FOR MAKING DIODES AND PRODUCTS RESULTING THEREFROM by J.M.N. Hanlet (Soc. Electronique Automatisme); U.S. Pat. 2,983,631, Issued May 9, 1961

The fabrication of high frequency surface barrier diodes is described. A thin layer of the semiconductor, e.g., Ge or Si, is evaporated in a vacuum onto thin heated strips of an alloy of iron and nickel. The frame holding the strips is then rotated by means of an electromagnet and granules of enamel are dropped onto the hot semiconductor surface which is now at a lower temperature. The frame is then returned to its original position and the excess granules fall off, leaving a "strainer" of enamel. Upon heating, the holes in the strainer do not exceed 5 to 7 microns in diameter. A counter electrode is then formed by evaporating an alloy of Sn and Cd onto the enamel-coated semiconductor layer. The diode is completed by attaching electrodes to the metal base and to the alloy. Some significant features of the device are its low hole storage, low junction capacitance, and the small effect of temperature on the reverse voltage. Several diodes can be fabricated at one time by masking certain regions during the evaporation process.

12,642 ON THE CAPACITIVE CHARACTERISTICS OF P-N JUNCTIONS by B.M. Vul (Lebedev Phys. Inst., Moscow); Soviet Phys.-Solid State, Vol. 3, pp. 148-149, July 1961

The basic laws governing the dependence of the capacitance of a p-n junction upon the distribution of ionized impurities within the junction are determined. Expressions for the slope of the capacitive characteristics of the junction and the coefficient of capacitive change are derived using the simplest model of a plane junction for which one of the parts (say the p-type) possesses a sufficiently low resistivity so that all voltages can be considered concentrated upon the n-type member.

12,643 PRODUCTION OF NEGATIVE TEMPERATURE STATES IN P-N JUNCTIONS OF DEGENERATE SEMICONDUCTORS by N.G. Basov, O.N. Krokhin, and Yu. M. Popov; Soviet Phys.-JETP, Vol. 13, pp. 1320-1321(L), Dec. 1961

The production of negative temperature states in degenerate p-n junctions is discussed. When a forward bias is applied to a junction so that it is destroyed, negative temperatures can be obtained in a thin layer (about the thickness of a diffusion length) near the junction. The Fermi quasi-levels corresponding to the nonequilibrium concentrations of electrons and holes must satisfy the relation $\mu_e + \mu_p > \Delta$, where μ_e and μ_p are the Fermi quasi-levels for electrons and holes and Δ is the width of

the forbidden band. If the junction is in a strongly degenerate semiconductor, the negative temperature can be produced before the potential barrier is completely destroyed. The negative temperature condition can be observed by changes in the I-V characteristic when the sample is illuminated with light of a suitable frequency.

12,644 ON THE QUESTION OF THE INFLUENCE OF "DEEP" IMPURITIES ON THE VOLT-AMPERE CHARACTERISTIC OF SEMICONDUCTING DIODES [in Russion] by P.M. Karageorgii-alkalev (Phys. Tech. Inst. AN Uzv. SSR); Izv. AN Uzv. SSR, Fiz.-Mate. Nauk, No. 2, pp. 12-28, 1961

Thin base diodes in which the dimensions of one of the homogeneous domains are comparable or less than the diffusion length of the minority carriers are discussed. It is necessary to take account of the influence of "deep" impurities in this case since it is associated mainly with the modulation of the size of the quasi-neutral domain in the thin base by the external voltage. As is shown, taking this into account affects the properties of the volt-ampere characteristic of the diode substantially.

12,645 HOT ELECTRON EMISSION FROM SILICON p-n JUNCTIONS PARALLEL TO THE SURFACE by J.L. Moll, N.I. Meyer, and D.J. Bartelink (Stanford U.); Phys. Rev. Lett., Vol. 7, pp. 87-90(L), Aug. 1, 1961

Measurements of the emission current from Si p-n junctions parallel to the emitting surface using a demountable vacuum system are reported. A method developed for thinning down the n-region is described. A mathematic model of the device and the theoretical expressions for the emitted current are discussed. It is shown that Shockley's theory fits fairly well with the experimental results (if the sources of experimental error are considered) but gives a surprisingly small mean free path for optical phonon excitation.

Fabrication of Junction Diodes with Fixed Back Resistances - See 12,670

12,646 SEMICONDUCTOR DEVICE AND METHOD OF MAKING SAME by M. Becker, M. Cutler, and J.R. Gliessman (Hughes Aircraft); U.S. Pat. 3,001,894, Issued Sept. 26, 1961

The fabrication of fast recovery time alloyed diodes is described. A wafer containing both n- and p-type impurities, with the segregation constant of the dominant impurity being lower than that of the other impurity, is used. A metal which is neither an acceptor nor a donor impurity in the semiconductor is deposited on its surface and the wafer is heated to a temperature above the eutectic temperature of the metal and semiconductor but below the melting point of the semiconductor. Upon cooling, a very thin high resistivity region of conductivity type opposite that of the original wafer is formed. A button of the solvent metal which forms on the regrown region serves as a contact to this region. A fast recovery time transistor can be fabricated by forming a similar junction on the other surface.

Fabrication of Alloyed High Temperature Si Diodes - See 12,673

12,647 A TREATMENT OF DIFFUSION ERRORS AFFECTING JUNCTION DEPTH by J.E. Reynolds (Motorola); IRE Trans., Vol. ED-8, pp. 377-381, Sept. 1961

An error treatment of the diffusion variables of time, temperature, and starting resistivity with regard to their effects upon junction depth is given. An analytical equation has been derived for engineering usage in determining the per cent erro in junction depth. A sample calculation using this equation is presented along with a method of estimating errors in junction depth due to heating and cooling in the diffusion cycle.

12,648 SEMICONDUCTOR DEVICES FOR PARAMETRIC AMPLIFICATION [in French] by P. Leclerc (Genl. Tel., France) Ann. Radioélect., Vol. 16, pp. 302-308, Oct. 1961

The construction of diodes for high performance parametric amplifiers is described. Such usage necessitates an extremely low series resistance which may be obtained through very precise alloying techniques or through standard diffusion processes. The limiting of the series resistance by controlling the thickness of high resistivity regions by diffusion is discussed.

12,649 VAPOR GROWN SEMICONDUCTOR DEVICE by J.C. Marinace and R.F. Rutz (IBM); U.S. Pat. 3,014,820, Issued Dec. 26, 1961

The preparation by vapor deposition techniques of abrupt junctions for use in tunnel diodes is described. The process is carried out in a sealed tube containing a source in a first zone and highly doped substrates on which a semiconductor film is to be deposited in a second zone. At the beginning of the reaction the two zones are kept at a high temperature; an unoccupied third zone following the substrates is kept at a lower temperature. A carrier vapor is also included in the tube. Following a period of time during which the impurity concentration in the vapor reaches the desired level and the surface of the substrate is vapor-etched, the temperature in the stubstrate zone is lowered to that of the third zone and the deposition reaction takes place.

12,650 SEMICONDUCTOR DEVICES by A.T. Starr (Intl. Stand. Elect.); U.S. Pat. 3,013,192, Issued Dec. 12, 1961

The fabrication of high frequency transistors and diodes is described. In the diode fabrication process, intrinsic polycrystalline Ge or Si and a type-determining impurity are simultaneously vacuum evaporated onto a Au plated Cu plate to form either an n- or p-type polycrystalline layer. A smaller, thinner polycrystalline layer of opposite conductivity type is then evaporated on the first layer, also by the simultaneous evaporation of intrinsic semiconductor and type-determining impurity to form a p-n junction. A thin Au layer is then evaporated on the second layer and a Au plated contact is welded to the Au layer by applying heat, e.g., by passing an electric current through the contact. A similar technique is used in the transistor fabrication process. High frequency devices are fabricated by this technique due to the low minority carrier lifetime of polycrystalline material.

Electrodeposited Ohmic Contacts for Si - See 12,677

12,651 SEMICONDUCTOR DEVICE by G. Eannarino and G. B. Finn, Jr. (Sarkes Tarzian); U.S. Pat. 2,981,873, Issued Apr. 25, 1961

Methods for producing semiconductor diodes which are sturdy and compact, reliable under severe environmental conditions, and suitable for production-quantity techniques are described. A p-n junction device is mounted within an open end cup-shaped electrically conductive housing. One side of the junction is connected to the housing while a resilient connector protruding from the open end of the housing is attached to the

pposite side of the junction. The semiconductor is enclosed ithin a relatively solid insulating material (epoxy resin). everal rectifiers may be formed on a single conductive mem- er by utilizing a series of recesses and the above mounting chniques to provide a three-phase half-wave rectifier in a ngle unit.

2,652 SEMICONDUCTOR DEVICE AND METHOD OF MAN- FACTURING SAME by C.E. Maiden and D.A. German lacific Semicon.); U.S. Pat. 2,998,558, Issued Aug. 29, 961

technique for encapsulating semiconductor junction diodes very small packages is described. The diode is immersed in low melting temperature glass which is kept at a temperature hich will not cause damage to the device. When the diode is moved from the glass a thin glass film forms on the device rface. A bare diode, or one on whose surface a thin coating polymeric organo-siloxane is produced, can be used.

,653 RECTIFIER UNIT by B. Storsand (Oerlikon Engrg.); S. Pat. 2,986,679, Issued May 30, 1961

air cooled rectifying unit consisting of individual rectifiers hich are screwed into cooling blocks with parallel faces is scribed. Cooling discs of a larger diameter than the cooling locks are placed next to the cooling blocks, and insulating scs are placed between the cooling discs. The entire unit is ld together by means of an insulated tension bolt passing rough the cooling blocks, cooling disks, and insulating disks. organic adhesive can be used between the cooling blocks d cooling disks to eliminate the air layer usually present.

,654 DRY RECTIFIER OF SMALL TYPE by H. Schneider iemens AG); U.S. Pat. 2,999,963, Issued Sept. 12, 1961

e assembly of a stack of Se rectifiers is described. The recti- rs are inserted in a U-shaped metallic housing with a metal te between each rectifier and an insulating plate at both ds of the stack. Spring and filler plates are also included if cessary. The ends of the package are completed by folding e lugs at both ends of each side of the housing. An insulat- g layer separates the rectifiers from the metallic housing. e housing is placed in a jig and an insulating cover is put in ce. The metallic plates separating the rectifiers protrude rough the cover to provide electrical contact to the rectifiers. gs on the sides are then simultaneously bent to hold the cover place. In this operation pressure is applied so that there is damaging stress on the rectifiers. The cover and sides are mly joined together by the final sealing step. Lugs extend- g from the bottom of the housing permit it to be securely stened to an electronic chassis.

,655 SELENIUM RECTIFIER by C.C. Geib and G.O. acson (Fansteel); U.S. Pat. 2,981,872, Issued Apr. 25, 1961

method for obtaining rectifiers having desired desensitized eas which allows them to be clamped under a substantial nge of pressures without damage is described. Thermoplastic terials used alone or in combination with kraft paper are roduced onto the surface of a Se layer at the time when the unter electrode is normally applied. Typical materials in- ude polystyrene, acrylate resins, cellulose plastics, vinyl ins, and other materials having the properties of melting or tening below the melting point of Se, suitable resistance to ectrical current flow, suitable adherence to Se, and ease in handling. The thermoplastic material used improves the dielectric properties of the kraft paper and endows the desensitized region with some desirable compressibility.

TRANSISTORS

12,656 RESEARCH AND DEVELOPMENT OF A 1000 Mc GERMANIUM AMPLIFIER TRANSISTOR by J. Biscoe (Philco); U.S. Gov. Res. Rep., Vol. 36, p. 35(A), Aug. 20, 1961 AD 258 261

An investigation leading to the fabrication of devices capable of 15.2 db of power gain at 1000 Mc is discussed. Typical units fabricated previously had about 12 db gain at 100 Mc. A study of the relationship between rb'Cc and power gain revealed the possibility of increasing the power gain (unneutralized) by changing the internal amplification factor of this device. The device is electrically stable, as shown by the life test results.

12,657 HF, VHF, AND UHF POWER AMPLIFIERS AND OSCILLATORS by J.T. Thompson (Hughes Aircraft); U. S. Gov. Res. Rep., Vol. 36, p. 32(A), Aug. 20, 1961 AD 258 037

Three useful devices for measuring transistor parameters are described. The General Radio 1607A bridge appears to be the most useful over the greatest parameter and frequency ranges. The Hewlett Packard 803 admittance meter and the MC Jones directional coupler are adequately treated, considering usefulness and range extensions toward transistor measurements. To complete the investigation of instrumentation, results of an extensive survey that covered all manufacturers of high frequency measuring equipment are listed and the few instruments usable for transistor work in the HF, VHF, and UHF regions are described. Ideas are extended toward the development of a worksheet approach to the general problem of amplifier design. One segment of the worksheet approach, the collector efficiency, is treated in detail both from an ideal case and an actual case that requires a numerical solution.

12,658 MEASUREMENT OF TRANSISTOR SWITCHING PARAMETERS by J.J. Sparks (Brit. Telecommun. Res.); Electronic Engrg., Vol. 33, pp. 387(L), June 1961

Conditions involved in the measurement of transistor switching parameters are discussed. Essential conditions that must be observed if true error-free measurements are to be obtained include: (1) rapid driving step voltage, (2) low generator resistance, (3) low base resistance, and (4) an adequate oscilloscope having a sufficient bandwidth and negligible input capacitance.

12,659 TRANSISTORS AND CIRCUITS THEREFOR by R.F. Rutz (IBM); U.S. Pat. 2,995,665, Issued Aug. 8, 1961

A point contact transistor whose base body includes a region of one conductivity type joined at a boundary junction to one or two other regions of opposite conductivity type is described. The thickness of the first region is made equal to or less than the diffusion length for the average lifetime of the minority carriers in that region. Several circuits utilizing this kind of transistor are included.

12,660 INTRINSIC-BARRIER TRANSISTOR TECHNIQUES (SILICON) by J.L. Buie, M.A. Clark et al. (Pacific Semicon.); U.S. Gov. Res. Rep., Vol. 36, p. S-23(A), Sept. 5, 1961 PB 152 306

A production basis for an n-p-i-n intrinsic-barrier transistor (a set of processes for modifying n-p-n transistors to incorporate a fourth region) is presented. The resulting transistors operate efficiently as oscillators at 70 Mc. Analysis of the diffused structure shows that by simple modifications the intrinsic-barrier structure can be built.

12,661 HIGH SPEED, HIGH CURRENT TRANSISTOR by R.F. Rutz (IBM); U.S. Pat. 2,981,874, Issued Apr. 25, 1961

A high speed, high current handling transistor is described. A combination of two electric fields in the base region operate to speed-up minority carrier transit time and to remove stored minority carriers and simultaneously enhance the emitter injection efficiency and the minority carrier transport factor. These fields are the result of a diffused base region having a graded resistivity and the result of a "p-n hook" collector. The graded base serves to provide an accelerating field to minority carriers in the base. The "p-n hook" provides an axially symmetric electric field in the base around the emitter by the flow of majority carriers from the collector to a ring base connection.

12,662 THEORETICAL CURRENT GAIN OF A CYLINDRICAL MESA TRANSISTOR by D.P. Kennedy and P.C. Murley (IBM); Solid State Electronics, Vol. 3, pp. 215-225, Nov.-Dec. 1961

An analytical investigation of the minority carrier transport problems encountered in a cylindrical mesa type of drift transistor is presented. For the cylindrical mesa transistor, computation of base region transport efficiency is considered as a boundary value problem; solution of this problem yields mathematical equations applicable to the design and development of practical semiconductor devices. This analytical method is applied to the problem of minority carrier transport across a solid cylinder type structure which approximates the transistor base region. Minority carrier losses representing a fundamental limitation upon transistor current gain are introduced through an assumption of bulk and surface-recombination mechanisms. Applications of this analysis are illustrated by establishing the common emitter current gain for typical junction transistors. The Si diffused transistor is shown to be less sensitive to surface recombination mechanisms and the existence of an optimum emitter radius for a semiconductor structure similar to the cylindrical hook collector is indicated.

12,663 NEGATIVE RESISTANCE SEMICONDUCTOR DEVICE STRUCTURE by S.L. Miller (IBM); U.S. Pat. 2,988,677, Issued June 13, 1961

A multiple junction semiconductor device is described which exhibits a negative resistance characteristic whose direction and slope is fully defined at all times. The device contains at least two rectifying junctions having relatively high and low reverse breakdown potentials, respectively. The low breakdown potential is formed between two adjacent highly doped regions of opposite conductivity, one of which is further connected to a lightly doped region of like conductivity. A diagrammatic illustration of the functioning of the device is given using an n-p-n and a p-n-p transistor arrangement.

12,664 BREAKDOWN VOLTAGE IN POWER TRANSISTORS by R. Greenburg (Motorola); Semicon. Prod., Vol. 4, pp. 21-25, Nov. 1961

A study of the cause of second breakdown in power transistors, the primary factor in determining the maximum reliable $V_{ce}-I_c$ limits, is presented. Second breakdown causes transistor destruction and is associated with the collector-base junction a controlled by the emitter-base junction. The exact action is not known but seems to be associated with a sudden concentr tion of current in a small ared causing the temperature to ex ceed the melting point of the Ge-In alloy. A collector-to-emitter short results. The envelope generated by the second breakdown locus determines an absolute maximum $V_{ce}-I_c$ limit for each transistor type. A maximum reliability area controlled in production by proper transistor design and testin lies inside the absolute maximum area. The test conditions ar discussed and suggestions for optimum performance are given. Since second breakdown can be triggered in a few microseco the absolute maximum area must be obeyed completely. Collector-to-base breakdown voltage, collector-to-emitter breakdown voltage, and punch-through voltage are discussed in an appendix.

Avalanche Conditions in Transistors - See 12,814

12,665 CERTAIN QUESTIONS ON THE ELECTRONICS OF ALLOYED SEMICONDUCTING TRIODES [in Russian] by G. Blinov and I.N. Vozhenin (Siberian Phys.-Tech. Inst.); Izv. VUZ Fiz., No. 5, pp. 55-64, 1961

Experimental and theoretical characteristics of semiconductin triodes for an arbitrary injection level are compared. It is observed that the condition of electrical neutrality in the bas is satisfied and that the influence of longitudinal electric fields in the base is insignificant for any injection level. The dependence of the effective carrier lifetime on the injection level is established and data that exist in the literature are analyzed.

12,666 A SIMPLIFIED APPROACH TO TRANSISTOR ADMITTANCES by J. Lindmayer and C. Wrigley (Sprague Elect.); Solid State Electronics, Vol. 3, pp. 278-290, Nov.-Dec. 1961

The use of simple admittance parameters which are valid for a limited frequency range to describe high frequency junction transistors is discussed. This is possible since the actual cutof frequency is much lower than the cutoff frequency arising fro the base transport. Two charges play the dominant role in de termining the admittances: the stored charge, and the portion of it reclaimable through the emitter during discharge. For a constant built-in field in the base region, the treatment is so simple that the admittance parameters can be determined by inspection. It is shown that the ratio of the transfer admittan is a real number for any transistor and all frequencies. This constant is determined in general for an arbitrary impurity dis tribution. The diffusion capacitances, as well as practical problems associated with their measurement, are discussed.

12,667 SUPERSATURATED TRANSISTOR SWITCHES by J.F. Gibbons (Stanford U.); IRE Trans., Vol. ED-8, pp. 443-452, Nov. 1961

The use of a simple one-dimensional transistor model to calcu late the ON characteristics of certain alloy switching transis tors is described. The model which includes nonlinear recomb nation and high-level injection effects, provides reasonably close predictions of the voltage drop across a closed transisto switch and the switch resistance when the transistor is operate in the intermediate area between low- and high-level conduc tion. The first section of the paper develops the transistor mo which is essentially Linvill's lumped model augmented to incl

he important one-dimensional effects that occur when the low-evel assumptions are violated. The second section presents he results of calculations based on this model and a comparison vith experimental values.

2,668 INFLUENCE OF WAFER THICKNESS AND CARRIER ECOMBINATION ON THE CUTOFF FREQUENCY OF ALLOY-UNCTION TRANSISTORS by S. Amer (Stand. Telephones Cables); Solid State Electronics, Vol. 3, pp. 304-308, Nov.-ec. 1961

he effect of wafer thickness and carrier recombination on the -cutoff frequency of the "intrinsic" transistor is discussed. irst, Moyjes' solution of the diffusion of minority carriers in symmetrical junction transistor is used to find the dc trans-ort factor. This is then converted to the ac case and finally n implicit equation is found for the cutoff frequency as a unction of wafer thickness θ and surface recombination veloc-ty S. It is shown that for S < 3000 cm/sec the influence of urface recombination is negligible. At very narrow basewidths he current density is very high at the emitter edge and this ecreases the diffusion length. The carrier's path (from slanted dge of emitter to slanted edge of collector) is longer than the eometrical basewidth. A reduction in wafer thickness de-reases this effect and thus increases the cutoff frequency in pite of increasing the current density at emitter edge. The ost important equations have been represented graphically for he particular case of the STC TK20 transistor.

2,669 THE CALCULATION OF CUTOFF FREQUENCIES OF INORITY-CARRIER TRANSPORT FACTORS IN DRIFT TRAN-ISTORS WHEN THE MOBILITIES ARE NOT CONSTANT by Sugano and F. Koshiga (U. Tokyo); Proc. IRE, Vol. 49, 1218(L), July 1961

he cutoff frequency of minority-carrier transport factor in a rift transistor is derived. For a p-n-p drift transistor, the mo-ility of holes is assumed to be $\mu_p = \mu_{p_0}(N_d/N_{d_0})^{-\nu}$, where μ_{p_0} is the hole mobility at the front of the collector junction, N_{d_0} is the density of donors at the front of the collector junc-ion, and N_d is the density of donors in the base. The transport actor β is then derived. A numerical calculation of β indi-ates that the cutoff frequency f_α is approximately equal to $3 f_{\alpha_0}$, where f_{α_0} is the cutoff frequency calculated when he mobility is assumed to be constant.

2,670 BACK RESISTANCE CONTROL FOR JUNCTION EMICONDUCTOR DEVICES by R.F. Rutz (IBM); U.S. Pat. 007,090, Issued Oct. 31, 1961

he fabrication of alloy junction transistors in which the emit-r and collector junctions have fixed values of back resistance described. The process is illustrated by means of an n-p-n ansistor. A very high resistivity n-type region is produced diffusion on the surfaces of a p-type wafer. An n-type emit-r and an n-type collector are alloyed through the high resis-ivity n-type skin to the p-type region. A base contact is then dered to a small undiffused p-type region at the surface. he electric field at the diffused surfaces reduces surface re-mbination and therefore increases α. The use of a high re-istivity skin to produce a fixed back resistance in junction odes is also discussed. By utilizing an appropriate geometry, is value can be made quite high.

,671 70 Mc, 1 WATT, SILICON TRANSISTOR by W.J. Freeman, III (RCA); U.S. Gov. Res. Rep., Vol. 36, p. 27(A), Aug. 20, 1961 AD 257 811

The development of a manufacturing process to establish a production line for a 70 Mc, 1 w Si transistor is discussed. The planar-constructed preproduction samples were fabricated and the results of some of the testing analyzed. Additional life test storage data for 3000 hours from the first group of planar transistors showed the desirability of this design. Illustrations showing the change of testing requirements with various parameters are presented for the planar device. An interesting effect observed during the initial stages of planar construction was that when the transistor junctions were reverse biased at collector currents of approximately 50 ma, the junctions broke down and pinpoints of light were observed along the base-collector and base-emitter junctions.

12,672 INDUSTRIAL PREPAREDNESS MEASURE ON 1 WATT 70 Mc GERMANIUM MESA TRANSISTOR by N.L. Lincoln (Motorola); U.S. Gov. Res. Rep., Vol. 36, p. 31(A), Dec. 5, 1961 AD 263 611

A 1 w, 70 Mc, pilot production run of a Ge mesa transistor is discussed. The high frequency and power requirements of the proposed device required the development of a completely new approach to the package and design of a mesa device. General mechanical and electrical descriptions are presented and the process technology is described in narrative form. The necessary equipment and the pilot production run are also described.

12,673 PRODUCTION OF HIGH TEMPERATURE ALLOYED SEMICONDUCTORS by R.E. Anderson (Texas Instr.); U.S. Pat. 2,985,550, Issued May 23, 1961

The fabrication of alloyed Si diodes and transistors that operate up to 150°C is discussed. Indium alloy dots are employed to form the appropriate junction areas by firing at 1100°C. Lead is then alloyed at 600°C to the portion of the In dot that is not alloyed to the Si. The resultant units are stable, both mechanically and electrically, to temperatures up to 150°C.

Fabrication of Alloyed Junction Transistors - See 12,646

12,674 METHOD OF PRODUCING TRANSISTORS by L.M. Nijland (Philips); U.S. Pat. 3,006,789, Issued Oct. 31, 1961

The fabrication of double diffused transistors in which ohmic contact to the base region is made by means of a diffused region is described. A p-type impurity such as boron with a very high solubility is first diffused into an n-type Si waver. The diffused layer is removed from all but one surface and a second diffusion utilizing Al and Sb is carried out. Since the solubility and diffusion coefficient of boron are both 100 times greater than those of Sb, the Sb has no effect on the boron-diffused layer. The p-type diffused base region and the boron layer contact each other. A depression is cut through the boron layer into the n-type collector region and ohmic contacts are soldered to the emitter and collector regions and to the boron-diffused layer. If the boron layer is formed as previously described and the Al and Sb diffusion are carried out before and after, respectively, making the depression through the boron layer, a very low resistance collector contact results. The process can also be used with other semiconductors, e.g., p-type Ge. In this case, As is used for the first diffusion and Sb and In for the second diffusion.

Diffusion Errors Affecting Junction Depth - See 12,647

Fabrication of High Frequency Junction Transistors by Vacuum Evaporation Techniques - See 12,650

12,675 INDIUM ANTIMONIDE TRANSISTORS by H.L. Henneke (Texas Instr.); Solid State Electronics, Vol. 3, pp. 159-166, Nov.-Dec. 1961

The design fabrication and electrical characteristics of an n-p-n InSb transistor which operates at 77°K are discussed. An analysis of the expected HF performance is presented and a comparison is made to a p-n-p Ge transistor. Because of its high electron mobility, the InSb transistor should have a base transit time 1/26 that of a similar Ge transistor. Although these ultimate capabilities have not been approached, transistors with f_t as high as 300 Mc and β's of 500 have been observed. Switching speeds approaching those of the best state-of-the-art Ge transistors have been measured.

12,676 CONDUCTOR CONNECTED TO THE ALLOYING AREA OF A CRYSTALODE, E.G., A TRANSISTOR OF THE ALLOY TYPE by W. Klossika (Telefunken); U.S. Pat. 2,998,555, Issued Aug. 29, 1961

A mechanically-strong electrode for use in alloyed junction transistors is described. The electrode consists of a strip of 80 per cent Ag - 20 per cent Cu which is tinned at both ends. The flat side of one end of the strip is soldered to the emitter or collector by means of a soldering iron. The other end is spot welded to one of the leads of a conventional transistor header. The electrode is bent so that sections of it are parallel to the transistor surface and to the header at both the emitter and collector.

12,677 A LOW-RESISTANCE OHMIC CONTACT FOR SILICON SEMICONDUCTOR DEVICES by S.L. Matlow and E.L. Ralph (Hoffman Electronics); Solid State Electronics, Vol. 2, pp. 202-208, May 1961

A method of obtaining a low-resistance ohmic contact to lapped Si by a displacement plating of Au followed by an electrodeposition of Cu is described. The contact resistance is found to be less than that obtained using unfired autoreductive electroless Ni. The bonding strength of the contacts as determined by a torque test is found to be quite good. The mechanism of the displacement plating is discussed from the viewpoint of the factors found to influence the plating rate and adherence. A figure of merit indicating the conditions necessary for good adherence is defined. The contact resistance is found to be a linear function of the displacement plating time. A hypothesis to explain these observations is offered.

12,678 PELTIER COOLING OF SEMICONDUCTOR COMPONENTS by R. Carey and R. Marlow (Texas Instr.); U.S. Gov. Res. Rep., Vol. 36, p. 27(A), Sept. 20, 1961 AD 259 106

The status of Peltier cooling as applied to semiconductor components is described. Five Peltier cooler-semiconductor component devices were designed, constructed, and evaluated. One of these devices is capable of maintaining the case temperature of two high frequency Si transistors at 35°C while each transistor is dissipating 150 mw and operating at an ambient temperature of 85°C. Recommendations for further study include miniaturization of the Peltier cooler, lower current coolers, and development of Peltier coolers located inside the transistor case.

12,679 SEMI-CONDUCTOR DEVICE by J. Pritchard and G. Brookes (Philips); U.S. Pat. 2,998,556, Issued Aug. 29, 1961

A technique for stabilizing the electrical characteristics of transistors is described. The transistor is sealed with boron oxide in one form or another. The boron oxide may be applied on the transistor and its immediate vicinity, e.g., by dipping the device into butyl borate and exposing the device to the atmosphere for about one-half hour. The process may be repeated to obtain a desired thickness of the coating. The envelope is filled with a filler such as silicone vacuum grease and is sealed. Alternatively, the device package may be filled with a form of boron oxide, e.g., bouncing putty. If the boron oxide or boron oxide-containing material has a high water content, it is heated before the device is sealed. After sealing, the device is subjected to a stabilizing heat treatment at 70° to 150°C. Several examples of the use of the technique on Si and Ge alloyed junction transistors are given.

12,680 ON THE QUESTION OF THE USE OF CERTAIN ORGANIC COATINGS TO PROTECT THE SURFACES OF SEMICONDUCTING DEVICES [in Russian] by V.F. Synorov and T.G. Davydova (Siberian Phys.-Tech. Inst., Tomsk U.); Izv. VUZ Fiz., No. 6, pp. 74-80, 1961

The influence of certain coatings on the parameters of semiconducting devices is clarified and a method of selecting coatings for the protection of the semiconductor surface from external effects while retaining the required values of the device parameters is developed. Butyl metacrylate and epoxide resin compounds were used. Dibutyl phthalate was used as a plasticizer and hexamethylene diamine was the hardener. Experiments show that coatings of completely different composition exert an analogous effect on the parameters of fused Ge triodes. In a first approximation, the mechanism of this effect can be explained by the change in the value of the surface potential during the adsorption of the polar molecules of the coating by the Ge surface.

MAGNETOELECTRIC DEVICES

12,681 A NOTE ON HALL PROBE RESOLUTION by H. Koehler, B. Kostyshyn, and T.C. Ku (IBM); IBM J. Res. and Dev., Vol. 5, pp. 326-327(L), Oct. 1961

The relationship between the output of a rectangular Hall probe used for measuring magnetic fields and the actual magnetic field is investigated. The technique expresses the Fourier coefficients of the expansion of the actual field as functions of the coefficients of the output of the probe. With the resulting corrections applied, agreement within one or two per cent of the theoretical field is attained. The case of the field due to current in straight wires is given particular attention.

12,682 FEEDBACK AMPLIFICATION IMPROVES HALL-EFFECT MULTIPLIERS by R.A. Greiner (U. Wisconsin); Electronics, Vol. 34, pp. 52-55, Aug. 25, 1961

Improvements in the operation of Hall-effect multipliers are described. To reduce distortion in the output voltage, a feedback amplifier is used to drive the field coil current in phase with the input signal. Reduction of common-mode signals and null voltage cancellation is achieved by adding a dc component to the field coil signal. With 100 ma dc in the coil, the phase shift between the output Hall voltage and the signal applied to the crystal driver was less than four degrees from 20 cps to 20 k

AGNETOELECTRIC DEVICES (Cont'd)

he distortion in the output signal was less than one per cent ver this frequency range.

2,683 HALL VOLTAGE GENERATORS FOR AMPLIFIER AND SCILLATOR PURPOSES by F. Kuhrt and K. Maaz (Siemens G); U.S. Pat. 2,988,707, Issued June 13, 1961

method of providing practical power amplification and oscillation generation based upon the Hall effect is discussed. he material forming the semiconductor Hall plate and the idth of the field gap provided in the closed magnetic system re so adapted that the quotient of the carrier mobility of the miconducting material and the gap width is larger than 10^6 m/vsec. An example of the design of a Hall generator using n InAs plate, having a mobility of 23,000 cm^2/vsec and a eld gap of 20 μ providing a ratio of 11.5×10^6 cm/vsec, is ven; the device provided an amplification factor of 10. Exnples of amplifying and oscillating circuits using Hall generors are included together with modifications using two Hall enerators in single and double field gaps.

OTHER CONDUCTIVE DEVICES

2,684 CRYOSAR MEMORY DESIGN by R.C. Johnston Lincoln Lab.); U.S. Gov. Res. Rep., Vol. 36, p. 21(A), ug. 5, 1961 AD 257 183

he cryosar and its applications in computer memories are dissed. The compensated cryosar is a negative-resistance twominal device utilizing a bulk effect in Ge at liquid He temeratures. Its use in computer memories due to its bistable haracteristics and ease of fabrication in large arrays is dissed. It is pointed out that careful consideration of device nd circuit parameters must be exercised if a successful large emory is to be achieved.

2,685 SEMICONDUCTOR BAND-PASS FILTERS by S.N. evine and J.J. Sein (RCA); 1961 IRE Intl. Conv. Rec., Part pp. 133-140

detailed analysis of semiconductor filters which utilize iterd impurity distributions or variations in geometry is given. he analysis is extended to filters which employ applied elecic fields that are periodically varied along the length of the ructure. Filters of these types are tunable by means of a dc as and have a bandwidth of the order of five per cent about e center frequency. With materials characterized by suffiently high resistivity and minority carrier lifetime, operating equencies in the range of 10^4 to 10^6 cps can be achieved. he performance of filters constructed by alloying techniques om high-resistivity p-type silicon with minority carrier lifemes of 10^{-3} to 10^{-4} seconds is presented in detail.

PHOTODEVICES

2,686 IMPURITY ACTIVATED ALLOY INFRARED DETECTORS K.S. Ling (RCA); U.S. Gov. Res. Rep., Vol. 36, pp. 20-(A), July 20, 1961 AD 256 516

theoretical analysis of three types of detector materials is prented. Theory predicts that Au doped Ge-Si alloy material ith the long wavelength threshold at 7 microns should have gher detectivity at the operating temperature of liquid nitrogen than has been realized with other detectors for this wavelength range. The Zn doped Ge-Si alloy material has high detectivities in the 8 to 13 micron atmospheric window at the operating temperature of 50°K. Equipment and procedures for preparing monocrystalline Ge and Ge-Si alloy are described in detail. Cell fabrication techniques and equipment and a method for evaluating the cells are also described. The theory of the performance of the Ge and Ge-Si alloy system is given. A detailed analysis of cell response with respect to infrared radiation and an analysis of conductivity with respect to impurity concentration are presented.

12,687 VAPOR DEPOSITED POLYCRYSTALLINE SILICON SOLAR CELLS by J.D. Heaps, O.N. Tufte, and A. Nussbaum (Honeywell Res. Ctr.); IRE Trans., Vol. ED-8, p. 560(L), Nov. 1961

Results of experiments in the construction of polycrystalline Si solar cells are described. Single crystal Si is used as a substrate for the deposition of a Si layer by the thermal decomposition of trichlorosilane ($SiHCl_3$) in the presence of hydrogen. For the substrates investigated, a deposit was always obtainable in the 900° to 1100°C range, with deposited layers varying from 0.001 to 0.030 in. Ga is then diffused into the deposited layer with a surface concentration of about 10^{18} cm^{-3}, followed by the diffusion of phosphorous with a surface concentration of 10^{20} cm^{-3}. The maximum open circuit voltage obtained with the cells is 0.3 volts (25°C), with the open circuit voltage of most cells lying between 0.23 and 0.3 volts. The highest efficiency obtained is 0.9 per cent, the efficiencies of most cells being somewhere around 0.6 per cent. The fabrication techniques are described and an explanation of the behavior of the cell is given.

12,688 ENERGY CONVERSION SYSTEMS REFERENCE HANDBOOK. VOLUME V. DIRECT SOLAR CONVERSION by W. Evans and W.R. Menetrey (Electro-Optical Systems); U.S. Gov. Res. Rep., Vol. 36, p. 22(A), Aug. 20, 1961 AD 257 788

The performance characteristics of a photovoltaic converter used to convert solar radiation directly to dc electrical energy are discussed. Empirical and analytical relationships are derived which present expected efficiencies of conversion as a function of temperature, solar insolance, and other factors. The effects of environmental degradation due to meteoroids and the Van Allen belts are discussed. The present and anticipated state-of-the-art of fabrication techniques is presented, along with the advantages of using concentrating mechanisms for increasing the solar illumination level. A discussion of the state-of-the-art and practical and theoretical limitations of the photoemissive generator is also included. It does not appear at present that the photoemissive generator offers competition to the photovoltaic cell.

12,689 THE POTENTIALITIES OF SILICON AND GALLIUM ARSENIDE SOLAR BATTERIES by T.S. Moss (Roy. Aircraft Estab.); Solid State Electronics, Vol. 2, pp. 222-231, May 1961

The theory of the spectral response of a p-n junction solar battery unit is given and detailed comparisons of the expected performance of Si and GaAs units are made. Data now available on absorption in GaAs show that it is a particularly favorable material because of its very steep absorption edge. The low effective masses and correspondingly low densities of states in GaAs are also advantageous. The efficiency of practical Si units is unlikely to exceed 15 per cent even with intensive

development, whereas GaAs units with efficiencies of about 20 per cent should be achievable in the near future and the performance may ultimately approach 25 per cent, even if (as assumed) the carrier lifetimes stay well below those for Si.

12,690 A NEW RADIATION-RESISTANT HIGH-EFFICIENCY SOLAR CELL by G. Mandelkorn, C. McAfee et al. (USASRDL); U.S. Gov. Res. Rep., Vol. 36, p. S-50(A), Aug. 20, 1961 PB 171 842

Details of a phosphorus-diffusion process for fabricating high-efficiency Si solar cells are presented. The phosphorus-diffused cells not only have high efficiencies but also a radiation resistance that is superior to commercial cells by at least an order of magnitude. Data on the electrical characteristics and radiation resistance of the cells are analyzed, and possible application of the new cells to satellites and atomic powered batteries is considered.

12,691 ELECTROLUMINESCENT FERROELECTRIC (ELF) SOLID STATE DISPLAY (Westinghouse); U.S. Gov. Res. Rep., Vol. 36, p. 30(A), Sept. 5, 1961 AD 258 598

The design and development of a solid state display panel consisting of a multitude of small individual cell structures are discussed. Brightness and current were measured for several specimens of ZnS:Cu,Cl films at temperatures of 77° to 330°K. Measurements on all the new ceramic material received to date were completed, utilizing both standard and fringing electrodes.

12,692 PROPOSED METHOD FOR CONTROLLING AND MINIMIZING REFLECTIONS FROM A SURFACE by R.H. Mattson (U. Minnesota); IRE Trans., Vol. ED-8, pp. 386-389, Sept. 1961

The use of a p-n junction to control the reflection of electromagnetic radiation from a surface is discussed. The device is made in such a way that the junction is parallel to the surface upon which the electromagnetic radiation is impinging. If the p-region is very narrow, the wave will penetrate through it into the depletion region. If the n-region is of high conductivity, the wave is deflected from it. If the depletion layer width is right for the frequency considered, the reflected wave will interact with the impinging wave to give the desired effect. By changing the bias applied to the junction, a tuning effect can be obtained. A detailed analysis of the proposed device is given. Some practical limitations to creating the device are described, but the concept and method of analysis could be useful for creating microwave tuning and control components.

Light Beam Modulators - See 12,540

THERMAL DEVICES

12,693 MANGANESE OXIDE THERMISTORS (Air Info. Div.); U.S. Gov. Res. Rep., Vol. 36, p. 23(A), Aug. 20, 1961 AD 257 908

Measurements of the electrical and thermal properties of thermistors made of manganese oxides and confirming the hypothesis that the specimens are actually solid electrolytes are reported. Theoretical formulas are derived for the temperature dependence of the coefficient of heat conductivity and therm EMF. Empirical laws are determined to characterize the dependence of the resistance of specimens on temperature, and the dependence of the charge-carrier mobility in the specime on activation energy. In thermistors made of manganese oxid oxygen ions also take an active part in the process of heat tr port. In the presence of a temperature gradient in a thermist semiconducting substance, a nonuniform concentration of oxy gen ions appears which leads to the appearance of an EMF in the thermistor.

12,694 NEW THERMALLY VARIABLE BEAD RESISTOR by V. Tannery and R.G. West (Motorola); J. Appl. Phys., Vol. 32 p. 1402(L), July 1961

The construction of a bead thermistor from $BaTiO_3$ is discussed When doped with the proper ions, the ferroelectric $BaTiO_3$ becomes a semiconductor at room temperature and has a posit temperature coefficient of resistivity when heated through the tetragonal-cubic transition temperature. The latter temperature may be moved higher or lower by partially substituting Pb^{2+} or Sr^{2+}, respectively, for Ba^{2+}. The thermistor has three properties not found in negative temperature thermistors: (1) is voltage stable in the PTC region, (2) it has a large negativ ac resistance in the PTC region, and (3) it has large power handling capacity for a bead of small mass.

12,695 NEW CONCEPTS IN THERMOELECTRIC DEVICE DE SIGN by W.H. Clingman (Texas Instr.); 1961 IRE Intl. Conv Rec., Part 6, pp. 174-182

Irreversible thermodynamics is applied to an analysis of therm electric device design. This method is useful when the effi-ciency and performance coefficient are important. To optimi the design for a given set of materials and technology, the ef fects of the thermal circuit and electrical circuit on entropy production within the device are considered. Methods of cho ing the basic design concept for the thermoelectric part of th system are presented. Then optimization of the dimensions of each of the individual thermocouples and materials is discusse and the effect of thermal resistance between the thermoelectr junctions and the heat source and sink on the entropy produc-tion within the entire system is considered.

12,696 THE PERFORMANCE OF A CONVECTIVELY COOLE THERMOELEMENT USED FOR POWER GENERATION by C. M Rollinger and J.E. Sunderland (Northwestern U.); Solid State Electronics, Vol. 3, pp. 268-277, Nov.-Dec. 1961

The differential equations which describe the steady-state ter perature distribution in a thermoelement with constant proper ties and with convective heat transfer from its longitudinal surface are solved by analytical methods. The closed-form analytical solutions are applied to a single element thermo-electric generator to determine the effect of surface heat tra fer upon the power output and efficiency over a range of valu for the heat-transfer parameters. The results show that in all cases the surface heat transfer increased the power output unc matched load conditions; in many cases both the power outpu and the thermal efficiency were increased through the use of surface heat transfer. The conclusion is drawn that surface heat transfer can be beneficial in many applications.

12,697 DEVELOPMENT OF A SEMICONDUCTOR FILM-TYPE THERMOCOUPLE ENERGY CONVERTER (Honeywell Re Ctr.); U.S. Gov. Res. Rep., Vol. 36, p. 24(A), Aug. 20, 1961 AD 258 075

HERMAL DEVICES (Cont'd)

e development and properties of an oxide thermoelectric nerator are discussed. The unit proves the effectiveness of ide thermoelectrics in applications where voltage at low rrents is required.

FERRO- AND FERRIMAGNETIC (FERRITE) DEVICES

,698 MINIATURIZED, TEMPERATURE STABLE, COAXIAL JUNCTION CIRCULATORS by J. Clark and J. Brown berry Microwave); IRE Trans., Vol. MTT-9, pp. 267-269, ay 1961

e design of a coaxial Y-junction, C-band circulator is dis- ssed. Exclusive of connectors the device is only 1.5 inch diameter, 0.75 inch in height, and weighs approximately 75 ounces. In order to make the junction a circulator at a ven frequency, the magnitude of the bias field, the dielec- c constant, and the height of the dielectric sleeves must be justed. Temperature stability is achieved by the use of mperature favorable" materials such as medium- to high- rcentage Gd substituted YIG. For most frequencies in the crowave spectrum the ferrimagnetic materials employed in Y-junction circulator can be biased in a low-loss region h a field that is either above or below that required for rimagnetic resonance. From the standpoint of miniaturiza- n, below-resonance operation is desirable.

,699 PULSE-OPERATED CIRCULATOR SWITCH by L. Frei- rg (Lockheed); IRE Trans., Vol. MTT-9, p. 266(L), May 61

means of eliminating the holding current which keeps a rite circulator, used as a microwave switch, in the switched tion is considered. Where switching speeds are of no con- quence the best microwave material for the frequency and ication may be used in the circuit and a switchable mag- ic material external to the circuit can be used to supply bias requirements. An actual construction of such a switch escribed and further points are discussed.

.700 ON THE DESIGN OF PUSH-PULL MAGNETIC AM- IERS by V.L. Benin; Automn. Remote Control, Vol. 22, . 338-343, Oct. 1961

ethod of designing push-pull magnetic amplifiers which mits direct determination of the optimum parameters with- successive approximations is described. The accuracy is vermined by the accuracy of the theory of linearized mag- ic amplifiers. The specific volume of steel in the amplifier minimized and the optimum ac change multiple is determined. e curve of the minimum normalized specific volume of steel the core as a function of the dc magnetic field strength is n used to determine the design parameters. A bridge mag- ic amplifier using Sh-32 cores made of E-42 transformer el was designed analytically. The difference between the mputed and experimental values of load current was 4 per nt.

romagnetic Parametric Amplifiers - See 12,783

701 MAGNETIC CORE LOGICAL DEVICES by E.A. Brown M); U.S. Pat. 2,991,455, Issued July 4, 1961

gical devices in which a single magnetic core can perform logical operations (AND, OR) are described. This magnetic core depends on two principles: subdivided cross-sectional areas are formed, and auxiliary fluxes are established by means of suitable core windings. One embodiment of the device is utilized in an AND device responsive only to coexisting input signals. Another utilization is an AND device responsive only to coexistent sampling signals. A third application is an OR device responsive to sampling signals supplied to one of several windings.

12,702 MAGNETIC DEVICE by K.D. Broadbent (Hughes Aircraft); U.S. Pat. 2,993,197, Issued July 18, 1961

Multiaperture magnetic cores and circuits utilizing them are discussed. Each core has two apertures, the ratio of aperture diameters being 6:1. Three wires are threaded through the smaller aperture; two of these wires control the magnetic states in two regions of the core and the third provides an output from the core. A wire for controlling the magnetic state in a third region of the core is also threaded through the larger aperture. A magnetic flip-flop utilizing two of these cores and a shift register constructed with a number of these flip-flops are described. A highly desirable feature of the shift register is that information can be moved in one direction only without the use of diodes.

12,703 CONDUCTION PROPERTIES OF PERMALLOY TAPE RING CORES WITH SMALL BANDWIDTH AND RECTANGULAR HYSTERESIS LOOP [in German] by P. Kupec (Tech. Hochsch., Muenchen); Arch. Elekt. Uebertragung, Vol. 15, pp. 257-272, June 1961

The B = b(H, t) function of tape ring cores of Permalloy with a known electrical history is determined. For this purpose the change of induction which occurs when the core is controlled by a square-wave pulse field H of different amplitude is measured. From these measurements characteristic functions are derived which allow a calculation of the time dependence of the secondary voltage and current with an arbitrary load on the transformer-connected ring core. The example of an ohmic load and control by square-wave current pulses is fully calculated and compared with experimental results.

Theory of Wall-Stepping Film Storage Devices - See 12,517

12,704 LOW FLUX DENSITY FERROMAGNETIC MATERIAL by J.M. Brownlow (IBM); U.S. Pat. 2,986,522, Issued May 30, 1961

Ferrite cores which can be switched from one state to another with a small amount of flux change are described. The low flux density reduces the heating effect in the devices and increases their switching speed. The ferrites have the formula $Cr_w Mn_x Ni_y Fe_z O_4$, where $w + x + y + z = 3$ and $w = 0.4\text{-}1.2$, $x = 0.7\text{-}1.6$, $y = 0.1\text{-}0.4$, and $z = 0.6\text{-}1.3$. The preparation and properties of some specific ferrite compositions are described.

12,705 COPPER CONTAINING FERRITE CORES by P. Geldermans, P. van den Ban, and G.L. Holthaus (Philips); U.S. Pat. 2,988,508, Issued June 13, 1961

Methods of manufacturing an annular magnet core having an outer diameter not greater than 4 mm, which is particularly suited for memory applications are described. The cores consist of a ferromagnetic material made from mixtures of Fe_2O_3, MnO, and CuO. In preparation, the mixture is preheated between 600°-1000°C to form a reaction product which is refined

and molded into the form of a ring. The rings are sintered in an oxygen-containing atmosphere by heating between 1150°-1350°C, after which they are cooled. In the cooling process from 700°C to room temperature, the oxygen content is lowered from that used in the sintering operation. Two detailed examples showing the method of processing and testing are included. Tables showing the variation in the properties of the rings under varying compositions of Cu-Mn-Fe-O and firing temperatures are included.

Magnetic Modulators - See 12,811

12,706 LOW-LEVEL GARNET LIMITERS by F.R. Arams, S. Okwit (Cutler-Hammer) and M. Grace (Airtron); Proc. IRE, Vol. 49, pp. 1308-1313, Aug. 1961

S- and L-band low level passive limiters and limiter-preselectors using polished single crystals of narrow line width YIG are described. The S-band limiter employs unsubstituted YIG and has an insertion loss of 0.6 db, a limiting threshold of -26 dbm, and a dynamic range greater than 30 db. The L-band limiter used Ga-substituted YIG crystals which, when ground into spheres, exhibits extremely narrow line widths. The L-band limiter has an insertion loss of 1.1 db, a limiting threshold of -21 dbm, and a dynamic range greater than 25 db. A tuning range from 1120-1305 Mc is obtained. Data on frequency sensitivity and SWR are given which indicate a high off-band rejection and fair power handling capability. A leading edge spike of 0.1 μsec duration has been observed. The decline of the various components of the magnetic susceptibility tensor can be used to construct other novel types of limiters. The operation of three such devices — electronically tunable preselectors, cavity type and comb type limiters — is described and experimental data are given.

12,707 AN INVESTIGATION AND EVALUATION OF VARIOUS CORE CONFIGURATIONS AND MATERIALS FOR OPTIMUM TRANSFORMER DESIGN by C. F. Rains, R. C. McMaster et al. (Battelle); U.S. Gov. Res. Rep., Vol. 36, pp. S-16–S-17(A), Aug. 20, 1961 PB 154 974

Ac core loss and permeability equipment corresponding to ASTM designation A-34-48 is described. The average reading or flux voltmeter was calibrated and core-loss tests were made on seven sets of Epstein samples. Core-loss tests at temperatures from about 80° to 1381°F were made of four E I laminated cores. The core loss was found to decrease as much as 60 per cent from room temperature to 1000°F. Two-, four-, and fourteen-mil oriented Si-Fe Epstein samples were tested at frequencies of 60, 100, and 200 cps. The percentage rise of core loss at 10,000 gauss from 60 to 200 cps was approximately 1.7 times greater for the 14-mil sample than for the 2-mil sample. A study was made of the effect on the core loss of different stacking arrangements and clamping pressures of E I laminated cores. The laminations were assembled in groups of one, two, three, and four. While various clamping pressures indicated no trend, it was found that the larger the number of laminations in a group the greater the core loss.

12,708 MODES IN RECTANGULAR GUIDES LOADED WITH A TRANSVERSELY MAGNETIZED SLAB OF FERRITE AWAY FROM THE SIDE WALLS by G. Barzilai and G. Gerosa (U. Rome); U.S. Gov. Res. Rep., Vol. 36, p. S-52(A), Aug. 5, 1961 PB 155 539

The characteristic equation describing the general modal spectrum for a rectangular guide partially filled with a slab of ferrite transversely magnetized and situated away from the side walls is derived. This equation is solved numerically for particular cases and for modes of zero and first order with respect to the dependence along the direction of the dc magnetic field. Some experiments to verify the theoretical results which show good agreement with the theory are presented.

PARAMAGNETIC DEVICES (Masers and Lasers)

12,709 ELECTRO-OPTICAL DEVELOPMENTS HIGHLIGHT NEREM by T. Maguire (Electronics); Electronics, Vol. 34, pp. 73-77, Nov. 10, 1961

Advances in gaseous and solid-state optical masers and modulation concepts presented at NEREM are reviewed. An experimental modulator using electro-optical effects in crystals of dihydrogen phosphate is described. About 2 kw is required to produce a peak phase retardation of 1.9 radians in the output of a maser operated on a pulsed basis at 9250 Mc. A photoklystron, which mixes two coherent light signals to yield a coherent microwave output, was announced. Pulsed optical masers have been used to produce optical harmonics. A ruby maser output has been passed through a red filter and focused inside crystalline quartz, with the emergent beam sampled by a quartz prism spectrometer equipped with red insensitive spectrographic plates. A dense image is obtained at the second harmonic.

12,710 MASER by D.I. Bolef and P.F. Chester (Westinghouse); U.S. Pat. 2,993,176, Issued July 18, 1961

A maser utilizing paramagnetic materials having anisotropic g-values is described. In previous masers either the frequency of the electromagnetic energy had to be swept through resonance or the external magnetic field varied. In the maser described the conditions for resonance are dependent upon the angle the crystal makes with the external field. By rapidly changing the angle, an inverted population distribution may be produced suitable for amplifying electromagnetic energy fed into a resonant cavity containing the paramagnetic material. In practice the material rotated has many crystals which are oriented at different angles so that some crystals will always be at an angle suitable for amplification.

12,711 RESEARCH ON PARAMAGNETIC RESONANCES by R.L. Kyhl and M.W.P. Strandberg (MIT); U.S. Gov. Res. Rep., Vol. 36, p. S-26(A), Aug. 5, 1961 PB 154 390

Gain and oscillation obtained from a paramagnetic crystal at 9 kMc by 180 degree pulse inversion are reported. Two energy levels and a single transition frequency in the spectrum of chromium in potassium cobalticyanide were used. The inversion pulses were of 10 mμsec duration. The oscillations showed an anomalous time dependence. A three-level maser was excited with ~1 μsec pumping pulses. The resulting oscillations showed a double decay with the longer time constant approaching 1 msec.

12,712 RESEARCH ON PARAMAGNETIC RESONANCES by R.L. Kyhl and M.W.P. Strandberg (MIT); U.S. Gov. Res. Rep., Vol. 36, p. 35(A), Aug. 20, 1961 AD 258 264

Research to obtain and investigate amplification by inverting the population of a paramagnetic mechanical system is discussed.

ome properties of spin-lattice relaxation constants are described. Limitations of electron magnetic-resonance detector nsitivity and quantitative spin determination are discussed. he observation of crossover transitions is reported.

2,713 RESEARCH ON PARAMAGNETIC RESONANCES by L. Kyhl and M.W.P. Strandberg (MIT); U.S. Gov. Res. ep., Vol. 36, p. 29(A), Nov. 5, 1961 AD 261 917

xperiments on reactance compensation of reflection type of avity masers are discussed. Measurements to determine optium ruby concentration and results obtained by using the ouble-cavity technique are described. Parallel experiments n unilateral broadband masers of the transmission type conining circularly polarized cavities have still not developed converging adjustment procedure for the excessive number of teracting tuning parameters. It is suggested that there is uch engineering work to be done before the system can be ed reliably as a part of a radio astronomy telescope or a persensitive laboratory spectrograph. A bandwidth greater an 100 Mc is obtained with a single ruby cavity.

2,714 ON THE PROBLEM OF PULSED OSCILLATIONS IN UBY MASER by G. Makhov (U. Michigan); U.S. Gov. Res. ep., Vol. 36, p. 27(A), Dec. 5, 1961 AD 263 339

is shown that the mechanism responsible for pulsed oscillaons in ruby maser is contained in the paramagnetic material nd bears a connection with ENDOR (electron-nuclear double sonance) interactions existing in ruby. This discovery refutes e theory commonly held that the pulsed mode is the result of ementary interaction between the inverted population of the ectron-spin system of the paramagnetic substance and the sonant cavity. The pulsed mode of oscillation is accounted r by suggesting that, in the case of the interaction between e electron-spin system and the resonant cavity, the instabilty producing pulsed oscillations is contained in the spin system. is instability results from the interaction between Cr electrons nd distant Al^{27} nuclei, and affects the pumping rather than the gnal transition.

2,715 TRANSIENT PHENOMENA IN RUBY MASER by F. ito (Nippon Elect.); J. Phys. Soc. Japan, Vol. 16, pp. 2-2593(L), Dec. 1961

ime lag (t_a) observed between the application of a pump gnal and the appearance of transient oscillations in an X-band ree-level ruby maser is discussed. The time lag has been easured as a function of the peak value of the pump power) and of the pump frequency (F). It was found that t_a inreased when either P or F decreased and that the amplitude of e oscillations decreased with a decrease in P. When the temerature was lowered from 4.2° to 2°K, t_a increased slightly. l measured values of t_a were on the order of a few hundred ec.

2,716 X-BAND LADDER-LINE TRAVELING-WAVE MASER G.I. Haddad and J.E. Rowe (U. of Michigan); U.S. Gov. s. Rep., Vol. 36, p. S-14(A), Nov. 5, 1961 PB 154 833

n X-band ruby traveling-wave maser (TWM) in which the RF ructure consists of a double-ridge ladder line and the signal coupled into and out of the structure with coaxial lines is scussed. The pump power propagates in a waveguide mode d the device operates at and below liquid He temperatures. The TWM is operated at the push-pull point with a pump frequency of 24 kMc and an approximate signal frequency of 9.65 kMc. Gross gains of 15 db have been obtained and bandwidths as high as 130 Mc are observed. General factors to be considered in the design of a broadband TWM are outlined and the choice of an RF propagating structure is considered in detail.

12,717 A RUBY LASER EXHIBITING PERIODIC RELAXATION OSCILLATIONS by R.E. Johnson, W.H. McMahan, F.J. Oharek, and A.P. Sheppard (Martin); Proc. IRE, Vol. 49, pp. 1942-1943(L), Dec. 1961

A ruby optical maser with confocal ends and an optical axis oriented 90 degrees to the cylinder axis is described. The ruby, measuring 2 inches in length and 1/4 inch in diameter, was centered in a GE FT-524 flash tube within a MgO reflector; one face was 2 per cent transmitting and the other heavily silvered. The threshold energy required was 1350 joules, as opposed to 2030 joules required for a zero-degree oriented ruby with flat ends under the same conditions. Total pulse duration was approximately 700 μsec with an initial pulse rise time of less than 0.2 μsec; the output was linearly polarized with a half-power beamwidth of 7.6 degrees. An important point to realize is that the relaxation oscillations generated were of a periodic nature; it is felt that this feature will enhance the usefulness of an optical maser in an optical ranging application using correlation techniques, and in Doppler ranging using ruby lasers.

12,718 DIRECT OBSERVATION OF MICROWAVE-FREQUENCY BEATS DUE TO PHOTOMIXING OF RUBY-OPTICAL-MASER MODES by B.J. McMurtry and A.E. Siegman (Stanford U.); U.S. Gov. Res. Rep., Vol. 36, p. 44(A), Dec. 20, 1961 AD 264 455

Observations of microwave signals produced by photomixing of near-neighbor axial-mode components in the output spectrum of a ruby optical maser (laser) are discussed. The observations were made by focusing the laser output onto the oxide cathode of an operating 2500-4000 Mc traveling-wave tube. Mixing (heterodyning) between the simultaneous, discrete optical frequencies in the laser output occurs in the TWT cathode, producing microwave amplitude modulation of the beam current. This amplitude modulation is amplified in the helix section producing easily observable microwave signals in the TWT output. Within the TWT bandwidth, discrete signals were observed at 1800 ±20, 2410 ± 3, 3000 ±20, and 3600 ±20 Mc, representing the "photo-beats" between third-through sixth-nearest neighbors in the laser-mode spectrum. This method of observation is a powerful tool for study of optical masers and also has significant implications for communications employing microwave-modulated light.

12,719 OPTICAL MASER ACTION OF Nd^{+3} IN A BARIUM CROWN GLASS by E. Snitzer (Am. Optical); Phys. Rev. Lett, Vol. 7, pp. 444-446(L), Dec. 15, 1961

Optical maser action observed in a glass optical maser which operates at room temperature is described. The maser had an output consisting of a number of sharp lines in a wavelength interval of about 30 A centered at ~1.06 μ. Nd^{+3} was used as the active ion, with the concentration of Nd_2O_3 varying from 0.13 to 2.0 wt per cent. The device utilized clad rods consisting of cores of Ba crown glass (59 wt per cent SiO_2, 25 per cent BaO, 15 per cent K_2O, and 1 per cent Sb_2O_3) having an index of refraction of 1.54 and cladding of ordinary

soda-lime-silicate glass with an index of refraction of 1.52. Several reasons for utilizing the clad rods are pointed out.

12,720 FEEDBACK MODULATION WITH A RUBY OPTICAL MASER by R.J. Collins and P. Kisliuk (Bell Labs.); Bull. Am. Phys. Soc., Ser. II, Vol. 6, p. 414(A), Nov. 24, 1961

Modulation of the optical feedback in a ruby maser to increase the output peak power is discussed. A pulsed ruby optical maser was constructed with detached mirrors allowing a shutter to be placed between the ruby and one mirror. In this way, a variable delay could be introduced between the application of the pumping source and application of the optical feedback. The rate of restoration of feedback can be fast compared to the buildup time of maser oscillation; comparable to the duration of a single "spike," or slow compared to the duration of a spike. Results for the case in which the peak powers were increased by a factor of ~10 are discussed. A study of the spiking behavior of a ruby maser in the absence of pumping radiation was made by delaying the application of feedback until after the pumping source had been extinguished.

12,721 OPTICAL MASER ACTION IN THE R_2 LINE IN RUBY by F.J. McClung, S.E. Schwarz, R.W. Hellwarth, I.J. D'Haenens (Hughes Res. Labs.), and F.J. Meyers (Hughes Aircraft); Bull. Am. Phys. Soc., Ser. II, Vol. 6, p. 511(A), Dec. 27, 1961

Optical maser action observed in the R_2 line of ruby was discussed. Because of a fast thermal relaxation between the two E levels it is not usually possible to satisfy the maser conditions at R_2 when R_1 is masering. However, if the R_1 line can be suppressed from masering even at high inversions, the R_2 line can be made to maser by the appropriate selection of operating conditions. This has been accomplished for end plates by using multilayer dielectric interference filters which have high transmission at R_1 and low transmission at R_2. The necessary filter conditions and the operating characteristics were described.

12,722 SOLID-STATE MASER RESEARCH by E.D. Reed (Bell Labs.); U.S. Gov. Res. Rep., Vol. 36, p. 30(A), Aug. 20, 1961 AD 257 969

Research covering five different subjects in the field of solid state masers is discussed. The subjects are: (1) a study of the optimum ruby orientation for traveling-wave maser applications, (2) an experimental program on a new maser material consisting of Gd in $CaWO_4$ (in particular the inherent gain of this material at low microwave frequencies is being studied, (3) an experimental study of broadening the effective ruby linewidth by shaping the applied dc magnetic field, (4) the continuation of a theoretical treatment of harmonic spin coupling, and (5) a study of paramagnetic resonance properties of Co-doped Al_2O_3.

12,723 OPTICAL TECHNIQUES FOR ELECTRONIC ENGINEERS by R.M. Benrey (MIT); Electronics, Vol. 34, pp. 47-53, Oct. 20, 1961

Optical principles and techniques useful to electronic engineers are summarized. Practical and applied optics and the techniques included under classical optics which are of concern to engineers are discussed. Lens design, optical quality, and the system limitations imposed by diffraction phenomena are explained. The properties of solid state and gaseous masers are compared and their limitations are discussed. A glossary of commonly used optical terms is included.

12,724 SOLID STATE MASER AMPLIFIER by R.C. Fletcher, H.E.D. Scovil, and H. Seidel (Bell Labs.); U.S. Pat. 3,001,141, Issued Sept. 19, 1961

A solid state amplifier which makes use of stimulated emission of radiation is described. An inverted population of energy levels or negative temperature in the medium is continuously maintained by the application of pumping power of frequency not significantly greater and in some cases less than that of the signal frequency. The medium is a paramagnetic substance whose population of electron spins is capable of at least four discrete energy levels of successively higher energies designated E_1, E_2, E_3, and E_4 respectively. The separations between the E_1 and E_2 and between E_3 and E_4 are each made to correspond to frequencies in a useful operating range, typically the microwave range. Application of spin lattice relaxation times between different levels is employed to maintain the desired excited states. The effects of doping the operating material with a paramagnetic salt possessing the necessary energy levels and spin-lattice relaxation times are discussed. Modifications to the basic form of solid state maser discussed are Faraday light rotation effect, and a means of utilizing magnetic susceptibility changes in the medium to modulate a carrier wave.

12,725 THE RUBY MASER. A PRACTICAL MICROWAVE AMPLIFIER by J.J. Cook, M.E. Bair, and L.G. Cross (U. Michigan); U.S. Gov. Res. Rep., Vol. 36, p. 29(A), Nov. 20, 1961 AD 262 709

The ruby maser is shown to be a stable, reliable, low-noise microwave amplifier. Results of the study indicate that performance improvements up to 14 db can easily be obtained. Test results of an engineering and development program to package the maser for use in a radio telescope demonstrated the feasibility of using the ruby maser as a compact, practical, and dependable field unit. The theory of operation of the maser is discussed and its potential use for ground surveillance, missile and satellite tracking, and space communications is described.

12,726 SOLID-STATE MASER AMPLIFIER, X-BAND by T.H. Maiman (Hughes Aircraft); U.S. Gov. Res. Rep., Vol. 36, p. S-14(A), Nov. 5, 1961 PB 155 561

The design and performance of a complete X-band maser receiver are described. Novel design features include a ruby-filled cavity which is fabricated from a solid block of ruby and coated with silver. An internal 12-oz permanent magnet provides the required magnetic field. Achievement of substantial miniaturization in maser design is reflected in the overall weight and size, which are 25 lb and 1/3 cu ft, respectively. This maser was successfully operated at temperatures from 1° to 100°K. At 4.2°K the gain-bandwidth product is 105 Mc and the overall receiver noise temperature is 25°K.

Maser-Parametric Low Noise Preamplifiers - See 12,785

12,727 A ZERO-FIELD X-BAND MASER SPECTROMETER by N. McAvoy, M.R. Kagan, and V.W.T. Townsend (Melpar); Bull. Am. Phys. Soc., Ser. II, Vol. 6, p. 298(A), Apr. 24, 1961

An X-band paramagnetic resonance spectrometer using a maser as either an oscillator or detector was discussed. A zero-field maser using Fe^{3+} doped Al_2O_3 is employed. Theoretical and experimental evaluations were given comparing the sensitivities

ARAMAGNETIC DEVICES (Masers and Lasers) (Cont'd)

f a conventional spectrometer with a maser-type spectrometer. his theoretical treatment included a four-part circulator with cillator-detector combinations. The design problems introuced by using detectors and sources with less than the blackody noise were also discussed.

DIELECTRIC DEVICES

2,728 NIOBIUM SOLID ELECTROLYTIC CAPACITORS by N. hwartz, M. Gresh, and S. Karlik (Bell Labs.); J. Electroem. Soc., Vol. 108, pp. 750-758, Aug. 1961

he suitability of Nb as an anode for solid electrolytic capacirs is discussed. Field crystallization of the amorphous NbO m is a determining factor for the properties of these capacirs. Purity of the porous anodes as dependent on the sintering nditions, formation temperature and voltage, and formation ectrolytes, parameters all known to control the initiation of ystallization, are correlated with the initial and life test operties of these capacitors. The initial properties of Nb lid electrolytic capacitors prepared under optimum conditions mpare favorably with equivalent tantalum components. Hower, with the current purity of Nb powder, only units with erating voltages up to 20 v survive a life test at 85°C. The ilures of capacitors rated at higher voltages are attributed to e partial crystallization of the amorphous film during formaon.

,729 APPLICATION CHARACTERISTICS OF SOLID TANTAUM CAPACITORS by R. Rhodes (IBM); 1961 IRE Intl. Conv. c., Part 6, pp. 254-266

estructive testing of tantalum capacitors and circuit applicaon information when high current power supplies present the ssibility of large current flow in case of component failure discussed. Component failure frequently leads to package ilure. Several possible kinds of package rupture are illusted photographically. The mechanism of solid tantalum caitor failure is found to be momentary breakdown followed avalanche until the oxide film is destroyed. Fusing proved be the most practical protective feature.

,730 CHARACTERISTICS OF THE SPACE-CHARGE-LIMITED ECTRIC DIODE AT VERY HIGH FREQUENCIES by J. Shao d G.T. Wright (U. Birmingham); Solid State Electronics, l. 3, pp. 291-303, Nov.-Dec. 1961

e incremental admittance of the space-charge-limited dictric diode is calculated. It is shown that for all frequenes the admittance can be represented as a conductance and ceptance in parallel. At very high frequencies, transit time ects reduce the forward conductance to 0.667 of the low quency value and increase the input capacitance to 1.33 of low frequency value. At low frequencies, such that transit e effects can be neglected, the reverse biased capacitance constant and equal to the geometrical electrode capacitance; forward biased capacitance is constant and equal to 0.75 the reverse biased capacitance. There are no negative reance effects at any frequency. Experimental measurements ve been made on space-charge-limited CdS diodes over the quency range 50 - 1000 Mc. These confirm the theoretical alysis and support the physical model used for describing ce-charge-limited current in solids.

OTHER SOLID STATE DEVICES

12,731 SUPERCONDUCTING MAGNETS by R.H. Kropschot and V. Arp (Natl. Bu. Stand.); Cryogenics, Vol. 2, pp. 1-15, Sept. 1961

The attainment of high fields with superconducting magnets and the fundamentals of superconductivity are discussed. A detailed treatment of wire-wound solenoids which employ elemental and alloy superconductors is supplemented with graphic data. Special design considerations (such as forces on magnets, time constants, field distribution, and operational precautions) and the economic factors affecting the application of high field magnets are considered.

12,732 FREQUENCY MIXING WITH SUPERCONDUCTING ELEMENTS by S. Shapiro (A.D. Little); U.S. Gov. Res. Rep., Vol. 36, p. 94(A), Aug. 20, 1961 AD 258 087

Two approaches to the problem of frequency mixing using superconducting elements are examined. One point of view involves the nonlinear effects associated with the superconducting-normal phase transition. The other treats the electrodynamics of superconductors with particular attention to possible nonlinear effects associated with a body maintained within the superconducting state. The details of an experimental program designed to investigate the latter effects are given. Discussion of recent developments, especially in the observation of tunneling between superconductors, indicates the directions in which the aims of this study might be further pursued.

12,733 CRYOGENIC INDUCTORS MAY BECOME POWER SOURCE by A. Hemel (Illinois Inst. Tech.); Electronics, Vol. 34, pp. 96-97, Nov. 10, 1961

The possibility of storing energy in cryogenically cooled inductors is described. The energy storage of a one henry coil with 10^5 amp flowing is 1390 kwh or 1680 hp-hr. Average current densities of 100 amp/cm^2 in the superconducting state have been observed in Nb_3Sn with superconductivity persisting in magnetic fields of 88 kilogauss. A conceivable arrangement to extract the energy from the coil and to recharge the cryogenic inductor is suggested.

12,734 DEPLETION LAYER TRANSDUCER — A NEW HIGH FREQUENCY ULTRASONIC TRANSDUCER by D.L. White (Bell Labs.); 1961 IRE Intl. Conv. Rec., Part 6, pp. 304-309

A high frequency (830 Mc) high efficiency depletion layer ultrasonic transducer is described. The ultrasonic waves are generated or detected by a thin, flat, high resistance layer (such as a p-n junction or rectifying metal to semiconducting contact) in an extrinsic piezoelectric semiconductor. When an ac voltage is applied to the material, the depletion layer behaves in a manner similar to an extremely thin piezoelectric crystal bonded to the conducting substrate. Since this depletion layer can be generated on the surface of the transducer, the problems of handling very thin piezoelectric plates are avoided.

Effects of Stress of Piezoelectric Ceramics Utilized in Transducers - See 12,458

Piezoelectric Generation of an Electrical Impulse - See 12,457

12,735 MINIATURE PIEZOELECTRIC GAGES FOR MEASURING TRANSIENT PRESSURE ON AIRFOILS by W.E. Baker and W.O. Ewing, Jr. (Aberdeen Proving Gnd.); U.S. Gov. Res.

Rep., Vol. 36, p. 114(A), Aug. 20, 1961 AD 258 017

The design, construction, and test of miniature piezoelectric pressure gauges for measuring blast-induced transient pressures on the surface of airfoils mounted on rocket sleds are discussed. The results of pressure calibrations, vibration testing, and shock tube testing indicate that the gauges are probably suitable for the purpose for which they were designed.

12,736 A CERAMIC BAND-PASS TRANSFORMER AND FILTER ELEMENT by A. Lungo and F. Sauerland (Clevite); 1961 IRE Intl. Conv. Rec., Part 6, pp. 189-203

A ceramic band-pass transformer for use in IF circuitry is described. Fabricated of a highly stable piezoelectric ceramic, this component takes the form of a small multiple-electrode disk operating at the first overtone of the radial mode. The electrode configuration in the form of a ring and dot provides an impedance transformation. Also, being a resonant device, a frequency band-pass characteristic is provided. A simplified equivalent circuit of the ceramic transformer is presented along with an analysis of the circuit. Reference is made to two well-known impedance transforming networks (the L-section and the π-network) which are used to explain the circuit behavior of the ceramic transformer.

12,737 CRYSTAL FILTERS by S. Malinowski and D. Schennberg (Motorola); U.S. Gov. Res. Rep., Vol. 36, p. 33(A), Nov. 20, 1961 AD 262 927

The inductively coupled lattice equivalent is found both theoretically and experimentally to be applicable to the construction of VHF wideband crystal filters. A step-by-step design procedure is illustrated. A complete description of the filter including component values and test equipment is given; all the test data are presented. The experimental results of a filter with crystals exhibiting spurious manifestations are compared with the results of a theoretical study. The behavior under high drive of a crystal filter is investigated theoretically and experimentally. Methods of measuring crystal parameters and simple tuning procedures are described.

12,738 A CONTRIBUTION TO THE ANALYSIS OF INVERSE MAGNETOSTRICTION [in Czech] by M. Gabler (Lab. Theory Info. Automn., Acad. Sci. CSR); Elektrotech. Casopis, Vol. 12, No. 9, pp. 580-590, No. 10, pp. 625-639, 1961

Qualitative relations expressing the phenomenon of inverse magnetostriction in transducers on the basis of the active ferromagnetic medium energy minimum are derived. The form of this ferromagnetic medium and the load of the output winding, where voltages proportional to mechanical stresses are induced, are taken into consideration. The characteristics of such transducers are discussed and experimental material confirming the theoretical results is given. Using these results, the conditions of work and the realization of the stated transmitters can be determined.

12,739 LOW TEMPERATURE COEFFICIENT ULTRASONIC SOLID DELAY LINES by P.A. Bauer (Corning); Solid State J., Vol. 2, pp. 23-29, Dec. 1961

A glass ultrasonic delay line which is relatively temperature-independent is described. Delays of 4 to 10,000 μsec at operating frequencies from one to 60 Mc are possible employing ultrasonic solid delay lines. The glass provides several advantages over more conventional delay line media: temperature stability, smaller size, lighter weight, better spurious signal level, increased bandwidth, and lower cost in some applications. The delay lines are useful for application in missile and satellite navigational systems, pulse compression radars, ultra stable clock circuits and as radar PRF staggers. Essential delay line properties are presented in both tabular and graphic forms equations for the delay time of a delay line are given.

BASIC SOLID STATE DEVICE CIRCUITS

GENERAL

12,740 NETWORK SYNTHESIS USING SIGNAL FLOW GRAPHS by E. Kushel (Polytech. Inst. Brooklyn); U.S. Gov. Res. Rep., Vol. 36, p. 36(A), Oct. 5, 1961 AD 260 572

A technique for the synthesis of driving point emittance functions through the use of signal flow graphs is described. The method is shown to be completely general. A signal flow graph is drawn after an examination of the driving point function. This flow graph is related to a realizable network. The values of elements in the branches of the network are found from a consideration of loop gains in the flow graph. The theory involved is first illustrated in terms of the synthesis of two element type circuits, then the general RLC case is treate

12,741 TIME RESPONSE CHARACTERISTICS OF LINEAR NE WORKS AND TRANSFORMATION METHODS IN NETWORK SYNTHESIS by J.D. Brule and B.P. Shah (Syracuse U. Res. Inst.); U.S. Gov. Res. Rep., Vol. 36, p. 91(A), Aug. 20, 1961 AD 257 822

An attempt to use the criterion of least-squared error to determine analytically the shifts of the locations of the poles and residues of a transfer function in order to meet a time domain specification is discussed. A first approximation is obtained with the help of existing methods, and successive steps are carried out using the first two terms of the Taylor Series expansion of the first approximation. In the process, orthogonal vector functions are formed by linear combinations of the part derivative functions. The use of FORTRAN for programming the problem for the IBM 650 data processing machine is illustrated.

12,742 TRANSFER FUNCTION SYNTHESIS OF ACTIVE RC NETWORKS by E.S. Kuh (U. California); U.S. Gov. Res. Re Vol. 36, p. S-18(A), Sept. 20, 1961 PB 156 845

A general method of synthesizing voltage transfer functions w complex poles and zeros using RC elements and a practical tr sistor amplifier is presented. The method allows specified source and load resistances. The overall network has a comm ground and is economical in terms of the number of elements.

12,743 THE USE OF WEIGHT FUNCTIONS IN THE TRANSI ANALYSIS OF NONLINEAR CIRCUITS by C.S. Yen (Stanfor U.); U.S. Gov. Res. Rep., Vol. 36, p. 29(A), Aug. 20, 19 AD 257 943

The solution of a second-order differential equation for a non

linear electric circuit is discussed. Using the principle of variation of parameters a given equation is reduced to two first-order differential equations. A weight function method is then applied to these two equations. The result of this analysis is presented by two transient-response curves. Three systems of equations are studied. For the first two systems, the results obtained are either better than or comparable to those of the Kryloff and Bogoliuboff method. Some improvement of the Kryloff and Bogoliuboff method, using the results of the weight function method, is considered, and excellent results are obtained. The third system is an example of use of the undamped frequency in the assumed solution, which is a generalization of the Kryloff and Bogoliuboff method. For the single-term approximation, error increases with increasing nonlinearity due to the presence of higher harmonics.

12,744 CONVOLUTION Z-TRANSFORM METHOD TO CERTAIN NONLINEAR DISCRETE SYSTEMS by E.I. Jury and M. A. Pai (U. California, Berkeley); U.S. Gov. Res. Rep., Vol. 36, p. S-22(A), Aug. 20, 1961 PB 155 452

The convolution Z-transform method is used to obtain an explicit solution of certain nonlinear difference equations. The explicit solution is often desired for system design as well as for obtaining the response for large intervals of time. In these difference equations, which describe the physical discrete systems, it is assumed that the nonlinearities are small. This is necessitated by the form of solution applicable to the use of the convolution method. The advantage of the method is to systematize the procedure for the solution as well as to obtain results in a closed form. The convergence of the solution is discussed as well as applications to certain examples. The examples chosen are feedback sampled-data systems with nonlinearities in the forward and feedback paths, respectively. Explicit solution in a closed form is obtained for the error as well as the output response. These results compare favorably with the numerical solution of the nonlinear difference as a recurrence relationship.

12,745 MICROMINIATURE COMPONENTS AND PACKAGING TECHNIQUES by S.M. Stuhlbarg and L.P. Sweaney; 1961 IRE Intl. Conv. Rec., Part 6, pp. 3-17

A comprehensive market analysis on microminiature components, including visits with more than 300 cognizant engineers and scientists, followed by a mail survey and several presentation years is discussed. The results of this analysis indicate that there is an expanding market for reliable, discrete microcomponents, and that the advent of functional circuitry utilizing thin film and semiconductor techniques will not diminish this market for a number of years. A number of wafer and pellet-shaped microcomponents are discussed including tantalum and ceramic capacitors, carbon and metal oxide film resistors, and silicon rectifiers. Various packaging techniques which lend themselves to production mechanization are described. A unique program is outlined in which development activities, reliability analyses, and pilot production functions are integrated to provide prototype sample lots having incrementally reducing failure rates.

12,746 A DOT COMPONENT PACKAGING SYSTEM FOR ELECTRONICS by A.E. Hawley, E.A. Klein, and S. Rubin (Hughes Aircraft); 1961 IRE Intl. Conv. Rec., Part 6, pp. 18-28

A new microminiature electronics packaging design philosophy and an application to a digital system are discussed. The package utilizes the new miniature "dot" components mounted in ceramic wafers. The "dot" components are 0.05 inch in diameter and 0.03 inch thick. Component connections are made by multilayer deposition techniques and connections to modules are made by a novel pressure connection method. A unique and compact heat transfer scheme is described. The design example contains 2260 components in an approximately 1.25 inch cube. The component density of the package (including all thermal interconnection and structural provisions) is 2,080,000 per cubic foot. Repairability is such that component replacement is possible and module replacement in the field is practical. The package is designed to function at temperatures to 96°C with 100°C components, can be sealed against contamination, and is sufficiently rugged to withstand space environments. The major design features are shown in eleven illustrations; numerical data and comparison with other packaging schemes are shown in two tables.

12,747 RESEARCH ON VARIOUS PHENOMENA FOR THE PERFORMANCE OF CIRCUIT FUNCTIONS by E.J. Scheibner and A.L. Bennett (Georgia Inst. Tech.); U.S. Gov. Res. Rep., Vol. 36, p. 91(A), Aug. 20, 1961 AD 257 864

An investigation of various solid-state phenomena and effects which might have an application in electronic systems is discussed. Technical articles on fifty-two phenomena and effects are presented. Each article includes a definition, a detailed description, and a short bibliography. Eighteen other related effects are also covered.

12,748 ANALYSIS OF CIRCUITS CONTAINING VARIABLE CAPACITANCE DIODES by D.R. Anderson and B.J. Leon (Hughes Res. Labs.); 1961 IRE Intl. Conv. Rec., Part 4, pp. 182-190

A method of analysis for circuit models consisting of a capacitive diode imbedded in an arbitrary linear time-invariant network is presented. The diode characteristics assumed have been verified by careful measurement. Both the simplifying assumption of ideal filters in the linear circuit and that of a two-term Taylor series for the diode characteristic are avoided. The main points of this method are: (1) a useful set of a priori conditions on the circuit and its excitation that guarantee operation within the capacitive range of the diode, (2) a method for finding the periodic response for the circuit used as a frequency multiplier, and (3) a method for evaluating the parameters in the linear time-variant model that characterizes the small signal performance of parametric amplifiers. An estimate for the errors introduced by this linearization is given.

12,749 PROPERTIES AND REALIZATION OF CERTAIN VARIABLE NETWORKS by N. Herbst (Cornell U.); U.S. Gov. Res. Rep., Vol. 36, p. 28(A), Sept. 5, 1961 AD 258 528

A survey of available physical network elements that reveals the practicality of an extension of network theory to include variable elements is presented. Semiconductor variable capacitors seem especially practical. Several connections of these capacitors are analyzed, and the series back-to-back is shown to be best with respect to eliminating signal effects upon the capacitance. Single-element-kind networks are considered in detail. Necessary and sufficient realizability conditions upon the driving-point impedances of lossless networks with one variable element are then derived and a realization procedure is developed. The realization for lossless networks is extended to include networks with one variable reactive

element and one resistance. A set of necessary and sufficient conditions for the realizability of driving-point impedances of these networks is developed and a realization procedure which leads to a set of canonic forms for such networks is presented. The technique is also adapted to allow realization of certain variable transfer functions.

12,750 TUNNEL DIODE THEORY AND APPLICATIONS by R. Nanavati, W.H. Card et al. (Syracuse U.); U.S. Gov. Res. Rep., Vol. 36, p. 40(A), Oct. 5, 1961 AD 260 776

Research concerned with tunnel diode theory and applications is discussed. Effort devoted to the related objective of developing a better understanding of the behavior of negative resistance devices in general is also described. The basic theory of the tunnel diode is presented including most of the presently known essential elements.

12,751 STABILITY CRITERIA FOR TUNNEL DIODES by L.I. Smilen and D.C. Youla (Polytech. Inst. Brooklyn); Proc. IRE, Vol. 49, pp. 1206-1207(L), July 1961

Various stability criteria for a tunnel diode are collated and discussed. The necessary conditions for a tunnel diode to be potentially stable are $r/R < 1$ and $L/R^2C < F(\theta)$; the sufficient conditions are $r/R < 1$ and $L/R^2C < 1$, where r and L are the series resistance and inductance, C and -R the parallel capacitance and resistance in the equivalent circuit of a tunnel diode.

$$F(\theta) = \frac{\theta^3}{(1+\theta^2)(\theta - \tan^{-1}\theta)} \quad \text{and} \quad \theta = \sqrt{\frac{r/R}{1-(r/R)}}\,.$$

12,752 TUNNEL-DIODE POWER by G. Dermit (Genl. Tel. Electronics); Solid State Electronics, Vol. 3, pp. 208-214, Nov.-Dec. 1961

An expression for nearly linear tunnel-diode power is derived. This expression is based on the fact that the time constant RC of tunnel junctions is a sensitive function of the impurity concentration in the semiconductor material, whereas the series RC product is a very slow varying function of impurity concentration. Tunnel-diode operation in the nearly linear range is specified with the aid of a single chart which applies to all materials and to arbitrary values of series resistances. A set of semicircles represents the power-inductance product per unit voltage-swing squared. Another set of quarter circles of the same chart specifies the LC products.

12,753 THEORY OF THE ESAKI DIODE FREQUENCY CONVERTER by R.A. Pucel (Raytheon); Solid State Electronics, Vol. 3, pp. 167-207, Nov.-Dec. 1961

A simple two-port admittance matrix, which represents the small signal conversion properties of a tunnel diode and whose elements are certain coefficients of the periodic time-dependent diode conductance produced by the pump, is derived. In terms of these coefficients and other diode parameters, expressions for such useful conversion properties as the load conditions necessary for circuit stability, the minimum noise figure, the maximum gain-bandwidth product, the necessary conditions for a positive mixer conductance at the RF and IF ports, and the pump loading necessary for self-excitation are derived. Under proper conditions partial noise cancellation can occur because of correlation effects arising from the nonstationarity of the shot-noise process in the pumped diode. Most of the theoretical results are illustrated by the data obtained from a detailed Fourier analysis applied to an actual high-frequency tunnel diode characteristic. These calculations show that the lowest noise figure and the highest gain-bandwidth product are obtained when the diode is biased in its negative conductance region.

12,754 APPLICATIONS OF THE CONSTANT-CURRENT DIODE by T.K. Hemingway (English Elect. Aviation); Electronic Vol. 34, pp. 60-63, Oct. 20, 1961

Circuit applications of experimental constant-current diodes are described. The diode reduces the effect of variation in supply voltage and spurious feedback. The presently available diodes are suitable for use only at laboratory temperatures. Results show that improvements and component-reduction can be achieved in low-frequency circuits. In decoupling circuits and voltage stabilizers, previously unobtainable results are easily achieved. However, little work has been done in regard to quantity manufacture of the diodes. Different circuit applications of constant-current diodes are described in detail and the results are compared to conventional circuits.

12,755 TRANSISTOR CIRCUITS by A.P. Stern (GE); Handbook Automn., Computatn., and Control, Vol. 3, John Wiley and Sons, 1961, pp. 27-01 — 27-112

A detailed consideration of the application of transistors to electronic circuitry is given. The basic circuit properties of the transistor are examined, and the h, z, and y type equivalent circuits are derived. Temperature effects are considered together with the various techniques of bias stabilization. Both low- and high-frequency amplifiers are studied; the equivalent circuit for each is given and the design equations for both types are tabulated. The properties of wideband (video) amplifiers and bandpass amplifiers are illustrated by several commonly used circuits; formulae for the design of coupling networks for tuned amplifiers are tabulated. Various types of dc amplifiers are illustrated, followed by a discussion of oscillators, modulators, mixers, and detectors. Design techniques for transistor switches, flip-flops, and monostable multivibrators are illustrated und applications to logic and computer circuitry are shown. A discussion of power supplies and power converters and an extensive selection of references to transistor circuit design are included.

12,756 RESEARCH DIRECTED TOWARD THE STUDY, ANALYSIS AND DESIGN OF TRANSISTOR CIRCUITS by A.W. Carlson (Transistor Appl.); U.S. Gov. Res. Rep., Vol. 36, p. 33(A), Aug. 20, 1961 AD 258 138

A 34-section nonlinear line using reverse biased junction diodes for voltage dependent shunt capacitance is described. The line is to be used to investigate proglems raised in interpreting the mathematical solution of the lossless uniform distributed nonlinear line given in AD 238 929 (see also Abstract 7084). A two-transistor free-running sawtooth generator having a linear portion and a rapid recycle is described. In one version of the circuit, one of the transistors performs as a blocking oscillator and as an emitter follower to give a low impedance output for the signal. A counter using a closed loop shift register having one inversion in the loop was also investigated. This type of operation has advantages at high count rates and also gives a reduction in active elements.

12,757 COMPUTER-DERIVED CURVES SIMPLIFY TRANSISTOR CIRCUIT DESIGN by D. McLaren (Martin); Electronics, Vol. 34, pp. 48-54, Nov. 3, 1961

he use of computer-derived curves in the design of transistor ircuits is described. The only information required to use the urves is the value of gain and stability desired. The equations sed are linear, making it possible to interpolate and extrap- late between sets of curves. The curves will provide compo- ent values and the optimum operating point. Two examples e given to illustrate the use of the curves. The various pa- ameters of frequency-sensitive transistors and their derivations e also given.

2,758 AVALANCHE TRANSISTOR CIRCUITS by W.M. enebry (U. Illinois); U.S. Gov. Res. Rep., Vol. 36, p. 26 A), Aug. 20, 1961 AD 257 748

n investigation of avalanche transistor circuits is presented. hese circuits offer several features which are desirable in fast ounting systems: (1) simplicity, (2) versatility, (3) fast re- ponse, and (4) large charge gain. The investigation was con- erned with the evolution of avalanche circuits which retain e desirable features but which do not suffer from the two de- cts of the basic avalanche circuit, i.e., low duty cycle and pulse propagation delay which is nonlinearly dependent upon put. Several transistor types which are suitable for fast ava- nche circuits are compared and comments are made about the pplication of these transistors. Several useful circuits which ay be constructed with avalanche transistor techniques are so described.

2,759 A NEW GAIN AND POWER CONCEPT IN TRANSIS- ORS WITH CIRCUITS EXTENDING THE FREQUENCY RANGE NTO THE MICROWAVE REGION by R. Zuleeg (Hughes Air- raft) and V.W. Vodicka (Lenkurt); 1961 IRE Intl. Conv. Rec., art 4, pp. 191-201

e operation of certain types of drift transistors at frequencies yond the maximum defined limit is discussed. Beyond

$$f_{max} = \sqrt{\alpha_o f_c / 8\pi r_b' C_c}$$

ds are available in which power gain and harmonic power eration are possible. Practical circuits are presented for eration in the microwave region. A theory which describes e transit-time effects of minority carriers across the base gion of the drift transistor at frequencies above cutoff is de- ed. Circuit performance of the transistors is described for equencies between 500 Mc and 3.6 kMc.

2,760 EXTEND TRANSISTOR FREQUENCY; Electronics, l. 34, p. 25, Nov. 3, 1961

new operating mode which increases the HF gain of transis- s, reduces interstage matching problems, and improves se- ctivity and stability is described. Gains of 20 db have been ieved. Inductances in the emitter circuit are neutralized a small variable capacitor between emitter and ground, th a dc path provided by an RF choke. The capacitor is ad- ted to the operating frequency which is independent of the ecific transistor as long as it is below the intrinsic cutoff quency of the transistor junction. No improvement can be ained if the cutoff frequency is limited by the transistor ction.

2,761 A DESIGN TECHNIQUE FOR HIGH SPEED TRANSIS- R CIRCUITS by W.A. Doesschate, Jr. (Raytheon); Raytheon ctronic Prog., Vol. 6, pp. 8-13, Nov.-Dec. 1961

Circuit layout techniques necessary for high-speed transistor circuits are discussed. The cost and complexity of using a co- axial air transmission line method is described and an alternate strip transmission line system which consists basically of two flat conducting plates precisely spaced with a flat center con- ductor running down the center between the two plates is intro- duced. Even this system is not well suited for changing lumped parameters and a circuit construction revolving about the use of copper laminated breadboard is given. The copper clad board greatly reduces the inductive properties of the ground section of the circuit. Normal breadboard construction is lim- ited by factors of skin effect and the restriction of current flow to two directions along a wire; with a Cu ground plane, currents can flow in any direction whatever and interaction is at a mini- mum. A comparison of output waveshapes of an avalanche pulse generator circuit indicates that the Cu clad-board method is a transition between the standard breadboard methods and the special HF techniques. The Cu clad-board method may be used to lay out a circuit to check its operation and component choice previous to its construction in strip line or coaxial lay- outs.

12,762 NETWORK THEORY OF SEMICONDUCTOR HALL PLATE CIRCUITS by J.M. Garg (Polytech. Inst. Brooklyn); U.S. Gov. Res. Rep., Vol. 36, p. 93(A), Aug. 20, 1961 AD 257 934

A study of the properties and synthesis of passive electrical networks which contain Hall plates as nonreciprocal elements is reported. Network representations of these elements which are dissipative and linear and exhibit nonreciprocity, and their optimum performance when used in a suitable connection with other conventional network elements are the major topics stressed.

AMPLIFIERS

12,763 AMPLIFIERS by R. O. Maze (Minn.-Honeywell); Handbook Automn., Computatn., and Control, Vol. 3, John Wiley and Sons, 1961, pp. 21-01 to 21-49

A survey of the various types of amplifiers and their comparative advantages is given. Among those considered are vacuum tube and semiconductor amplifiers, dielectric and plasma amplifiers, magnetic amplifiers, and electromechanical amplifiers. Factors such as size, weight, efficiency, cooling requirements, reliabil- ity, and power supply requirements are considered, and the common fields of application for each device are indicated. Characteristics of rotary and pneumatic amplifiers are discussed, and the use of pneumatic amplifiers in control circuits is indi- cated. Data on modulators for control applications are tabu- lated, and the use of modulators and demodulators in dc ampli- fiers is considered.

12,764 MULTISTAGE TRANSISTOR AMPLIFIER by R.W. Brad- miller (Avco); U.S. Pat. 3,001,145, Issued Sept. 19, 1961

A transistor multiple stage amplifier employing negative dc feedback and automatic gain control is discussed. An alternate p-n-p — n-p-n arrangement simplifies AGC and feedback net- works. The negative feedback voltage is developed across a dc load resistor in the last amplifying stage and is applied to the base of the first transistor amplifier. An automatic gain control signal is applied from an appropriate AGC stage to the same point. Neutralization is not required by the stages since

the ac load impedance is reduced by direct coupling of the collector to the base. The LC ratio of the tuned circuits is smaller than that usually employed, which minimizes the effect of inherent internal capacity. Application of dc load resistors in the emitter circuits degenerates the dc gain so that the dc characteristics of the transistors are made nearly independent of the transistor internal parameters. Any commercially available transistor suitable for amplifying the desired frequency band may be used in the circuit. The amplifying circuit has great utility in intermediate frequency amplifiers found in superheterodyne receivers.

12,765 TUNED TRANSISTOR AMPLIFIER by W. Minner (Telefunken); U.S. Pat. 2,997,658, Issued Aug. 22, 1961

A circuit which eliminates the effect of the transistor collector capacity on the output resonant circuit is described. A resistor, shunted by a choke, is inserted between the collector and the resonant circuit. The series circuit of the collector capacitance and the resistor operates as a shunt circuit. A collector capacitance variation of 2.5 to 5 μμf is converted to an effective capacitance variation of 1.69 to 1.79 μμf by proper choice of the resistor.

Design of Amplifiers - See 12,657

12,766 BANDWIDTH LIMITATIONS AND SYNTHESIS PROCEDURES FOR NEGATIVE RESISTANCE AND VARIABLE REACTANCE AMPLIFIERS by R.M. Aron (Calif. Inst. Tech.); U.S. Gov. Res. Rep., Vol. 36, p. S-17, Sept. 20, 1961 PB 156 874

The bandwidth limitation on the reflection coefficient of circuits containing a reactance limited negative conductance such as a tunnel diode is derived. The insertion loss method of modern network theory is adapted to the synthesis of low pass ladder equivalents of amplifiers containing these elements. Amplifiers which have a considerable bandwidth advantage over simple single tuned circuits, and which approach the ultimate bandwidth limit as rapidly as possible as the number of passive components is increased, are demonstrated. Fundamental bandwidth limitations of three-frequency nonlinear reactance amplifiers, parametric amplifiers, and noninverting upconverters are found. A low-pass ladder equivalent circuit and the insertion loss method are shown to be useful tools for synthesis of these amplifiers. Considerable bandwidth advantage over single-tuned circuits is again demonstrated.

12,767 TRANSISTOR STABILIZATION CIRCUIT by J.L. Jensen (Minn.-Honeywell); U.S. Pat. 2,997,657, Issued Aug. 22, 1961

A method to equalize current flow in parallel-connected amplifiers is described. A pair of transistors have their input circuits parallel-connected to a transformer winding. A second transformer in the output circuit, with a center-tapped primary connected series-opposing, has a center-tapped secondary connected in the transistor input circuits. Any inequality in the current output of the two transistors produces a resultant mmf in the output winding, inducing a feedback voltage in the secondary to equalize the transistor currents.

12,768 TEMPERATURE-SENSITIVE BIAS NETWORK by E.W. Grant (Statham Instr.); U.S. Pat. 3,005,958, Issued Oct. 24, 1961

A two-stage amplifier suitable for amplifying the modulated output of a dc transducer is described. Each stage consists of a common emitter followed by a grounded collector or emitter follower circuit. An ac feedback is used to improve temperature stability and a dc feedback may be employed to increase linearity. A temperature compensating network utilizing temperature-sensitive resistors is connected in the base-bias circuit of the first stage to compensate for variations in conductance of the remaining stages. The circuit is shown incorporated in a system which provides an amplified demodulated output of a transducer modulated carrier signal.

12,769 ELECTRONIC HYBRID AMPLIFIERS FOR INDUSTRIAL TEMPERATURE APPLICATIONS by R.J. Redding (Constructors J. Brown, Ltd.); Control, Vol. 4, pp. 95-98, Nov. 1961

Hybrid dc amplifiers for use with thermocouples and resistance thermometers are described. The amplifiers are of the industrial type and are limited to a frequency response of one-tenth the frequency of the ac supply voltages. Impedance matching between tubes and transistors is accomplished by use of a current transformer in which the primary current is controlled by the transistor stage operating at high voltage in the starvation mode and the secondary current appears across the grid to cathode of the output tube connected as an electrometer.

12,770 DESIGN OF A TRANSISTORIZED 60 MC, WIDE BAND I-F AMPLIFIER FOR WIDE TEMPERATURE RANGES by A. Ossoff (Emertron); Solid State J., Vol. 2, pp. 40-46, Sept. 1961

The design of a transistorized miniature 60 Mc IF amplifier utilizing silicon tetrodes is described. The amplifier affords a 3 db bandwidth of 20 Mc and excellent gain, bandwidth, and AGC characteristics from -65° to +100°C. Excluding transistors all components utilized were designed for operation from -65° to +200°C. The procedures utilized are separated into dc circuit design, measurement of parameters, ac circuit design, transformer design, and gain-temperature compensation. Performance data of the final design and a description and photographs of the package are presented.

12,771 RESEARCH DIRECTED TOWARD THE STUDY OF LINEAR AMPLIFICATION USING SWITCHES by A.W. Carlson (Transistor Appl.); U.S. Gov. Res. Rep., Vol. 36, p. 33(A), Aug. 20, 1961 AD 258 135

Research on the use of switches as power amplifiers is described. The switch is controlled by a signal to produce a duration modulated pulse train which is then passed through a low pass filter to recover the amplified signal. The method is capable of high efficiency in conversion of dc source power to signal power, the efficiency approaching 100 per cent with lossless switches in the proper circuit. The distortion is low if the pulse repetition rate is sufficiently higher than the cutoff frequency of the filter and if the signal modulating the pulse train falls in the filter pass band.

12,772 GENERAL CONSIDERATIONS ON DIFFERENCE AMPLIFIERS by G. Klein and J.J. Zaalberg van Zelst; Philips Tech. Rev., Vol. 22, pp. 345-351, 1960/1961

After a reference to various medical and technological applications of difference amplifiers, the requirements to be met by such amplifiers are discussed. A definition is given of the rejection factor and the discrimination factor which describe the most important characteristics of these amplifiers. For a two-stage amplifier these factors are calculated from those of the

two stages separately. It is shown that the requirements to be met by a good difference amplifier are satisfied if the first stage is given a high rejection factor and a high discrimination factor. This makes it possible to use fairly simple circuits for the subsequent stages.

12,773 SOME TYPES OF LOW NOISE AMPLIFIER by R. Hearn, R.J. Bennett, and B.A. Wind (Plessey); J. Brit. IRE, Vol. 22, pp. 393-403, Nov. 1961

The need for amplifiers with optimum noise performance is discussed. Particular reference is made to the requirements of space communication. The application of vacuum tubes, transistors, masers, parametric amplifiers, and tunnel diodes to the problem of obtaining a low-noise receiver in the frequency range 100 to 1000 Mc is described and the advantages and disadvantages of each device are pointed out. Experimental results, with a brief outline of the underlying theory, are given for a varactor amplifier used as a preamplifier to a UHF receiver. Results are also given for a transistor employed as a self-oscillating mixer showing conversion gain and a low noise figure. Consideration is then given to the application of these devices to the various frequency ranges and means of optimizing parametric amplifier noise figures.

12,774 TRANSISTOR AMPLIFIER by K.S. Knol and H. van de Weg (Philips); U.S. Pat. 3,001,146, Issued Sept. 19, 1961

A transistor amplifier having a high signal-to-noise ratio is discussed. Noise produced by the transistor varies with frequency and with the value of impedance connected to the transistor input electrodes. The noise decreases as this impedance approaches a purer resistance character and passes through a minimum at a given value of the impedance. A network is described which, in combination with the internal resistance of the signal source viewed from these input electrodes, constitutes the optimum frequency-dependent impedance required for minimum noise within the signal frequency range. The input impedance to minimize noise should have a small phase angle in the range of frequencies to be covered and a magnitude approximately inversely proportional to frequency. One control mechanism illustrated consists of a T-type filter employing two series inductances and a shunt capacitor mutually ganged together. The inductance is varied in inverse proportion to the $\sqrt{2}$ power of the signal frequency and the capacitor inversely to the square root.

12,775 TRANSISTORIZED SELECTIVE AMPLIFIERS USING RC NETWORKS by E. Dell'Oro (Transitron); Electronic Engrg., Vol. 33, pp. 734-736, Nov. 1961

The design procedure for a low-power selective amplifier using a twin-T network instead of a conventional LC network is presented. To simplify the calculations, the bandwidth is restricted to the 3 db points and the phase shifts introduced by the twin-T network, the RC coupling, and the transistors are ignored. The basic design approach is to apply negative voltage feedback through a twin-T network to a high-gain amplifier. Emitter followers are used for input and output stages to provide the required impedances. The twin-T components must have tolerances of ±0.5 per cent for the circuit to function correctly.

Selective Amplifiers - See 12,828

12,776 SERIES-ENERGIZED CASCADED TRANSISTOR AMPLIFIER by K.H. Beck (Minn.-Honeywell); U.S. Pat. 2,999,984, Issued Sept. 12, 1961

A circuit which permits large output voltage excursions without transformation is described. In addition, a means for adding the power outputs of a number of transistors without requiring close matching of their characteristics is provided. The circuit consists of a plurality of direct coupled common-base transistor amplifying stages. The circuit input, the emitter-collector circuit of each of the transistors, and the circuit energizing source are connected in a direct series circuit with the load. The base of each transistor is connected by means of a separate resistance network to the dc source. The resistance of each base network is selected with respect to the parameters of the associated transistor, the load resistance, and the stage location to provide for equal contribution by each stage to the load voltage or load power or to provide for an equal power output from each transistor.

Cascade Amplifiers - See 12,800

12,777 DEVELOPMENT OF TUNABLE C-BAND REACTANCE AMPLIFIERS (Airborne Instr. Lab.); U.S. Gov. Res. Rep., Vol. 36, p. 25(A), Oct. 20, 1961

The design, development, and fabrication of tunable C-band reactance amplifiers are considered. The amplifiers were designed to meet the following criteria: (1) a tunable frequency range (5250 to 5750 Mc), (2) a bandwidth greater than 50 Mc, (3) a power gain greater than 20 db, (4) a noise figure less than 4 db at room temperature, (5) a phase stability of less than 1 degree, and (6) a gain stability of less than 1 db. Three possible simple means of tuning the amplifier are discussed. The effect of pump power and pump frequency variations on the gain and phase stability of the amplifier is investigated.

12,778 ON THE POSSIBILITIES OF USING MICROWAVE SELF-OSCILLATORS AS REGENERATIVE AMPLIFIERS. Part II. AMPLIFIERS OPERATING AS A FOUR-TERMINAL NETWORK [in Russian] by I.V. Lebedev, C. Chun-Mou (Moscow Power Inst.); Izv. VUZ Radiotek., Vol. 4, No. 6, pp. 629-639, 1961

The fundamental parameters of a resonant self-oscillator (not pre-excited) which operates in the amplifier region with two coupling elements under input matching conditions are analyzed. The role of the load mismatch and the influence of mismatching the amplifier input on the gain coefficient and on the frequency bandwidth are described. A comparison of four-terminal network type amplifiers with similar two-terminal network type amplifiers is presented.

12,779 APPLICATION OF SEMICONDUCTOR DIODES TO LOW-NOISE AMPLIFIERS, HARMONIC GENERATORS, AND FAST-ACTING TR SWITCHES by J.C. Greene, J. Kliphuis, and L. Susman (Airborne Instr. Lab.); U.S. Gov. Res. Rep., Vol. 36, p. 27(A), Aug. 5, 1961 AD 257 084

Detailed information on the work performed on an L-band voltage-tunable amplifier is reported. The primary design goals for this amplifier were: (1) voltage tunability over a frequency range in excess of 10 per cent and (2) a noise figure of less than 2 db. An experimental model was designed and evaluated. This model had a gain of 15 db and an average amplification bandwidth of about 25 Mc that could be tuned from

1150 to 1350 Mc by varying only the pump frequency. By varying both the pump frequency and the dc bias applied to the varactor diode, the amplifier pass band could be tuned from 1100 to 1500 Mc with a constant gain of 14 db.

12,780 THE TUNNEL DIODE STRAIGHT AMPLIFIER AS A LOW-NOISE PRESTAGE IN THE UHF-DOMAIN [in German] by H. Rieck and R. Maurer (Telefunken); Arch. Elekt. Uebertragung, Vol. 15, pp. 495-507, Nov. 1961

The signal and noise behavior of an amplifier cascade that consists of a tunnel diode straight amplifier as a prestage, followed by a conventional triode amplifier, are discussed. The transducer gain, insertion gain, and bandwidth of the tunnel diode straight amplifier are calculated as well as the minimum overall noise figure that can be attained if no secondary condition exists, or if the bandwidth of the prestage is prescribed. The conditions for a low-noise tunnel diode are derived. Experimental results at 500 and 600 Mc are in fair agreement with the theory.

12,781 CONSTANT-OUTPUT-FREQUENCY, OCTAVE TUNING RANGE BACKWARD-WAVE PARAMETRIC AMPLIFIER by S. Okwit and E.W. Sard (Airborne Inst. Lab.); IRE Trans., Vol. ED-8, pp. 540-549, Nov. 1961

A varactor diode backward-wave parametric amplifier which operates in a new mode that yields a constant-output frequency as the amplification frequency is electronically tuned over an octave signal tuning range is described. A theoretical discussion of the design considerations is presented and applied to the construction of an LF model (1.5 to 3.3 Mc). Experimental data on the important amplifier characteristics correlate well with theory. The amplifier yields stable gains in excess of 20 db over a greater-than-octave tuning range, and the output frequency (which is taken at the idler) has less than a ±1.6 per cent variation over the octave band. The overall effective receiver input-noise temperatures were measured and agreed well with theory, being about 160°K at the LF end of the band and increasing to 300°K at the HF end.

12,782 A THEORETICAL INVESTIGATION OF A TRAVELING WAVE PARAMETRIC AMPLIFIER by A. Sorenssen (Norwegian Def. Res. Estab.); U.S. Gov. Res. Rep., Vol. 36, p. 40(A), Oct. 5, 1961 AD 260 750

A mathematical treatment of the wave phenomena in a traveling wave parametric amplifier is presented. The waves are described by two coupled differential equations of the 2nd order. By the elimination of one of the unknowns a 4th order differential equation arises. There are four waves of the signal frequency and four waves of the idler frequency, in contrast to linear transmission lines where there are only two waves on a single frequency. The influence of the reflected waves on the stability of the amplifier is investigated and oscillation criteria are given. Some methods to prevent oscillation are suggested.

12,783 RESEARCH ON MILLIMETER FERROMAGNETIC TYPE PARAMETRIC AMPLIFIER by R.A. Moore and M.L. Laflen (Westinghouse); U.S. Gov. Res. Rep., Vol. 36, p. 41(A), Oct. 5, 1961 AD 260 790

Mechanisms involved in the modified semistatic mode of parametric amplification are discussed. Particular attention is given to the pump power efficiency. Although the power required by the medium is a very small fraction of a watt, the pump efficiency is so low that a power of several watts is required by the cavity. An alternate configuration is proposed in which a ferrimagnetic rod serves to support the electromagnetic as well as the magnetostatic resonances. This configuration should result in a more efficient utilization of the pump power. The propagation properties of electromagnetic waves along a longitudinally magnetized circular cylinder of ferrimagnetic material were investigated for this application. The properties of narrow-line-width garnets were measured by resonant cavity techniques except at the gyromagnetic resonan frequency. Line width measurements were conducted on a Magic-T bridge.

12,784 SEMICONDUCTOR DIODE AMPLIFIER by H.W. Abbott and L.D. Wechsler (GE); U.S. Pat. 2,997,659, Issued Aug. 22, 1961

A diode amplifier which provides both voltage and current gain is described. A storage diode and capacitor are series-connected with a rectifier in parallel with the series combination. Current gain is achieved by controlling the storage diode reverse impedance with a small forward current. Since the voltage level of the input signal controls the division of forward current between the storage diode and the rectifier, voltage gain is obtained. An overall power gain of 74 db has been achieved with six ac coupled diode amplifiers. A push-pull amplifier and a flip-flop circuit are described.

Transistor Amplifiers - See 12,755

Hall Generator Amplifiers - See 12,683

Magnetic Amplifiers - See 12,700

12,785 AIRBORNE MASER FEASIBILITY STUDY by O.G. Owens and H.R. Senf (Hughes Res. Labs.); U.S. Gov. Res. Rep., Vol. 36, p. S-23(A), Aug. 5, 1961 PB 155 102

The results of a feasibility study of low-noise preamplifiers for an airborne X-band receiver are given. Several classes of masers and parametric amplifiers were considered. The overall system noise temperature, pump frequency, and pump power associated with the use of each type of amplifier are estimated. The recommended receiver front-end consists of a traveling-wave maser cooled by a closed-cycle helium refrigerator, a conventional mixer and IF preamplifier, and a crystal-controlled solid-state local oscillator. Tentative values for the outline dimensions, weights, input power requirements, and other physical characteristics needed to accomplish a coordinated plan for the design of the complete airborne communication terminal are presented. Isometric drawings showing a recommended physical arrangement of the components of the receiver front-end mounted on the antenna structure within the radome are provided.

Maser Amplifiers - See 12,724 and 12,726

12,786 A DUAL CHANNEL TRANSISTOR POWER AMPLIFIER by A.B. Bereskin (U. Cincinnati); IRE Trans., Vol. AU-9, pp. 197-203, Nov.-Dec. 1961

The design and performance characteristics of a dual-channel transistor power amplifier capable of delivering 30 w per channel at less than one per cent intermodulation distortion is described. The circuit employs three common emitter stages with as much as 25 db overall voltage feedback. A low level transistor driver is direct coupled to a second stage complementary

AMPLIFIERS (Cont'd)

driver; this stage is in turn coupled through a driver transformer to the push-pull output stage. The secondaries of the driver transformer and the two windings of the output transformer are bifilar wound to avoid conduction transfer notches. Thermal compensation is included in the output stage to provide bias stabilization. The low-level frequency response curve was within 1/2 db of a Gaussian response curve from 10 cps to 50 kc. Information on the layout and construction of the amplifier is also included.

12,787 HIGH-INPUT-IMPEDANCE TRANSISTOR AMPLIFIER by G.F. Montgomery (Dept. of Commerce); U.S. Pat. 2,995,712, Issued Aug. 8, 1961

A transistor amplifier with an input impedance of 50 to 100 megohms and a gain of approximately unity from 10 cps to 20 kc is described. Two high-gain transistors are connected in cascade with a floating power supply. A modified Darlington circuit is used with the emitter resistor bypassed and the second stage collector connected to ground and through a resistor to the power source. An output capacitor isolates the power supply from ac ground. A feedback path through the emitter bypass capacitor and the collector resistance reduces the shunting effect of the input transistor collector resistance and biasing network.

12,788 CURRENT AMPLIFIER FOR LOW IMPEDANCE OUTPUTS by E.W. Grant (Statham Instr.); U.S. Pat. 3,005,957 Issued Oct. 24, 1961

A circuit which amplifies an input signal to produce an output signal of greater current magnitude at substantially the same voltage level is described. The circuit utilizes an impedance bridge containing a Zener diode in one leg and an emitter-follower transistor in the other leg; the remaining legs consist of an emitter-follower and a resistor which may be temperature-sensitive for purposes of temperature compensation. The current-amplification of the circuit is limited by the magnitude of the load impedance; in a typical circuit, for a signal input of 25 μa at 1.18 v, an output of 72 ma at 1.02 v was obtained. An additional resistance may be inserted in series with the Zener diode to aid in balancing the bridge and provide compensation for the temperature characteristics of the Zener diode.

OSCILLATORS

12,789 VHF AND UHF CRYSTAL CONTROLLED OSCILLATORS by S.N. Witt, Jr. and H.W. Denny (Georgia Tech.); U.S. Gov. Res. Rep., Vol. 36, p. 31(A), Aug. 20, 1961 PB 257 993

Four VHF transistorized oscillator units are described. Detailed analyses of temperature and voltage effects on one of the units and typical short-term frequency variations of all of the units are discussed. Efforts were made to determine the causes of the observed short-term frequency variations. The oscillator units operate in the frequency range from 100 to 175 Mc. Seven VHF transistorized amplifiers are described with schematic diagrams and photographs. Power gains as great as 21 db were obtained. Six frequency multiplier units are also described. All of the units are designed either to double or triple the input frequency. Output frequencies as high as 470 Mc are reported. Additional amplification was required between the transistorized oscillator units and the multipliers in most cases. The problems of intrumentation in the measurement of oscillator characteristics are discussed.

12,790 HIGH SPEED TRANSISTOR MULTIVIBRATOR by M.M. Fortini (Philco); U.S. Pat. 2,997,605, Issued Aug. 22, 1961

A high-speed saturating multivibrator is described. Rapid turn-off is achieved by dispelling the stored minority carriers by reverse biasing the transistor base and by providing a low impedance drainage path. An additional biasing potential effects rapid turn-on of the nonconducting stage. Auxiliary switching transistors are used to apply the biasing potentials and to provide a low impedance path for the minority carriers. A pulse rise time of 1.3 μsec has been obtained. A scale-of-two binary counter which operates to 55 Mc is described.

12,791 MULTIVIBRATOR CIRCUIT HAVING A BISTABLE CIRCUIT DRIVING AND TRIGGERED BY A RELAXATION CIRCUIT by T.P. Sylvan (GE); U.S. Pat. 2,997,665, Issued Aug. 22, 1961

A multivibrator circuit which permits independent wide range adjustment of the output is described. Each output of a conventional multivibrator is series connected through a resistance and a diode to a single timing capacitor. A unijunction transistor connected across the timing capacitor provides a discharge path. The capacitor charges alternately through the diode and resistor paths to the breakdown voltage of the unijunction transistor. When the transistor fires, the capacitor discharges, developing a voltage pulse across a resistor in one base lead. This pulse is used to trigger the multivibrator. The output pulse width is adjusted by varying the resistance in the capacitor charge path.

12,792 TRANSISTORIZED MULTIVIBRATOR CIRCUIT ADAPTED TO OSCILLATE FOR ONLY A PREDETERMINED TIME by P. Emile, Jr. (U.S. Army); U.S. Pat. 3,005,963, Issued Oct. 24, 1961

A free-running transistor multivibrator adapted to generate a predetermined number of pulses in response to each trigger pulse is described. This is accomplished by, first, choosing the magnitude of the coupling capacitors so as to take advantage of the "lost charge" effect, and second, by making the charging time of the capacitors through the collector resistors only slightly less than the discharge time of these capacitors through the base resistances. If the magnitude of the capacitors is restricted such that the removal of the charge required to cut off the transistors causes a significant voltage drop in these capacitors, the discharge time required for the capacitor to return to the slightly negative value which will turn the transistor on again is reduced. The effect is cumulative and the oscillations will die out after a predetermined time or after a predetermined number of pulses. It is shown that the "charge loss" effect may be accentuated by incorporating semiconductor diodes in the circuit.

12,793 TRANSISTOR OSCILLATOR CONTROL CIRCUITS by D.L. Hileman (Thompson RW); U.S. Pat. 3,003,121, Issued Oct. 3, 1961

An oscillator control circuit using a new operating region of transistors is described. When the collector voltage drops below the base voltage, the resultant forward biasing of the base-collector junction provides regenerative action. Free-running and single-shot multivibrators, oscillators, and frequency dividers using this principle are described. An RC network is connected to the base. The capacitor voltage increases until

the base voltage exceeds the collector voltage. Regenerative switching then occurs, discharging the capacitor. An oscillator is produced by connecting an inductor in series with the capacitor and connecting a voltage limiting diode between the collector and emitter.

12,794 TRANSISTOR OSCILLATOR by J.A. Greefkes (N.A. Philips); U.S. Pat. 3,003,120, Issued Oct. 3, 1961

A stabilized transistor oscillator with less than one per cent distortion is described. The oscillator has a power output of 23 mw and a frequency range to 20 kc. Current from a transistor connected as a constant current source is supplied to a second transistor, where it is passed by the collector or base depending on the biase voltage. The current-source transistor has a tuned circuit in its base and the second transistor has coupled windings in its base and collector circuits. When the base potential exceeds the collector potential the input current flows to the base winding producing negative feedback. When the collector voltage exceeds the base voltage, current flows through the collector winding producing positive feedback.

Transistor Oscillators - See 12,755

Hall Generator Oscillators - See 12,683

SWITCHING CIRCUITS

12,795 ANNOTATED BIBLIOGRAPHY ON THE MINIMIZATION OF BOOLEAN FORMULAS AND SWITCHING CIRCUITS (Parke Math. Labs.); U.S. Gov. Res. Rep., Vol. 36, p. 63 (A), Oct. 5, 1961 AD 260 552

More than two hundred titles of papers and several books which deal with the problems encountered in the minimization of Boolean formulas and switching networks, or with mathematical results that have been directly useful in the study of such problems, are reported. Although fairly complete, this list does not pretend to be exhaustive. Whenever possible without undue amount of labor, a short abstract of the paper is given; often, this abstract is (or is summarized) from the one given by the author or by a reviewer.

12,796 TRANSFORMER DRIVE FOR SWITCHING TRANSISTORS by J.R. Dyke (Computer Dev.); Electronic Engrg., Vol. 33, pp. 737-739, Nov. 1961

An investigation of the problems encountered in using a transformer drive for switching transistors is presented. Major secondary current effects are: (1) pulse sag, (2) turn-on of the transistor by a spurious pulse, (3) double-pulsing when the on-time ratio is greater than 0.85, and (4) decrease in pulse amplitude with longer on-times. Spurious pulses and double-pulsing are caused by the charge and discharge of the stray capacitance, transformer capacitance, and transistor input capacitance. A diode in series with a resistor, connected across the secondary with the diode conducting when the transistor base is positive, eliminated these effects. The on-time ratio can be improved by use of a resistor across the secondary. The analysis is developed and the equations are derived from the equivalent circuit.

12,797 STATIC SWITCHING DEVICES by G. Marks and E. Demers (Kidde, Walter); U.S. Gov. Res. Rep., Vol. 36, p. S-22(A), Sept. 5, 1961 PB 156 769

Experimental data and theoretical considerations leading to the choice of a circuit design of a basic static relay resulting in reliable operation are discussed. These considerations include the heat problem, required power gain, reliable snap-action actuation, isolation, and fast and chatter-free operation. A simple modification of the basic relay circuit to operate in a latching mode is described. Here the latching is accomplished by biasing the input circuit of the basic relay into the "backlash" region between input operate voltage and input release voltage. A method of obtaining latching by means of positive feedback and the design of a polar relay based on two basic relays are also given.

12,798 DESIGN OF A TRANSISTOR SWITCH TAKING INTO CONSIDERATION THE TOLERANCES OF THE COMPONENTS [in German] by P. Veith; Regelungstech. Praxis, Vol. 9, pp. 413-418, Oct. 1961

Equations which can provide the upper and lower limits of the resistances required for a switching transistor network are discussed. Graphic representation of the mathematical relationships indicate the influence of the tolerances of the voltages, currents, resistances, and also of the transistor characteristics upon the two states of the transistor switch. From the equations and diagrams those measures which will maximize the performance of the transistor switch are realized. The theoretical results are clearly summarized in a table and a numerical example of a calculation based upon these values is included.

Switching Circuit:
Theory - See 12,839
Analysis - See 12,840

12,799 TRANSISTOR TRIGGER CIRCUIT by W.A. Lawrence, Jr. (Bell Labs.); U.S. Pat. 2,999,172, Issued Sept. 5, 1961

A transistor pulsing circuit with a high trigger sensitivity and enhanced pulse repetition frequency is described. Modifications of the basic blocking oscillator are given. A diode is connected to the feedback capacitor and poled to present a low impedance during the capacitor discharge cycle. Another diode is connected in series with the feedback capacitor and poled to present a high impedance to the passage of the input signal current. The former modification serves to decrease the recovery time and the latter minimizes attenuation and loading of the input trigger signal source.

12,800 AMPLIFYING TRIGGER CIRCUIT by J.A. Baird (Bell Labs.); U.S. Pat. 3,002,109, Issued Sept. 26, 1961

A trigger circuit which is also adapted to serve as an amplifier for signal amplitudes below that at which triggering occurs is described. In one application three amplifiers are connected in cascade. One amplifier serves as part of a stabilizing negative feedback loop. Two of the amplifiers of opposite conductivity are connected by a positive feedback loop. A reverse biased diode is provided in the positive feedback loop to prevent transmission as long as the amplitude of the input signal applied to the circuit is below a predetermined threshold level. The circuit then behaves as a conventional linear cascade amplifier. If the signal amplitude exceeds the threshold level, the positive feedback loop will be switched on by conduction of the series diode. The transistor amplifiers are then rapidly driven to a state of maximum current conduction, producing a large amplitude load voltage and current. The duration of the current depends upon adjustable circuit parameters.

12,801 AN ANALYSIS OF THE D-C DESIGN CONSIDERATIONS OF A TRANSISTORIZED SCHMIDTT TRIGGER. Part I. by J. Corsiglia (Interstate Electronics); Semicon. Prod., Vol. 4, pp. 29-32, Nov. 1961

The design requirements of a transistorized Schmidtt trigger are analyzed and a vacuum tube and a transistorized trigger are compared. The voltage level at the lower trigger point is not the same as for the upper trigger point because of hysteresis, or dead band, caused by different circuit parameters for the two stages. The input must be direct-coupled to obtain good squaring action. A consideration of the input-output voltage characteristics of closed-loop amplifiers indicates that a dead band, or hysteresis, must exist to provide a negative resistance region to ensure fast transition. Equations are derived for calculation of the upper and lower trip points and the effect of parameter variation is discussed.

12,802 TUNNEL DIODES FOR LOW-LEVEL TRIGGERS by Samaun (Bandung Inst. Tech., Indonesia); Electronics, Vol. 34, pp. 52-53, Nov. 24, 1961

A sensitive low-level circuit using a tunnel diode to drive a Schmitt trigger is described. The tunnel diode is dc biased close to its maximum current, providing an effective load line of less than one ohm. The trigger current sensitivity has been experimentally measured as 6.5 μa. The output is used to trigger a transistorized Schmitt trigger circuit. Temperature stabilization is necessary for practical use. The circuit is useful as an integral discriminator, but no simple arrangement has yet been found for use as a differential discriminator.

Magnetic Flip-Flops - See 12,702

12,803 PORTABLE, WIDE-RANGE, TRANSISTORIZED GATE FOR ACOUSTIC RESEARCH by C.E. Fox and H.V. Hillery (U. Texas); J. Acoust. Soc. Am., Vol. 33, p. 1681(A), Nov. 1961

A highly portable transistorized gate developed for use in acoustic research and development was discussed. When the gate is used with an oscillator and a power amplifier, electrical pulses are generated. The gate includes controls which permit continuous variation of pulse widths from below 1 msec to above 100 msec at repetition rates from 5 msec to several seconds per pulse. The gate also produces a variable delay pulse for triggering an oscilloscope at any time between the end of one pulse and the start of the next pulse, thus permitting precise study of echoes. Controls are included in the gate circuit to force each pulse to be initiated at the same selected voltage level of the gated signal so that all pulses have identical pulse fronts. Frequencies ranging from 5 cps to over 1 Mc can be gated. The rejection ratio is over 60 db up to 100 kc. The gate has been constructed from readily obtainable, inexpensive components.

Gating Circuits - See 12,843

12,804 BINARY COMPARER by W. Michele (Burroughs); U.S. Pat. 2,989,734, Issued June 20, 1961

A system for comparing the identity of two binary expressions is described. A bistable element (ferroelectric or ferromagnetic) having a substantially rectangular hysteresis loop is used as a storage element. Each bit of the first binary word to be compared is fed into a series of pairs of bistable elements, one bit per pair; each bit of the second binary word is similarly fed into the same pairs of bistable elements, but in an opposite sense. Similar bits in any pair of bistable elements will leave the pair in its original state, whereas dissimilar bits will cause the pair to assume a second state. Shift pulses are used to switch the pairs of bistable elements to the same reference state. The dissimilarity of any pair of characters will result in an output signal or signals being generated in output circuits associated with the bistable elements.

12,805 TEMPERATURE COMPENSATED VOLTAGE COMPARISON CIRCUIT by J.R. Judkins (U.S. Navy); U.S. Pat. 3,005,918, Issued Oct. 24, 1961

A dc voltage comparison circuit utilizing a temperature compensated single silicon voltage comparison diode is described. The two voltages to be compared are connected through a resistive network to the anode and cathode of the comparator diode. A reference voltage developed across two silicon diodes is connected to the anode of the comparator to compensate for the threshold voltage of this diode; as the threshold voltage of the comparator diode changes with temperature, the reference voltage will change in an inverse direction, re-establishing the desired conduction characteristics in the comparator diode. An ac voltage signal is fed to the anode of the comparator diode and taken from the cathode where it is fed through an amplifier to the desired indicating circuitry. When the two input signals are exactly equal, only the positive half of the ac signal will pass through the diode; at all other conditions, different ratios of positive and negative signals will pass, thus providing a measure of the relative amplitudes of the dc input signals.

12,806 SOLID STATE COMMUTATOR STUDY (GE); U.S. Gov. Res. Rep., Vol. 36, p. 34(A), Sept. 5, 1961 AD 258 789

The establishment of techniques for the design of a solid state commutator utilizing photoconductive and electroluminescent cells is considered. The operating characteristics of these components were investigated to determine their capabilities as elements of a switching device. The most feasible types of photoconductor switching networks were analyzed and the development and measurements of each are described. Properties particularly considered are the ON/OFF output ratio, attenuation, capability of handling large numbers of inputs, linearity, and noise level. An 8-channel commutator utilizing the developed T-section switch and binary grouping output, was constructed and tested. Bandwidth and minimum signal levels are discussed in terms of the design predictions.

12,807 APPLICATIONS OF TUNNEL DIODES IN SWITCHING CIRCUITS by T. Kunihiro (U. Illinois); U.S. Gov. Res. Rep., Vol. 36, pp. S-20-21(A), Nov. 20, 1961 PB 171 993

The general considerations for switching circuits are presented. The methods used to realize the three basic requirements by using tunnel diodes are stated. A set of basic circuits is presented and some experimental results are given. Other miscellaneous applications are discussed.

Tunnel Diode Switching Circuits - See 12,845

12,808 TRANSISTOR SWITCHING CIRCUIT by A.M. Gindi (IBM); U.S. Pat. 3,007,061, Issued Oct. 31, 1961

A transistor switching circuit capable of switching high voltages through a load but using only standard low voltage transistors is described. The circuit consists of two or more transistors connected in cascade and a load connected in series with the transistor arrangement. The switching signal is coupled to the base

of one of the transistors, while the bases of the remaining transistors are connected to an RC network which provides a time delay in switching. In the absence of a switching signal all the transistors are nonconducting and the load voltage divides across the transistors. Upon application of the switching signal, all the transistors become conductive, the time constant networks insuring less-than-breakdown voltages across the transistors during the transition. At the termination of the switching signal the transistors again become nonconductive and the time constant network prevents the voltages across the transistors from exceeding their breakdown levels. Since the turn-on and turn-off times of the transistors are overlapping, the switching time for the unit approaches that of a single transistor switch.

12,809 TRANSISTOR SAMPLING RELAY by R.D. Olson (Hughes Aircraft); Static Relays for Electronic Circuits, Engineering Publishers, 1961, pp. 184-192

Characteristics of an SPST relay exhibited by transistor collector-to-emitter resistance between the cutoff and saturated states are reported. Resistance changes between several megohms and a few hundred ohms in the respective states are possible. To prevent the control voltage from summing with the switched signal a transformer coupled floating circuit is used. The theory of operation is developed for the basic relay circuit. Applications and extensions of the circuit discussed are: a DPST relay, an SPST relay, a low level limiter, and a phase detector. Characteristics and important parameters are given and some suitable transistors are mentioned. Sampling rates up to 100 kc with presently available transistors are possible.

12,810 STATIC SWITCHING DEVICES by R. Gilbert (Kidde, Walter); U.S. Gov. Res. Rep., Vol. 36, p. 31(A), Sept. 5, 1961 AD 258 667

A signal switching relay using a symmetrical transistor as the contact is described. The relay gives good performance for low level signals at frequencies in or below the audio range. A drive circuit for a low level relay using a diode bridge as the contact was also developed. A current rating of 3 amps at 85°C was established for the current relay.

Transistor Switching Circuits - See 12,755, 12,844, and 12,848

SIGNAL CONVERTERS

12,811 SENSITIVE MAGNETIC MODULATOR WITH TWO-PHASE INPUT by F.I. Kerbnikov and M.A. Rozenblat; Automn. Remote Control, Vol. 22, pp. 323-329, Oct. 1961

The circuit and theory of a two-phase magnetic modulator using perpendicular magnetic fields and a square-wave power supply are discussed. Filters in the control and power supply circuits are eliminated and a practically pure sinusoidal output is provided. A two-phase transistor converter supplies two square wave voltages shifted 90 degrees in phase to provide two transverse fields. A voltage amplification factor of 386 for the idling stage was obtained with parasitic second harmonic voltage in the output equal to an input signal of the order of 4 (10^{-16}) w.

Transistor:
Modulators - See 12,755
Detectors - See 12,755

12,812 RECENT ADVANCES IN MICROWAVE MIXERS by J. J. Chacran (Sage Labs.) and R. Tenenholtz (Microwave Assoc.); 1961 IRE Intl. Conv. Rec., Part 3, pp. 139-146

The latest advances in two of the main types of microwave mixers, i.e., wide RF bandwidth coverage with conventional low-frequency IF output and medium or wide RF bandwidth coverage with high-frequency IF output, are reviewed. In the wide RF bandwidth category, octave coverage has been achieved with both waveguide and coaxial systems. In the case of high IF mixers, IF center frequencies from UHF to X-band have been obtained with IF bandwidths up to 40 per cent. In addition, several mixers have been developed with the RF frequency at a lower frequency than the IF center frequency. Several different mixers are discussed in detail. Final results of some typical units are given.

Frequency Mixing with Superconducting Elements - See 12,732

12,813 TUNNEL-DIODE CONVERTER ANALYSIS by C.S. Kim (GE); IRE Trans., Vol. ED-8, pp. 394-405, Sept. 1961

An analysis of tunnel-diode converters for two different conditions of operation is presented. In the first, the converter is self-oscillating; in the second, the local oscillator (LO) voltage is provided from an external source. Two classes of self-oscillating converters are presented. The first operates on the fundamental of the oscillation frequency and the other operates on the second harmonic. Assuming that the dynamic conductance of a tunnel diode changes only as a function of the local oscillator voltage, and expressing this conductance in a Fourier series, a 3 x 3 conductance matrix is obtained. Utilizing this matrix, expressions for gain, bandwidth, and noise figures are obtained. The analysis includes the image frequency termination. In the expressions for noise figure, the cross-correlation terms, produced by the amplitude change of the dc equivalent shot-noise current due to the LO voltage, are also included.

Transistor Converters - See 12,755

WAVE GENERATORS

12,814 USE OF THE TRANSISTOR UNDER AVALANCHE CONDITIONS [in French] by P. Chapouille (Compg. Genl. Tel., France); Ann. Radioélect., Vol. 16, pp. 277-292, Oct. 1961

After a brief exposition of the Kidd-Hasenberg-Webster avalanche transistor theory, some experimental developments in transistors are discussed. The $I_c = f(V_{co})$ characteristics of various transistors were taken and different types of pulse generators were constructed. Rise times of the order of 1 nsec were obtained with a peak power of 360 w. Certain relations controlling the operation of a pulse generator are given; the peak power available and the energy involved during a pulse are closely examined. A few applications based on these fundamental circuits are described, including a pulse frequency divider circuit.

12,815 PULSE GENERATOR WITH MEANS FOR PRODUCING PULSES INDEPENDENT OF LOAD CONDITIONS by W.

WAVE GENERATORS (Cont'd)

ilberg, B. Gnoth, and U. Eckert (Telefunken); U.S. Pat. ,997,600, Issued Aug. 22, 1961

, pulse generator for the production of current pulses which re independent of the load is described. Two emitter-coupled ansistors have their collectors connected to a common induct- nce with the load in the collector circuit of one. The load ansistor is normally off with the other transistor normally on. triggered blocking oscillator switches the load transistor on, ausing the conductivity states to reverse. Because of the slow esponse of the inductance, the load current is almost independ- nt of the magnitude of the load for a period of time. A feed- ack transformer maintains the load transistor in conduction for predetermined time period.

2,816 CURRENT PULSE GENERATOR by A. Kaiser, C. ishler, and Trumbull (Sperry Rand); U.S. Pat. 3,001,091, sued Sept. 19, 1961

transistor circuit capable of producing relatively high cur- nt pulses having a flat pedestal, short rise and decay times, d small storage periods is described. A cascade arrangement base alternating n-p-n and p-n-p transistors is employed ch that during quiescent periods all the transistors are non- nductive. All transistors are rendered simultaneously con- ctive with application of a positive input pulse to the cir- it. A theoretical analysis of the equivalent output amplifier rcuit is presented. The device is applicable for driving a low pedance load with a high current pulse such as a circuit for iving an inhibit plane of a coincident current ferrite core emory.

,817 TRANSISTOR PULSE GENERATOR by D.J. Hamilton ughes Aircraft); U.S. Pat. 3,002,110, Issued Sept. 26, 61

triggered transistor pulse generator which provides an output nal whose time duration is independent of load variations is scribed. The first transistor of the circuit serves as a blocking illator or signal generator to control the second transistor ich provides an output signal. Minority carrier storage time the second transistor is reduced by application of an inductor ially connected with a diode placed in parallel with the itter-base circuit of the second transistor. The device is table for providing an output pulse of constant time duration marily dependent upon the quasi-stable time period of the transistor in response to a clock pulse signal input.

,818 TRANSISTORIZED RING-TYPE PULSE GENERATOR J.M. Marzolf (Naval Res. Lab.); U.S. Gov. Res. Rep., l. 36, p. 26(A), Oct. 20, 1961

ransistorized ring-type pulse generator which provides a etitive sequence of high-power timed pulses in separate out- circuits suitable for triggering purposes is described. A le range of timing intervals can be obtained and positive or gative polarity is possible. This circuit can be employed for iming or a delay application.

819 TRIGGERED PULSE GENERATOR WITH STEERING CUIT TO CONTROL OPERATION OF TIMING LOOP by A. Starr, Jr. (Burroughs); U.S. Pat. 3,004,173, Issued t. 10, 1961

table and precise triggered pulse generator suited for opera- n involving a high duty factor is described. The circuit com- prises a pulse timing section having a current feedback path and a steering section. During the quiescent operating state the steering section prevents current from flowing in the feedback loop of the pulse timing section. When a trigger pulse is received by the steering section, current is switched into the feedback loop and an output pulse is initiated in the pulse timing section. After a length of time determined by the constants of the pulse timing section, the steering section opens the feedback loop and the circuit returns to its quiescent state. The basic circuit and modifications adapted for increased precision and stability and for high duty cycles are given.

12,820 TRANSISTOR PULSE GENERATOR by L.M. Smith (Bell Labs.); U.S. Pat. 3,007,058, Issued Oct. 31, 1961

A monostable pulse generator using a single point contact transistor in the grounded emitter configuration is described. The collector is connected by a capacitor to the primary winding of a transformer which has its secondary winding in series with a diode connected to the base of the transistor. The diode is biased to be normally conducting, thus holding the transistor in the "off" state. A trigger pulse at the input renders the diode momentarily nonconducting, thus turning on the transistor. The resulting voltage pulse appearing at the collector is fed back to the base diode to maintain it in the nonconducting state until the capacitor charges sufficiently to reduce the secondary voltage and allow the diode to conduct. If the subsequent capacitative discharge current is then made to exceed the current which the transistor supplies to an output load connected to the collector, the turn-"off" delay due to storage of minority carriers in the transistor is materially reduced. This results in a very stable output pulse duration. The load current capacity of the generator may be increased by connecting two such pulse generators in parallel. Due to the nature of the interconnections between the transistors, both units will turn "off" at approximately the same time.

Pulse Generators - See 12,792

12,821 LINEAR SWEEP CIRCUIT ARRANGEMENTS by A. Martinez (Marconi Wireless); U.S. Pat. 3,001,086, Issued Sept. 19, 1961

A "bootstrap" transistor linear sweep circuit is described. A preliminary theoretical discussion of the conventional transistor "bootstrap" circuit is given. In known arrangements the charging circuit includes the output load resistance which makes it difficult to secure the required full recharging of the coupling condenser when the flyback period is short. A circuit is given in which a unilaterally conducting device is included in series with the collector-emitter path of the second transistor in a "flyback" period charging circuit of the second condenser. This arrangement overcomes the above mentioned defect with little or no cost. Two alternate sweep arrangements are presented.

12,822 GENERATING TANGENTIAL SWEEPS FOR INFRARED MAPPING by J.L. Woika (HRB-Singer); Electronics, Vol. 34, pp. 64-66, Oct. 13, 1961

A transistorized tangential waveform generator is described. Generation is obtained by simple and direct adjustment of positive-slope waveshapes formed by straight line segments of a three-segment ramp function. A positive step function is applied to an RC network to charge the capacitance through a high impedance path, the voltage across the capacitor providing the waveform; two parallel constant-current sources supply

the charging current. By controlling the outputs of the current sources the waveform can be adjusted. A 6 msec sweep showed no noticeable deviation from linearity in any section of the waveform. More complex waveforms can be generated by using more current sources and a negative ramp generator.

Sawtooth Generators - See 12,756

12,823 TEST SIGNAL GENERATOR WITH CIRCUIT MEANS TO SEPARATELY ADJUST RISE AND FALL TIME OF THE OUTPUT PULSES by F. Herzfeld (RCA); U.S. Pat. 3,007,055, Issued Oct. 31, 1961

A test signal generator which develops a generalized trapezoidal waveform whose rise-, plateau-, decay-, and quiescent-time are independently adjustable is described. An asymmetrical square wave is generated by a flip-flop circuit that is controlled by two variable delay circuits. The square wave is adapted to gate a linear ramp generator circuit providing a rising leading edge. This in turn drives a special circuit which follows input signals monotonically. The special circuit also provides a decreasing linear ramp or trailing edge of a predetermined desired decay-time when the input decays faster than the rate of linear decay determined by the special circuit.

Transistor Wave Generators - See 12,755

PULSE CIRCUITS

Pulse Generators - See Wave Generators

12,824 MAGNETIC CORE PULSE CIRCUITS by E.W. Bauer (IBM); U.S. Pat. 2,992,415, Issued July 11, 1961

A magnetic core pulse delay circuit is described. Pulse multiplier and pulse supplying circuits utilize magnetic elements in producing either a single timed output pulse or several discrete output pulses in response to an input pulse applied. These circuits depend on a magnetic core element which is driven by quantified pulses. Several new methods of adjusting the number and timing of output pulses from a pulsing circuit through the use of a magnetic element are described.

12,825 CIRCUITRY FOR INDEPENDENTLY DELAYING THE LEADING AND TRAILING EDGES OF AN INPUT PULSE by J.H. Guenther (Genl. Dynamics); U.S. Pat. 3,007,060, Issued Oct. 31, 1961

A circuit which performs the functions of wave shaping and time-delay is described. Upon reception of a pulse of sufficient amplitude to activate the Schmidt-type input trigger circuit, a square-wave pulse is produced which passes to the control circuitry through a buffer stage. This pulse then charges a control capacitor at a fixed rate, triggering the output circuit (also of the Schmidt-type) at a predetermined voltage level. The output remains in the triggered state until the input pulse falls below the triggering amplitude of the input circuit. The control capacitor then discharges until its voltage falls below the output triggering level at which time the output ceases. Thus the distorted input pulse is converted into a rectangular output pulse delayed in time.

12,826 SIGNAL TRANSMISSION CIRCUIT by R.W. Beckwith U.S. Pat. 2,999,948, Issued Sept. 12, 1961

A signal transmission circuit which, in response to signals of alternating polarity, can affect at least three control operation is described. The transmission system includes two unilaterally conducting diodes for coupling respective output terminals. Two RC filters couple the first and second output terminals to a reference potential point so that an alternating input signal appears as a unidirectional output (of the same polarity) between each of the terminals and the reference point. The device described is employed to receive signals of opposite or alternating polarity and transmit them as signals of the same polarity to separate utilization units.

OTHER CIRCUITS

12,827 NEGATIVE IMPEDANCE REPEATERS OR NEGISTORS by J.F. Brouwer (Philips Telecommun. Ind.); Philips Telecommun. Rev., Vol. 23, pp. 1-20, Oct. 1961

The principles and applications of transistorized negative impedance repeaters or "negistors" are discussed. Special attention is paid to the multipurpose network which enables the negistor to be used in widely varying transmission media. The principles of design are given, together with a short description of the projected applications of the device. The characteristics and the operation of the negistor are treated in detail and the stability conditions under which the negistor can be used are examined with the aid of several graphs.

12,828 THEORY AND APPLICATION EXAMPLES OF A COMPONENT WITH DISTRIBUTED RESISTANCE AND CAPACITANCE [in German] by W. Minner (Telefunken); Arch. Elekt. Uebertragung, Vol. 15, pp. 537-599, Nov. 1961

Theory and examples of applications of a distributed RC component are presented. The component can be considered as a cascade connection of an infinite number of RC filter sections consisting of a series arm resistance and a shunt arm capacitance. The electrical performance of this component is calculated by the theory of homogeneous damped line. The equivalent π circuit and associated matrix parameters are given; the results are summarized in diagrams. As a typical application of the component a low-pass filter is designed. An oscillator is calculated using the component in the feedback path of a transistor amplifier. By means of a bypass capacitor between input and output the component becomes a surpression filter. The connection of this surpression filter in the feedback path of a transistor amplifier gives a selective amplifier as shown by a further example.

12,829 APPLICATION OF THE POTENTIAL ANALOGY TO BODE'S LINEAR-PHASE FILTER DESIGN by E.H. Luthman (Stanford U.); U.S. Gov. Res. Rep., Vol. 36, pp. 28-29(A), Aug. 20, 1961 AD 257 941

The increasing importance of the design of linear-phase filters to the network synthesizer is discussed. Research is concerned with the design techniques for such filters by investigating the possibility of applying the potential analogy to Bode's well-known method of parameter determination for linear-phase filters. The potential analogy is applied to two typical Bode filters: the first has three critical frequencies in the transmission band and one in the transition region, while the second has five critical frequencies in the transmission band and one in the transition region. Flux plots for a negatively charged plate lying in the passband region of the frequency axis and positive charges located in the finite p-plane are drawn. The method of quantizing the negative charges on an equipotential is

mployed, from which a quantized image transfer function for ach filter is obtained. The phase and attenuation characteristics of these transfer functions are studied and compared with imilar characteristics of other linear-phase filter designs. everal realizing techniques are applied to these transfer functions and the resulting networks are shown.

emiconductor Bandpass Filters - See 12,685

uby Laser for Doppler Ranging Applications - See 12,717

iezoelectric Bandpass Filters - See 12,736

rystal Filters - See 12,737

APPLICATIONS OF SOLID STATE DEVICES

COMMUNICATIONS AND RELATED APPLICATIONS

2,830 THE APPLICATION OF A HAMMING ERROR CORECTING CODE TO A STANDARD TELETYPE EQUIPMENT y R.W. Levell (Ministry of Aviation); J. Brit. IRE, Vol. 22, p. 377-389, Nov. 1961

n apparatus which has been added to a standard telegraph quipment to allow for automatic detection and correction of rrors in the signals received over a teleprinter link is describ. The signal is derived from a standard paper tape reader. he code characters are read off in blocks of two; for each ock the start and stop signals normally associated with each aracter are removed and the remaining digits are transmitted line together with a synchronizing digit and four parity eck digits. The parity digits are generated by the coder acding to a scheme devised by Hamming (Bell Sys. Tech. J., r. 1950). They are added to each block of information gits so that, when the decoder is fully synchronized, it is le to detect the existence and location of an error and can erefore correct it. The additional transmitting and receiving uipment is described in great detail. The electronic portion he apparatus has been fully transistorized and a unit conuction system, using printed circuit boards, has been employ-

2,831 MICROWAVE TEST EQUIPMENT AND ITS APPLICAONS by B. Leibowitz and E. Levy (Polarad); Electrical sign News, Vol. 6, pp. S2-S19, Nov. 1961

ost of the fundamental microwave measurements and their ociated test equipment are discussed in detail. Block diams are employed to indicate typical test setups. The frency region considered extends from 300 to 300,000 Mc. sically all microwave measurements can be classified under e of three parameters: phase, frequency, and amplitude. odivisions of these parameters include the detection of power, measurement of impedance and admittance, wavelength, noise figure, attenuation, antenna patterns, and frequency ctrum analysis. Examples of a typical power meter, phase ter, and a Q meter accompany the article.

crowave Power Meters - See 12,882

12,832 MICROWAVES — PAST, PRESENT, AND FUTURE by K. Tomiyasu (GE); Electronic Ind., Vol. 20, pp. 90-93, Nov. 1961

An historical discussion of microwave techniques and a forecast of future potentiality for microwaves are presented. The technical developments which have emerged are described with emphasis on ferrites, varactor diodes, high power microwave, phase shifters, and microwave, optical and infrared masers. The microwave infrared gap is still relatively unfilled awaiting the development of more powerful sources and more sensitive detectors. Applications of microwaves in the fields of technology such as radio, physics, and optics are given.

12,833 SOLID STATE CONTROL OF MICROWAVES by R.W. Damon (Microwave Assoc.); Electronic Ind., Vol. 20, pp. 115-116, Nov. 1961

Methods for improving transmission rates, reduction of weight and size, and increased reliability of microwaves are discussed. Typical performance capabilities of available solid state devices are given. Switches have been constructed with the capability of handling 150 watts peak and several watts cw. Limiters with bandwidths of from 5 to 30 per cent with power ratings of 5 kw peak and duplexers of approximately the same capabilities are described. A discussion of diode switching theory is presented with a variable reactance type diode (varactor) used as an example. The switches are very small in size and weight, have switching speeds on the order of nanoseconds, and require little driving power to obtain switching action (only tens of milliwatts).

Microwave Mixers - See 12,812

12,834 REPRODUCE INSTRUMENTATION FOR PROJECT 6.2 OPERATION PLUMBBOB by J.C. Hoadley (Diamond Ord. Fuze Labs.); U.S. Gov. Res. Rep., Vol. 36, p. 106(A), Sept. 5, 1961 AD 259 036

A magnetic tape recording system developed to measure magnetic components of the electromagnetic field associated with nuclear detonation is described. The instrumentation is considered satisfactory for the reproduction of data taken with this recorder, specifically those data recorded on Project 6.2 Operation Plumbbob. (The system was also applicable for reproducing Hardtack tapes.) A seven-channel reproduce system was designed and constructed with capabilities to reproduce magnetically-recorded signals over a frequency range from several cycles to over 200 kc within ±1 db, play back an AM and FM channel simultaneously, obtain quick-look data reduction in the field, and accomplish complete data analysis in the laboratory.

12,835 MAGNETIC READING DEVICE by S.M. Rubens (Sperry Rand); U.S. Pat. 2,995,631, Issued Aug. 8, 1961

A magnetic reading device capable of reading a magnetic record which is either entirely stationary or moving relatively slow with respect to the reader head is described. The head consists of a closed tubular-shaped core of highly magnetic material (e.g., Mumetal, or a ferromagnetic ferrite) which is joined at right angles to a two-legged core of similar material. An air gap is formed between the legs of the core to detect magnetic records on the medium being scanned. A source of high frequency ac is connected to the tubular-shaped core to vary the permeability of the core and the reluctance of the air gap. Because of the shape of the reading head, the flux induced

by this signal does not cross the air gap or alter the magnetic record. A magnetic record appearing in the air gap establishes a flux in the two-legged core. Because of the varying reluctance caused by the ac source, the flux linkages established by the magnetic record vary at a rate twice that of the ac source. This signal may be detected by means of a suitable winding linking the core.

Stereo Amplifier - See 12,786

Tape Playback-Correct System - See 12,872

COMPUTERS

DIGITAL COMPUTERS

12,836 MOLECULAR COMPUTER OCCUPIES 6.3 CU INCHES by J.M. Carroll; Electronics, Vol. 34, pp. 30-31, Oct. 27, 1961

A microminiature general-purpose digital computer using molecular electronic circuits is described. The computer weighs 16 oz, occupies 6.3 cu in and requires 16 w. It is a serial, binary, fixed-point machine with a word length of 10 bits and sign. The computer uses synchronous logic timed by an external 100 kc clock and is addressed by an external digital keyboard or paper-tape reader. Three types of semiconductor networks are used: flip-flops, NOR circuits, and logic drivers. A flip-flop shift register provides 16 words of instruction storage and 16 words of temporary storage. The computer is a single-address machine using an 8-bit instruction word. Fifteen commands are available. The computer has an accumulator, A and R registers, with the A register in temporary storage.

12,837 SUPERCONDUCTIVE COMPUTERS — COMMONPLACE IN TEN YEARS? by T. Maguire (McGraw-Hill); Electronics, Vol. 34, pp. 45-51, Nov. 24, 1961

New approaches to the design of superconductive memories with cycle times of a few nanosec are described. To overcome the time limitation of transistor drivers, tunnel diode and cryosar drivers are under investigation. The cryosar is a semiconductor device which operates on the basis of impact ionization of impurities — a bulk effect — in a liquid helium environment. Operation time is 10 nanosec. The effect of edges in two-hole memory cells is eliminated in a continuous plane memory with a three nanosec storage time. Trapped-flux phenomena are used to effectively punch normal areas in a continuous superconducting film to store a persistent current. Because of the shielding action of the superconducting plane, no delta noise is exhibited. A packing density of $10^7/in^3$ is possible. An associative or content-addressable memory, addressed directly by its stored contents, is under development. The use of simultaneous logic in each cell to select a specific cell allows storage of a record without specifying any memory address. Each record is identified by a key, permitting a simultaneous memory search. Retrieval time is approximately 0.2 μsec with comparable clear and write times.

12,838 ELECTROLUMINESCENT-PHOTORESPONSIVE COMPUTER ELEMENT RESEARCH - Staff Report (Westinghouse); U. S. Gov. Res. Rep., Vol. 36, p. 125-126(A), Sept. 20, 1961 AD 259 395

The development of an electroluminescent-photoresponsive (EL-PR) computer element with μsec switching speed, an impedance ratio of 50 to 1, off to on, and a power gain > 1 is described. Existing EL-PR devices and materials as well as anticipated advances in these fields are discussed. This investigation revealed that either the μsec switching speed and the 50 to 1 impedance ratio or the power gain > 1 and the 50 to 1 ratio could be achieved with existing materials. However, the realization of all three criteria will require a major breakthrough either in the form of EL materials with greater efficiency or a PC device with inherent gain.

Transistor Computer Circuits - See 12,755

12,839 SOLID-STATE LOGICAL TRANSDUCERS by F.E. Battocletti, A.C. Thomas et al. (Ohio State U.); U.S. Gov. Res. Rep., Vol. 36, p. 29(A), Sept. 5, 1961 AD 258 579

The classification of all binary switching functions of a given number of input variables into equivalence classes by rearrangement and negation of the input variables is discussed. Several theorems describing properties of the switching functions which result in various types of symmetries of the functions under input rearrangement and negation are presented. The analysis is based on the representation of the switching function in terms of sets of vectors from a finite dimensional vector space over the field of integers modulo 2. This approach makes use of the properties of the groups of transformations on the vector space which are related to the input rearrangements and negations. One type of solid-state logic unit investigated was the field-effect transistor with two control gates located concentrically around the source terminal. Another approach to the problem of realizing multiple input logic functions is to employ four-layer diodes coupled internally in a single piece of semiconductor. A number of four-layer diodes were fabricated and tested with external coupling.

12,840 ITERATIVE SWITCHING NETWORKS COMPOSED O COMBINATIONAL CELLS by W. Kilmer (Montana State Coll U.S. Gov. Res. Rep., Vol. 36, pp. S-24-25(A), Aug. 5, 19 PB 155 481

The one-dimensional case of an n-dimensional iterative switching network consisting of a number of identical logic cells uniformly interconnected through discrete information channels along each of n axis directions in space is discussed. The presentation is limited to the ℓ-dimensional case, or the case of a linear cellular array, where cells are combinational the information channels between them are bilateral, and switching is done synchronously with unit delay through each cell. These constraints are justified by demonstrating the behavioral equivalences which exist between corresponding combinational-cell and sequential-cell networks. Three classes networks are formed according to whether or not information flowing in one direction along the cellular array is dependent upon that flowing in the other direction. A synoptic discussion of Hennie's steady-state analysis results is given for the three classes, and the relative merit and character of the class having mutually dependent information flow is discussed. The main part of the paper deals with this class as the only one which can exhibit stable-state memory properties, and proves several important theorems concerning these properties. A transposition of some of Hennie's previous results is given as a start on the transients and cycling problems.

12,841 A TRANSISTOR BINARY DIGITAL LOGIC SYSTEM E.B. James (Computer Dev.); Electronic Engrg., Vol. 33,

pp. 740-742, Nov. 1961

A basic logic unit which can perform any of the standard logical operations (AND, OR, NOT) and which permits a complete computing system to be built using only one type of unit is described. The basic unit is a two-transistor bistable circuit with the logical operations carried out in the diode networks interconnecting the units. The logic unit stores the logic function until a positive pulse is applied to a drive input. The unit has a fanout of 20. Satisfactory operation has been achieved at pulse rates up to 50 kc. A practical circuit design, using worst-case techniques, is given. By suitable timing a single unit can be made to carry out more complex logic functions. An example of a computing assembly is given.

12,842 LOGIC CIRCUIT by G.F. Frank (GE); U.S. Pat. 2,995,735, Issued Aug. 8, 1961

A bistable multivibrator with "least state" memory is described. The circuit contains two transistors cross-connected in the conventional manner as a flip-flop. A saturable magnetic core structure having two cores immediately adjacent to each other is used as the memory element. Each of the cores is encircled by a different impedance winding connected in series with the emitter circuit of one of the transistors. A third saturating winding connected between the two collectors encircles both cores; the polarity of the windings is such that the cores are saturated in one direction when one transistor is conducting and in the other direction when the other transistor is conducting. In the event of failure and subsequent restoration of power the remnance of the core structure favors current flow through the transistor which was last conducting by causing the winding in series with the other transistor to present a high impedance to current flow.

12,843 PULSE AMPLIFIER GATING MEANS CONTROLLED BY COINCIDENT OR SHORTLY PRIOR PULSE by J.W. Skerritt (IBM); U.S. Pat. 3,007,059, Issued Oct. 31, 1961

A transistor gating circuit which consists of a pulse amplifying circuit together with a gating control circuit is described. The two circuits are connected through diodes which inhibit the operation of the amplifying circuit in the absence of a proper conditioning signal from the control circuit. The gating circuit presents a high input impedance to incoming control signals and has been operated at a pulse repetition frequency in excess of 5 Mc. The control section of the circuitry is capable of conditioning up to twenty pulse amplifying sections and may be connected up to twenty inputs through a conventional diode OR circuit to provide the logical OR function. The amplifying circuit may similarly be connected to multiple inputs to provide the logical AND function. Thus up to twenty gating circuits, each including a transistor, may be controlled by a single control circuit utilizing one transistor.

12,844 HOW TO SELECT THE RIGHT TRANSISTOR FOR SWITCHING APPLICATIONS by J. Hiltebeitel and P. Thomas (Philco); Electrical Design News, Vol. 6, pp. 68-81, Nov. 1961

Two of the most commonly employed building blocks, the inverter and the flip-flop, which are interconnected to form an overall system, are described. Pertinent transistor properties needed to obtain optimum performance from these two building blocks in different types of transistor logic circuits are discussed. Transistors for use in direct coupled logic circuits should possess low maximum V_{sat}, high minimum V_{be} with a very narrow spread in this parameter, moderately high h_{fe} and low I_{cbo}. A transistor to be used in stabistor coupled logic circuits should possess a narrow spread in V_{be} (on), moderately high h_{fe} and moderately low I_{cbo}. Great detail is presented on each basic configuration including circuit diagrams and some characteristic curves. Other configurations given include resistor transistor logic, resistor capacitor transistor logic, and diode transistor logic circuits. Typical transistors are offered as examples for the respective coupled logic circuits and "rules of thumb" are given for parameter variations.

Transistor Logic Circuits - See 12,755

12,845 TUNNEL DIODE CIRCUITS FOR SWITCHING THIN FILM MEMORIES by P.C. Davis (MIT); U.S. Gov. Res. Rep., Vol. 36, p. 26(A), Aug. 5, 1961 AD 257 015

A theoretical investigation of the tunnel diode as a source of high-speed current pulses capable of switching thin film memories in the order of tens of nsec is presented. Break-point models of the characteristic curve are constructed and piecewise linear analysis is used to predict and extrapolate experimental results. Three basic circuits were chosen as drivers for various load forms and levels. These were tried in the laboratory and results are given. Each of these circuits utilized a novel quick-recovery feature which was responsible for about one-half to two-thirds of the sum of the diode peak currents necessary for a given load current. The recovery time was made equal to the pulse width, which was 20 nsec. The triggering delay time was approximately one-half the pulse width for all three circuits. It is concluded that tunnel diodes can be used to drive thin magnetic films in strip lines at the speed desired.

12,846 MAGNETIC NEITHER NOR CIRCUIT by J.A. Kauffmann and R.M. Tomasulo (IBM); U.S. Pat. 2,985,868, Issued May 23, 1961

A NEITHER-NOR logical switching circuit which employs magnetic cores is described. Each core may be set, in accordance with the number of input variables connected thereto, at different rates of speed. The circuit is adapted to receive input pulses over a selectable time interval and to produce an output indication at a selectable time. An inhibit core is employed to oppose the voltage induced in the output winding of the input core whenever it is set by an input voltage. In the circuit described the necessity for providing a separate input core, characteristic of prior magnetic NEITHER-NOR devices, is eliminated.

Multiaperture Magnetic Core Logic Devices - See 12,701

12,847 MAGNETIC CORE BINARY COUNTER CIRCUIT by H.D. Crane (Burroughs); U.S. Pat. 2,995,663, Issued Aug. 8, 1961

Binary counter circuits using ferrite magnetic cores are described. The basic types of cores and the logical function each performs are illustrated. The various counting circuits formed from these cores are then shown. The basic circuit utilizes a trigger circuit which can be set in two alternative stable states by successive inputs. The trigger circuit consists of a straight transfer core circuit and an "exclusive OR" core circuit connected in a closed loop such that the inputs and outputs of each core are interconnected. The trigger input is applied to the second input of the "exclusive OR" circuit. A counter is formed by adding an AND core circuit which compares the input

with the stable conditions of the flip-flop. The AND circuit produces an output on alternate inputs corresponding to the state of the flip-flop in one of its two stable conditions. The output from the AND circuit may be used as a carry signal coupled to the input of a successive counter stage to form a divider chain.

12,848 ELECTROMAGNETIC STORAGE AND SWITCHING ARRANGEMENTS by G.R. Hoffman and M.A. Maclean (IBM); U.S. Pat. 2,991,457, Issued July 4, 1961

Transistorized switching circuits which may be used as binary counters are described. The basic circuit is composed of a single core of magnetic material (e.g., a ferrite core) with "0" and "1" input coils. An output coil is connected into the collector circuit of a transistor which serves as a pulse shaping amplifier operating in the saturation mode. The transistor remains in the "off" state until a pulse of sufficient magnitude to change the state of the core appears at the input terminals; the pulse is then amplified by the transistor and appears across the load resistor connected in the emitter circuit. An additional coil may be connected in the emitter circuit to provide regenerative action; in this case a short pulse will be sufficient to change the state of the core. Various modifications allow this second circuit to be used as a binary counter of both unidirectional and composite pulses. A chain of five binary counters of this type has been operated at an input pulse rate of $2 \cdot 10^5$ pulses/sec. Power transistors of the junction type have been used in this application with peak currents of up to 150 ma and base drive currents of up to 20 ma without exceeding the rated 50 mw dissipation.

Counters - See 12,756 and 12,790

12,849 OPERATION OF THE DIODE MATRIX CODER by W. A. Bellmer (Polytech. Inst. Brooklyn); U.S. Gov. Res. Rep., Vol. 36, p. S-39(A), Aug. 5, 1961 PB 155 709

Improvements made on the preliminary design considerations for a diode-matrix transducer and the construction of a medium size device are reported. The physical characteristics of this device with associated input producers and output recorder are described to serve as a maintenance reference. Programming methods are provided for each function of the device and examples are given. The coder performs all functions reliably except the decoder, which presents problems due to a form of feedback produced by the program.

12,850 BORROWING CIRCUIT OF A BINARY SUBTRACTIVE CIRCUIT AND ADDER by H. Yamada (Kokusai Denshin Denwa Kabushiki Kaisha, Japan); U.S. Pat. 2,988,277, Issued June 13, 1961

The application of a parametrically excited resonator circuit (parametron) to "borrowing" circuits for binary subtractive and adder circuits is described. The resonator consists of two nonlinear reactive cores whose input windings are in-phase and whose output windings are counter-phase. The latter are connected to a capacitative resonant circuit such that an input signal at frequency 2f causes an output signal at frequency f to appear across the output terminals. This output signal is either in phase with the input signal or 180° out of phase and remains in a given state as long as excitation is applied to the input. Various applications of the circuit are shown, including signal transmission, delay circuitry, and serial and parallel subtractive circuitry.

12,851 CODED DIGIT ADDER by W.G. Edwards (Natl. Cash Register); U.S. Pat. 2,991,009, Issued July 4, 1961

A coded decimal adder circuit which adds the binary signals representing decimal digits in a parallel fashion is described. The adder circuit is composed of two simultaneously operating adder units, one of which responds to the two coded decimal digits in the binary number system and the other of which responds to one of the coded decimal digits in the binary number system and to the other as converted to the binary "excess 6" number system. The adder unit responding to the digit in the "excess 6" number system provides the binary sum output when the decimal equivalent sum is greater than the digit nine and the adder unit responding to both digits in the binary system provides the sum output when the decimal equivalent sum is equal to digit nine or less. Gates controlled by the decimal carry-out digit from the adder unit having an input in the "excess 6" system pass the correct sum represented in the binar system, as obtained from one adder unit or the other, to the output. The addition of a pair of binary coded decimal digits may thus be accomplished during each clock period of the computer.

12,852 SERIAL BINARY ADDERS by W.F. Steagall (Sperry Rand); U.S. Pat. 2,987,252, Issued June 6, 1961

Improved serial adders for binary digital numbers employing magnetic amplifiers are discussed. A plurality of magnetic amplifiers are interconnected to form half adder devices and thes in turn are interconnected through further magnetic amplifiers to effect a full adder capable of performing serial binary addition. Both the basic complementing and noncomplementing magnetic amplifiers are described in detail. A complementing magnetic amplifier will give an output when no input is presented or will give no output when there is an input. A noncomplementing amplifier is one which will give an output only when an input is present. Applications of the basic magnetic amplifier circuits are discussed. A number of waveform diagra are employed to supplement the discussion.

12,853 MATRIX ADDER by A.F. Collins (IBM); U.S. Pat. 2,995,303, Issued Aug. 8, 1961

A matrix adder composed of magnetic cores having substantial rectangular hysteresis loop characteristics is described. The cores are arranged in the form of a 10 x 11 matrix and core selection is based on the absence of switching current, as opposed to the conventional coincident current scheme. Input data are represented in "2 out of 5" code form in which the b values are weighted 0, 1, 2, 3, and 6; inherent translation to decimal from the 2 out of 5 code form is accomplished within the core. The adder is controlled to provide a sum for each operation involving the entry of two quantities, the entries being effected by appropriate drive lines to two out of four co trol windings, namely true, complement, carry, and no-carry The sum of the two input values is arrived at upon the selecti of a core which lies at the intersection of a selected column and a selected row of cores in the adder matrix. Selective switching is achieved by differentiation between "relaxed" a "saturated" remnance states.

12,854 MAGNETIC MEMORY DEVICE by R.W. Hughes and D.G. Fawcett (Intl. Tel. and Tel.); U.S. Pat. 2,993,196, Issued July 18, 1961

A nondestructive parallel-serial readout for a magnetic memo system is described. The memory is composed of a series of magnetic cores arranged in a row-column matrix. A read-wri

pulse generator drives a selected row to a one-half saturation condition; a second read-write pulse generator is connected to the columns through appropriate delay and logic circuitry to drive the selected cores to full saturation for readout and simultaneously generate a feedback signal to restore the cores to their original condition. The cores are saturable magnetic elements having substantially rectangular hysteresis loops and the logic circuitry (inverter and AND gate) uses vacuum tube elements.

12,855 MAGNETIC CORE MEMORY by R.S.C. Cobbold (Min. Natl. Def., Canada); U.S. Pat. 2,995,733, Issued Aug. 8, 1961

A coincident current magnetic core memory of the parallel type is described. Words are stored in the memory in a row of cores in one plane and a read wire is provided for each core in the row in order to read out the word in parallel. Each core is threaded by two coincidence current wires, a read wire and an inhibit wire. The coincidence current wires thread the cores by rows and the inhibit and read wires thread the cores by columns. The wires are arranged so that no two cores are threaded by the same two coincidence current wire and read wire, or by the same two coincidence current wires and inhibit wire. All conductors are threaded through the core in a rectangular system and no conductors are threaded through the core at angles other than 90 degrees with respect to other conductors. This arrangement of conducting wires has the advantage of minimizing inductive pickup between conductors, facilitating individual core replacement, and being easily adaptable to semi-automatic production techniques. The cores themselves are stacked in planes and the orientation is such that the axes of the cores in the upper plane are substantially at right angles to the axes of the cores in the lower plane.

12,856 MAGNETIC MEMORY WITH NON-DESTRUCTIVE READOUT by N.S. Prywes (RCA); U.S. Pat. 2,988,730, Issued June 13, 1961

Static magnetic memory circuitry for electrical switching and information storing and transfer functions is described. The basic circuit is composed of an even number of magnetic cores (either two or four) with the four windings on the cores arranged in a bridge circuit; an energy storage device (capacitor) is connected across one of the windings of the bridge circuit. The input is applied across the second diagonal and encounters either a high- or a low-impedance depending on the preset magnetization of the core. Various circuits utilizing the basic circuitry are shown, including a storage register, an AND gate, a bistable circuit, and a binary counter.

12,857 DATA STORAGE UNIT by N.J. Albanes (IBM); U.S. Pat. 2,989,731, Issued June 20, 1961

A magnetic drum storage unit for a high-speed digital computer is described. Data is stored on the surface of the drum in channels, each of which is divided into a predetermined number of sections arranged in an interlaced manner; reading or writing may commence in a pre-chosen channel of the drum and continue if necessary in succeeding channels. Signals are available identifying the channel and the first and last character positions therein. Variable length records may be stored and a character is written on the drum when an end of record is encountered. Illustrations of the mechanical layout of the drum and its associated control circuitry are included.

12,858 DISC FILE MEMORIES by H.J. McLaughlin (Bryant Computer); Instr. and Control Sys., Vol. 34, pp. 2063-2068, Nov. 1961

A disc file memory with a surface capacity of 15×10^6 bits and a head positioning time of 100 msec is described. The memory consists of 24 discs with each surface serviced by six magnetic heads, each of which can assume any of 128 positions. The heads are positioned by a hydraulic mechanism. Switching between the 288 heads is accomplished electronically in 10 to 50 μsec. A bit density of 270 per in and a speed of 900 rpm are used. Timing tracks control data writing by gating NRZ information into recording circuits. An index track marks the zero (datum position) on each track. A single bit in a track can be changed. Each track operates at a fixed clock frequency with bit interlacing used for submultiples of the clock rate and track interlacing for multiples of the clock frequency. Serial and parallel operation is described.

12,859 FORMING SEMI-PERMANENT MEMORIES WITH METAL CARD STORAGE by J. Yamato and Y. Suzuki (Nippon Tel. and Tel.); Electronics, Vol. 34, pp. 136-141, Nov. 17, 1961

A semi-permanent metal card memory, which provides electrical readout only, is described. The memory is built on the principle that the electromagnetic coupling between two coils is considerably reduced if a metal shield is inserted between them. The memory content is contained on punched metal cards with a rectangular 4.5 x 10 mm hole for a ONE. Good results have been obtained from an experimental memory of 20,000 bits. An inproved memory now under development will provide a capacity of 14,700 words of 32 bits each, with a cycle time of 67 μsec and a volume of 0.6 cc per bit. The memory is electrically stable since it is a static device.

Core Drivers - See 12,816

12,860 SHIFTING REGISTERS by F. Goatcher (EMI); U.S. Pat. 2,994,070, Issued July 25, 1961

A two core unit shifting register in which amplification is provided in the shifting paths to reduce degeneration of the information is described. A series of magnetizable cores (e.g., ferrite cores) is coupled by links, each of which links one core with the succeeding core. The properties of the hysteresis loop are utilized, and the binary digits "0" and "1" are assigned to the opposite stages of remnance magnetism in the cores. Advancing pulses are also coupled to the cores such that a first core in the "1" state is changed to the "0" state by the pulse, and the next core is changed from the "0" to the "1" state through the linking action. No change occurs in either core if an advancing pulse is applied when the first core is in state "0". Digital information is fed in time-serial manner to the first core of the register so that this core assumes the state representative of the value of each digit in turn, each digit being propagated to the next core by advancing pulses applied to the first core midway between digit times. Advancing pulses are applied to all odd-numbered cores at the same time and to each intervening core at digit times; the result is that each core is shifted by a distance of two cores in each digit interval.

12,861 TRANSFER CIRCUIT by F. Stern-Montagony (IBM); U. S. Pat. 2,994,854, Issued Aug. 1, 1961

Transfer circuitry for a magnetic core shift register is described. The shift register uses magnetic core elements with three

windings. A shift pulse applied to the register changes the state of all cores previously in the "one" state to the "zero" state and subsequently charges a capacitor in the transfer circuit between cores. On removal of the shift pulse the capacitor discharges through the second winding of the shifted core in such a direction as to confirm this core in its "zero" state; discharge current also flows through the second and third winding of the succeeding core in such a direction as to establish this core in its "one" state. Each shift pulse thus advances the binary information one core at a time.

12,862 DATA STORAGE SYSTEM by G.L. Richards (Genl. Dynamics); U.S. Pat. 2,995,734, Issued Aug. 8, 1961

A ferrite-core shift register with internal logic circuitry is described. The register consists of a number of storage unit stages with one or more cores in each stage. Each stage has its own internal logic system which is independent of all apparatus other than substantially identical logic systems individual to the next adjacent stages of a given shift register. The stages are arranged in a serial fashion, each stage having a permanent and a temporary storage unit, both of which are controlled by clock pulses. Signals incoming to any one stage are held within the permanent storing unit of that stage until an impulse is applied to the read input of the storage unit. Signals pass from the permanent to the temporary storage unit of a given stage, thence to the input of the succeeding stage under control of appropriate switching pulses. Data signals are held in particular stage until the succeeding stage has been cleared to receive them; output signals are not spilled to the load until all stages of the register have been filled.

Magnetic Core Shift Registers - See 12,702

12,863 BIRTH, LIFE AND DEATH IN MICROELECTRONIC SYSTEMS by B. Widrow, W.H. Pierce, and J.B. Angell (Stanford U.); U.S. Gov. Res. Rep., Vol. 36, p. 33(A), Sept. 20, 1961 AD 259 538

An adaptive vote taker which compares the outputs of paralleled redundant system parts in a binary system and determines the most probable answer based on past performance of the separate parts is described. Initially, the vote-taker assigns equal significance to each redundant part and (in a binary system) requires that a simple majority of the parts be correct. With experience, the vote-taker continually reduces the weight of the outputs from those parts that make mistakes. Thus the vote-takers act as automatic repairmen which delete defective parts of a system. The heart of the adaptive vote-taker is an element providing variable gain with memory; a variable resistor with memory (memistor) which uses electrochemical deposition or removal of copper to achieve the variable memory has been successfully applied.

12,864 FUNCTIONAL CONVERTER WHICH READS GRAPHICAL FUNCTIONS FROM THE TAPE OF SELF-WRITING INSTRUMENTS [in Russian] by A.I. Petrenko (Kiev Polytech. Inst.); Izv. VUZ Radiotek., Vol. 4, No. 6, pp. 711-718, 1961

A photo-optic electronic unit which reads graphical functions from the tapes of self-recorders for the subsequent insertion of the data in a computer machine or use in automatic units is described. The basis of the instrument is a new pulse tracking system which permits obtaining minimum dynamic errors in reproduction. Fundamental relations for the synthesis and construction of such units are presented.

12,865 INFORMATION RECORD READING SYSTEM by M. M. Astrahan (IBM); U.S. Pat. 2,994,853, Issued Aug. 1, 1961

A system for reading a record in which information is contained in the form of a mark-space code is described. The reader contains two transducers separated from each other by a distance less than the length of one digital position. The leading transducer produces a signal corresponding to the mark-space coding in each successive digital position while the lagging transducer generates a delayed timing signal. The timing signal is used to identify the digital position while the logic circuitry in the leading transducer circuit generates the value of the digital position on the appearance of each timing pulse. The system has the advantages of allowing a wide tolerance in the alignment between the reading head and the coded document and of permitting a variable reading velocity.

ANALOG COMPUTERS AND OTHER DATA SYSTEMS

12,866 AN IMPROVEMENT IN THE RELIABILITY OF ANALOG CIRCUITRY THROUGH THE APPLICATION OF REDUNDANCY by A.A. Sorensen (Space Tech. Labs.); U.S. Gov. Res. Rep., Vol. 36, p. 34(A), Oct. 5, 1961 AD 260 459

Results obtained by the application of redundancy to various types of analog circuitry are summarized. Comparisons are made between several possible techniques after the application of both passive and active switching redundancy. Formulas which enable the designer to find out the actual reliability improvements that may be expected from redundancy are derived.

12,867 ELECTRONIC COMPUTER MULTIPLIER CIRCUIT by H. Schmid (Genl. Precision); U.S. Pat. 2,995,305, Issued Aut. 8, 1961

A transistorized four quadrant time-division multiplier of the analog type is described. A sawtooth wave is superimposed on the first variable to be multiplied and the resultant signal is fed to a limiter which utilizes three transistors in the grounded emitter configuration. The limiter produces a square-wave pulse train which is time-modulated by the input signal voltage to be multiplied. The time-modulated pulse train is then fed to a switch composed of two transistors connected emitter-to-emitter. The switch limits the amplitude excursions of each pulse in accordance with the value of the second variable to be multiplied. Since one variable modulates the time duration of each pulse while the other modulates the amplitude, the area of the pulse is proportional to the product of the two variables. The pulses are then applied to a filter which produces a steady output voltage proportional to this product. Feedback may be used to ensure the provision of an accurately time-modulated signal.

12,868 THE TRANSPONDER-NEW LINK IN DATA DIGITIZING by W.A. Stanke (Electro-Logic); ISA J., Vol. 8, pp. 43-45, Nov. 1961

A new converter which offers an inexpensive method for analog-to-digital conversion of low-level transducer signals is described. A three-winding magnetic core converts analog inputs into a pulse of duration proportional to the input voltage level. The transponder design parameters can be adjusted to suit the application. Input voltage requirements are 100 μv full scale or greater, with a source impedance of not more than 1000 ohms.

The conversion rate is 800 cps or less and the pulse duration may vary from 0.5 to 1.5 msec or greater. By converting to the digital mode very early in the system, full exploitation of the advantages of pulse-counting techniques — accuracy, reliability, simplicity, small size and low power requirements — are possible.

12,869 ANALOG TO DIGITAL ENCODER by E.M. Jones (Baldwin Piano); U.S. Pat. 2,986,726, Issued May 30, 1961

A system for obtaining a vernier reading from a code member such as a digital code disc converter is described. Using this system it is possible to obtain from a sixteen digit code disc quanta equivalent to those derived from a twenty digit code disc. The system is applicable to any code member, circular, rectilinear, cylindrical, conical or otherwise. Sinusoidal signals are utilized to derive thirty-two quanta per sine wave. These signals are derived from auxiliary equipment associated with a reference circle having a large number of divisions. These quanta are then correlated or integrated with other quanta obtained in the normal manner from a code member. Details of the system are discussed and supplemented by several diagrams and illustrations.

12,870 CYCLIC DIGITAL-TO-ANALOG CONVERTER by F.S. Macklem (Servo); U.S. Pat. 2,986,727, Issued May 30, 1961

A digital-to-analog converter capable of processing complex numbers is described. A voltage dividing network of resistance elements which are selectively changeable by a plurality of switches is provided. Each switch is controlled by single-digit pulsating signals from a digital-transmission system. Component elements and the excitation of the voltage-dividing network are selected to provide an output voltage in correspondence with the input binary data. For converting cyclic numbers directly or to complex numbers, the voltage dividing network is energized by an alternating-current carrier to provide a pair of complementary voltages for the two deflection systems of a cathode-ray tube. The angular displacement and magnitude of the scope is the analog of the complex number conversion of the input cyclic numbers.

12,871 SINGLE-BIT DELTA MODULATING SYSTEMS by A. Schroder and M. Kozuch (Intl. Tel. and Tel.); Electronics, Vol. 34, pp. 125-129, Nov. 17, 1961

A delta modulation method for transmitting analog signals digitally and then recovering the analog information is described. Delta pulses represent binary decisions determined by the polarity of the difference between the modulating signal and the approximation of the signal. A difference circuit in the encoder subtracts the output of a pulse integrator from the modulating signal. A feedback loop constantly corrects the integrated signal to a close approximation of the modulating signal. The decoder contains an identical integrator and a low-pass filter to remove frequency components outside the desired pass band. The encoder clock frequency establishes a periodic pulse pattern when there is no modulation. The delta process is better than pulse-coded modulation for line rates up to 40,000 bits per sec. The delta modulation process is suitable for signals requiring good envelope delay characteristics and in the conversion of telemetry signals.

12,872 DATA PROCESSING SYSTEM by J.F. Bucy, Jr., H. Jones, J.A. Morrison, Jr., and L.J. Spieker (Texas Instr.); U.S. Pat. 2,994,851, Issued Aug. 1, 1961

A system for automatic multi-channel playback of reproducibly recorded data in order to obtain data corrected to a common time base is described. The system is used to make static and dynamic time delay corrections to magnetically recorded seismic data so that each trace can be aligned with respect to a reference trace. Time corrections are made by a magnetic recording delay line, equipped with two magnetic drums. Each drum, in addition to a recording head and an erase head, contains detecting heads equally spaced around its periphery. The first drum rotates at a constant speed with each detecting head then representing a finite delay time. The detecting heads have individual inhibit and gate circuitry and selection of a particular head is made by a programming section. Depending on which detecting head is conducting, data is delayed and then fed to the second drum. The second drum rotates at a different constant speed, providing a different delay time. Signals from the second drum are recorded directly on a visual type chart.

POWER APPLICATIONS

12,873 THE VOLTAGE SOURCE WITH BUILT IN STABILITY by Staff Engineers (Minn.-Honeywell); Instrumentation, Vol. 14, pp. 13-15, Fourth Quarter, 1961

An extremely stable voltage or current source capable of replacing the standard cell is described. There are three stages in the unit. In the rectification stages, ac line voltage is reduced by a step-down transformer and converted to dc by a diode rectifier. A resistor Zener-diode combination serves as the first regulation stage. The second regulation stage cascades the first, using a Zener diode in a bridge network. The bridge supplies current output to the desired load through a temperature compensating resistor assembly and a current limiting adjustable resistor. With ambient temperature constant the output will be within 0.3 per cent for supply voltage between 107 - 127 v. The maximum variation in output over the temperature range (89° ± 50°F) is ±1500 microvolts. Nominal output voltages available are 1.029 and 4.200.

12,874 DESIGN TECHNIQUES FOR REGULATED STATIC CONVERTERS by W.A. Manahan (Space Tech. Labs.); U.S. Gov. Res. Rep., Vol. 36, pp. S-26-27(A), Aug. 5, 1961 PB 156 343

Developments of static converters to exploit available components in terms of reliability, efficiency, size, weight, and power are summarized. The report defines converters as devices which invert (modulate), ac transform, and rectify (demodulate) the input dc. Efficient and reliable circuits utilizing push-pull, magnetically coupled, transistor multivibrators are analyzed. DC line voltage regulators which can be efficiently mechanized by using switching techniques without sacrifice of transistor voltage rating are shown. DC voltage regulators which add a controlled voltage to the line voltage such that average dc voltage is constant are also described. Switched regulators with pulse width modulation control provide efficient regulation but require filters, and their design is discussed. The relationship between the reliability problem associated with thermal runaway and the temperature at which the power transistors become thermally divergent is shown. A state-of-the-art device and a bibliography of applicable literature is given.

12,875 DESIGN TECHNIQUES FOR STATIC INVERTERS by A.A. Sorensen (Space Tech. Labs.); U.S. Gov. Res. Rep.,

Vol. 36, p. S-27(A), Aug. 5, 1961 PB 156 342

The current state-of-the-art of static inverters utilizing semiconductors as power handling components is summarized. Design criteria are evaluated in terms of aircraft or missile electrical power systems. Various methods for the generation of variable dwell-time, stepped wave used in pulse-duration modulation are described. The advantages and disadvantages of inverters which utilize either bridge or parallel inverter power stages are discussed. Switching patterns were analyzed to optimize the efficiency of the power transistor in a switching mode. An advanced design static inverter which utilizes the state-of-the-art knowledge is presented.

12,876 SPEED-UP CIRCUITS IMPROVE SWITCHING OF TRANSISTOR INVERTERS by A.G. Lloyd (Bread-Boards); Electronics, Vol. 34, pp. 92-93, Nov. 10, 1961

The use of additional capacitors and transformer windings to increase inverter switching speed is described. The increased switching speed reduces transistor dissipation and lowers the ripple in the dc output. Cross-coupled positive-feedback capacitors increase the high-frequency gain of the feedback loop, and provide the energy storage to drive the OFF transistor fully on when the core saturates. A speed-up transformer winding provides increased switching speed without excessive power loss in the base-drive resistors. Switching times of 4 μsec have been observed for 2N174's and 2 μsec for some types of Ge power transistors.

12,877 SATURABLE CORE TRANSISTOR OSCILLATOR by J. L. Jensen (Minn.-Honeywell); U.S. Pat. 2,997,664, Issued Aug. 22, 1961

A dc to ac power supply which maintains a stable output frequency in spite of variations in supply potential or load is described. Two emitter-coupled junction transistors have their collectors connected to a center-tapped primary with the load across the secondary. The bases are connected to the center-tapped secondary of a saturable transformer. The saturable transformer primary has a Zener diode clipping circuit connected across it and is series connected with a primary winding of the output transformer. The clipper circuit provides a constant feedback voltage, holding the output frequency relatively constant since the time required to saturate the core is kept constant. A feedback winding in the load circuit controls the conductivity of the transistors as a function of load current.

Transistor Power Supplies - See 12,755

Power Generation Control System - See 12,879

CONTROL APPLICATIONS

12,878 THE LOGICAL SPECIFICATION OF CONTROL REQUIREMENTS by S. Alexander (English Elect.); Electronic Engrg., Vol. 33, pp. 732-734, Nov. 1961

A system in which electrical, mechanical, and chemical engineers can specify their control needs in logical form is proposed. The control engineer can then design the control system using the same logic. The logical specification is based on Boolean algebra. The terms are broken down into: AND, NOT, OR (inclusive OR), OR ELSE, IF AND ONLY IF, IF-THEN. The use of the different terms is expalined and the use of the system is illustrated in the logical design of a simple system.

12,879 DIGITAL COMPUTER — CONTROL DIRECTS PHILADELPHIA ELECTRIC'S GENERATING SYSTEM by J.R. Stauffer (Phila. Elect.); Instrumentation, Vol. 14, pp. 4-9, Fourth Quarter, 1961

A description of an electric generating and dispatching system which is completely solid-state (employing no motors, servos, slidewires or vacuum) and which is directed by a digital computer is given. The computer performs the primary function of allocating generation at minimum cost. Its calculations are based on such data as incremental cost curves, fuel costs, and performance characteristics of generating units, as well as transmission losses. A brief description of how the system works is given including a schematic of the digital computer-directed economic dispatch system, and also of typical steam station equipment. The computer also operates on a time-sharing basis in computing data for interconnection billing and is available for systems studies and calculations.

12,880 APPLYING DEAD-TIME COMPENSATION FOR LINEAR PREDICTOR PROCESS CONTROL by D.E. Lupfer and M.W. Oglesby (Phillips Petrol.); ISA J., Vol. 8, pp. 53-57, Nov. 1961

A practical linear predictor control system that has been applie to a chemical reactor for automatic control of production rate is discussed. Process dynamics are given and the predictor control system is derived employing a flow type block diagram. The process compensation block has a pulse type transfer function. Three pulse generators were designed for study: one to give exact linear predictor control, one designed around a first order approximation dead time model, and one designed around a second-order approximation dead-time model. An analog simulation study was made and the results are shown graphically. The predictor control system offers significant improvement ove conventional control but there was little to be gained by appli cation of dead-time model greater than the first order.

Control Amplifiers - See 12,763

INSTRUMENTATION

12,881 HIGH VOLTAGE MEASUREMENT BY ADP CRYSTAL PLATE by S. Namba (Inst. Phys. Chem. Res., Japan); Rev. Sci. Instr., Vol. 32, pp. 595-597, May 1961

High voltage measurement based on the electro-optical effect of an ADP crystal plate is described. When voltage is applied across a uniaxial ADP crystal, the crystal becomes biaxial. Fo the field E_z in the z direction across a z-cut crystal plate, the axes of the index ellipsoid are rotated by -45° in the xy plane independent of E_z and birefringence along the z axis becomes proportional to E_z, then the retardation of light in the z direc tion becomes proportional to applied voltage across the crystal plate. Therefore, the applied voltage can be obtained by photoelectric measurement of the optical retardation.

12,882 A HALL EFFECT MICROWAVE POWER METER by A.D Rugari (Griffiss AF Base); U.S. Gov. Res. Rep., Vol. 36, p. 29(A), Aug. 5, 1961 AD 257 311

The measurement of Hall voltages at frequencies of 3500 and

9050 Mc and its application to the measurement of microwave power are described. The Hall crystals used were fabricated from indium arsenide and indium arsenide phosphide. These materials were chosen because they possess a large electron mobility at room temperature, and thus exhibit a pronounced Hall effect capability. The results obtained show approximately two orders of magnitude of improvement over other reported work in this area and are believed to be the first reported measurement of a Hall voltage at microwave frequencies using the intermetallic compounds. The design of a Hall effect microwave power meter capable of accurately measuring from 1 to 250 w of CW power at S-band frequencies is described.

12,883 THERMAL DRIFT IN MICROWAVE POWER METERS by R.F. Pramann (Hewlett-Packard); Electronic Ind., Vol. 20, pp. 102-104, Nov. 1961

A method of achieving a realistic design goal of 100 times less detector mount drift in microwave power measurements than previously available is discussed. Ambient heat which affects the bolometer element limits the usefulness of 100 μw ranges found on commonly available devices. Isolation of the bolometer mount by temperature control is impractical since only one-hundredth degree centigrade change would cause a 3 mw drift. An alternate method which employs two coupled bridges, each containing thermistors, is described. Each bridge is designed with feedback to maintain balance. Both thermistors are biased by a common power source. Microwave current applied to the first thermistor, in the first bridge, would be communicated to the second bridge, and a dc current of equal magnitude would be applied to a thermistor in that bridge. The dc current is easy to meter and state in terms of microwave power. Circuit details are given; stable sensitivity on the order of 1 μw is possible.

Maser Spectrometer - See 12,727

12,884 RADIO FREQUENCY CALORIMETRY by P.G. Vargushkin, W.T. Cronenwett et al. (Electro-Mech.); U.S. Gov. Res. Rep., Vol. 36, p. 118(A), Oct. 5, 1961 AD 260 529

Theoretical and experimental investigations in the field of radio-frequency power measurements are described. Particular attention is devoted to the calorimeter, since it is the only instrument currently available which is capable of being calibrated without recourse to auxiliary standards. Prototype models of calorimeters were constructed for both high and low power ranges. Pertinent design criteria and performance data are presented for static and flow-type calorimeters.

12,885 LOW-LEVEL RF POWER MEASUREMENTS by J. O'Neil (Sperry Gyro.); Elect. Design News, Vol. 6, pp. S28-S31, Nov. 1961

A simplified method of measuring low-level RF power which will decrease both measuring time and cost and will dispel any doubt of accuracy at low-levels is described. A self-balancing bridge of the Wheatstone type is employed in which the unknown leg contains a power-sensitive device (e.g., a bolometer). The output of an audio amplifier is used to supply the "line voltage" to the bridge, while the input to the audio amplifier is obtained from the "null voltage." Equal amounts of RF and AF power will cause the same resistance change in the bolometer. The output of the audio oscillator decreases with the application of RF power, and the indicating meter records this decrease in applied AF voltage, calibrated to equivalent RF power. An SPDT RF switch between the RF circuit and the bolometer is employed. The meter is zeroed with an equivalent Z_{af} connected to the bolometer to insure proper impedances, switched to the RF circuit for the power reading and then switched back to the zero position. Some circuit analysis and details of the method are given.

12,886 INDUSTRIAL PREPAREDNESS MEASURE FOR THERMISTOR BOLOMETER INFRARED DETECTORS by I. Meltzer (Servo Corp. Am.); U.S. Gov. Res. Rep., Vol. 36, p. 17(A), Aug. 5, 1961 AD 257 491

Manufacturing methods for a mass production facility capable of producing a representative variety of qualified thermistor bolometers are discussed. The following parts have been manufactured: (1) flakes for all eight series, (2) heat sinks for all eight series, (3) Ge windows and lenses, and (4) housing for the bolometers. Resistance and peak voltage data were recorded and are presented graphically.

12,887 RESEARCH ON THE DETECTION OF INFRARED EMISSION FROM SATELLITE VEHICLES by F.F. Hall, Jr., C.V. Stanley, and T.P. Dixon (ITT Fed. Labs.); U.S. Gov. Res. Rep., Vol. 36, p. 17(A), Aug. 5, 1961 AD 257 170

A 20-inch aperture infrared radiometer designed to detect infrared emission from satellite vehicles is described. The radiometer designed to detect infrared emission from satellite vehicles is described. The radiometer may be equipped with either cooled lead sulfide or cooled indium antimonide detectors. Radiation modulation is accomplished by space filter type chopper discs enabling angular resolution of 1167 waves per radian to aid in background suppression. A nodding Newtonian folding mirror provides for scanning the 1/4 x 1/4 degree instantaneous field over ±2.5 degrees in the search-acquisition mode of operation. A memory oscilloscope is used to correlate low level signals by their ordered appearance in repeated line scans. Infrared irradiance measurements from orbiting satellites are presented. It is shown that other satellites must have been significantly cooler than 500°K to escape detection due to their passive radiation only. Techniques are described for predicting satellite orbits and optimizing search scan procedures. Infrared background measurements for daytime, twilight, and night sky conditions are presented.

12,888 RESEARCH ON THE DETECTION OF FAR INFRARED RADIATION by B.R. Curtis (Thomson RW); U.S. Gov. Res. Rep., Vol. 36, p. S-54(A), Aug. 5, 1961 PB 154 302

The study, design, and construction of equipment for the measurement of thermal radiation in the three millimeter (3000 μ) region of the electromagnetic spectrum are discussed. The radiometer constructed is described. The design incorporates techniques for the measurement of both the absolute intensity and the polarization of radiation received from various objects. Experimental tests and investigations of the feasibility of the design are also presented.

Impurity Activated Alloy Infrared Detectors - See 12,686

12,889 THE CALCULATION OF TEMPERATURE DIFFERENCES FROM RESISTANCE THERMOMETER MEASUREMENTS USING A DIGITAL COMPUTER by L.J. Challis (U. Nottingham); Cryogenics, Vol. 2, pp. 23-25, Sept. 1961

Details of precise temperature difference measurements using

resistance thermometers and data analysis employing a digital computer are presented. Equations are derived for the temperature difference and the resulting resistance difference between two carbon resistance thermometers. Interpolation formulae are also derived. A quadratic expression is given which can be made to give reasonable agreement with the calibration data. The first part of the digital program is concerned with the reading in of the experimental values and with the determination of the best values of the constants in the interpolation formulae. The second part of the program is used to calculate the value of the actual temperature difference. As the mean temperature is unknown the method of successive approximations is used. The computed values of the temperature difference are of sufficient accuracy if ΔT is greater than about 2×10^{-2}°K. The method of programmed calculations is useful for measurements of thermal conductivity and Kapitza resistances.

12,890 STABILIZED SCINTILLATION COUNTER by S.A. Scherbatskoy (Geophys. Measurements); Rev. Sci. Instr., Vol. 32, pp. 599-600(L), May 1961

A simple cheap scintillation counter spectrometer which possesses very high stability and requires no precision regulated voltage is described. The calibration of the spectrometer remained constant for a period of one year of typical use, and the total drifts in the calibration was 50 kev in the 2 Mev region. Use of small flashing glow discharge tube in place of an auxiliary crystal as the source of standard light pulses gave very good results. Very high stability was also observed with a single channel sweeping type spectrometer. The arrangement had been successfully used with geophysical instruments which were transported from location to location and operated from small motor-generator power supplies.

12,891 PROSPECTS OF SEMICONDUCTOR RADIATION DETECTORS [in Italian] by G. Fabri (CISE Lab., Segrate); Energia Nucleare, Vol. 8, pp. 337-341, Mar. 1961

The use of Ge and Si as radiation detectors is discussed. Their electrical properties are highly sensitive to nuclear particles. Whenever a charged particle penetrates into a semiconductor, it creates electrons and holes which can be collected if in the presence of an electric field. In a reversed bias junction this process allows the detection of ionizing particles. An analysis of different methods for producing surface junctions is carried out. Experimental results of energy resolutions in semiconductor detectors are more satisfactory than those available with ionization chambers.

12,892 EXPERIENCE AT HARWELL WITH SURFACE-BARRIER DETECTORS by G. Dearnaley (Atomic Energy Res. Estab.); IRE Trans., Vol. NS-8, pp. 11-16, Jan. 1961

A simple and reliable technique for the construction of surface barrier detectors in Si and Ge is described and their characteristics, sensitive depth, working life, and damage by radiation are reported. Various detector structures have been investigated; their applications to nuclear physics are discussed.

12,893 PERFORMANCE OF SILICON SURFACE BARRIER DETECTORS WITH CHARGE SENSITIVE AMPLIFIERS by J.L. Blankenship and C.J. Borkowski (Oak Ridge Natl. Lab.); IRE Trans., Vol. NS-8, pp. 17-20, Jan. 1961

Si surface barrier diode detectors of 1 cm^2 and 25 mm^2 sensitive area are described. These detectors have given pulse height spectral resolutions of 17 and 13-1/2 kev (FWHM) respectively, for 5.5 mev alpha particles. Reverse currents at 500 volts bias were less than 1×10^{-6} amps/cm^2 with breakdown in excess of 1000 volts. A charge sensitive amplifier contributes 3-1/2 and 10 kev noise (FWHM) with an input capacitive loading of 20 and 180 pf, respectively.

12,894 HIGH RESOLUTION STUDY OF NUCLEAR REACTIONS BY P-N JUNCTION DETECTORS by G. Amsel, P. Baruch, and O. Smulkowski (Lab. Phys. l'École Norm. Supér.); IRE Trans., Vol. NS-8, pp. 21-28, Jan. 1961

Problems arising from the use of p-n junctions for the detection of particles emitted in nuclear reactions are studied. The mechanism that insures the distinction between particles uses a "diffusion zone" as an anticoincidence detector. An electrostatic deflection system protects the junction against ionic bombardment. Maximum resolution is achieved by the use of slit-shaped detectors. Typical spectra obtained in course of the study of the reactions $O^{16}(d,d)O^{16}$, $O^{16}(d,\alpha)N^{14}$, $O^{18}(d,\alpha)N^{16}$, $O^{18}(p,\alpha)N^{15}$, are presented. Alpha-ray groups 70 kev apart have been separated.

12,895 IMPROVEMENTS IN ENCAPSULATED SILICON JUNCTION ALPHA DETECTORS by R.W. Jackson, P.P. Webb, and R.L. Williams (RCA Victor); IRE Trans., Vol. NS-8, pp. 29-34, Jan. 1961

The development of an encapsulated Si junction particle detector for general use is discussed. Because soldering to the thin front layer raises problems in the achievement of high stability, low leakage, and low noise at high voltages, the depletion layer depths obtainable in encapsulated units with high resistivity material do not approach those obtainable in unencapsulated units in vacuum. A representative measurement gave a resolution of 0.6 per cent with a window area of 5 sq mm (junction area 20 sq mm) and depletion layer depth of 180 μ.

12,896 TRANSISTOR FORM OF NUCLEAR PARTICLE DETECTOR by R.L. Williams and P.P. Webb (RCA Victor); IRE Trans., Vol. NS-8, pp. 35-43, Jan. 1961

A transistor nuclear particle detector fabricated from 20,000 ohm-cm, p-type Si is discussed. By using a thick (10 mils) wafer of this resistivity Si, a bias voltage of 30 to 40 v extends the depletion layer almost completely through the wafer, leaving a thin p-region. A particle entering the device through the collector depletion layer produces ionization in this layer which is quickly swept out. The charge separation is such that the emitter is forward biased and a transistor pulse current flows subsequent to the collector diode current. The current time characteristics of the device are shown and the gain of the device is considered both for light radiation and particle pulse signals.

12,897 APPLICATION OF SOLID STATE DETECTORS TO HIGH ENERGY PHYSICS by G.L. Miller, B.M. Foreman, L.C.L. Yuan (Brookhaven Natl. Lab.), P.F. Donovan, and W.M. Gibson (Bell Labs.); IRE Trans., Vol. NS-8, pp. 73-78, Jan. 1961

An investigation of diffused Si junctions up to 1.5 cm diameter for the detection of minimum ionizing particles is discussed. An analyzing magnet and counter telescope of the Brookhaven Cosmotron were employed. The use of detectors at high energies depends on obtaining good signals from minimum ionizing events. This minimum occurs at relativistic velocities and

orresponds to an energy loss of approximately 1.7 Mev gm^{-1} m^2 for all particles. Detectors for this application must have large area, reasonably thick depletion layers, and a low eries resistance to insure fast rise time. The signal-to-noise tio obtained is ~10:1 and the resolution ~30 per cent.

2,898 SEMICONDUCTOR PARTICLE COUNTERS AT LOW EMPERATURES by F.J. Walter, J.W.T. Dabbs, and L.D. oberts (Oak Ridge Natl. Lab.); IRE Trans., Vol. NS-8, pp. 9-82, Jan. 1961

he behavior of Ge and Si semiconductor surface-barrier coun-rs in the temperature range 0.2° to 300°K is discussed. When e Ge is cooled below 10°K, the pulse height changes abrupt-by a factor of 5. In cooling the Si to -20°C factors of 100 ere noted. An important feature of Si counters is their ability resolve α-particle fine structure under good conditions. A mple model describing the observed behavior is shown and ountings suitable for low temperature applications are de-ribed.

2,899 dE/dx AND E SEMICONDUCTOR DETECTOR SYSTEMS OR 25-MEV He^3 AND ALPHA PARTICLES by H.E. Wegner . California); IRE Trans., Vol. NS-8, pp. 103-111, Jan. 61

in semiconductor detectors whose space-charge region fills e volume of the detector have been constructed. These de-tors measure α particles and can also be used for high-ergy particles to measure dE/dx. A combination detector easuring both dE/dx and E of a particle is described. Per-mance with 21- and 25-Mev He^3 and α particles is shown. is combination allows various mass particles produced in a gh-energy reaction to be completely separated. Construc-n of 0.002 in counters is described and their advantages e discussed. Energy resolution characteristics for NaI scin-lation detectors and semiconductor detectors are compared high-energy He^3 and α particles.

olution of Hall Probes - See 12,681

,900 108-MC PRECISION FREQUENCY GENERATOR by Schwab and H.D. Tanzman (USASRDL); U.S. Gov. Res. ., Vol. 36, p. 31(A), Aug. 20, 1961 AD 257 999

ystem to supply a minimum of 10 w, 108-Mc signal with a quency stability of 1×10^{-9}/sec for a period of thirty min-s is described. The system is housed in a standard relay rack contains an ultra-precise 1-Mc crystal oscillator, frequency ltipliers, power amplifier, and power supplies. Test results dicate a frequency stability of 5×10^{-10} for a sampling per-d of 1 second in the interval of 30 minutes. The system is cribed and testing techniques are outlined.

ENERGY CONVERSION

Solar Energy Converters - See 12,688

Si and GaAs Solar Batteries - See 12,689

Vapor Deposited Si Solar Cells - See 12,687

12,901 PERFORMANCE OF THE TAP-100 THERMOELECTRIC CONVERTER by J.E. McCormick (Griffiss AF Base); U.S. Gov. Res. Rep., Vol. 36, p. 21(A), Aug. 5, 1961 AD 257 312

Design and fabrication data on the TAP-100 thermoelectric converter are reported. Details of performance of the equipment are included. The device was operated to failure with the test program being divided into three parts as follows: (1) a preliminary evaluation during which several short runs were conducted so that loading and fuel consumption data could be obtained for various hot junction temperature levels; (2) a life test of the device; and (3) final testing, conducted just prior to disassembly. After testing the device was disassembled and the failure mechanics were analyzed. Results indicated that failure was caused by a combination of numerous internal shorts and severe junction breakdown.

12,902 THERMOELECTRIC ELEMENT FOR CIRCUIT COOLING by M. Nagata and Z. Abe (Hitachi); Electronics, Vol. 34, pp. 54-55, Oct. 13, 1961

A lower-than-ambient constant temperature chamber using a five-element thermoelectric converter is described. The temperature inside the chamber is sensed by a thermistor bridge and the bridge output voltage is compared with a reference temperature setting voltage. The difference voltage is amplified and used to control current to the thermoelectric converter. By using a thermoelectric converter, chamber temperature can be maintained below, as well as above, ambient. For a control current of 5 amp, the thermal time constant is 41 seconds. The equivalent input drift of a one-stage HJ17D grounded-emitter direct-coupled amplifier, using no temperature compensating circuitry, was less than 0.1 μa or 100 μv over a period of several hours when operated in the chamber at 18°C.

12,903 THE APPLICATION OF THERMOELECTRIC SPOT COOLING TO ELECTRONIC EQUIPMENT by W.R. Stubstad (Collins Radio); 1961 IRE Intl. Conv. Rec., Part 6, pp. 38-46

The design, application and basic theory of nine Bi_2Te_3 thermoelectric spot coolers are discussed. The units pumped 5 watts of heat over a 30°C temperature difference with a coefficient of performance exceeding 0.5. Shock tests and mechanical evaluations are reported and a brief discussion of design calculations is included.

Peltier Coolers for Transistors - See 12,678

Thermoelectric Energy Converters - See 12,697

SUBJECT INDEX

A

$A^{III}B^{V}$ Compounds, Susceptibility of 12,523
Absorbed Oxygen on Photo-EMF of PbS, Effect of 12,580
Absorption in:
  Ag_2O, Infrared 12,547
  Al 12,543
  Al, Photon 12,543
  Alkali and Alkali Earth Aluminates, Infrared 12,548
  Aluminate, Infrared 12,548
  BeO Films 12,552
  BiI_3 12,554
  CdS, Magnetic Field Effects on 12,541
  CdSe 12,542
  CO (Solid), Infrared 12,549
  CO (Solid) in Solid Matrices 12,550
  Diamond, Infrared 12,546
  $ErCl_3$-$LaCl_3$ 12,553
  Ge, Electric-Field Modulated 12,540
  Group V Trioxide Films 12,552
  KBr, Irradiation Effects on 12,450
  KCl and KBr, Color Center 12,544
  KH_2PO_4 and KD_2PO_4 12,436
  NaCl, Irradiation Effects on 12,450
  PbO Films 12,552
  Quartz, Acoustic 12,626
  Rutile 12,551
  Semiconductors, Infrared 12,545
  SnO and SnO_2 Films 12,552
  TaO_5 Films 12,552
  ZrO_2 Films 12,552
Absorption (Reabsorption) in Crystals 12,539
Acceptors in InSb, In Dislocation 12,288
Acoustic Absorption in Quartz 12,626
Activation Energies of TlSe 12,481
Adders 12,851, 12,852
Adders, Magnetic Core Matrix 12,853
Admittance:
  Parameters for HF Transistors 12,666
  of Space-Charge-Limited Dielectric Diodes 12,730
Adsorption Effects on Surface:
  Energy in Ni 12,355
  Self-Diffusion in Ni 12,355
Alkali Aluminates, Infrared Absorption in 12,548
Alkali Earth Aluminates, Infrared Absorption in 12,548
Alkali Halides,
  Dislocation Generation in 12,291
  Lattice Potential for 12,433
  Positron Lifetimes in 12,439
Alloyed High Temperature Si Semiconductors, Fabrication of 12,673
Aluminate, Infrared Absorption in 12,548
Aluminum,
  Absorption in 12,543
  Dislocation Diffusion Activation Energy of 12,294
  Dislocations:
    in Czochralski Grown 12,289
    and Substructures Produced during Solidification of 12,304
  Luminescence in 12,562
  Precipitation of He along Dislocations in 12,303
Aluminum Superconductors, Plastic Deformation Effects on 12,493
Aluminum Antimonide-Indium Antimonide, Thermomagnetic Effects in 12,608
Aluminum Nitride, Preparation and Properties of 12,388
Aluminum-Zinc,
  Resistivity of 12,474
  Resistivity Changes Due to Formation of G.P. Zones in 12,475
Ammonium Dihydrogen Phosphate, Photoelastic Constants of 12,620
Ammonium Ion in NaCl-Type Crystals, Diffusion of 12,363
Amplification in Masers 12,711, 12,712
Amplifiers 12,657, 12,755, 12,763, 12,786
Amplifiers,
  Bandwidth Limitations in 12,766
  Cascade 12,776, 12,800
  Current 12,788
  dc 12,769
  Differential 12,772
  Diode 12,784
  Elimination of Collector Capacitor Effects in 12,765
  Feedback 12,778
  Hall Generator 12,683
  High-Input Impedance 12,787
  IF Wideband 12,770
  Linear 12,771
  Low Noise 12,773, 12,774
  Magnetic 12,700
  Maser 12,724, 12,726
  Multistage 12,764
  Parametric: 12,777, 12,779, 12,781, 12,782
    Ferromagnetic 12,783
  Push-Pull 12,784
  Selective 12,775, 12,828
  Stabilization Circuit for 12,767
  Temperature Compensating Bias Networks for 12,768
  Tunnel Diode 12,780
Analog:
  Circuitry, Theory of 12,866
  Multiplier Circuits 12,867
Analog-Digital-Analog Transmission Systems 12,871
Analog-Digital Converters 12,868, 12,869
AND:
  Gate 12,856
  Logic Circuits 12,843
Anelastic Relaxation Process, Lognormal Distribution Function for 12,614
Anisotropic Conductors, Resistivity Measurements on 12,472
Annealing of:
  Defects in Ionic Crystals 12,263
  Quenched Ag 12,416
  SiO Films 12,415
  Vacancies in Au, Pressure 12,272
Anthracene Films, Photoconductivity and Electrical Conductivity of Evaporated 12,579
Anthranilic Acid Films, Dark Conductivity in 12,577
Anti-Ferroelectric Transitions 12,454
Antimony, Dislocation Generation by Spark Discharge in 12,292
Antimony Single Crystals, Etch Grooves in 12,411
Antimony Telluride, Dislocation Loops in 12,307
Antimony Trioxide Films, Absorption in 12,552
Antimony Trisulfide, Switching Effect in 12,446
Arithmetic Circuits, Parametron 12,850
Arsenic Trioxide Films, Absorption in 12,552
Avalanche:
  Pulse Generators 12,814
  Transistor Circuits 12,758

B

Backward-Wave Parametric Amplifiers 12,781
Band-Splitting in the Spectra of Cubic Crystals Subjected to Oriented Deformation 12,555
Band Theory of Molecular Crystals 12,426
Barium Sulfate, Charge Centers in 12,443
Barium Titanate,
  Permittivity of 12,445
  Radiation Effects on 12,449
Barium Titanate Bead Thermistors, Fabrication and Properties of 12,694
Barium Titanate-Calcium Titanate, Radiation Effects on 12,449
Barium Titanate-Lead Titanate, Radiation Effects on 12,449
Barium Titanates, Static Stress Effects on 12,458
Base Characteristics of Transistors 12,665
Bauschinger Effect, Measurement of 12,417
Benzophenone Films, Dark Conductivity in 12,577
Beryllium Oxide Films, Absorption in 12,552
Bias Networks for Amplifiers, Temperature Compensating 12,768
Binary Comparator Circuits 12,804
Binding:
  Energy for Vacancies and Solute Atoms in Au-Pd Solid Solutions 12,267
  Properties, Thermal Effects on 12,598
Bismuth,
  Dislocation Generation by Spark Discharge in 12,292
  Effective Mass of Holes and Fermi Energy of 12,464
  Thermal Conductivity of 12,602
Bismuth in Pb-Tl, Self-Diffusion of 12,354
Bismuth-Antimony-Selenium-Tellurium, Growth and Thermoelectric Properties of Crystals in 12,385
Bismuth Telluride,
  Scattering and Galvanomagnetic Effects in 12,467
  Thermal Conductivity of 12,599
Bismuth Telluride Thermoelectric Coolers 12,903
Bismuth Tri-iodide, Absorption and Luminescence in 12,554
Bismuth Trioxide Films, Absorption in 12,552
Body-Centered Cubic Lattices, Order-Disorder Transformation in 12,250
Bolometers, Infrared 12,886
Bonds in Chlorides, NQR Studies of 12,424
Borates, NMR Studies of B^{11} in 12,536
Boron in Si,
  Diffusion of 12,360
  Dislocation Generation by Solute Diffusion of 12,290
Boron-Diffused Si, Slip Patterns in 12,372
Brass,
  Dislocations in α- 12,308
  Order-Disorder Transformation in β- 12,250
Breakdown in:
  Dielectrics 12,448
  Dielectrics, Thermal dc 12,447
  Nonpolar Semiconductors 12,497
  Sb_2S_3 12,446
  Transistors 12,664

C

Cadmium, Dislocations in α- 12,308
Cadmium in GaAs, Diffusion of 12,349
Cadmium Selenide, Absorption in 12,542
Cadmium Selenide-Zinc Selenide, Energy Gap of 12,429
Cadmium Sulfide,
  Absorption in 12,541
  Carrier Properties of 12,441
  Photoelectric Emission from 12,585
  Surface Etch Pits on 12,410
Cadmium Telluride, Photoelectric Emission from 12,585
Cadmium Telluride-Mercury Telluride, Preparation and Properties of 12,246
Calcite, Color Centers in 12,278
Calcium Fluoride, Ion-Ion Interaction in 12,425
Calcium Fluoride with Rare Earth Dopants, Growth of 12,404
Capacitance of Junctions 12,642
Capacitors,
  Breakdown Characteristics of 12,729
  Nb 12,728
Carbon:
  Boats, Growth of GaAs Using 12,379
  in Si,
    Diffusion of 12,361
    Impurity Analysis Method for Determining 12,335
  in Ta, Solid Solubility of 12,248
Carbon Monoxide (Solid),
  Absorption in 12,550
  Infrared Absorption in 12,549

Carrier Transport: 12,468
in Drift Transistors 12,662
Cascade Amplifiers 12,776, 12,800
Ceramic Filters, Bandpass 12,736
Cesium Antimonide, Photoelectric Effect in 12,581
Cesium Chloride, Lattice Vibrations in 12,435
Charge:
Centers in $BaSO_4$ 12,443
Distribution in Dielectrics 12,444
Storage in Phosphors, Measuring Equipment for 12,568
Chemical Control System 12,880
Chlorides, Bonds in 12,424
Chromium, Thermal Expansion of 12,613
Circuit Layout Techniques, Transistor-Breadboard 12,761
Circuitry, Solid State Phenomena Applied to 12,747
Circuits,
Analysis of 12,743, 12,744
Avalanche Transistor 12,758
Design of 12,756
Diode 12,754
Hall Plate 12,762
Transistor 12,755, 12,757
Tunnel Diode 12,750
Varactor 12,748, 12,749
Circulator Switches, Ferrite 12,699
Circulators, Ferrite C-Band 12,698
Coatings for Devices, Organic Protective 12,680
Cobalt, Preparation of Ferromagnetic Thin Films of 12,394
Cobalt Films,
Magnetic Anisotropy in 12,514
Phase Transformation in Thin 12,252
Resonance and Magnetization of 12,515
Cobalt-Based Alloy, Diffusion of W in 12,359
Cobalt (III) Acetylacetonate, Polarized Spectra of 12,556
Cobalt Ferrites, Thermomagnetic Properties of 12,609
Cobalt-Manganese Spinels with Admixtures, Resistivity and Structure of 12,486
Cobalt Oxide, Stoichiometry Deviations in 12,370
Coders, Diode Matrix 12,849
Coercivity of Au-Co 12,369
Color:
Center:
Absorption in KCl and KBr 12,544
Formation, Model for 12,274
Centers, Excitation of 12,557
Centers in:
Calcite 12,278
KBr-Tl, Diffusion of 12,279
KCl,
A- 12,273
Bleaching of 12,276, 12,277
Production of 12,275
Coloring of PbO, Photoelectric 12,583
Commutators, Photoelectronic 12,806
Comparators,
Binary 12,804
dc Voltage 12,805
Compounds from Nonstoichiometric Melts, Growth of Semiconducting 12,381
Computer:
Circuits - See also Specific Circuit
Corrective Circuitry 12,863
Power Generation Control System 12,879
Computers,
Electroluminescent-Photoresponsive 12,838
Microminiature 12,836
Superconductive 12,837
Concentration Profile of P in Si, Diffusion 12,346
Conduction:
Electrons, Zone Theory of 12,428
Mechanism in Ultra-Thin Films 12,471
Conductivity of:
CdS 12,441
Evaporated Anthracene Films 12,579
Ge, Low Temperature 12,479
Conductivity of: (Cont'd)
Group II Titanates 12,484
Mn-Zn Ferrites, Temperature Dependence of 12,485
Ni-Doped Polymer Carbons 12,489, 12,490
NiO, Temperature-Pressure Dependence of 12,480
PbS Layers, Microwave Temperature Dependence of 12,476
Rb-B Glasses, Concentration Dependence of 12,488
Rutile, Temperature Dependence of 12,606
Zeolites 12,487
ZnO 12,438
Contacts, Ohmic 12,677
Control:
Amplifiers 12,763
Circuitry, Logic Specification of 12,878
System,
Chemical 12,880
Power Generation 12,879
Converters,
Analog-Digital 12,868, 12,869
Digital-Analog 12,870
Solar Energy 12,688
Thermoelectric 12,697, 12,901
Tunnel Diode 12,813
Converters: 12,755
- See also Inverters
Coolers, Thermoelectric 12,902, 12,903
Copper,
Emission Lines of 12,560
Energy Dependence of Defects in 12,262
Interstitials in 12,280
Self-Diffusion Coefficient of 12,353
Copper Alloys, Stacking Fault Energies of 12,329
Copper-Gold, Deformation Effects on Structure of 12,251
Copper Manganese Aluminum, Anisotropy of 12,522
Cores,
Characteristics of Permalloy Ferrite 12,703
Fabrication of Ferrite Memory 12,705
Counters, Binary 12,790, 12,847, 12,848, 12,856
Creep Buckling Time, Determination of 12,418
Critical Field of Group V-b Metal Superconductors 12,494
Cryogenic Energy Storage 12,733
Cryosar Drivers 12,837
Cryosars, Design and Applications of 12,684
Crystal:
Filters 12,737
Growth:
- See Growth of
Patterns 12,375
Imperfections in a Si Single Crystal, X-ray Study of 12,256
Orientation, Computer Study of 12,406
Crystalline Stable Free Radicals, Susceptibilities of 12,525
Crystallites, Effect of Mean Free Path on Optical Constants of Spherical Metal 12,588

Cuprous Oxide,
Energy Band Structure of 12,431
Infrared Luminescence of 12,569
Refractive Index of 12,590
Cuprous Oxide Films, Space Charge in 12,502
Current Amplifiers 12,788
Czochralski Method of Crystal Growth 12,378

D

Data Processing System 12,872
dc Amplifiers, Hybrid 12,769
Defect Structure of:
α-Nb_2O_5 12,269
Irradiated Si and LiF 12,368
Defects,
Field Ion Microscopic Analysis of 12,257
Stress Induced Point 12,261
Theory of 12,260
Defects in:
Ag 12,416
Cu, Energy Dependence of 12,262
Deformation:
Produced Residual Stress in α-Brass 12,417
on Structure of Cu_3Au, Effects of 12,251
Degenerate Junctions,
Negative Temperatures in 12,643
Tunneling in 12,640
Delay Lines, Glass 12,739
Dendrites, Growth of Sapphire 12,402
Dendritic Formation during Single Crystal Pulling 12,378
Detectors 12,755
Detectors,
Infrared 12,886, 12,887, 12,888
Radiation 12,891, 12,892, 12,893, 12,894, 12,895, 12,896, 12,897, 12,898, 12,899
Devices,
Pressure Effects on 12,629
Radiation Effects on 12,630
Diamond,
Infrared Absorption in 12,546
Lattice Wave Dispersion Curves of 12,546
Diamonds, Growth of 12,401
Dielectric:
Constant of $BaTiO_3$ 12,445
Diodes, Admittance of Space-Charge-Limited 12,730
Loss in:
LiF 12,452
NaCl 12,451
Properties of:
Ceramic Ferroelectrics, Irradiation Effects on 12,449
KBr and NaCl, Irradiation Effects on 12,450
Relaxation: 12,454
Processes, Lognormal Distribution Function for 12,614
Dielectrics,
Breakdown in 12,447, 12,448
Charge Distribution in 12,444
Electret Organic (Wax) and Inorganic (Ceramic) 12,442
Thermal Conductivity in 12,601
Differential Amplifiers 12,772
Diffused:
Ge, Reduction of Surface Impurity Concentration of 12,348
Transistors, Fabrication of 12,674
Diffusion,
Anelastic Measurement of 12,345
Double- 12,343
Dynamics of 12,341
Diffusion:
Errors Affecting Junction Depth 12,647
along Grain Boundaries, Radiochemical Analysis of 12,333
Techniques for Parametric Diodes 12,648
Diffusion in:
α-AgCd 12,345
Anisotropic Crystals, Vacancy 12,270
Cu, Self- 12,353
Evaporating Solid 12,344
GaAs 12,351
Ni, Effect of Impurity Adsorption of Surface Self- 12,355
Order-Disorder System 12,342
Pb-Tl 12,354
Semiconductor Compounds, Bibliography of 12,358
Si 12,350
Diffusion of:
Ag and In in Zn 12,352
Boron in Si 12,360
Carbon in Si 12,361
Cd in GaAs 12,349
Color Centers in KBr-Tl 12,279
Li^+-B^- Ions in Si 12,365
NH_4 Ions in NaCl-Type Crystals 12,363

Diffusion of: (Cont'd)
Ni in Ag 12,356
Phosphorus in:
Si 12,690
Si, Concentration Profile of 12,346
Sn in InSb 12,357
Thallous Ions in KBr 12,362
W in Co-Based Alloy 12,359
Zn in:
GaAs 12,349
InSb 12,357
Diffusionless Transformations 12,295
Digital-Analog Converters 12,870
Diode:
Amplifiers 12,784
Circuits 12,754
Circuits, Variable Capacitance 12,748, 12,749
Diodes,
I-V Characteristics of 12,644
Ag-Bonded Ge: Fabrication and Properties of 12,634
Alloyed Junction: Fabrication of 12,646
Dielectric: Admittance of Space-Charge-Limited 12,730
Diffused 12,648
Glass Encapsulation of 12,652
Gold-Bonded 12,635
Junction:
Fabrication of:
Alloyed High Temperature Si 12,673
High Frequency 12,650
Fixed Back Resistance 12,670
Packaging of 12,651
Point Contact:
GaP 12,632
Whiskers for 12,633
Surface Barrier: Fabrication and Characteristics of 12,641
Tunnel:
Characteristics of 12,753
GaAs 12,636, 12,637
Magnetic Field Dependence in InSb 12,639
Power Evaluations in 12,752
Stability Criteria for 12,751
Tunneling in 12,638
Discriminators, Integral 12,802
Dislocation:
Cross Slip and Cross Climb 12,319
Distribution in Ge 12,306
Generation by:
Solute Diffusion in Si 12,290
Spark Discharge 12,292
Interaction with Domain Structure 12,321
Jogs, Elastic Self- and Interaction Energies of 12,320
Loop Formation by Vacancy Condensation 12,293
Loops, Quenched-In 12,294
Loops in Sb_2Te_3 12,307
Model of a Twin 12,325
Motion,
Abrupt-Kink Model of 12,310
Forces Resisting 12,325
Loop-Edge 12,313
"Lorentzian" Force Mechanism of 12,311
Motion: 12,312
in Grain Boundaries 12,323
during Plastic Deformation 12,330
Pile-Up, Fatigue Dependence of 12,299
Strain Hardening in fcc Metals 12,302
Structure 12,308
Walls, Dilatational Strain Field of Edge 12,295
Dislocations,
Field Ion Microscopic Analysis of 12,257
Theory of:
Continuous 12,283
Preferential Etching at 12,405
Dislocations:
on Bending Characteristics in MgO, Effect of 12,301
between PbS-PbSe Films, Misfit 12,305
Produced during Solidification of Aluminum 12,304
to Tensile Strength of LiF, Contribution of 12,297
to Yield Stress, Contribution of Temperature Dependent Locking of 12,300
Dislocations in:
Al 12,289
Al, Precipitation of He along 12,303
Alkali Halides, Breakdown Generation of 12,291
Anisotropic Media, Motion of 12,309
Ge,
Etching Analysis of 12,284, 12,285
Strain Generation of 12,287
InSb, Edge 12,288
LiF,
Charged 12,296
Polygonization of 12,318
MgO,
Fracture Depencence on 12,298
Motion Activation Energies of 12,316
Mica 12,322
NaCl,
Charged 12,296
Motion Activation Energies of 12,316
NaI, NMR Analysis of 12,286
Ni-Cr, Formation and Motion of 12,315
Visco-Elastic Media, Motion of 12,314
Zn, Edge 12,317
Disorder in Fe_3Al, Electrical Measurement of 12,249
Display Panels, Electroluminescent 12,691
Domain:
Motion in Ferrites 12,511
Structure, Dislocation Interaction with 12,321
Structure in Mg-Mn Ferrites 12,516
Wall Interactions in Ferromagnetics 12,517
Domains in Thin Magnetic Films 12,512
Donors in InSb, Sb Dislocation 12,288
Drift:
Transistors 12,661
Transistors,
Frequency Cutoff in 12,669
Minority Carrier Transport in 12,662
Drivers,
Core 12,816
Cryosar and Tunnel Diode 12,837

E

Effective Mass of Holes in Bi 12,464
Elastic:
Compression in NaI, NMR Analysis of 12,286
Constants, Pulse Echo Technique for Measuring 12,616
Constants of:
Ag 12,616
TiC and TiB_2 12,617
Modulus of NaCl 12,618
Properties of Ge 12,615
Solid, Wave Propagation in 12,627
Electrets, Organic (Wax) and Inorganic (Ceramic) 12,442
Electrochemical Polishing of Ge and Si Wafers 12,407
Electrodeposited Ohmic Contacts 12,677
Electrodes, Junction Transistor 12,676
Electroluminescence of:
GaP Point Contact Diodes 12,632
ZnS 12,563
ZnS:(Cu,Al) 12,565
ZnS:(Cu,Cl) 12,564, 12,691
Electroluminescent:
Display Panels 12,691
Photoresponsive Computers 12,838
ZnSe Phosphors, Preparation of 12,389
Electromagnetic:
Elastic Solid, Wave Propagation in 12,627
Memory Units 12,859
Electron:
Bombardment Floating Zone Melting, Gun for 12,382
Density in ZnO 12,438
Irradiation-Induced Expansion in InSb 12,420
Electron: (Cont'd)
Microscope Analysis of Vacancy Agglomerates 12,266
Mobility in InAs 12,465
Scattering, Phonon: 12,469
and Impurity 12,468
States, Zone Theory of 12,428
Transport 12,468
Emission:
of Ge Films, Vacuum Measurements of 12,584
from High-Melting Compounds, Infrared 12,558
Lines of:
Cu 12,560
Zn and Zn-Sb Compounds 12,560
ZnO and ZnS 12,560
from Si Junctions 12,645
Spectrum of Ga-Doped Ge 12,559
Encapsulation of Junction Diodes, Glass 12,652
Encoders, Photoelectric 12,864
Energy:
Band Structure of:
Cu_2O 12,431
Rutile 12,606
TeSe 12,432
Zr-O 12,427
Converters,
Solar 12,688
Thermoelectric 12,697, 12,901
Gap of:
Binary $(ZnSe)_x$-$(CdSe)_y$ Systems, Reflection Spectrum Determination of 12,429
$GeSe_2$ 12,482
$SnSe_2$ 12,482
Storage, Cryogenic 12,733
Epitaxial Ag Films on Rocksalt, Growth and Structure of Thin 12,391
Erbium Chloride-Lanthanum Chloride, Absorption and Fluorescence in 12,553
Erbium Ethylsulphate, Susceptibility of 12,526
Etch:
Grooves in Sb Single Crystals 12,411
Pits on CdS Crystals, Color Photographs of Surface 12,410
Etches for Dislocation Analysis in Ge 12,284, 12,285
Etching:
at Dislocations, Theory of Preferential 12,405
of Si, Photosensitive 12,409
Evaporation Coefficient of Crystal Surfaces, Surface Pressure Dependence of 12,24
Excitation:
Efficiencies of Phosphors, Ultraviolet 12,567
of F-Centers and Excitons 12,557
Exciton:
Formation in Semiconductors 12,545
Spectra in CdSe 12,542
Excitons, Excitation of 12,557

F

Fabrication of:
Alloyed High Temperature Si Devices 12,673
$BaTiO_3$ Bead Thermistors 12,694
Diffused Transistors 12,674
Hall Effect Devices 12,683
HF Junction Diodes and Transistors 12,650
InSb n-p-n Transistors 12,675
Intrinsic Barrier Transistors 12,660
Junction Transistors and Diodes Having Fixed Back Resistance 12,670
Faraday Effect in Ferrites, Ultrahertzian 12,518
Fatigue in:
InSb Single Crystals 12,299
Ti and Ti Alloys, Interstitial Atom Effect on 12,282
Faults in Sodium Azide, Radiation and Mechanical Induced 12,421
Feedback:
Amplifiers 12,778
Oscillators 12,793

Fermi Energy of Bi 12,464
Ferrimagnetic Structure of Fe_7Se_8 12,255
Ferrite:
- See also Magnetic
Circulator Switches 12,699
Circulators 12,698
Cores,
Characteristics of Permalloy 12,703
Low Flux Density 12,704
Loaded Waveguides 12,708
Memory Cores, Fabrication of 12,705
Ferrites,
Fabrication of Superconductive 12,393
Magnetization of Square Loop 12,511
Preparation of:
High Resistivity Nickel 12,397
Mn-Zn Square Loop Ferrites 12,399
Relaxation Phenomena in Mn-Zn 12,520
Thermomagnetic Properties of 12,609
Ultrahertzian Faraday Effect in 12,518
Ferrites:
for Computer Memories, Composition of 12,396
with High Temperature Independent Initial Permeabilities, Preparation of 12,395
for Microwaves, Preparation of 12,398
Ferroelectric:
Contact-Pressure Effects in MnO_2 12,453
Properties of Sr-Bi(TiO_3) 12,455
Transitions 12,454
Ferroelectrics, Shock Waves in 12,623
Ferromagnetic:
Co and Fe-Co Films, Preparation of 12,394
Parametric Amplifiers 12,783
Properties of Thin Films 12,512
Resonance, Kubo Expansions in 12,519
Ferromagnetics, Domain Wall Interactions in 12,517
Ferromagnets, Dislocation-Domain Structure Interactions in 12,321
Field:
Effect in Semiconductors 12,501
Ion Microscopy in Analysis of:
Crystal Structure 12,258
Structure 12,257
Film:
Memory Units, Switching Circuits for 12,845
Resistors, Ni-Cr 12,631
Storage Devices, Theory of Wall-Stepping 12,517
Films,
Absorption of 12,552
Conduction Mechanism in 12,471
Hysteresigraph for Magnetic 12,510
Magnetic Properties of 12,512
Optical Properties of 12,538
Reflection from 12,593
Resistive: Electrical Properties of 12,440
Filters,
Bandpass Piezoelectric Ceramic 12,736
Crystal 12,737
Design of 12,829
RC Component 12,828
Semiconductor Bandpass 12,685
Flip-Flops, Magnetic Core 12,702
Floating Zone Growth of Semiconductor Crystals 12,383, 12,384
Flow Graph Network Synthesis 12,740
Fluorescein Films, Dark Conductivity in 12,577
Fluorescence in $ErCl_3$-$LaCl_3$ 12,553
Fluorine^{19} in MgF_2, NMR of 12,535
Four-Point Resistivity Measurements on Anisotropic Conductors 12,472
Fracture in:
MgO, Slip Distribution Effects on 12,298
Solids, Theory of 12,622
Frequency:
Cutoff in:
Alloy Junction Transistors 12,668
Drift Transistors 12,669
Generators, Precision 12,900
Range of Transistors, Extension of 12,759

G

Gain Extension in Transistor Circuits 12,760
Gallium,
Thermal Conductivity of 12,602
Thermoelectric Power of 12,605
Gallium-Doped Ge, Emission Spectrum of 12,559
Gallium Antimonide, Stoichiometric Deviations in 12,371
Gallium Antimonide and Arsenide, Abrasion Surface Damage Determination of 12,408
Gallium Antimonide-Indium Antimonide, Susceptibility of 12,523
Gallium Arsenide,
Diffusion in 12,351
Diffusion of Zn or Cd in 12,349
Floating Zone Purification of 12,336
Impurities in 12,334
Gallium Arsenide:
Crystal Growth Using Carbon Boats 12,379
Solar Cells 12,689
Tunnel:
Diodes 12,636, 12,637
Diodes, Tunneling in 12,638
Gallium Nitride, Preparation and Properties of 12,388
Gallium Phosphide Point Contact Diodes, I-V and Electroluminescence Characteristics of 12,632
Galvanomagnetic:
- See also Magnetoelectric
Effects in Bi_2Te_3 12,467
Properties of Carriers at Ge Surfaces 12,466
Garnet Limiters, Characteristics of Low-Level 12,706
Garnets,
Growth of Large Single-Crystal Yttrium-Iron 12,400
Magnetic Properties of Y-Ho 12,521
Gating Circuits 12,803, 12,843
Generators,
Precision 12,900
Pulse 12,814, 12,815, 12,816, 12,817, 12,818, 12,819, 12,820
Sawtooth 12,756
Sweep 12,821
Tangential Waveform 12,822
Germanium,
Absorption Modulation in 12,540
Conductivity at Low Temperatures of 12,479
Crystal Growth of Heavily Compensated 12,377
Diffusion in 12,344
Dislocation:
Analysis by Etching of 12,284, 12,285
Distribution in 12,306
Dislocations as Function of Strain in 12,287
Elastic Properties of 12,615
Emission Spectrum of Ga-Doped 12,559
Galvanomagnetic Properties of 12,466
Mobility in 12,466
Photoelastic Effect in 12,592
Photoelectric Kinetics in 12,582
Protective Coatings for 12,680
Reduction of Surface Impurity Concentration of Diffused 12,348
Resistivity and Hall Constant of Li-Doped 12,478
Stress in 12,306
Textural Properties of Thin Films of 12,374
Vacancy Aggregates in Quenched 12,265
X-Ray Scattering in 12,419
Germanium:
Crystal Growth,
Nomographs for 12,376
Temperature Gradient during 12,306
Donors, Photoionization and Zeeman Spectra of 12,470
Films, Optical and Photoemission Properties of 12,584
Wafers, Electrochemical Polishing of 12,407
Germanium Selenide, Resistivity and Hall Coefficient of 12,482
Germanium-Silicon Infrared Detectors 12,686
Glass:
Optical Maser 12,719
Ultrasonic Delay Lines 12,739
Glasses, Conductivity of Rb-B 12,488
Globars, Infrared Emission from 12,558
Gold,
Vacancy:
Agglomerates in 12,266
Migration in 12,272
Gold:
Plate, Sputtering Rate of 12,414
Thin Films, Deposition and Structure of 12,390
Gold-Bonded Diodes 12,635
Gold-Cobalt,
Co Precipitates in 12,369
Coercivity of 12,369
Gold-Palladium Solid Solutions, Binding Energy for Vacancies and Solute Atoms in 12,267
Grain:
Boundaries, Dislocation Motion in 12,323
Boundary Sliding, Stress Effects on 12,324
Graphite, Twinning in 12,327
Group:
II Titanates, Conductivity of 12,484
II-VI Single Crystals, Vapor Phase Growth of 12,387
III-V Compounds,
Czochralski Method for Growth of 12,380
Surface Damage in 12,408
Susceptibility of 12,523
V-b Metal Superconductors, Critical Field and Thermal Conductivity of 12,494
Growth:
Patterns of Crystals 12,375
Twins in InSb 12,326
Growth of:
- See also Preparation of
Al, Czochralski 12,289
CaF with Rate Earth Dopants 12,404
Crystals:
of Alloy System Bi-Sb-Se-Te 12,385
by Czochralski Method 12,378
Diamonds 12,401
Epitaxial Ag Films on Rocksalt 12,391
GaAs Crystals in Carbon Boats 12,379
Ge 12,377
Ge, Temperature Gradient during 12,306
Group:
II-VII Single Crystals from Vapor Phase 12,387
III-V Compounds by Czochralski Method 12,380
Iron Single Crystals by Zone Melting 12,392
Large Single-Crystal YIG 12,400
Sapphire Whiskers 12,402
Semiconducting Compounds from Nonstoichiometric Melts 12,381
Semiconductor Crystals by Floating Zone 12,384
Si:
Crystals by Floating Zone Method 12,383
and Ge Crystals, Nomographs for 12,376
Synthetic Mica Crystals 12,403

H

Hall:
Coefficient of:
$SnSe_2$ and $GeSe_2$ 12,482
TlSe 12,481
Constants of:
Ge, Temperature Variation of 12,478
Ni-Doped Polymer Carbons 12,489, 12,490
Effect:
in CdS 12,441
Devices, Fabrication and Application of 12,683
Multipliers 12,682
Plate Circuits 12,762
Probes, Characteristics of 12,681
Hamiltonian, Two-Dimensional Spin Wave 12,509

Heat:
Capacity of Tb 12,596
Conductivity - See Thermal Conductivity
Content of:
MgO 12,595
ZrO and $ZrSiO_3$ 12,595
Transfer in Microminiature Circuitry 12,746
Helium Precipitation along Dislocations in Al 12,303
Heusler Crystals, Magnetic Anisotropy of 12,522
High:
Frequency Oscillators 12,789
Impedance Amplifiers 12,787
Voltage, Measurement of 12,881
Voltage Switching Circuits 12,808
Holes in Bi, Effective Mass of 12,464
Holmium Sulfate, Susceptibility of 12,526
Hybrid Amplifiers, dc 12,769
Hydrocarbons (Solid), Thermally Induced EMF in Irradiated 12,607
Hysteresigraph for Magnetic Films 12,510

I

Impurities, Analysis of 12,331, 12,332
Impurities in:
GaAs Grown in Quartz Boats 12,334
LiF, Crystal Nucleation Affected by 12,405
Impurity:
Adsorption on Surface:
Energy in Ni, Effect of 12,355
Self-Diffusion in Ni, Effect of 12,355
Analysis, Radiochemical 12,333
Concentration, Evaluation of 12,347
Concentration of Diffused Ge, Reduction of Surface 12,348
Diffusion in Semiconductor Compounds, Bibliography of 12,358
in Si, Analysis of Carbon 12,335
Indium in Zn, Diffusion of 12,352
Indium Antimonide,
Diffusion of Zn and Sn in 12,357
Edge Dislocations in 12,288
Electron Irradiation-Induced Expansion in 12,420
Resistivity and Magnetoelectric Properties of 12,499
Twins in 12,326
Indium Antimonide:
Films, Optical Properties and Preparation of 12,589
from Nonstoichiometric Melts, Growth of 12,381
Single Crystals, Fatigue in 12,299
Transistors, Design and Properties of 12,675
Tunnel Diodes, Magnetic Field Dependence in 12,639
Indium Antimonide and Arsenide Abrasion Surface Damage, Determination of 12,408
Indium Arsenide, Electron Mobility in 12,465
Indium Sulfide, Twinning in β- 12,328
Information Readers 12,865
Infrared:
Absorption in:
Ag_2O 12,547
Alkali and Alkali Earth Aluminates 12,548
Diamond 12,546
Semiconductors 12,545
Solid CO 12,549
Detectors 12,886, 12,887, 12,888
Detectors, Ge-Si 12,686
Emission from High-Melting Compounds 12,558
Luminescence of Cu_2O Surface Layers 12,569
Injection Level in Transistors 12,665
Intermetallic Compounds, Determination of Abrasion Surface Damage in Some III-V 12,408
Internal Friction in:
α-AgCd 12,345
α-Iron 12,628
NaCl 12,618
Steel 12,323
Interstitials in:
Cu, Stability of 12,280
LiH and NaCl 12,281
Ti, Fatigue Dependence on 12,282
Intrinsic Barrier Transistors, Fabrication and Operation of 12,660
Inverters,
Design and Survey of 12,874
High Speed 12,876
Saturable Core-Transistor 12,877
Survey of 12,875
Ion-Ion Interactions in CaF_2, Closed Shell 12,425
Ion Radical Salts, EPR Studies of Spin Correlation in 12,532
Ionic:
Conductivity of Zeolites 12,487
Crystals,
Charge Distribution in 12,444
Defect Annealing in 12,263
Lattice Vibrations in 12,435
Plasticity of 12,330
Structures, Charge Centers in Crystalline 12,443
Iron,
Dislocation Motion in 12,314
High Field Magnetic Properties of 12,505
Internal Friction in α- 12,628
Iron:
Single Crystals by Zone Melting, Production of 12,392
Whiskers, Field Ion Microscope Analysis of 12,258
Iron-Aluminum Solid Solution Alloys, Crystallographic Order in 12,247
Iron-Boron Interactions in Si 12,367
Iron-Cobalt, Preparation of Ferromagnetic Thin Films of 12,394
Iron Selenide, Superstructures of 12,255
Irradiation-Induced Expansion in InSb, Electron 12,420
Ising fcc Ground State 12,508

J

Junction Depth, Diffusion Errors Affecting 12,647
Junctions,
Capacitance of 12,642
Degenerate:
Negative Temperatures in 12,643
Tunneling in 12,640
Effects of High Dislocation Density on Properties of Shallow p-n 12,372
Emission from 12,645
Vapor Deposition: Preparation of 12,649

L

Laser Action in Ruby 12,721
Lasers,
Glass 12,719
Growth of CaF_2 Crystals for 12,404
Observation of Signals from 12,718
Output Peak Power of 12,720
Periodic Relaxation in Ruby 12,717
Lasers:
- See also Masers 12,717
Discussed at 1961 NEREM Conference 12,709
Lattice:
Constants of:
$NaNO_2$, Temperature Dependence of 12,254
Si 12,253
Expansion, Irradiation Induced 12,281
Potential in:
Alkali Halides 12,433
Ruby 12,530
Strains, Generation and X-Ray Measurement of 12,259
Vibration Spectra 12,545
Vibrations, Formulation of 12,434
Vibrations in:
KH_2PO_4 and KD_2PO_4 12,436
Methyl and Methyl-d3 Cyanide Films 12,437
Lattice: Vibrations in: (Cont'd)
NaCl and CsCl 12,435
Pb, Image of Fermi Surface in 12,430
Solid CO 12,549
Wave Dispersion Curves of Diamond 12,546
Lattices, Order-Disorder Transformation in bcc 12,250
Lead, Lattice Vibrations of 12,430
Lead in Pb-Tl, Self-Diffusion of 12,354
Lead Monoxide Films, Absorption in 12,552
Lead Oxide, Photoelectric Coloring in 12,583
Lead Sulfide, Photo-EMF of 12,580
Lead Sulfide Layers, Conductivity of 12,476
Lead Sulfide-Lead Selenide Films, Dislocations between 12,305
Lead Telluride, Neutron:
Irradiation Effects on 12,423
Radiation Effects on 12,422
Lead-Thallium,
Diffusion of Bi in 12,354
Self-Diffusion of Pb and Tl in 12,354
Lead Zirconate-Lead Titanate,
Piezoelectric:
Properties and Preparation of 12,456
Pulse Generation by 12,457
Radiation Effects on 12,449
Static Stress Effects on 12,458
Lifetime:
- See also Recombination
Effects in Superconductivity 12,491
Lifetimes of Positrons in Metals and Alkali Halides 12,439
Light:
Beam Modulators 12,540
Scattering in Crystalline Polymers 12,591
Limiters, Garnet 12,706
Linear Amplifiers 12,771
Lithium Ion Drift in Si 12,366
Lithium Fluoride,
Charged Dislocations in 12,296
Defect Structure in 12,368
Dielectric Losses in 12,452
Dislocation Contribution to Tensile Strength of 12,297
Polygonization of Dislocations in Bent 12,318
Lithium Fluoride Crystal Nucleation, Effect of Impurities on 12,405
Lithium Hydride, Interstitial Defects and Lattice Expansion in 12,281
Logic:
Circuits 12,755, 12,839, 12,840, 12,841, 12,844, 12,847
Circuits,
AND and OR 12,843
NEITHER NOR 12,846
Devices, Magnetic Core 12,701
Specification of Control Circuitry 12,878
Low:
Distortion Oscillators 12,794
Noise Amplifiers 12,773, 12,774, 12,779
Luminescence, Theory of 12,561
Luminescence - See also Electroluminescence
Luminescence of:
AgCl 12,570
Al, Shock-Induced 12,562
BiI_3 12,554
Cu_2O Surface Layers, Infrared 12,569
KBr 12,566
KI:Tl 12,571
NaCl-Ni Phosphors 12,574
Phosphors, Reabsorption Mechanisms Involving 12,539
Plastic Scintillators 12,575
ZnO 12,573
ZnS:Mn 12,572

M

Magnesium Fluoride, NMR of F^{19} in 12,535
Magnesium-Manganous Ferrites, Domain Structure in 12,516

Magnesium Oxide,
Dislocation Motion Activation Energy in 12,316
Dislocations and Bending in 12,301
Heat Content of 12,595
Magnetic:
- See also Ferrite
Amplifiers 12,700
Anisotropy:
in Co Films 12,514
of Cu_2MnAl 12,522
Core:
Logic Devices 12,701
Matrix Adder 12,853
Cores, Fabrication and Applications of 12,702
Drum Data Storage Unit 12,857
Field at Nuclei in Rare Earth Metals 12,506
Films, Hysteresigraph for 12,510
Modulators 12,811
Moment, Measurement Apparatus for 12,504
Properties, Measurement Coils for High Field 12,505
Properties of Y-Ho Garnets 12,521
Reading Device 12,835
Relaxation Processes, Lognormal Distribution Function for 12,614
Rotatory Power Variation in Ferrites 12,518
Structure, Ising fcc Ground State of 12,508
Transformer Cores, Testing of 12,707
Magnetism in Transition Metal Alloys 12,507
Magnetization of:
Co Films 12,515
Ni Films 12,513
Square Loop Ferrites, Irreversible Change of 12,511
Magnetoelectric:
- See also Galvanomagnetic
Measurement Device, High Pressure 12,498
Properties of InSb, Annealing Effects on 12,499
Magnetostrictive Devices, Theory of 12,738
Magnets, Superconducting 12,731
Manganese in TiO_2, Paramagnetic Resonance of 12,533
Manganese Arsenide, High Field Magnetic Properties of 12,505
Manganese Dioxide, Ferroelectric Contact-Pressure Effects in 12,453
Manganese Oxide, Stoichiometry Deviations in 12,370
Manganese Oxide Thermistors, Electrical and Thermal Properties of 12,693
Manganese Zinc Carbide, Resistivity of 12,483
Manganese-Zinc Ferrites,
Conductivity of 12,485
Relaxation Phenomena in 12,520
Maser:
Action in Ruby, Optical 12,721
Amplifiers, X-Band 12,726
Parametric Preamplifiers 12,785
Spectrometer 12,727
Masers - See also Lasers
Masers,
Amplification in 12,712
Calcium Tungstate 12,722
Characteristics and Applications of Ruby 12,725
Gain and Oscillation 12,711
Linewidth and Spin Coupling in 12,722
Optical Techniques for 12,723
Pulsed Oscillations in Ruby 12,714
Reactance Compensation of Ruby 12,713
Resonance Conditions in 12,710
Ruby 12,722
Theory of 12,724
Time Lag in Ruby Three-Level 12,715
Traveling-Wave 12,722
X-Band Ruby Traveling-Wave 12,716
Mean Free Path on Optical Constants of Spherical Metallic Crystallites, Effect of 12,588
Measurement of High Voltage by ADP Crystals 12,881
Memory:
Elements, Preparation of Ferrites for 12,396
Readout 12,854
Units,
Cryosar 12,684
Disc File 12,858
Magnetic Core 12,854, 12,855, 12,856
Metal Card Electromagnetic 12,849
Switching Circuits for Thin Film 12,845
Transistor-Core 12,842
Mercuric Oxides, Susceptibility of 12,537
Mercury Telluride, Thermal EMF of 12,246
Mercury Telluride-Cadmium Telluride, Preparation and Properties of 12,246
Metal:
Crystals, Plasticity of 12,330
Oxide Films, Space Charge in 12,502
Metallic Contacts, Superconductivity Theory of 12,492
Metals,
Positron Lifetimes in 12,439
Strain Hardening in fcc 12,302
Methyl and Methyl-d3 Cyanide Films, Vibrational Spectra of 12,437
Mica, Dislocations in 12,322
Mica Crystal Growth, Synthetic 12,403
Microminiature:
Circuitry 12,746
Components, Survey of 12,745
Computers 12,836
Microwave:
Amplifiers, Ruby Maser 12,726
Mixers 12,812
Power Meters 12,882, 12,883
Test Equipment 12,831
Microwaves,
Solid State:
Control of 12,833
Device Applications in 12,832
Tuning and Control of 12,692
Mixers, Microwave 12,812
Mobility:
of Carriers in Ge 12,466
of CdS 12,441
in InAs, Electron 12,465
Modulators 12,755
Modulators,
Light Beam 12,540
Magnetic 12,811
Molecular Crystals, Band Theory of 12,426
Molybdenum,
Defects in 12,257
Zone Refining of 12,337
Monte Carlo Calculation of Order-Disorder Transformation in bcc Lattices 12,250
Multiple Junction Transistors 12,663
Multiplier Circuits, Analog 12,867
Multipliers, Hall Effect 12,682
Multistage Amplifiers 12,764
Multivibrators 12,790, 12,791
Multivibrators, Free Running 12,792
Multiwaveform Generators 12,823

N

Néel Points in Thin Magnetic Films 12,512
Negative:
Impedance Repeaters 12,827
Temperatures in Degenerate Junctions 12,643
Negistors 12,827
NEITHER NOR Logic Circuits 12,846
Nernst-Ettingshausen Effect in InSb-AlSb 12,608
Network Synthesis 12,740, 12,741, 12,742
Neutron Irradiation on PbTe, Effects of 12,423
Nichrome Films, Electrical Properties of 12,440
Nichrome-Silicon Films, Electrical Properties of 12,440
Nichrome-Silicon Oxide Films, Properties of 12,440
Nickel,
Effect of Impurity Adsorption on Surface:
Energy in 12,355
Self-Diffusion in 12,355
Nickel:
in Ag, Diffusion of 12,356
Alloys, Stacking Fault Energies of 12,329
Films, Magnetization of 12,513
Nickel-Chromium, Dislocations in 12,315
Nickel-Chromium Thin Film Resistors 12,631
Nickel-Cobalt, Vacancy Agglomerates in 12,266
Nickel-Copper, Vacancy Agglomerates in 12,266
Nickel Ferrites, Preparation of High Resistivity 12,397
Nickel Oxide,
Conductivity of 12,480
Stoichiometry Deviations in 12,370
Vacancies in 12,480
Niobium:
Capacitors 12,728
Superconductors, Critical Field and Thermal Conductivity of 12,494
Niobium Oxide, Defect Structure of 12,269
Niobium Pentachloride, NQR Studies of Bonds in 12,424
Niobium-Zirconium, Superconducting 12,496
Nitrogen in Ta, Solid Solubility of 12,248
Nonlinear Circuits,
Analysis of 12,744
Transients in 12,743
Nuclear:
Magnetic Resonance:
Analysis of Dislocations in NaI 12,286
of F^{19} in MgF_2 12,535
Studies of B^{11} in Borates 12,536
Quadrupole Resonance Studies of Bonds in Chlorides 12,424
Relaxation in Solids 12,534
Nuclei in Rare Earth Metals, Magnetic Fields at 12,506

O

Ohmic Contacts, Electrodeposited 12,677
Optical:
Constants of Spherical Metallic Crystallites, Effect of Mean Free Path on 12,588
Properties, Reversibility Principle Formulation of 12,538
OR Logic Circuits 12,843
Order-Disorder:
of Cu_3Au 12,251
Transformation in Body-Centered Cubic Lattices 12,250
Organic:
Compounds, Dark Conductivity in 12,577
Electrets 12,442
Films, Vibrational Spectra of Methyl and Methyl-d3 Cyanide 12,437
Protective Coatings for Devices 12,680
Solids,
EPR Studies of Spin Correlation in 12,532
Susceptibilities of 12,525
Organics, Thermally Induced EMF in Irradiated 12,607
Orientation of Crystals, Computer Study of 12,406
Oscillators 12,755
Oscillators,
Feedback 12,793
Hall Generator 12,683
High Frequency 12,789
Low Distortion 12,794
Multivibrator 12,790, 12,791, 12,792
Oxide Monocrystals, Deviations from Stoichiometry of 12,370
Oxygen in:
Si, Measurement of 12,366
Ta, Solid Solubility of 12,248

P

Packaging, Microminiature Circuitry 12,746
Packaging of:
  Diodes 12,651
  Junction Diodes, Glass 12,652
  Rectifiers 12,653, 12,654, 12,655
Paramagnetic:
  Resonance, Amplification by 12,712
  Resonance:
    in the Analysis of Impurities 12,332
    Line Splitting in Inhomogeneous Fields 12,529
    of Mn in TiO_2, Hyperfine Structure of 12,533
    in $NaNO_2$ 12,531
    in Semiconductors 12,528
  Salts, Spin Absorption in 12,527
Parametric:
  Amplifiers 12,777
  Amplifiers,
    Backward-Wave 12,781
    Bandwidth Limitations in 12,766
    Ferromagnetic 12,783
    Low Noise 12,779
    Traveling Wave Type 12,782
  Diodes,
    Diffusion Techniques for 12,648
    Fabrication and Properties of 12,634
Parametric-Maser Preamplifiers 12,785
Parametron Arithmetic Circuits 12,850
Peltier:
  Coolers for Transistors 12,678
  Effect in Two-Phase Alloys 12,600
Penetration of Ag into Quartz 12,364
Permalloy Ferrite Cores, Characteristics of 12,703
Phase Diagram of:
  Sn-S System 12,243
  Zr-Co-O and Zr-Ni-O Systems 12,244
Phase Transformation, Diffusionless 12,295
Phase Transformation in:
  Fe, Alpha-Gamma 12,392
  Thin Co Films 12,252
Phenylanthranilic Acid Films, Dark Conductivity in 12,577
Phonon Scattering 12,469
Phosphors,
  Charge Storage in 12,568
  Preparation of Red ZnSe Electroluminescent 12,389
  Reabsorption and Luminescence in 12,539
  Ultraviolet Excitation Efficiencies of 12,567
Phosphorus in Si,
  Diffusion of 12,690
  Diffusion Concentration Profile of 12,346
  Dislocation Generation by Solute Diffusion of 12,290
Photo-Electronic Switching Circuits 12,806
Photo-EMF:
  of PbS, Absorbed Oxygen Effects on 12,580
  in Semiconductors 12,501
Photoconduction, Theory of 12,576
Photoconductivity of:
  Evaporated Anthracene Films 12,579
  HgTe-CdTe 12,246
  Organic Compounds 12,577
  of Semiconductors, Capacitive Field Effects on 12,578
Photoelastic:
  Constants of Ammonium Dihydrogen Phosphate 12,620
  Effect in Ge and Si 12,592
  Stress-Birefringence of Rb-Halides 12,619
Photoelectric:
  Coloring in PbO 12,583
  Effect in Cs_3Sb 12,581
  Emission from CdS and CdTe 12,585
  Theory, Universal Speed of Recombination Concept in 12,582
Photoinelasticity in AgCl 12,621
Photoionization Spectra of Ge Donors 12,470
Photomagnetic Effect, Transversal 12,587
Photon Absorption in Al 12,543
Photoprotons from Si^{28}, Fine Structures of 12,586
Photosensitive Etching of Si 12,409
Piezoelectric:
  Ceramics, Static Stress Effects on 12,458
  Filters, Bandpass 12,736
  Generation of an Electrical Impulse 12,457
  Lead Zirconate-Titanate, Properties and Preparation of 12,456
  Pressure Gauges 12,735
Piezoelectricity of Quartz, Strain Dependence of 12,459
Planar Transistors, Si 12,671
Plastic:
  Deformation, Dislocation Motion during 12,330
  Deformation Effects on Superconducting Properties of Al 12,493
  Flow in Metals, Ferroelectric Contact-Pressure Effect Measurements on 12,453
  Scintillators 12,575
Plasticity of Ionic and Metal Crystals 12,330
Plating, New Method for Measurement of Sputtering of 12,414
Platinum, Resistivity of 12,477
Point:
  Contact:
    Diodes,
      GaP 12,632
      Whiskers for 12,633
    Transistors 12,659
  Defects, Stress Induced 12,261
Polarization:
  of $NaNO_2$, Spontaneous 12,254
  in Solids 12,534
Polarized Spectra of Co(III) Acetylacetonate 12,556
Polishing of Ge and Si Wafers, Electrochemical 12,407
Polymer Carbons,
  Conductivity and Hall Constants of 12,489, 12,490
  Preparation of 12,490
Polymers, Crystalline: Light Scattering in 12,591
Positron-Electron Study of Electronic Structure 12,439
Positron Lifetimes in Metals and Alkali Halides 12,439
Potassium Bromide,
  Absorption in 12,544
  Dielectric Properties of 12,450
  Diffusion of Thallous Ions in 12,362
  Luminescence of 12,566
  Model for V_1 Center Formation in 12,274
Potassium Bromide:Tl, Color Center Diffusion in 12,279
Potassium Chloride,
  A Centers in 12,273
  Absorption in 12,544
  Color:
    Center Bleaching in 12,276
    Centers in 12,275, 12,277
  Vacancy Pair Mobility in 12,271
Potassium Iodide:Tl, Luminescence in 12,571
Potassium Phosphate, Lattice Vibrations and Absorption in 12,436
Power:
  Amplifiers, Dual Channel 12,786
  Evaluations in Tunnel Diodes 12,752
  Generation Control System 12,879
  Meters,
    Microwave 12,882, 12,883
    RF 12,884, 12,885
  Supplies 12,755, 12,873
  Transistors, Breakdown in 12,664
Preamplifiers,
  Maser-Parametric 12,785
  Tunnel Diode 12,780
Precipitation of Co in Au-Co 12,369
Preparation of:
  - See also Growth of
  AlN and GaN 12,388
  Ferrites:
    with High Temperature Independent Initial Permeabilities 12,395
Preparation of: Ferrites: (Cont'd)
    for Microwaves 12,398
  Ferromagnetic Thin Films 12,394
  HgTe-CdTe Solid Solutions 12,246
  High Resistivity Nickel Ferrites 12,397
  InSb Films 12,589
  Lead Zirconate-Titanate 12,456
  Mn-Zn Square Loop Ferrites 12,399
  Red ZnSe Electroluminescent Phosphors 12,389
  Semiconducting Polymer Carbons 12,490
  Si from SiI_4 12,386
  Square Loop Ferrites 12,396, 12,399
  Superconductive Ferrites 12,393
  Tunnel Junctions by Vapor Deposition 12,649
Pressure:
  Effects on Devices 12,629
  Gauges, Piezoelectric 12,735
Pulse:
  Amplifier Gating Circuit 12,843
  Delay Circuits 12,824
  Distributor Circuits 12,826
  Echo Technique for Measurement of Elastic Constants 12,616
  Generators 12,792, 12,814, 12,815, 12,816, 12,817, 12,818, 12,819, 12,820
  Shaping Circuits 12,825
Purification:
  - See also Zone Refining
  of GaAs, Floating Zone 12,336
  Methods for Surface Studies 12,413
  of Precipitated TiO_2 12,340
Push-Pull Amplifiers 12,784

Q

Quartz,
  Acoustic Absorption in 12,626
  Penetration of Ag into 12,364
  Ultrasonic Attenuation in 12,625
Quartz Piezoelectricity, Strain Dependence of 12,459

R

Radiation:
  Detectors,
    Junction 12,894, 12,895, 12,897
    Semiconductor 12,899
    Si and Ge 12,891
    Surface Barrier 12,892, 12,893, 12,898
    Transistor 12,896
  Effects:
    on Devices 12,630
    in PbTe, Neutron 12,422, 12,423
Radio-Frequency Coil Modification for Floating Zone Method 12,384
Radiochemical Analysis of Impurities 12,333
Radiometers, Infrared 12,887
Ranging with Ruby Lasers 12,717
Rare Earth:
  Dopants, Growth of Single Crystals of CaF_2 with 12,404
  Metals, Magnetic Field at Nuclei in 12,506
Reabsorption in Crystals 12,539
Readers, Information 12,865
Reading Device, Magnetic 12,835
Readout, Memory 12,854
Recombination,
  Irreversible Thermodynamic Formulation of 12,460
  Surface 12,463
Recombination:
  - See also Lifetime
  of Li^+-B^- Ions in Si 12,365
  in Semiconductors, Impurity Center 12,461
  in Si, Irradiation Effects on 12,462
Rectifiers, Packaging of 12,653, 12,654, 12,655
Reflection:
  of Ge Films, Vacuum Measurements of 12,584
  Spectrum Determination of Energy Gap of Binary $(ZnSe)_x$-$(CdSe)_y$ 12,429
  from Thin Films 12,593

Refraction in Crystalline Polymers 12,591
Refractive Index of:
Cu2O 12,590
InSb Films 12,589
Refrigeration, Thermoelectric 12,902
Regenerative Amplifiers 12,778
Registers, Storage 12,856
Relaxation:
Phenomena in Mn-Zn Ferrites 12,520
Processes, Lognormal Distribution Function for 12,614
Repeaters, Negative Impedance 12,287
Resistive Films, Electrical Properties of 12,440
Resistivity:
- See also Conductivity
Changes Due to Formation of G.P. Zones 12,475
Measurements, Specimen Size and Probe Criteria for 12,473
Measurements on Anisotropic Conductors 12,472
Resistivity of:
Al-Zn Alloys 12,474
Co-Mn Spinels with Admixtures 12,486
Ge, Temperature Variation of 12,478
InSb, Annealing Effects on 12,499
Mn3ZnC 12,483
Pt, Temperature Effects on 12,477
SnSe2 and GeSe2 12,482
TlSe 12,481
Resistors,
Ni-Cr Thin Film 12,631
Temperature Effects on 12,477
Resonance Conditions in Masers 12,710
Rubidium-Boron Glasses, Conductivity of 12,488
Rubidium Halides, Photoelastic Stress-Birefringence of 12,619
Ruby, Crystal Field Structure of 12,530
Ruby:
Lasers, Periodic Relaxation in 12,717
Maser Amplifiers, X-Band 12,726
Masers 12,713, 12,714, 12,716, 12,718, 12,720, 12,721, 12,725
Rutile,
Absorption in 12,551
Paramagnetic Resonance of Mn in 12,533
Thermoelectric and Conductivity Properties of 12,606

S

Sampling Switches 12,809
Sapphire Whiskers, Growth of 12,402
Sawtooth Generators 12,756
Scattering,
Phonon: 12,469
and Impurity 12,468
Scattering in:
Bi2Te3, Kinetics of 12,467
Crystalline Polymers, Light 12,591
Scintillation Counters 12,890
Scintillators, Plastic 12,575
Selective Amplifiers 12,775, 12,828
Selenium, Thermal Conductivity of Tl Doped 12,603
Selenium Rectifiers, Packaging of 12,654, 12,655
Semiconducting Compounds from Nonstoichiometric Melts, Growth of 12,381
Semiconductor Compounds, Diffusion in 12,358
Semiconductors - See also Specific Semiconductor
Semiconductors,
Breakdown in Nonpolar 12,497
Field Effect and Photo-EMF in 12,501
Infrared Absorption in 12,545
Paramagnetic Resonance in 12,528
Zone Refining of 12,339
Shift Registers, Magnetic Core 12,702, 12,860, 12,861, 12,862
Shock Waves in Ferroelectrics 12,623
Silica, Ultrasonic Attenuation in 12,624
Silicon,
Carbon Impurity Analysis Method for 12,335
Crystal Imperfections in 12,256
Defect Structure in 12,368
Silicon, (Cont'd)
Diffusion:
in 12,344, 12,350
of Boron in 12,360
of Carbon in 12,361
Concentration Profile of P in 12,346
of Li+-B- Ions in Si 12,365
of Phosphorus in 12,690
Dislocation Generation by Solute Diffusion of Boron and Phosphorus in 12,290
Fe-B Interactions in 12,367
Lattice Constants and Thermal Expansion Coefficients of 12,253
Li Ion Drift in 12,366
Paramagnetic Resonance in 12,528
Photoelastic Effect in 12,592
Photosensitive Etching of 12,409
Recombination in Irradiated 12,462
Slip Patterns in Boron-Diffused 12,372
Thermal Conductivity of 12,599
Silicon:
Crystal Growth,
Floating Zone Method for 12,383
Nomographs for 12,376
from SiHCl3, Vapor Deposition of 12,687
from SiI4, Preparation of 12,386
Solar Cells 12,689, 12,690
Surfaces, Impurity Contamination in 12,412
Wafers, Electrochemical Polishing of 12,407
Silicon28, Photoproton Fine Structure of 12,586
Silicon Carbide-Molybdenum Silicide, Infrared Emission from 12,558
Silicon Carbide-Silicon Nitride-Molybdenum Silicide, Infrared Emission from 12,558
Silicon Monoxide Films, Annealing of 12,415
Silicon Tetraiodide, Preparation of Si from 12,386
Silver,
Annealing of Quenched 12,416
Defects in 12,416
Diffusion of Ni in 12,356
Elastic Constants of 12,616
Temperature Dependence of Rolling Textures in High Purity 12,373
Silver:
Alloys, Stacking Fault Energies of 12,329
Films on Rocksalt, Growth and Structure of Thin Epitaxial 12,391
into Quartz, Penetration of 12,364
in Zn, Diffusion of 12,352
Silver-Bonded Ge Diodes, Fabrication and Properties of 12,634
Silver Cadmium, Diffusion and Internal Friction in 12,345
Silver Chloride,
Dislocation Generation in 12,291
Luminescence in 12,570
Photoinelasticity in 12,621
Silver Oxide, Infrared Absorption in 12,547
Silver-Zinc, Order-Disorder Transformation in β- 12,250
Slip:
Distribution in MgO, Fracture Dependence on 12,298
Patterns in Boron-Diffused Si 12,372
Sodium Azide, Faults in 12,421
Sodium Chlorate, Thermal Expansion Coefficients of 12,611
Sodium Chloride,
Absorption of 12,450
Charged Dislocations in 12,296
Defect Annealing in 12,263
Dielectric:
Loss in 12,451
Properties of 12,450
Dislocation Motion Activation Energy in 12,316
Elastic Modulus of 12,618
Interstitial Defects and Lattice Expansion in 12,281
Lattice Vibrations in 12,435
Thermal Expansion of 12,612
Vacancies in 12,268
Sodium Chloride-Type Crystals, Diffusion of NH4 Ions in 12,363
Sodium Chloride Vacancy Pair Mobility in 12,271
Sodium Chloride-Nickel Phosphors, Luminescence of 12,574
Sodium Iodide, NMR Analysis of Dislocations and Axial Compression in 12,286
Sodium Nitrite,
Lattice Constants and Polarization of 12,254
Paramagnetic Resonance in 12,531
Solar:
Cells,
Characteristics of 12,688
Fabrication of 12,687
GaAs 12,689
Si 12,689, 12,690
Energy Converters 12,688
Solid:
Solubilities in Ta 12,248
Solutions of HgTe-CdTe 12,246
State Phenomena Applied to Circuitry 12,747
Solidification of Al, Dislocations and Substructures Produced during 12,304
Space-Charge-Limited Dielectric Diodes, Admittance of 12,730
Space Charge in Metal Oxide Films 12,502
Specific:
Heat, Anomalies in 12,598
Heat of:
MgO 12,595
Ti-Mo Superconductors 12,597
ZrO and ZrSiO3 12,595
Spectrographic Analysis of Impurities 12,332
Spectrometer, Maser 12,727
Spin:
Absorption in Paramagnetic Salts 12,527
Correlation in Ion Radical Salts, EPR Studies of 12,532
Spin-Wave:
Hamiltonian, Solutions to Two-Dimensional 12,509
Resonance in Co Films 12,515
Spinels, Twinning in 12,328
Spot Coolers, Thermoelectric 12,903
Sputtering, New Method for Measurement of Plating 12,414
Square Loop Ferrites,
Composition of 12,396
Preparation of Mn-Zn 12,399
Stability Criteria for Tunnel Diodes 12,751
Stacking Fault Energies of Cu, Ag, and Ni Alloys 12,329
Stanic Oxide Films, Absorption in 12,552
Stereo Amplifiers 12,786
Stoichiometric Deviations in:
GaSb 12,371
Oxide Monocrystals 12,370
Storage:
- See also Memory
Devices, Theory of Wall-Stepping Film 12,517
Units, Magnetic Drum 12,857
Strain Hardening in fcc Metals 12,302
Strength of Solids, Theory of 12,622
Stress, Contribution of Temperature Dependent Locking of Dislocations to Yield 12,300
Stress:
in α-Brass, Deformation Produced Residual 12,417
Effects on Grain Boundary Sliding 12,324
Strontium-Bismuth Titanate, Ferroelectric Properties of 12,455
Structure of:
Co-Mn Spinels with Admixtures 12,486
Cu3Au, Deformation Effects on 12,251
Deposited Au Thin Films 12,390
Methyl and Methyl-d3 Films 12,437
Ruby, Electronic 12,530
Sulfur-Tin System, Phase Diagram of 12,243
Superconducting:
Al, Plastic Deformation Effects on 12,493
Ferrites, Fabrication of 12,393

Superconducting: (Cont'd)
Group V-b Metals, Critical Field and Thermal Conductivity of 12,494
Magnets 12,731
Nb-Zn Alloys 12,496
Ti-Mo, Specific Heat of 12,597
Vanadium Films 12,495
Superconductive Computers 12,837
Superconductivity,
Lifetime Effects in 12,491
Nonlinear Effects in 12,732
Superconductivity in the Neighborhood of Metallic Contacts, Theory of 12,492
Superstructures of Fe_7Se_8 12,255
Surface:
Barrier Diodes, Fabrication and Characteristics of 12,641
Concentration, Evaluation of 12,347
Energy:
in Ni, Effect of Impurity Adsorption on 12,355
of Zeolites 12,487
Evaporation from Crystals, Surface Pressure Dependence of 12,245
Impurity Concentration of Diffused Ge, Reduction of 12,348
Recombination 12,463
Self-Diffusion in Ni, Effect of Impurity Adsorption on 12,355
States, Conductivity Measurements of 12,578
Studies, Purification Methods Used in 12,413
Surfaces,
Stabilization of Transistor 12,679
Thermal Transfer from 12,696
Susceptibilities of Crystalline Stable Free Radicals 12,525
Susceptibility, Measurement of 12,503
Susceptibility of:
Er and Ho Ethylsulphates 12,526
GaSb-InSb 12,523
Mercuric Oxides 12,537
Weakly Magnetic Materials 12,524
Sweep Circuits, Linear 12,821
Switches, Ferrite Circulator 12,699
Switching:
Characteristics of Transistors 12,667
Circuits 12,755, 12,797, 12,798, 12,839, 12,840, 12,844, 12,848
Circuits,
Bibliography on 12,795
Comparator 12,805
Current 12,810
Gate 12,803, 12,843
High Voltage 12,808
Photoelectronic 12,806
Sampling 12,809
Transformer Drive for 12,796
Trigger 12,799, 12,800, 12,801, 12,802
Tunnel Diode 12,807, 12,845
Effect in Sb_2S_3 12,446
Parameters, Measurement of Transistor 12,658

T

Tangential Waveform Generators 12,822
Tantalum, Solid Solubilities in 12,248
Tantalum:
Capacitors, Breakdown Characteristics of 12,729
Superconductors, Critical Field and Thermal Conductivity of 12,494
Tantalum Chloride, NQR Studies of Bonds in 12,424
Tantalum Pentoxide Films, Absorption in 12,552
Tape:
Playback-Correct System 12,872
Recording System 12,834
Teletype Equipment, Error Correcting System for 12,830
Tensile Strength of LiF 12,297
Terbium, Heat Capacity of 12,596
Ternary Phase Diagrams of Zr-Co-O and Zr-Ni-O Systems 12,244
Tetracyanoguinodimethane, Studies of Spin Correlation in 12,532
Textures in:
Ag, Temperature Dependence of 12,373
Ge Films 12,374
Thallium in Pb-Tl, Self-Diffusion of 12,354
Thallium Selenide,
Activation Energies of 12,481
Energy Band Structure of 12,432
Resistivity and Hall Coefficient of 12,481
Thallous Ions in KBr, Diffusion of 12,362
Thermal:
Conductivity in:
Dielectrics 12,601
Two-Phase Alloys 12,600
Conductivity of:
Bi 12,602
Bi_2Te_3 12,599
Ga 12,602
Group V-b Metal Superconductors 12,494
Se with Tl Additives 12,603
Si 12,599
Sn 12,602
Distributions from Surfaces 12,696
Effects on Binding Properties 12,598
EMF in:
Irradiated Hydrocarbons 12,607
MnO 12,693
Expansion: 12,610
Coefficients: 12,611
of Si 12,253
of Cr 12,613
of NaCl 12,612
Properties of Solids 12,594
Thermionic Properties of ZrC-UC 12,500
Thermistors,
Fabrication and Properties of $BaTiO_3$ Bead 12,694
MnO 12,693
Thermoelectric:
Cooler 12,902, 12,903
Devices, Design of 12,695
Energy Converters 12,697, 12,901
Materials, Preparation and Evaluation of 12,340
Power of Ga 12,605
Properties, Measurement of 12,604
Properties of:
Alloy System Bi-Sb-Se-Te 12,385
PbTe 12,422
Rutile 12,606
Thermoelements, Thermal Transfer from 12,696
Thermomagnetic:
Effects in InSb-AlSb System 12,608
Properties of Ferrites 12,609
Thermometers, Low Temperature 12,889
Thorium Chloride, NQR Studies of Bonds in 12,424
Tin, Thermal Conductivity of 12,602
Tin in InSb, Diffusion of 12,357
Tin Selenide, Resistivity and Hall Coefficients of 12,482
Tin-Sulfur System, Phase Diagram of 12,243
Titanates, Conductivity of Group II 12,484
Titanium and Ti Alloys, Fatigue in 12,282
Titanium Boride, Elastic Constants of 12,617
Titanium Carbide, Elastic Constants of 12,617
Titanium Dioxide,
Paramagnetic Resonance of Mn in 12,533
Purification of Precipitated 12,340
Stoichiometry Deviations in 12,370
Titanium Tetrachloride, NQR Studies of Bonds in 12,424
Transducers, Depletion Layer 12,734
Transformer Cores, Testing of 12,707
Transients in Nonlinear Circuits 12,743
Transistor:
Circuits 12,755, 12,756, 12,757
Circuits,
Avalanche 12,578
Breadboard Layout Techniques for 12,761
Gain Extension in 12,760
Electrodes 12,676
Switching Parameters, Measurement of 12,658
Test Sets 12,657
Transistors,
Admittance Parameters for High Frequency 12,666
Avalanche Conditions in 12,814
Base Characteristics of 12,665
Double Diffused 12,674
Drift: 12,661
Frequency Cutoff in 12,669
Minority Carrier Transport in 12,662
Extension of Frequency Range in 12,759
Frequency Cutoff in 12,668
Ge Mesa 12,672
HF Ge 12,656
Injection Levels in 12,665
Intrinsic Barrier: Fabrication and Operation of 12,660
Junction:
Fabrication of:
Alloyed 12,646, 12,673
High Frequency 12,650
Fixed Back Resistance of Junctions in 12,670
InSb n-p-n 12,675
Multiple Junction 12,663
Peltier Coolers for 12,678
Planar 12,671
Point Contact 12,659
Power: Breakdown in 12,664
Protective Coatings for 12,680
Stabilization of the Surfaces of 12,679
Switching Characteristics of 12,667, 12,798
Transition Metal Alloys, Magnetism in 12,507
Transmission of Ge Films, Vacuum Measurements of 12,584
Transmittance of InSb Films 12,589
Traveling Wave:
Masers, Ruby 12,716
Type Parametric Amplifiers 12,782
Trigger:
Circuits 12,799, 12,801
Circuits,
Amplifying 12,800
Tunnel Diode 12,802
Tungsten, Defects in 12,257
Tungsten in Co-Based Alloy, Diffusion of 12,359
Tunnel:
Diode:
Amplifiers 12,780
Circuits 12,750
Converters 12,813
Drivers 12,837
Switching Circuits 12,807, 12,845
Trigger Circuits 12,802
Diodes,
Characteristics of 12,753
GaAs 12,636, 12,637
Magnetic Field Dependence in InSb 12,639
Power Evaluations of 12,752
Stability Criteria for 12,751
Junctions by Vapor Deposition, Preparation of 12,649
Tunneling:
Theory 12,640
in Tunnel Diodes 12,638
Twinning in Graphite 12,327
Twins, Dislocation Model of 12,325
Twins in:
β-In_2S_3 12,328
InSb, Growth of 12,326

U

Ultrasonic:
Absorption in Quartz 12,626
Attenuation in:
Quartz 12,625
Silica 12,624
Delay Lines, Glass 12,739
Transducers, Layer 12,734

V

Vacancies in Fe_7Se_8 12,255

Vacancies:
in NaCl, Quenching of Cation 12,268
in NiO, Concentration of 12,480
and Solute Atoms in Au-Pd Solid Solutions, Binding Energy for 12,267
Vacancy:
Agglomerates, Electron Microscope Analysis of 12,266
Aggregates in Quenched Ge 12,265
Diffusion: 12,294
in Anisotropic Crystals 12,270
Distributions 12,264
Migration in Au, Pressure Effects on 12,272
Pairs in KCl and NaCl, Mobility of 12,271
Vanadium:
Films, Superconducting 12,495
Superconductors, Critical Field and Thermal Conductivity of 12,494
Vapor:
Deposition, Preparation of Tunnel Junctions by 12,649
Deposition of Si from $SiHCl_3$ 12,687
Phase Growth of Single Crystals of II-VI Compounds 12,387
Varactor Circuits 12,748, 12,749
Variable Waveform Generators 12,823
Visco-Elastic Media, Motion of Dislocations in 12,314
Voltage Comparators, dc 12,805

W

Wave:
Generators 12,755
Generators, Tangential 12,822
Propagation in Electromagnetic Elastic Solid 12,627
Waveguides, Ferrite Loaded 12,708
Whiskers, Field Ion Microscope Analysis of 12,258
Whiskers for Point Contact Diodes 12,633
Wideband Amplifiers, IF 12,770
Work Function of CdTe and CdS 12,585

X

X-Ray:
Scattering in Ge 12,419
Stress Measurement 12,259
Study of Crystal Imperfections in Si 12,256

Y

Yttrium-Holmium Garnets, Magnetic Properties of 12,521
Yttrium-Iron Garnets, Growth of Large Single-Crystal 12,400

Z

Zeeman Spectra of Ge Donors 12,470
Zeolites, Conductivity and Surface Energy of 12,487
Zinc,
Diffusion of Ag and In in 12,352
Dislocation:
Generation by Spark Discharge in 12,292
Motion in 12,313
Edge Dislocations in 12,317
Zinc in:
GaAs, Diffusion of 12,349
InSb, Diffusion of 12,357
Zinc-Aluminum Alloys, Resistivity of 12,474
Zinc-Manganese Ferrites, Relaxation Phenomena in 12,520
Zinc Oxide,
Conductivity and Electron Density in 12,438
Luminescence of 12,573
Zinc Selenide Red Electroluminescent Phosphors, Preparation of 12,389
Zinc Selenide-Cadmium Selenide, Energy Gap of 12,429
Zinc Sulfide, Electroluminescence in 12,563
Zinc Sulfide:Cu:Al, Electroluminescence in 12,565
Zinc Sulfide:Cu:Cl, Electroluminescence in 12,564
Zinc Sulfide:(Cu,Cl), Electroluminescence in 12,691
Zinc Sulfide:Mn, Luminescence of 12,572
Zirconium Carbide-Uranium Carbide, Thermionic Properties of 12,500
Zirconium-Cobalt-Oxygen System, Phase Diagram of 12,244
Zirconium Dioxide Films, Absorption in 12,552
Zirconium-Nickel-Oxygen Systems, Phase Diagrams of 12,244
Zirconium Oxide, Heat Content of 12,595
Zirconium-Oxygen, Energy Band Structure of 12,427
Zirconium Silicate, Heat Content of 12,595
Zone:
Melting,
Gun for Electron Bombardment Floating 12,382
Production of Fe Single Crystals by 12,392
Purification of GaAs, Floating 12,336
Refining, Thermal Behavior in 12,338
Refining of:
Mo 12,337
Semiconductors 12,339
Theory for Conduction Electrons 12,428

REQUEST FOR PAPERS

Cambridge Communications Corporation has initiated publication of original review articles pertaining to the solid state. Manuscripts (with bibliographies) reviewing topics in the fields of solid state physics and metallurgy, solid state device technology, and circuit applications of solid state devices are requested. Interested parties should contact the Assistant Editor for further information.

Announcing the Availability of Bibliographic and Information Retrieval Services

Our highly experienced scientific abstracting staff, composed of people with substantial professional qualifications and representing many branches of the sciences, is ready to work with you in these areas.

For more detailed information, write a brief description of your problem or project and a member of our scientific staff will review it. Our reply will be prompt.

Write directly to:

Dr. Geoffrey Knight, Jr., President
Cambridge Communications Corporation
238 Main Street
Cambridge 42, Massachusetts

AUTHOR INDEX

Abbott, H.W. 12,784
Abe, K. 12,586
Abe, Z. 12,902
Aboullaev, G.B. 12,603
Achyuthan, K. 12,620
Addamiano, A. 12,388
Adsit, N.R. 12,324
Agaev, Ya. 12,608
Agranovich, V.M. 12,539, 12,601
Akhundova, S.A. 12,603
Albanes, N.J. 12,857
Albers, W. 12,243
Alderson, J.E. 12,571
Alexander, S. 12,878
Aliev, M.I. 12,603
Ali Zaidi, S.R. 12,604
Allred, W.P. 12,380
Amelinckx, S. 12,307
Amer, S. 12,668
Amorosi, D.M. 12,422, 12,423
Amsel, G. 12,894
Anders, E. 12,401
Anderson, D.R. 12,748
Anderson, P.B. 12,269
Anderson, R.E. 12,673
Andresen, H.G. 12,533
Andrianov, A.S. 12,566
Angell, J.B. 12,863
Ansel'm, A.I. 12,469
Aoyagi, K. 12,522
Arams, F.R. 12,706
Aron, R.M. 12,766
Arp, V. 12,731
Asanabe, S. 12,482
Asdente, M. 12,474
Astrahan, M.M. 12,865
Averkin, A.A. 12,498
Azároff, L.V. 12,256, 12,438

Bair, M.E. 12,725
Baird, D.H. 12,398
Baird, J.A. 12,800
Baker, W.E. 12,735
Balkanski, M. 12,332
Balygin, I.E. 12,364
Bardasis, A. 12,491
Barnes, R.S. 12,322
Barron, T.H.K. 12,435
Barry, D. 12,400
Bartelink, D.J. 12,645
Baruch, P. 12,894
Barzilai, G. 12,708
Basov, N.G. 12,643
Bates, L.F. 12,609
Batterman, B.W. 12,419
Battocletti, F.E. 12,839
Bauer, E.W. 12,824
Bauer, P.A. 12,739
Beck, K.H. 12,776
Beck, P.A. 12,317
Becker, M. 12,646
Beckwith, R.W. 12,826
Belfor, G.G. 12,444
Bellmer, W.A. 12,849
Benin, V.L. 12,700
Bennemann, K.H. 12,280
Bennett, A.L. 12,747
Bennett, R.J. 12,773
Benrey, R.M. 12,723
Bentle, G.G. 12,316
Bereskin, A.B. 12,786
Berlaga, R.Ya. 12,580
Berlincourt, D. 12,458
Berlincourt, T.G. 12,496
Bernhein, R.A. 12,444
Berry, B.S. 12,614
Bever, M.B. 12,251
Biloni, H. 12,304
Birnbaum, H.K. 12,261
Biscoe, J. 12,656
Black, J.F. 12,349
Blakely, J.M. 12,355
Blankenship, J.L. 12,893
Blinov, G.A. 12,665
Bocek, M. 12,330
Bogolomov, V.N. 12,498
Bokshteyn, S.Z. 12,333
Bolef, D.I. 12,710
Bonch-Bruevich, A.M. 12,565
Borgeaud, P. 12,253
Borkowski, C.J. 12,893
Borovikov, G.P. 12,559
Borzyak, P.G. 12,584
Boyle, W.S. 12,470
Bradmiller, R.W. 12,764
Bragg, R.H. 12,256
Braginski, A. 12,520
Brailsford, A.D. 12,310
Brandon, D.G. 12,257
Braun, J.H. 12,409
Bray, P.J. 12,286, 12,536
Breazeale, M.A. 12,620
Bril, A. 12,567
Brittain, J.O. 12,323, 12,324
Broadbent, K.D. 12,702
Brockhouse, B.N. 12,430
Brookes, G. 12,679
Brouwer, J.F. 12,827
Brown, E.A. 12,701
Brown, J. 12,698
Brown, L.M. 12,320
Brown, M.A.C.S. 12,540
Brownlow, J.M. 12,396, 12,399, 12,704
Brule, J.D. 12,741
Buchanan, C.L. 12,629
Bucklow, I.A. 12,382
Bucy, Jr., J.F. 12,872
Buehler, E. 12,337
Buford, J.T. 12,386
Buie, J.L. 12,660
Butcher, P.N. 12,639
Butler, J.N. 12,502
Buttrey, J.W. 12,368
Butusov, Yu.M. 12,428
Bykova, T.T. 12,580

Cahn, R.W. 12,249
Calverley, A. 12,494
Cape, J. 12,544
Card, W.H. 12,750
Carey, R. 12,678
Carlson, A.W. 12,756, 12,771
Carroll, J.M. 12,836
Caswell, H.L. 12,415
Chacran, J.J. 12,812
Challis, L.J. 12,889
Chang, R. 12,295, 12,316
Chapin, W.E. 12,630
Chaplin, R.L. 12,262
Chapouille, P. 12,814
Chasmar, R.P. 12,465
Chesnust, D.B. 12,532
Chester, P.F. 12,710
Christopher, M.E. 12,459
Christy, R.W. 12,275
Chun-Mou, C. 12,778
Clark, J. 12,698
Clark, M.A. 12,660
Clarke, F.J.P. 12,552
Cline, R.S. 12,373
Clingman, W.H. 12,695
Cobbold, R.S.C. 12,855
Cohen, J.B. 12,475
Cole, M. 12,382
Coleburn, N.L. 12,562
Collins, A.F. 12,853
Collins, R.J. 12,720
Conard, II, G.P. 12,394
12,725
Cook, J.J. 12,526
Cooke, A.H. 12,492
Cooper, L.N. 12,441
Coopmans, P. 12,514
Corciovei, A. 12,422,
Corelli, J.C. 12,423
Corli, J.A. 12,616
12,335
Cornet, C. 12,301
Cornet, I. 12,801
Corsiglia, J. 12,847
Crane, H.D. 12,456
Crawford, A.E. 12,884
Cronenwett, W.T. 12,725
Cross, L.G. 12,336
Cunnell, F.A. 12,452
Curien, H. 12,888
Curtis, B.R. 12,646
Cutler, M.

Dabbs, J.W.T. 12,898
Damon, R.W. 12,833
Danforth, W.E. 12,500
Danielian, A. 12,508
Davey, J.E. 12,374
David, J.P. 12,588
Davis, Jr., J.R. 12,446
Davis, P.C. 12,845
Davydova, T.G. 12,680
Dearnaley, G. 12,892
DeBlois, R.W. 12,505
Dekeyser, W. 12,296
Dekhtiar, I.Ia. 12,321
Delavignette, P. 12,307
Dell'Oro, E. 12,775
Demers, E. 12,797
Denny, H.W. 12,789
Dermit, G. 12,752
Deshpande, V.T. 12,611
Dew-Hughes, D. 12,287
D'Haenens, I.J. 12,721
Dieke, G.H. 12,553
Dillon, Jr., J.A. 12,413
Dimmock, J.O. 12,542
Dixon, T.P. 12,887
Doesschate, Jr., W.A. 12,761
Donachie, Jr., M.J. 12,259
Donald, D.K. 12,338
Donnay, G. 12,443
Donnay, J.D.H. 12,443
Donovan, P.F. 12,897
Dorn, J.E. 12,302
Douglas, T.B. 12,595
Downey, J.W. 12,244
Doyama, M. 12,416
Doyle, W.P. 12,552
Drickamer, H.G. 12,530
Drokin, A.I. 12,516
Ducret, L. 12,335
Duffy, Jr., W. 12,525
Duga, J.J. 12,299
Dumontet, P. 12,588
Dunkin, J.W. 12,627
Dyke, J.R. 12,796
Dylgerov, V.D. 12,516
Dymon, J.J. 12,398

Eannarino, G. 12,651
Eckert, U. 12,815
Edwards, J.O. 12,536
Edwards, P.L. 12,402
Edwards, W.G. 12,851
Eland, A.J. 12,410
Elbaum, C. 12,289
Emel'yanenko, O.V. 12,608
Emile, Jr., P. 12,792
Emrick, R.M. 12,272
Eringen, A.C. 12,627
Erofeichev, V.G. 12,476
Eshelby, J.D. 12,314
Evans, W. 12,688
Ewing, G.E. 12,549
Ewing, Jr., W.O. 12,735

Fabri, G. 12,891
Fawcett, D.G. 12,854
Feder, R. 12,249
Fedorovich, R.D. 12,584
Feldkeller, E. 12,512
Finn, Jr., G.B. 12,651
Finn, M.C. 12,288
Fisher, C. 12,382
Fitzgerald, T. 12,625
Flata, M. 12,629
Fletcher, G.C. 12,612
Fletcher, R.C. 12,724
Flinn, P.A. 12,250
Flodmark, S. 12,426, 12,427
Foreman, B.M. 12,897
Fortini, M.M. 12,790
Fox, C.E. 12,803
Frait, Z. 12,515
Frank, G.F. 12,842
Frankevich, E.L. 12,607
Freeman, Jr., D.C. 12,487
Freeman, III, W.J. 12,671
Freiberg, L. 12,699
Freise, E.J. 12,327
Friedberg, S.A. 12,483
Frisch, H.L. 12,468
Frisco, L.J. 12,448
Froemel, J.G. 12,403
Frohlich, H. 12,497
Frost, R.T. 12,422
Fu-ch'o, Pu. 12,519
Fuller, H.W. 12,517

Gabler, M. 12,738
Galkin, G.N. 12,462
Garg, J.M. 12,762
Gashimzade, F.M. 12,432
Gatos, H.C. 12,288, 12,408
Gaunt, P. 12,369
Gavrishchak, I.V. 12,246
Geguzin, Ya.E. 12,263
Geib, C.C. 12,655
Geldermans, P. 12,705
Gelling, W.G. 12,389
Genberg, R.W. 12,425
Georgobiani, A.N. 12,563
Gerber, J.F. 12,495
German, D.A. 12,652
Gerosa, G. 12,708
Gheorghita-Oancea, C. 12,579
Ghosh, P.K. 12,503
Ghosh, S.K. 12,535
Gibbons, J.F. 12,667
Gibson, W.M. 12,897
Gilbert, R. 12,810
Gilman, J.J. 12,617
Gindi, A.M. 12,808
Gjostein, N.A. 12,353
Gliessman, J.R. 12,646
Gnoth, B. 12,815
Goatcher, F. 12,860
Godik, E.E. 12,429
Goetzberger, A. 12,350
Goodyear, J. 12,328
Gorbacheva, I.E. 12,499
Gorkun, Yu.I. 12,473
Gossick, B.R. 12,340
Gould, J.R. 12,339
Grace, M. 12,706
Grandjean, C. 12,592
Grant, E.W. 12,768, 12,788
Greefkes, J.A. 12,794
Greenburg, R. 12,664
Greene, J.C. 12,779
Greiner, R.A. 12,682
Gresh, M. 12,728
Gribov, L.A. 12,434
Grinberg, A.A. 12,587
Gross, E.F. 12,541, 12,547
Grossweiner, L.I. 12,276
Gubkin, A.N. 12,442, 12,455
Guenther, J.H. 12,825
Gugelot, J.F. 12,395
Guggenheim, H. 12,404
Gulyaev, Yu.V. 12,461
Gutowsky, H.S. 12,444
Gyulai, Z. 12,375

Haanstra, J.H. 12,389
Haddad, G.I. 12,716
Hake, R.R. 12,496, 12,597
Hall, Jr., F.F. 12,887
Ham, F.S. 12,365
Hamaguchi, Y. 12,267
Hamilton, D.J. 12,817
Hamman, D.J. 12,630
Hanafy, Z. 12,537
Hanlet, J.M.N. 12,641
Happel, Jr., R.J. 12,402
Hardy, J.R. 12,546
Hashimoto, K. 12,481
Hawley, A.E. 12,746
Heaps, J.D. 12,687
Hearn, R. 12,773
Heller, W.R. 12,628
Hellwarth, R.W. 12,721
Heltemes, E.C. 12,596
Hemel, A. 12,733
Hemingway, T.K. 12,754
Hemmat, N. 12,376, 12,383
Henebry, W.M. 12,758
Henneke, H.L. 12,675
Herbst, N. 12,749
Herman, H. 12,475
Herzfeld, F. 12,823
Hilberg, W. 12,815
Hildebrandt, M. 12,521
Hileman, D.L. 12,793
Hillery, H.V. 12,803
Hillmann, H. 12,392
Hiltebeitel, J. 12,844
Hines, R.L. 12,390
Hirone, T. 12,356
Hoadley, J.C. 12,834
Hoekstra, W. 12,567
Hoffman, G.R. 12,848
Hoglen, J.J. 12,490
Holland, J.R. 12,406
Holland, L. 12,415
Holonyak, Jr., N. 12,637
Holthaus, G.L. 12,705
Honig, A. 12,528
Hooper, H.O. 12,286
Hoover, D.B. 12,297
Horner, D. 12,603
Hornig, D.F. 12,363
Hoshino, S. 12,254
Howard, R.E. 12,470
Howe, S. 12,289
Howie, A. 12,329
Hu, H. 12,373
Hughes, R.W. 12,854
Hulbert, J.A. 12,639
Hulme, K.F. 12,639
Hurle, D.T.J. 12,381

Iakovlev, V.A. 12,264
Iizima, S. 12,632
Il'in, V.E. 12,495
Indenbom, V.L. 12,306, 12,308
Isaacson, G.O. 12,655
Isler, W.E. 12,637
Ivanchik, I.I. 12,640
Izumi, K. 12,265
Izvozchikov, V.A. 12,583

Jablonowski, E.J. 12,395
Jackson, R.W. 12,895
Jacobson, R.L. 12,325
Jacox, M.E. 12,433
Jaeckel, R. 12,245
Jaffe, P.M. 12,565
Jain, S.C. 12,265
James, E.B. 12,845
James, W.J. 12,255
Janousek, V. 12,445
Jenkins, D.S. 12,635
Jensen, J.L. 12,765, 12,877
Johnson, C.A. 12,295
Johnson, L.D. 12,305
Johnson, R.E. 12,715
Johnson, T.L. 12,295
Johnston, R.C. 12,685
Jones, E.M. 12,865
Jones, H.J. 12,875
Jones, O. 12,385
Judkins, J.R. 12,805
Jury, E.I. 12,745

Kaderka, M. 12,455
Kagan, M.R. 12,725
Kaiser, A. 12,815
Kallmann, H. 12,565
Kaplyanski, A.A. 12,555
Kapshukov, I.I. 12,565
Karageorgii-alkalev, P.M. 12,645
Kard, P.G. 12,535
Karkhanin, Yu. I. 12,565
Karlik, S. 12,725
Kats, M.L. 12,565
Kauffmann, J.A. 12,845
Keating, D.T. 12,425
Kelley, A. 12,325
Kennedy, D.P. 12,665
Kerbnikov, F.I. 12,815
Kern, W. 12,335
Keyes, R.W. 12,615
Khansevarov, R.Yu. 12,575
Kikuchi, M. 12,635
Kikuchi, R. 12,345, 12,342
Kilmer, W. 12,845
Kim, C.S. 12,815
Kimura, M. 12,585
King, J.C. 12,625
Kishkin, S.T. 12,335
Kisliuk, P. 12,725
Kita, S. 12,635
Klein, E.A. 12,745
Klein, G. 12,775
Klemens, P.G. 12,475

iphuis, J. 12,779
ossika, W. 12,676
night, J.R. 12,379
hol, K.S. 12,774
howles, J.E. 12,511
obayashi, K. 12,586
oehler, H. 12,681
oehler, J.S. 12,416
ofstad, P. 12,269
oikov, S.N. 12,447
ojima, K. 12,273
ojima, T. 12,273
olbe, W.F. 12,278
olesova, V.A. 12,548
ondo, J. 12,506
onobeev, Yu.V. 12,539, 12,601
onstantinov, O.V. 12,541
opytina, M.V. 12,428
orenblit, I.Ya. 12,467
orsunskii, M.I. 12,559
osevich, A.M. 12,325
osevich, V.M. 12,292, 12,411
oshiga, F. 12,669
osman, M.S. 12,583
ostyshyn, B. 12,681
ovenskii, I.I. 12,359
ozuch, M. 12,871
rasner, S. 12,421
rasnopevtsev, V.V. 12,450
reingold, F.I. 12,547
retschmer, G.G. 12,589
rishnan, K.S. 12,268
rokhin, O.N. 12,643
ropschot, R.H. 12,731
roupa, F. 12,313, 12,320
rueger, H.H.A. 12,458
, T.C. 12,681
ucher, T.I. 12,344
uh, E.S. 12,742
uhrt, F. 12,683
ukushkin, L.S. 12,575
umihiro, T. 12,807
ürzler, J.E. 12,337
upec, P. 12,703
urbatov, L.N. 12,476
urova, I.A. 12,478
uskii, Yu. A. 12,463
uthel, E. 12,740
ushnerev, M.Ya. 12,486
ut, R.L. 12,711, 12,712, 12,713
ylie, N.R. 12,636

allen, M.L. 12,783
alterrere, J.P. 12,489
amiri, J. 12,535
anczerowicz, J. 12,454
anbert, L.M. 12,377
ang, I.G. 12,469
arabee, G.B. 12,412
arial, J. 12,610
arline, M.C. 12,288, 12,408
arrence, Jr., W.A. 12,799
asarev, A.N. 12,436
athenby, R. 12,526
atukin, V.N. 12,529
atsk, M.J.M. 12,526
atsedev, I.V. 12,778
atowitz, J.L. 12,468
atterc, P. 12,648
atowitz, B. 12,831
aupriere, B.M. 12,418
auder, A. 12,871
Leon, B.J. 12,748
Leslie, D.H. 12,496
Levchenko, A.A. 12,292
Levell, R.W. 12,830
Levine, S.N. 12,685
Levshin, V.L. 12,561
Levy, E. 12,831
Li, C.H. 12,298
Li, J.C.M. 12,319
Lidiard, A.B. 12,271
Lincoln, N.L. 12,672
Linde, V.R. 12,486
Lindmayer, J. 12,666
Ling, K.S. 12,686
Lipschuta, M.E. 12,401
Lipsite, H.A. 12,282
Litvinova, L.B. 12,559
Livingston, R. 12,531
Lloyd, A.G. 12,876
Logan, R.A. 12,247
Lomer, W.M. 12,507
Lowenthal, G.C. 12,477
Lungo, A. 12,736
Lupfer, D.E. 12,880
Lutes, O.S. 12,504
Luthman, E.H. 12,829
Luyckx, A. 12,441

Maaz, K. 12,683
MacDonald, A.L. 12,376, 12,383
Machlup, S. 12,459
Macklem, F.S. 12,870
Maclean, M.A. 12,848
Madatova, E.G. 12,321
Mader, S. 12,266
Mager, A. 12,392
Maguire, T. 12,709, 12,837
Maiden, C.E. 12,652
Maiman, T.H. 12,726
Makarov, V.P. 12,431
Makhov, G. 12,714
Maki, A.G. 12,550
Malinowski, S. 12,737
Manahan, W.A. 12,874
Mandelkorn, G. 12,690
Mannami, M. 12,265
Marais, A. 12,520
Marinace, J.C. 12,348, 12,649
Maringer, R.E. 12,299
Markin, B.I. 12,488
Marks, G. 12,797
Marlow, R. 12,678
Martinez, A. 12,821
Marzolf, J.M. 12,818
Matlow, S.L. 12,677
Matthews, J.W. 12,305
Matthias, B.T. 12,393
Mattson, R.H. 12,692
Matyas, M. 12,523
Maurer, R. 12,780
Maze, R.O. 12,763
McAfee, C. 12,690
McAvoy, N. 12,727
McClung, F.J. 12,721
McCormick, J.E. 12,901
McKeown, D. 12,414
McLaren, D. 12,757
McLaughlin, H.J. 12,858
McMahan, W.H. 12,717
McManus, G.M. 12,250
McMaster, R.C. 12,707
McMurtry, B.J. 12,718
Meessen, A. 12,581
Meltzer, I. 12,886
Mendelssohn, K. 12,494
Menetrey, W.R. 12,688
Merceron, T. 12,520
Meyer, N.I. 12,645
Meyers, F.J. 12,721
Mgebryan, O.I. 12,315
Michele, W. 12,804
Mikhail, H. 12,537
Miller, G.L. 12,897
Miller, S.L. 12,663
Milligan, D.E. 12,437
Miloslavski, V.K. 12,572
Minakova, S.V. 12,591
Minden, H.T. 12,378
Minner, W. 12,765, 12,828
Misarova, A. 12,445
Miselyuk, E.G. 12,284
Missman, Jr., R.A. 12,466
Mitoff, S.P. 12,480
Mitra, S.K. 12,302
Mitsuishi, T. 12,285
Miura, S. 12,356
Mohanty, G.P. 12,438
Moll, J.L. 12,645
Montgomery, G.F. 12,787
Moore, R.A. 12,783
Mori, R. 12,481
Moroz, L.M. 12,333
Morris, R.G. 12,599
Morrison, Jr., J.A. 12,872
Moss, T.S. 12,689
Mudholker, V.M. 12,611
Mueller, R.K. 12,326
Mullen, J.G. 12,270
Müller, E.W. 12,258
Mullin, J.B. 12,381
Mura, T. 12,283
Murley, P.C. 12,662
Murray, G.T. 12,303
Mykura, H. 12,355

Nabarro, F.R.N. 12,311
Nachtrieb, N.H. 12,354
Nagata, M. 12,902
Nagornaya, L.L. 12,575
Namba, S. 12,881
Nanavati, R. 12,750
Narasimhamurty, T.S. 12,619
Nasledov, D.N. 12,608
Natansohn, S. 12,398
Neshpor, V.S. 12,594
Neugebauer, C.A. 12,471, 12,513
Nevitt, M.V. 12,244
Newman, R.C. 12,361, 12,636
Newton, C.J. 12,417
Nicolas, J. 12,521
Nijland, L.M. 12,674
Nikitenko, V.I. 12,306
Nishimaki, N. 12,273
Niwa, H. 12,265
Nomura, K.C. 12,343
Norton, J.T. 12,259
Novikova, G.E. 12,591
Nowick, A.S. 12,614
Nussbaum, A. 12,687
Nyashin, Yu.I. 12,527

Oglesby, M.W. 12,880
Oharek, F.J. 12,717
Okazaki, A. 12,255
O'Keefe, J.G. 12,536
Okwit, S. 12,706, 12,781
Olson, E.R. 12,440
Olson, R.D. 12,809
Ondris, M. 12,515
O'Neil, J. 12,885
Ormont, B.F. 12,429
Osborne, P.W. 12,302
Ossoff, A. 12,770
Owens, E.B. 12,371
Owens, O.G. 12,785

Pacey, A.J. 12,609
Pai, M.A. 12,744
Paige, E.G.S. 12,540
Palatnik, L.S. 12,292
Parfianovich, I.A. 12,574
Paritskii, L.G. 12,576
Parker, E.R. 12,294
Parker, R. 12,397
Parkinson, D.H. 12,545
Pashaev, B.D. 12,602
Pasternák, J. 12,590
Pastur, L.A. 12,325
Pataki, G. 12,460
Paul, D.I. 12,509
Pearson, G.L. 12,358
Pell, E.M. 12,365, 12,366
Pelle, J.S. 12,331
Pen'kovski, V.V. 12,558
Penley, J.C. 12,277
Peperle, W. 12,245
Petitjean, C. 12,452
Petrenko, A.I. 12,864
Petty, R.L. 12,281
Phelps, D.H. 12,275
Phillips, W.D. 12,532
Pierce, W.H. 12,863
Pimentel, G.C. 12,549
Piper, T.S. 12,556
Piper, W.W. 12,387
Pohl, H.A. 12,489, 12,490
Polich, S.J. 12,387
Pollak, B.L. 12,439
Polyakov, L.M. 12,263
Popov, Yu. M. 12,643
Potter, R.F. 12,589
Pramann, R.F. 12,883
Pretzel, F.E. 12,281
Price, P.B. 12,313
Priest, J. 12,415
Primachenko, V.E. 12,501
Pritchard, J. 12,679
Prussin, S. 12,290
Prywes, N.S. 12,856
Pucel, R.A. 12,753
Puotinen, D.A. 12,385
Putner, T. 12,415

Quader, M.A. 12,345
Queisser, H.J. 12,350, 12,372

Rains, C.F. 12,707
Ralph, E.L. 12,677
Rao, K.R. 12,430
Redding, R.J. 12,769
Reddoch, A.H. 12,424
Redwood, M. 12,457
Reed, E.D. 12,722
Reinberg, A.R. 12,276
Reitz, J.R. 12,425
Remaut, G. 12,296
Rennert, J. 12,568
Resing, H.A. 12,354
Reynolds, C.E. 12,623
Reynolds, J.E. 12,647
Rhodes, R. 12,729
Richards, G.L. 12,862
Rieck, H. 12,780
Ringeissen, J. 12,570
Roberts, B.W. 12,617
Roberts, L.D. 12,898
Roberts, R.W. 12,400
Roessler, B. 12,251
Roginskii, S.Z. 12,486
Rollinger, C.N. 12,696
Romanov, V.A. 12,582
Roos, B. 12,427
Rosen, C.A. 12,449
Rosenstock, H.B. 12,598
Rosolowski, J.H. 12,352
Ross, V.F. 12,536
Singh, S. 12,553
Rowe, J.E. 12,716
Rowell, P.M. 12,494
Rozenblat, M.A. 12,811
Rozenshtein, L.D. 12,577
Rozhanskii, V.N. 12,308
Rubens, S.M. 12,835
Rubin, S. 12,746
Rugari, A.D. 12,882
Rutz, R.F. 12,649, 12,659, 12,661, 12,670
Ryvkin, S.M. 12,576

Sachse, H.B. 12,370
Saito, F. 12,715
Sakata, K. 12,606
Salem, T.M. 12,537
Salinger, G.L. 12,524
Samaun 12,802
Samsonov, G.V. 12,558
Sard, E.W. 12,781
Satyanarayana, B.S. 12,453
Sauerland, F. 12,736
Schear, J.J. 12,585
Scheibner, E.J. 12,747
Schennberg, D. 12,737
Scherbatskoy, S.A. 12,890
Schindler, M.J. 12,510
Schmid, Jr., A.P. 12,635
Schmid, H. 12,867
Schmit, J.L. 12,504
Schneider, A.D. 12,246
Schneider, H. 12,654
Schoeck, G. 12,293
Schol, K. 12,243
Schrieffer, J.R. 12,491
Schroeder, J.B. 12,600
Schwab, D. 12,900
Schwartz, C.M. 12,248
Schwartz, N. 12,728
Schwarz, S.E. 12,721
Scovil, H.E.D. 12,724
Scott, P.L. 12,534
Sears, G.W. 12,405
Seay, G.E. 12,623
Seeger, A. 12,260, 12,266
Seidel, H. 12,724
Sein, J.J. 12,685
Seitz, F. 12,274
Seitz, R.N. 12,425
Senf, H.R. 12,785
Serin, B. 12,493
Shah, B.P. 12,741
Shanavi, G.I. 12,442
Shao, J. 12,730
Shapiro, S. 12,732
Shaskol'skaya, M.P. 12,291
Shearin, P.E. 12,262
Shekhmamet'ev, R.I. 12,554
Shepherd, W.H. 12,367
Sheppard, A.P. 12,717
Shevlin, T.S. 12,604
Shibuya, I. 12,254
Shklyarevskii, I.N. 12,572
Shoda, K. 12,586
Shoji, M. 12,285
Shu-Chao, K. 12,291
Shukla, R.C. 12,433
Shuraleva, E.I. 12,574
Siegman, A.E. 12,718
Siina, S. 12,586
Silcox, J. 12,369
Silk, E.C.H. 12,322
Silverman, S.J. 12,384
Simsch, E. 12,266
Singh, S. 12,553
Sinha, P.P. 12,317
Sinha, S.K. 12,535
Skerritt, J.W. 12,843
Sloope, B.W. 12,391
Smakula, A. 12,278
Smilen, L.I. 12,751
Smith, G.E. 12,464
Smith, L.M. 12,820
Smith, M.S. 12,397
Smith, S.D. 12,546
Smulkowski, O. 12,894
Snitko, O.V. 12,501
Snitzer, E. 12,719
Soffer, B.H. 12,551
Solomon, R. 12,636
Solow, M. 12,562
Sorensen, A.A. 12,875, 12,876
Sorenssen, A. 12,782
Sparks, J.J. 12,658
Spieker, L.J. 12,872
Spitzer, W.G. 12,247
Stamires, D.N. 12,487
Stanke, W.A. 12,868
Stanley, C.V. 12,887
Starks, R.J. 12,386
Starr, A.T. 12,650
Starr, Jr., D.A. 12,819
Stauffer, J.R. 12,879
Steagall, W.F. 12,852
Steigman, G.A. 12,328
Stephens, D.R. 12,530
Stern, A.P. 12,755
Stern-Montagony, F. 12,861
Stewart, O.M. 12,248
Stokes, R.J. 12,298
Storsand, B. 12,653
Strandberg, M.W.P. 12,711, 12,712, 12,713
Straumanis, M.E. 12,253
Strauss, A.J. 12,371
Stubstad, W.R. 12,903
Stuhlbarg, S.M. 12,745
Sugano, T. 12,669
Sugihara, M. 12,522
Sullivan, D.L. 12,517
Sullivan, M.V. 12,407
Sunderland, J.E. 12,696
Susman, L. 12,779
Suzuki, Y. 12,859
Suzuoka, T. 12,356
Swann, P.R. 12,329
Swanson, M.L. 12,483
Sweaney, L.P. 12,745
Swenson, C.A. 12,596
Sylvan, T.P. 12,791
Synorov, V.F. 12,680
Sze, S.M. 12,357

Taimuty, S.I. 12,449
Takeuchi, T. 12,312
Tal'roze, V.L. 12,607
Tamai, T. 12,279, 12,362
Tanaka, K. 12,265
Tannenbaum, E. 12,346
Tannery, V.J. 12,694
Tanzman, H.D. 12,900
Tatsuzaki, I. 12,536
Tauchi, S. 12,285
Tenenholtz, R. 12,812
Teutonico, L.J. 12,309

Tharmalingam, K. 12,271
Thomas, A.C. 12,839
Thomas, P. 12,844
Thompson, C.T. 12,495
Thompson, J.T. 12,657
Thornton, P.H. 12,249
Tiller, C.O. 12,391
Tiller, W.A. 12,293
Tishler, C. 12,816
Tomasulo, R.M. 12,846
Tomboulian, D.H. 12,543
Tomiyasu, K. 12,832
Tomono, M. 12,285
Townsend, V.W.T. 12,727
Trapeznikova, O.N. 12,591
Truell, R. 12,625
Trumbore, F.A. 12,247
Trumbull 12,816
Tsertsvadeze, A.A. 12,557
Tsikin, A.N. 12,447
Tufte, O.N. 12,347, 12,687
Tuler, F.R. 12,261
Turner, J. 12,367
Tyablikov, S.V. 12,519
Tyapkina, N.D. 12,478

Ugai, Ya.A. 12,560

Vacek, K. 12,330, 12,570
Vajda, G.L. 12,440
van den Ban, P. 12,705
van der Burgt, C.M. 12,395
Vandewauwer, J. 12,441
van de Weg, H. 12,774
Van Laar, J. 12,585
Varlashkin, P.G. 12,884
Varshni, Y.P. 12,433
Vartanyan, A.T. 12,577
Vasicek, A. 12,593
Vasilevskaya, V.N. 12,284
Vassiliev, A. 12,521
Vaughan, D.A. 12,248
Vedder, W. 12,363
Veith, P. 12,798
Velikov, Yu.Kh. 12,621
Vennik, J. 12,296
Victor, A.C. 12,595
Vieland, L.J. 12,351
Vigneron, M.C. 12,518
Vlasenko, N.A. 12,572
Vodicka, V.W. 12,759
Volkov, S.D. 12,622
Vook, F.L. 12,420
Vorob'ev, Yu.V. 12,569
Votava, E. 12,252
Vozhenin, I.N. 12,665
Vul, B.M. 12,642

Wakefield, J. 12,361
Wald, M. 12,257
Walter, F.J. 12,898
Wang, D.Y. 12,282
Warekois, E.P. 12,408
Washburn, J. 12,297
Wasscher, J.D. 12,472, 12,471
Webb, M.B. 12,895,
Webb, P.P. 12,896
Wechsler, L.D. 12,784
Weeks, R.F. 12,624
Wegner, H.E. 12,899
Wei, L.Y. 12,357
Weise, E.K. 12,484
Wenden, H.E. 12,604
West, R.G. 12,694
Wheatley, J.C. 12,524
Wheeler, R.G. 12,542, 12,734
White, D.L. 12,613
White, G.K. 12,340
Whitehurst, H.B. 12,618
Whitworth, R.W. 12,863
Widrow, B. 12,562
Wiley, R.C. 12,500
Williams, A.J. 12,360
Williams, E.L. 12,895,
Williams, R.L. 12,896
Williams, S.E. 12,571
Wilson, D.V. 12,300
Wind, B.A. 12,773
Witt, Jr., S.N. 12,789
Witte, R.S. 12,277
Woika, J.L. 12,822
Woods, A.D.B. 12,430
Worden, E.C. 12,403
Wright, G.T. 12,730
Wright, L.G. 12,449
Wrigley, C. 12,666

Yamada, H. 12,850
Yamato, J. 12,859
Yaroshetskii, I.D. 12,576
Yen, C.S. 12,743
Yen-Wen, W. 12,291
Yoshimatsu, M. 12,318
Youla, D.C. 12,751
Yuan, L.C.L. 12,897

Zaalberg van Zelst, J.J. 12,772
Zaitseva, A.S. 12,436
Zakharchenya, B.P. 12,541
Zavaritskaya, E.I. 12,479
Záveta, K. 12,485
Zeldes, H. 12,531
Zelinin, Ya.M. 12,573
Zhilich, A.G. 12,431
Zhukovskii, A.P. 12,573
Zolotareva, Yu.M. 12,516
Zuleeg, R. 12,579

Pre-publication Announcement

A BOOK
OF CLASSIFIED
ABSTRACTS
ON

ORGANIC SEMICONDUCTORS

FEATURING

- Over 1000 Abstracts
- Subject Index
- Material Index
- Author Index

You save money by ordering now at the pre-publication price of $20.00

Payment will not be due until the book is issued in the Fall of 1962.

SEND YOUR ORDER TODAY TO

CAMBRIDGE COMMUNICATIONS CORPORATION
238 Main St., Cambridge 42, Mass.

Please enter our Pre-publication Order for ORGANIC SEMICONDUCTORS to be published in the Fall of 1962, at the special price of $20.00.

Name .....
Position .....
Company .....
Division, if any .....
Address .....
City ..... Zone ..... State.....

FOR SURFACE STUDIES

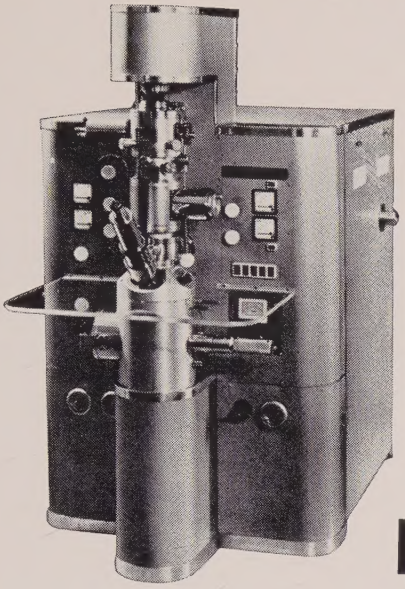

KE1

Trüb, Täuber Secondary Electron Emission Microscope

for direct viewing of metallic and semiconducting specimens by means of secondary electrons released from ion bombardment of the surface — featuring . . .

- Images free of distortion and deformation
- Enlargement up to 1500 X electronoptically
- Resolution 500–600Å
- Object temperature 150°–800° C
- Observable surface of the object 25 mm square
- Differentiation of the material

The Instrument Includes . . .

Electrostatic immersion objective
Ion beam system
Revolving contrast diaphragms
2 electromagnetic projectors
Observation chamber with fluorescent image screen
Recording chamber with plate cassette
High-intensity optical microscope
All-metal housing with vacuum equipment including diffusion pump
High-voltage equipment for 45 kV
Measuring instruments and control equipment

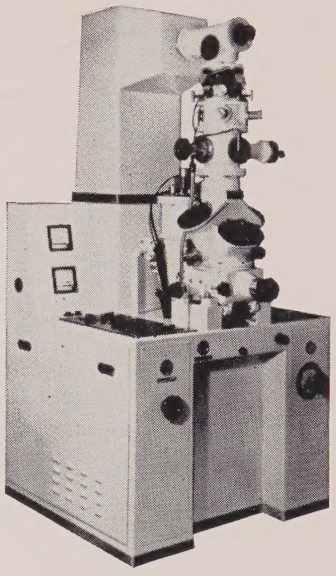

KD3

Trüb, Täuber Electron Diffractograph

for determining the crystalline structure of surfaces, thin layers, and extremely small quantities of material, including dynamic processes — featuring . . .

- Cold-cathode electron gun with practically unlimited life
- Simple design — dependable operation, extreme flexibility
- Balanced optical system
- High resolving power
- Large variety of specimen holders for various methods of investigation
- Devices for heating and cooling the test specimens (from liquid nitrogen to 1000°C)
- Devices for discharging, etching, surface evaporating
- Various cameras for photographic recording on plates and films
- Unique kinematic recorder

Specifications

Acceleration Voltage —	
continuously adjustable:	10 to 50 kV
ripple (fractional):	$\approx 10^{-4}$
stability:	$\pm 0.1\%$
Final vacuum:	approx. 2×10^{-5} mm Hg
Magnification with electronic lens:	75X
Minimum line width:	0.001 mm
Minimum diameter of beam for focussing on specimen, without additional diaphragms:	4μ

Distributed by:

NEW ENGLAND SCIENTIFIC INSTRUMENTS CO.

238 MAIN STREET · CAMBRIDGE 42, MASSACHUSETTS · KIrkland 7-2932

Electron Microscopes • Nuclear Induction Spectrographs • High Voltage Oscillographs • Precision Laboratory Instruments • Nuclear Track Microscopes

in'for·ma'tion re·triev'al, *n.* **1.** rapid location of technical information on specific topics.

information retrieval system for the solid state:

SOLID STATE ABSTRACTS ON CARDS

INSTRUCTIONS—OUTLINE—PRE-INDEX
for
SOLID STATE ABSTRACTS ON CARDS

PHYSICS
METALLURGY
ELECTRONICS

SEMICONDUCTORS
PHOSPHORS
MAGNETICS
DIELECTRICS
SUPERCONDUCTORS
METALS

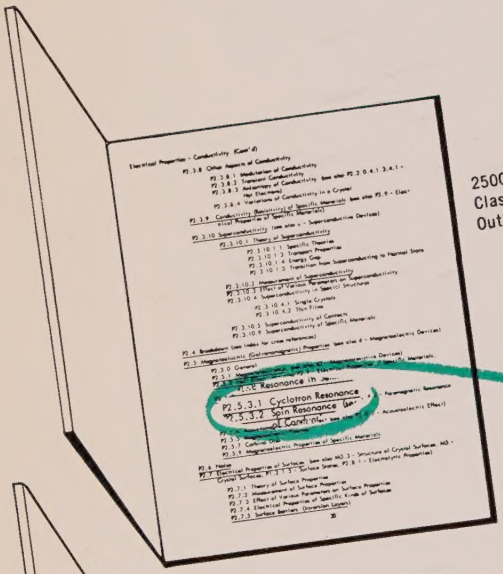

2500-Topic Classification Outline

Send for your free copy of our new 120 page book describing this unique system which is now being used in more than 300 solid state laboratories throughout the world.

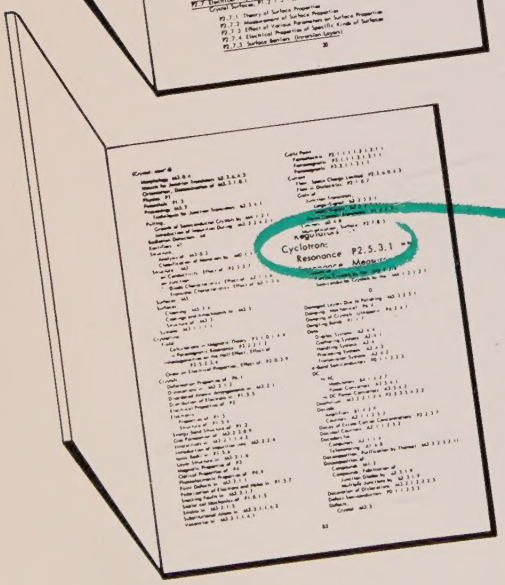

4000-Entry Alphabetical Pre-Index

Guide Card

P2.5.3.1 Cyclotron Resonance

10,000 abstract cards already available with regular monthly additions

P2.5.3.1.1

7318 PROPERTIES OF SEMICONDUCTORS WITH AN EXTREMUM LOOP I. CYCLOTRON AND COMBINATIONAL RESONANCE IN A MAGNETIC FIELD PERPENDICULAR TO THE PLANE OF THE LOOP by E. I. Rashba (Inst. of Physics, Kiev); Soviet Phys. – Solid State, Vol. 2, pp. 1109–1122, Dec. 1960

The absorption of radio waves in semiconductors having a specific band structure where an extremum is reached not at isolated points but over a curve in k-space is discussed. The frequencies and intensities of the transitions are computed. It is shown that as a result of the presence of spin-orbital bonds, transitions involving a change in spin due to the Lorentz force possess significant power

CAMBRIDGE COMMUNICATIONS CORPORATION

236 MAIN STREET • CAMBRIDGE 42, MASSACHUSETTS • **Tel. 491-0710**